

**Molecular analysis of insulin signaling mechanisms in
Echinococcus multilocularis and their role in the host-parasite
interaction in the alveolar echinococcosis**

**Dissertation zur Erlangung des
naturwissenschaftlichen Doktorgrades der
Bayerischen Julius-Maximilians-Universität
Würzburg**

**Vorgelegt von:
Christian Konrad
aus Würzburg**

Würzburg, Februar 2007

Eingereicht am:

Mitglieder der Promotionskommission:

Vorsitzender: Prof. Dr. Martin J. Müller

Gutachter: Prof. Dr. Matthias Frosch

Gutachter: Prof. Dr. Jürgen Kreft

Promotionskolloquium am:

Promotionsurkunde ausgehändigt am:

Ehrenwörtliche Erklärung

Hiermit erkläre ich, die vorliegende Dissertation selbstständig angefertigt und nur die angegebenen Quellen und Hilfsmittel verwendet zu haben. Diese Arbeit ist bisher in gleicher oder ähnlicher Form keinem anderen Prüfungsverfahren mit dem Ziel der Erlangung eines akademischen Grades vorgelegen, auch in anderen Fakultäten erfolgte noch keine vollständige oder teilweise Vorlegung.

Zürich, den 21.2.2007

Christian Konrad

Vielen Dank an.....

Prof. Dr. Matthias Frosch für die Möglichkeit der Promotion, die Übernahme des Gutachtens und die langjährige Unterstützung, die diese Promotion erst ermöglicht hat.

Prof. Dr. Jürgen Kreft für die wiederholte Bereitschaft als Gutachter aus der Fakultät für Biologie zur Verfügung zu stehen.

Prof. Dr. Klaus Brehm für die permanente Unterstützung und die vielen hilfreichen Diskussionen am Abend, die sehr zum Gelingen dieser Arbeit beigetragen haben. Ich werde nie das „Bist Du dir da sicher?“ oder „Wo ist denn die Kontrolle?“ vergessen. Auch weiß ich jetzt, wen ich bei „Wer Wird Millionär“ mit dem Telefonjoker anrufen würde und welches fränkische Wort doch mit einem „harden D“ geschrieben wird.

Moni Bergmann, der Protein-Fee, für das erfolgreiche Bewerben des Bio-RAD Systems und das stets offene Ohr bei Problemen aller Art.

Meiner Bench-Nachbarin Verena für ihre Hilfsbereitschaft und dem einen oder anderen Schwank. Ich gebe zu, Saarländer sind keine Pfälzer, aber fast....

Markus für die Metazestoden und die Einführung in deren Kultivierung. Ich danke Dir auch für die schönen Abende mit den Zerglingen, denen das Vespingas ausging....

Katja, Tina, Sabrina S., Florian, Ricardo und Julia für die schöne Zeit.

Bianca bzw. Calvin & Hobbes für die Aufmunterung als die EmMPK-1 mir Kummer bereitete und diverse Motivationsschübe zum Schreiben dieser Arbeit.

Dr. Alexandra Schubert-Unkmeir für die Möglichkeit an Neisserien zu arbeiten, die Zeit um diese Doktorarbeit zu schreiben und die fortlaufende Unterstützung.

Sabrina H. für sämtliche Blots von HBMEC-Zellen, auch wenn ich mir ziemlich sicher bin, dass sie dich im Schlaf verfolgen werden.

Giuseppe für die sizilianische Pizza.

Meiner Familie, die mich immer unterstützte.

Samuel, der mir seit über 10 Jahren ein sehr guter Freund ist.

Contents

<u>1 Abstract/ Zusammenfassung</u>	<u>1</u>
<u>2 Introduction</u>	<u>5</u>
2.1 The small fox-tapeworm <i>Echinococcus multilocularis</i>	5
2.1.1 Phylogeny	5
2.1.2 Life cycle	7
2.1.3 <i>E. multilocularis</i> – the causative agent of the alveolar echinococcosis	10
2.1.4 Epidemiology of the alveolar echinococcosis	11
2.2 Insulin/ Insulin-like-Growth-Factor I signaling	12
2.2.1 Hormones of the insulin superfamily	12
2.2.2 Insulin/ IGF-I signaling cascade in mammalian (human) cells	14
2.2.3 Insulin/ IGF-I signaling cascade in invertebrates	18
2.2.4 Insulin/ IGF-I signaling in <i>E. multilocularis</i>	20
2.3 Src-family kinases (non-receptor tyrosine kinases) and GAP-proteins	22
2.4 Molecular biology of <i>E. multilocularis</i>	23
2.4.1 <i>E. multilocularis</i> orthologs of mammalian signaling molecules	23
2.4.2 <i>In vitro</i> cultivation of <i>E. multilocularis</i> larval stages	24
2.4.3 Trans-splicing in <i>E. multilocularis</i>	25
2.4.4 Recombinant antigens	25
2.5 Aims	26

3 Results	27
3.1 Insulin promotes growth and survival of <i>E. multilocularis</i> metacystode vesicles <i>in vitro</i>	27
3.1.1 Insulin promotes growth and survival of <i>E. multilocularis</i> metacystode vesicles under axenic conditions	27
3.1.2 Immortal hepatocyte cell lines express insulin	28
3.1.3 Host albumin promotes survival of <i>E. multilocularis</i> metacystode vesicles <i>in vitro</i>	29
3.2 Insulin and IGF-I affect <i>E. multilocularis</i> metacystode vesicles on several levels	31
3.2.1 Insulin and IGF-I stimulate DNA <i>de novo</i> synthesis in <i>E. multilocularis</i> metacystode vesicles <i>in vitro</i>	31
3.2.2 Insulin and IGF-I induce protein phosphorylation in <i>E. multilocularis</i> metacystode vesicles <i>in vitro</i>	32
3.2.3 Host derived factors including Insulin and IGF-I activate a specific signal transduction pathway in <i>E. multilocularis</i> metacystode vesicles <i>in vitro</i>	33
3.2.4 Insulin stimulates <i>egfd</i> expression in <i>E. multilocularis</i> metacystode vesicles <i>in vitro</i>	37
3.3 EmIR - the <i>E. multilocularis</i> insulin receptor ortholog as potential transmitter of external signals	39
3.3.1 Southern blot analysis of <i>E. multilocularis</i> chromosomal DNA – EmIR is encoded by a single copy gene	39
3.3.2 Production of polyclonal antibodies directed against EmIR's ligand binding and intracellular domain	41
3.3.3 Western blot analysis of <i>E. multilocularis</i> metacystode vesicles for the expression of EmIR	46

3.3.4 Expression of EmIR in <i>E. multilocularis</i> larval stages under different growth conditions	49
3.3.4.1 <i>in vitro</i> activation of protoscolices affects the expression of EmIR	49
3.3.4.2 Expression of EmIR in <i>E. multilocularis</i> metacestode vesicles is upregulated by host derived factors	53
3.3.5 Immunohistochemical and electron microscopical analysis of the expression of EmIR in <i>E. multilocularis</i> larval stages	56
3.3.6 Expression of EmIR in a heterologous system	59
3.3.7 <i>in vitro</i> autophosphorylation of insulin stimulated EmIR	64
3.3.8 activation of EmIR in <i>E. multilocularis</i> metacestode vesicles by insulin	66
3.3.9 An inhibitor of human IR tyrosine kinase affects <i>E. multilocularis</i> metacestode vesicles <i>in vitro</i>	66
3.4 Insulin but not IGF-I can be detected in the hydatid fluid of <i>E. multilocularis</i> metacestode vesicles <i>in vitro</i> and <i>in vivo</i>	71
3.5 Protein <i>de novo</i> synthesis in <i>E. multilocularis</i> metacestode vesicles is upregulated by host derived factors different from insulin	76
3.6 Downstream signaling of EmIR in <i>E. multilocularis</i> larval stages	78
3.6.1 Expression of EmIR tyrosine kinase domain in a heterologous system	78
3.6.2 Identification of IR Orthologs in other Cestodes	81
3.6.2.1 Characterization of cDNAs from distinct cestodes encoding ligand binding and tyrosine kinase domain of IR orthologs	82
3.6.2.2 Amino acid sequence comparison of the IR ligand binding and tyrosine kinase domain of cestode IR orthologs	96

3.6.3 Identification of a possible EmIR downstream signaling cascade in <i>E. multilocularis</i> larval stages	102
3.6.3.1 Analysis of <i>emrhogap</i> cDNA	103
3.6.3.2 Structural features of EmRhoGAP	106
3.6.3.3 Analysis of <i>emfyn</i> cDNA	112
3.6.3.4 Structural features of EmFyn	115
3.6.3.5 Analysis of the expression of <i>emfyn</i> and <i>emrhogap</i> in <i>E. multilocularis</i> larval stages	123
3.6.3.6 Analysis of the expression of <i>emfyn</i> and <i>emrhogap</i> in insulin stimulated <i>E. multilocularis</i> metacestode vesicles	124
3.6.3.7 Interaction between EmFyn and EmIR <i>in vitro</i>	125
3.6.3.8 EmFyn and EmRhoGAP interact in the Yeast Two Hybrid	128
3.6.3.9 EmRhoGAP interacts with EmRap2 and EmRaf in the Yeast Two Hybrid	130
3.6.3.10 Src-family kinase inhibitors affect <i>E. multilocularis</i> metacestode vesicles <i>in vitro</i>	132
4 Discussion	134
5 Materials and Methods	142
5.1 Equipment	142
5.2 Consuming articles	142
5.3 Enzymes, commercial kits, chemicals and oligonucleotides	143
5.4 Working with RNA	144
5.4.1 Isolating total RNA from mammalian cells	144
5.4.2 Isolating total RNA from metacestode vesicles and protoscolices	144
5.4.3 DNase I treatment of isolated total RNA	145
5.4.4 Synthesis of first strand cDNA	145

5.5 Working with DNA	145
5.5.1 Isolation of chromosomal DNA from <i>E. multilocularis</i> larval stages	145
5.5.2 Isolation of plasmid DNA from bacteria	146
5.5.3 Determination of DNA concentration	146
5.5.4 Agarose – gelelectrophoresis	147
5.5.5 Purification of DNA from agarose gels, PCR and restriction digests	148
5.5.6 DNA precipitation	148
5.5.7 DNA – sequencing	148
5.5.8 Polymerase Chain Reaction (PCR)	149
5.5.9 Restriction digest of DNA	150
5.5.10 Ligation of DNA fragments	150
5.5.11 TOPO-TA and TA-cloning	151
5.5.12 Southern blot hybridization	151
5.6 General protein analysing methods	152
5.6.1 SDS-PAGE	152
5.6.2 Coomassie staining	153
5.6.3 Western blot	154
5.6.4 Determination of protein concentration	156
5.6.5 Protease inhibitors and phosphatase inhibitors	156
5.7 Working with bacteria	157
5.7.1 Bacterial strains	157
5.7.2 Media	157
5.7.3 Transformation of bacteria	158
5.7.4 Recombinant expression of proteins in <i>E. coli</i>	158
5.7.4.1 pBAD/Thio-TOPO [®] Vector and pBAD/TOPO [®] Vector (Invitrogen)	158
5.7.4.2 pGEX-3X – Glutathione - S - Transferase fusion proteins	161

5.7.4.3 Recombinant expression of ligand binding and intracellular domain of EmIR with the pBAD/Thio-TOPO [®] Vector in <i>E.coli</i> BL21	163
5.7.4.4 Expression of the extracellular and intracellular domain of EmIR with pGEX-3X in <i>E.coli</i> BL21	164
5.7.4.5 Longterm storage of purified proteins	165
5.8 Immunization of rabbits	165
5.9 Expression of <i>E. multilocularis</i> proteins in heterologous systems	166
5.9.1 Expression of EmIR in S2 (<i>Drosophila</i>) – cells	166
5.9.2 Expression of EmIR in mammalian cells – human embryonal kidney (HEK293) cells	168
5.9.3 Expression of EmFyn and EmRhoGAP in mammalian cells	174
5.9.4 Transfection of mammalian cells, lysis and immunoprecipitation	175
5.10 Yeast Two Hybrid analysis	176
5.10.1 Media, buffers and yeast strains	176
5.10.2 Matchmaker 3 GAL4 Two – Hybrid system	177
5.10.3 Yeast transformation and analysis of protein interaction	179
5.10.4 Cloning of Yeast Two Hybrid constructs	180
5.10.4.1 EmFyn constructs	180
5.10.4.2 EmRhoGAP constructs	181
5.10.4.3 EmIR and HIR constructs	181
5.11 Expression of <i>insulin</i> and <i>igf-I</i> in hepatocytes	183
5.12 Working with <i>E. multilocularis</i>	185
5.12.1 <i>E. multilocularis</i> isolates	185
5.12.2 Cultivation of <i>E. multilocularis</i> <i>in vivo</i>	185
5.12.3 <i>in vitro</i> cultivation of <i>E. multilocularis</i>	186
5.12.4 Isolation of protoscoleces	187

5.12.5 <i>in vitro</i> activation of protoscoleces	188
5.12.6 Protein synthesis and secretion into both the medium and hydatid fluid is upregulated by host factors	188
5.12.7 Phosphorylation of parasite proteins is induced by insulin and IGF-I	189
5.12.8 <i>in vitro</i> phosphorylation of EmIR	190
5.12.8.1 <i>in vitro</i> phosphorylation assay	190
5.12.8.2 Stimulation of in intact vesicles with insulin	192
5.12.8.3 Effect of HIR tyrosine kinase inhibitor HNMPA-(AM) ₃ on <i>E. multilocularis</i> metacestode vesicles	192
5.12.8.4 Effect of HIR tyrosine kinase inhibitor HNMPA-(AM) ₃ on EmMPK-1	193
5.12.8.5 EmMPK-1 is activated by human insulin as well as human IGF-I	193
5.12.8.6 Human insulin stimulates the expression of <i>egfd</i>	194
5.12.8.7 Immunohistochemistry and electron microscopy	196
5.12.8.8 Isolation of hydatid fluid and measuring of insulin and IGF-I concentration	197
5.12.8.9 Uptake of insulin-biotin	197
5.13 IR orthologs of other cestodes	198
<u>6 References</u>	<u>200</u>
<u>7 Publications</u>	<u>213</u>
<u>8 Curriculum vitae</u>	<u>217</u>

1 Abstract

The insulin receptor ortholog EmIR of the fox-tapeworm *Echinococcus multilocularis* displays significant structural homology to the human insulin receptor (HIR) and has been suggested to be involved in insulin sensing mechanisms of the parasite's metacestode larval stage. In the present work, the effects of host insulin on *Echinococcus* metacestode vesicles and the proposed interaction between EmIR and mammalian insulin have been studied using biochemical and cell-biological approaches. Human insulin, exogenously added to *in vitro* cultivated parasite larvae, (i) significantly stimulated parasite survival and growth, (ii) induced DNA *de novo* synthesis in *Echinococcus*, (iii) affected overall protein phosphorylation in the parasite, and (iv) specifically induced the phosphorylation of the parasite's Erk-like MAP kinase orthologue EmMPK1. These results clearly indicated that *Echinococcus* metacestode vesicles are able to sense exogenous host insulin which induces a mitogenic response. To investigate whether EmIR mediates these effects, anti-EmIR antibodies were produced and utilized in biochemical assays and immunohistochemical analyses. EmIR was shown to be expressed in the germinal layer of the parasite both on the surface of glycogen storing cells and undifferentiated germinal cells. Upon addition of exogenous insulin to metacestode vesicles, the phosphorylation of EmIR was significantly induced, an effect which was suppressed in the presence of specific inhibitors of insulin receptor-like tyrosine kinases. Furthermore, upon expression of EmIR/HIR receptor chimera containing the extracellular ligand binding domain of EmIR in HEK 293 cells, a specific autophosphorylation of the chimera could be induced through the addition of exogenous insulin. These results indicated the capability of EmIR to sense and to transmit host insulin signals to the *Echinococcus* signaling machinery. The importance of insulin signaling mechanisms for parasite survival and growth were underscored by *in vitro* cultivation experiments in which the addition of an inhibitor of insulin receptor tyrosine kinases led to vesicle degradation and death.

Based on the above outlined molecular data on the interaction between EmIR and mammalian insulin, the parasite's insulin receptor orthologue most probably mediates the insulin effects on parasite growth and is, therefore, a potential candidate factor for host-parasite communication via evolutionary conserved pathways.

In a final set of experiments, signaling mechanisms that act downstream of EmIR have been analyzed. These studies revealed significant differences between insulin signaling in

Echinococcus and the related cestode parasite *Taenia solium*. These differences could be associated with differences in the organo-tropism of both species.

Zusammenfassung

Der orthologe Insulinrezeptor EmIR des Fuchsbandwurmes *Echinococcus multilocularis* weist signifikante strukturelle Homologie zum humanen Insulinrezeptor (HIR) auf. Es wurde schon seit geraumer Zeit vermutet, dass EmIR an den Mechanismen beteiligt sein könnte, die es dem Metacestoden Larvenstadium des Parasiten erlauben Insulin zu detektieren. In dieser Arbeit wurden die Effekte von Wirtsinsulin auf *Echinococcus* Metacestoden-Vesikel und die vermutete Interaktion zwischen EmIR und Insulin von Säugern mittels biochemischer und zellbiologischer experimenteller Ansätze untersucht. Die exogene Zugabe von humanem Insulin zu *in vitro* kultivierten Parasitenlarven hatte folgende Effekte: (i) das Überleben und das Wachstum des Parasiten wurde signifikant stimuliert; (ii) die DNA *de novo* Synthese in *Echinococcus* wurde induziert; (iii) die generelle Proteinphosphorylierung des Parasiten wurde beeinflusst; (iv) die Phosphorylierung der orthologen Erk-like MAP Kinase, EmMPK1, des Parasiten wurde spezifisch induziert. Diese Beobachtungen zeigen deutlich, dass *Echinococcus* Metacestoden-Vesikel exogenes Insulin des Wirtes detektieren können und dass dieses Insulin einen mitogenischen Effekt auf den Parasiten hat. Um zu untersuchen, ob diese Effekte durch EmIR vermittelt werden, wurden anti-EmIR Antikörper hergestellt und in biochemischen experimentellen Ansätzen und immunohistochemischen Analysen eingesetzt. Es konnte gezeigt werden, dass EmIR in der Germinalschicht des Parasiten expremiert wird, sowohl an der Oberfläche von Glykogen-Speicherzellen als auch von undifferenzierten Germinalzellen. Nach der Zugabe von exogenem Insulin konnte eine signifikante Zunahme der Phosphorylierung von EmIR festgestellt werden. Diese Stimulierung konnte durch die Zugabe eines spezifischen Inhibitors für Insulinrezeptor-ähnliche Tyrosinkinasen unterdrückt werden. Desweiteren konnte mittels der Expression eines chimären EmIR/HIR-Rezeptors, der die extrazelluläre Ligandenbindungsdomäne von EmIR enthielt, in HEK293 Zellen gezeigt werden, dass die Zugabe von exogenem Insulin eine spezifische Autophosphorylierung der Chimäre induziert. Diese Ergebnisse bezeugen die Fähigkeit von EmIR Insulin-abhängige Signale des Wirtes einerseits zu detektieren und andererseits an die *Echinococcus* Signalwege weiter zu leiten. Die Bedeutung von Insulin-Signalmechanismen für das Überleben und das Wachstum des Parasiten konnte durch *in vitro* Kultivierungsexperimente aufgezeigt werden. Die Zugabe eines Inhibitors spezifisch für Insulinrezeptor Tyrosinkinasen verursachte die Degradation und den Tod der Metacestoden-Vesikel. Basierend auf den dargelegten molekularen Daten bezüglich der Interaktion zwischen EmIR und Insulin von Säugern erscheint es sehr wahrscheinlich, dass der orthologe Insulinrezeptor des Parasiten die Effekte von Insulin auf das Wachstum des Parasiten vermittelt. Aus diesem Grund ist EmIR ein

potentieller Kandidat für die Kommunikation zwischen Wirt und Parasiten mittels evolutionär konservierten Signalwegen.

Die Signalmechanismen unterhalb von EmIR wurden in abschließenden Experimenten untersucht. Diese offenbarten deutliche Unterschiede in der Weiterleitung von Insulin induzierten Signalen zwischen *Echinococcus* und dem verwandten parasitären Zestoden *Taenia solium*. Diese Unterschiede könnten mit dem unterschiedlichen Organtropismus beider Arten in Verbindung stehen.

2 Introduction

2.1 The small fox-tapeworm *Echinococcus multilocularis*

2.1.1 Phylogeny

All so-called helminths belong to the protostomia, while the vertebrates belong to the deuterostomia. The former are further divided into two groups, the ecdysozoa and the lophotrochozoa. The ecdysozoa are characterized by possessing an exoskeleton and that they grow by molting, while the other group is characterized by having the soft tissue in contact with the environment and having cilia for feeding and moving. The two major phyla comprising the helminths, the nematodes and the platyhelminthes, belong to the ecdysozoa and lophotrochozoa, respectively [11]. The phylogenetic positions as well as representatives of those two phyla are given in figure 1.

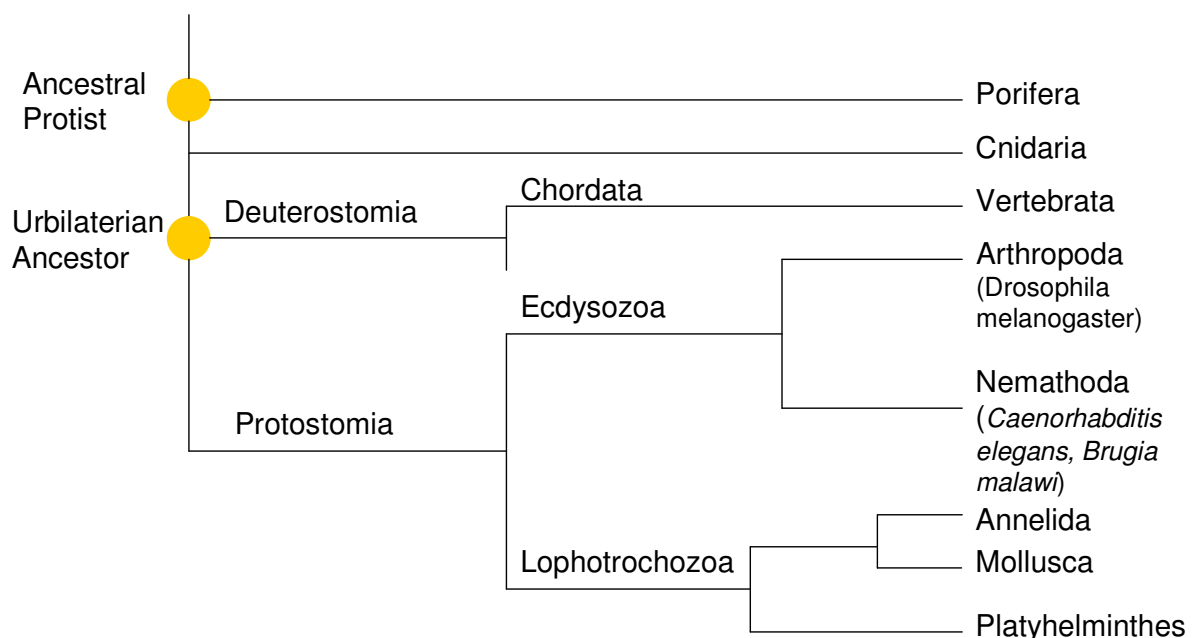


Fig. 1: Phylogenetic tree of the phylum platyhelminthes (adapted from S.C. Gilbert, Developmental Biology 6th edition 2000). The phylogenetic position of the phylum platyhelminthes, nematoda and arthropoda are shown. Important members of these phylums are given in brackets

With *Caenorhabditis elegans*, a model organism for parasitic nematodes as well as for developmental biology has been successfully established. Important human and veterinarian parasitic helminths of the genera *Echinococcus*, *Taenia* and *Schistosoma* (Fig.2) can be found among the platyhelminthes [12,179,180]. Until today, 5 species of the genus *Echinococcus* are known: *E. granulosus*, *E. multilocularis*, *E. vogeli* und *E. oligarthus* [13] and *E. shiquicus* [32]. But it has been discussed in recent years to grant two subspecies of *E. granulosus*, *E. granulosus equinus* and *E. granulosus ortleppi*, the status of species due to progress in molecular characterization [13]. In the following, a general overview of the biology of the genus *Echinococcus* will be given, with emphasis on *E. multilocularis*.

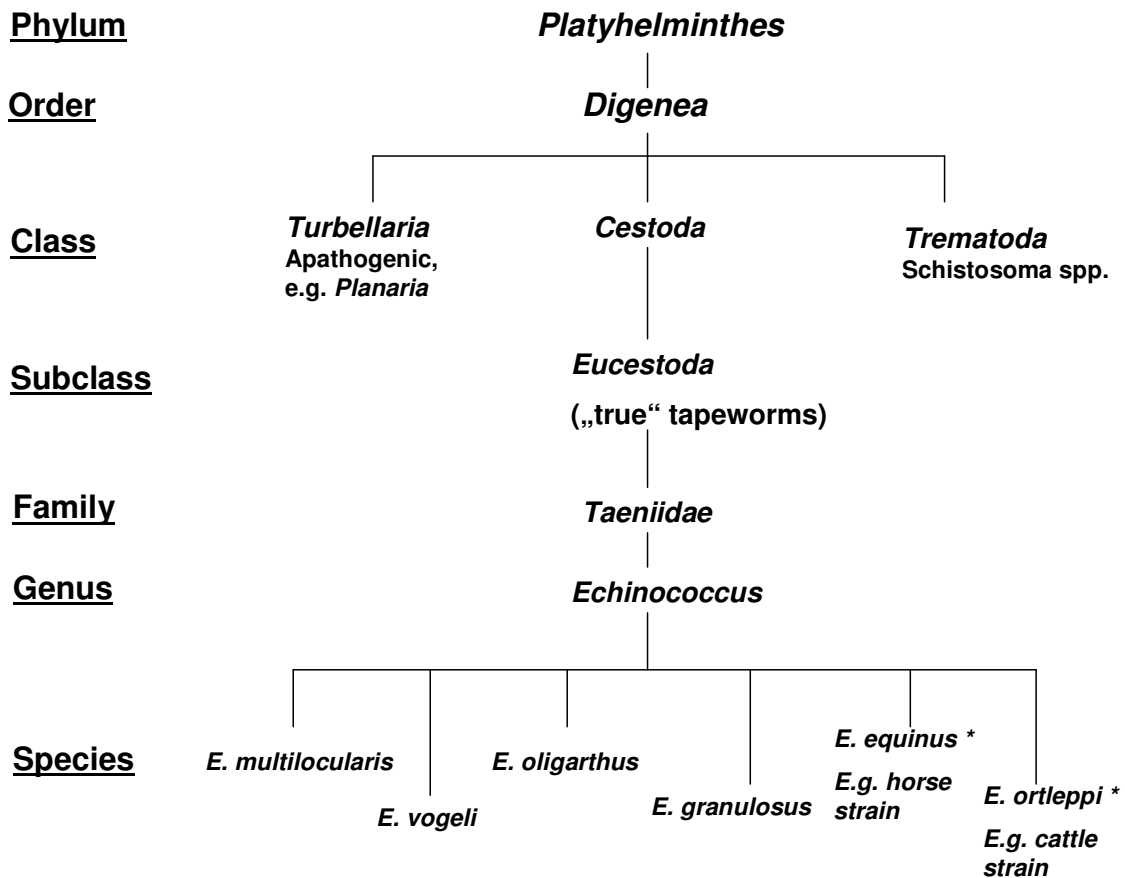


Fig. 2: Phylogenetic tree of the genus *Echinococcus*.

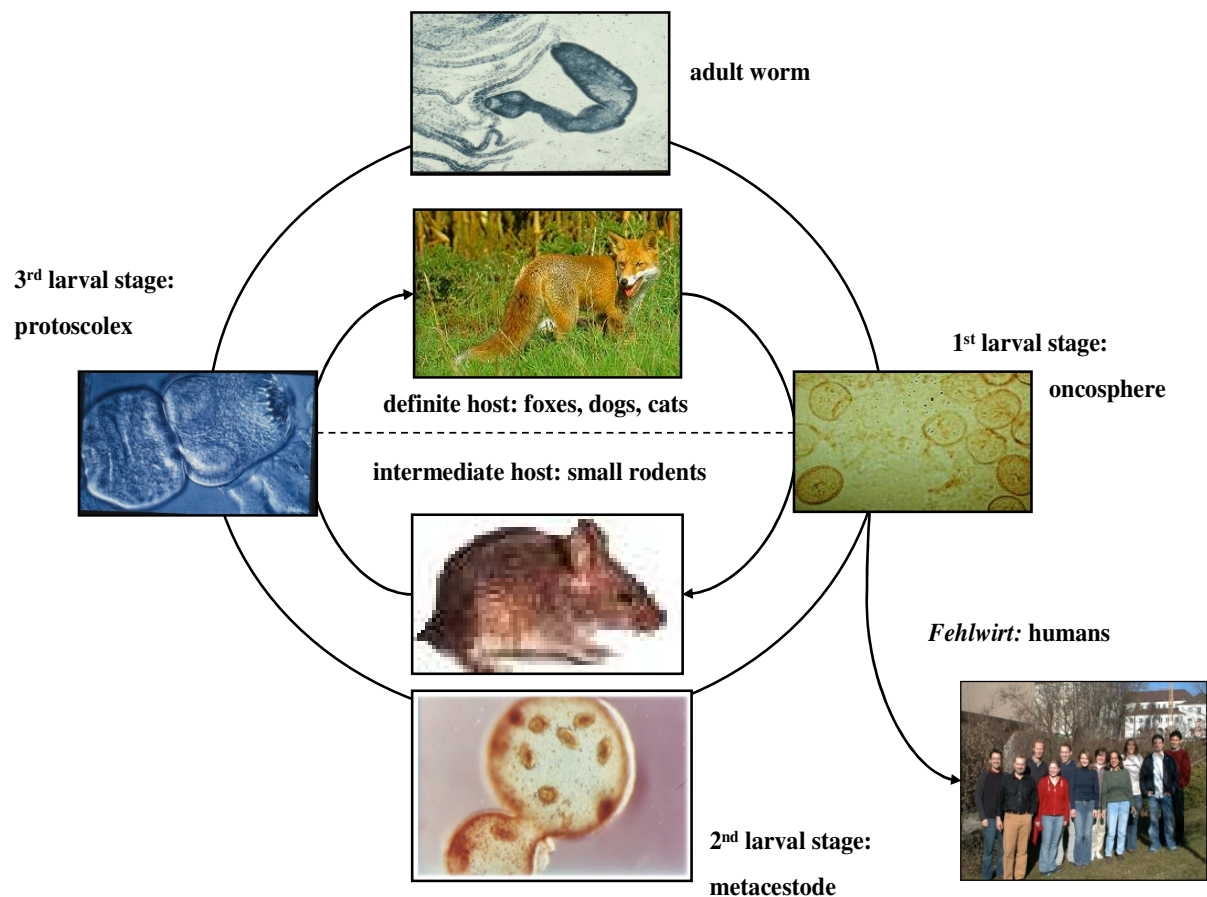
2.1.2 Life cycle

The species of the family *Taeniidae* are characterized by a specific hermaphroditic life cycle which involves two host switches. The carnivore final host harbors the adult worm in its intestine and infective eggs are shed with the faeces [14]. When the eggs are ingested by the intermediate host, the so-called oncosphere hatches which is capable to penetrate and invade the surrounding tissue and develops into the next larval stage, the metacestode. In turn, the third larval stage, the protoscoleces develop within the metacestode. In case the intermediate host becomes the prey of the final host, the protoscoleces are activated in its gut and develop into the mature worm, closing the life cycle [14]. Besides morphological differences, e.g. the number of hooks in the rostellum and shape of the oncosphere, the single species are discriminated on the basis of the final and intermediate host. *E. vogeli* parasitizes in dogs and small rodents [15] while *E. oligarthus* parasitizes in rodents and wildcats [15]. Both species are found in Central and Southern America [12]. In the case of the world wide distributed *E. granulosus*, the adult worm settles mainly in the intestine of dogs but also other carnivores, whereas sheep, pigs, goats, cattle, camels, horses and deer can be the intermediate hosts for the larval stage [14, 12]. Adult *E. shiquicus* are found in the Tibetan fox (*Vulpes ferrilata*) and hydatid cysts in the black lipped pika (*Ochotona curzoniae*) while human infections are not known [32].

The life cycle of *E. multilocularis* is schematically depicted in figure 3. The head structure of the adult worm possesses 4 suckers and a rostellum with which the worm settles in the final host's intestine. This head structure is followed by up to 5 proglottides contributing the most to the overall length of 2-3 mm of the adult worm [17]. The primary final hosts are red and polar foxes of the genus *Vulpes*, but also dogs and cats as final hosts are known. The intermediate hosts are generally small rodents, but also deer, moose, reindeer and bison [14, 18]. Fertilization of the eggs occurs by self-insemination and the mature eggs containing the first larval stage, the so-called oncosphere, develop in the terminal (gravid) proglottid. The mature eggs are released into the environment by shedding of the gravid proglottid with the faeces. The oncosphere is the infective agent for the intermediate host and are, within the egg, relatively resistant against external influences [17]. After ingestion through the intermediate hosts, the oncosphere becomes activated while passing stomach and intestine. It is assumed that the acidic pH and bile salts are involved in this activation process [19]. Since the composition of bile salts varies between vertebrate species, it is thought that bile salts are also in part involved in determining the parasite's host specificity [20]. Following its activation, the oncosphere penetrates the intestinal epithelium, enters the mesenterial veins leading into

the portal vein in which the oncosphere is transported by the blood flow to the liver. In most cases, the oncosphere develops within the liver to the second larval stage, the metacestode [69]. Neither the factors inducing and regulating this transformation nor the reason for the liver as primary infection site are known. The metacestode comprises a fluid filled vesicle (the hydatid cyst), which is separated from the environment by an inner germinal layer and an outer acellular laminated layer (Fig.46,47). The latter is mainly composed of carbohydrates [21,22] and contains high molecular weight glycans [23]. The presumed function of the laminated layer is protection against the intermediate host's immune system [24]. A point that is supported by the observation that the laminated layer persists in the intermediate host even after spontaneous exitus of the metacestode [21,22]. The metacestode grows in size by proliferation of the cells in the germinal layer and asexually by exogenous budding of daughter cysts, thereby infiltrating the surrounding tissue and leading to the characteristic sponge-like appearance within the infected organs. During this process, small vesicles, cell groups or even single cells can be detached from the parasitic tissue and be transported with the body fluids to other parts of the body, e.g. bones and brain [14,20,25]. The infiltrative growth of *E. multilocularis* metacestodes is a major difference to the growth of the metacestodes of *E. granulosus* which do not infiltrate the surrounding tissue [14]. The third larval stage, the protoscolex, develops from so-called brood capsules which form at the proximal side of the germinal layer approximately 6 weeks post-infection with the oncosphere. Within a metacestode, several protoscoleces develop thereby leading to the asexual reproduction of the parasite. The protoscolex in the metacestode is characterized by its invaginated head structures (Fig.37) [17]. When the intermediate host is ingested by the final host, the parasite's life cycle has closed. The metacestode is digested in the stomach which leads to the release of the protoscoleces. They evaginate their head structures and settle in the host's intestine [17]. The signals triggering the evagination are not clear yet, but the change in pH and bile salts seem to be involved [14]. At least *in vitro*, the evagination can be induced by incubating invaginated protoscoleces under low pH conditions and in the presence of bile salts (Fig.37) [8]. Approximately one week after settlement, the first proglottides are formed while the first oncospheres are synthesized after another five weeks [14].

Fig. 3: Life cycle of *E. multilocularis*. The adult stage of *E. multilocularis* persists mainly in the small intestine of foxes of the genus *Vulpes*. The first larval stage, the oncosphere, develops in the terminal (gravid) proglottide and is shed off with the faeces. When the oncosphere is taken up by the intermediate host, usually small rodents, it hatches and penetrates the intestinal wall and is transported by the blood stream into the liver. In this organ, the oncosphere develops into the second larval stage (metacestode). At a certain stage of development, the third larval stage (protoscolex) develops within the metacestode. The life cycle is closed when the intermediate host is eaten by the definite host. In its digestive tract, the metacestode is digested and the protoscolex becomes activated to develop into the adult worm. When the oncosphere is taken up by humans, the metacestode can develop also in the liver causing alveolar echinococcosis. Since humans generally do not become the prey of the intermediate host, the life cycle will not be continued. Humans are therefore considered as *Fehlwirt*.



2.1.3 *E. multilocularis* – the causative agent of the alveolar echinococcosis

Besides natural intermediate hosts, also humans can get infected with oncospheres from *E. multilocularis* (Fig.3). Since the parasite's life cycle can then not be continued, humans are regarded as dead end intermediate hosts or *Fehlwirt*. The liver is the major infected organ and the continuous growth of the metacestode leads to alveolar echinococcosis (AE). Depending on the progress of the infection, the larva can infiltrate vast parts of the liver. Other sites of infection are bones, lung and brain [14,20]. The parasite's growth in humans is significantly slower than in rodents and, in addition, brood capsules and protoscoleces usually do not develop (in less than 10% of all cases) [27,18]. Although spontaneous death of metacestodes occurs, the infection is generally detected in a progressed state due to the lack of symptoms. The estimated window period from the time point of infection to the diagnosis ranges from some years to decades which impairs the chance to determine the source of infection [28,29]. Therefore, several sources of infection are under discussion. Among them are the consumption of contaminated fruits and the contact with infected animals carrying the adult worms. For *E. granulosus*, it could be demonstrated that infectious eggs can be found in the coat of infected dogs [17]. This might also be the case for *E. multilocularis* and its final host, the fox. Another point might be swallowing dust containing eggs, e.g. during the harvest of crops [17].

The first symptoms of an *Echinococcus* infection resemble those of a hepatic infection, like a sore abdomen, vomiting and icterus. At this time, the larval stage has vastly proliferated by exogenous budding and growth in size leading to severe damaging of the liver by pressure necrosis and it is very likely that metastases have formed [12,18,20,25].

The diagnosis of AE occurs via a combination of imaging and serology by employing ultrasonographic/computer tomography and the detection of antibodies in the patient's serum which are directed against parasite proteins (e.g. Elp/Em10) [18,30]. If left untreated, virtually 100% of the patients die within 10-15 years from diagnosis [18,31]. The only possible way for curing patients is the complete resection of the parasite tissue. The available drugs for the treatment of AE – benzimidazoles like albendazol – have only a parasitostatic effect. Hence, in cases without the option of surgery or incomplete resection, the benzimidazoles must be taken life long [28,30]. A further option is liver transplantation in patients with unresectable liver lesions. But the immunosuppression may lead to a faster growth of remaining parasite material [18].

2.1.4 Epidemiology of the alveolar echinococcosis

E. multilocularis is almost exclusively distributed over the Northern Hemisphere with Central Europe, Russia, Western China, North Japan, North Africa and the subarctic regions of Alaska and Canada being the most important regions [18,33]. Within these regions, AE is considered the most severe parasitic infection [34]. Recent studies indicate that *E. multilocularis* is spreading which might be in part due to the rabies vaccination of foxes which could increase the possibility of infection by increasing the foxes' lifespan [35]. In the late 1980s, areas endemic for *E. multilocularis* were only known for Germany, Austria, Switzerland and France. By the end of 1999, foxes were tested positively for adult worms not only in the already known countries but also in Belgium, Czech Republic, Slovakia, Liechtenstein, Luxembourg and Denmark, while the metacestode could be identified in rodents in Slovenia, Bulgaria, Romania (Fig.4) [36]. Together with the increased distribution of infected foxes, an increase of AE cases is expected for the next decade [17]. It is under current discussion if the emerging of foxes in urban areas could increase the risk of infection. Hofer et al. could show that 61 out of 129 foxes captured in Zürich were infected with the adult stage of *E. multilocularis* [37]. Due to the large window period between the infection and the diagnosis of the infection, this question will only be answerable in a couple of years and the general risk of infection is only hardly determinable [28]. But the high prevalence of *E. multilocularis* in foxes seems to correlate with higher rates of human infections. Recent data indicates that 60-65% of autochthonous infections in Germany occurred in high endemic areas, although the total number of known infections was only 203 [38]. With 80 and 200 cases per 100,000 inhabitants, higher rates of infection are known for high endemic areas in Russia and China, respectively. It is assumed that the close contact between humans and dogs in combination with its stronger role as final host causes these increased infection rates [34].

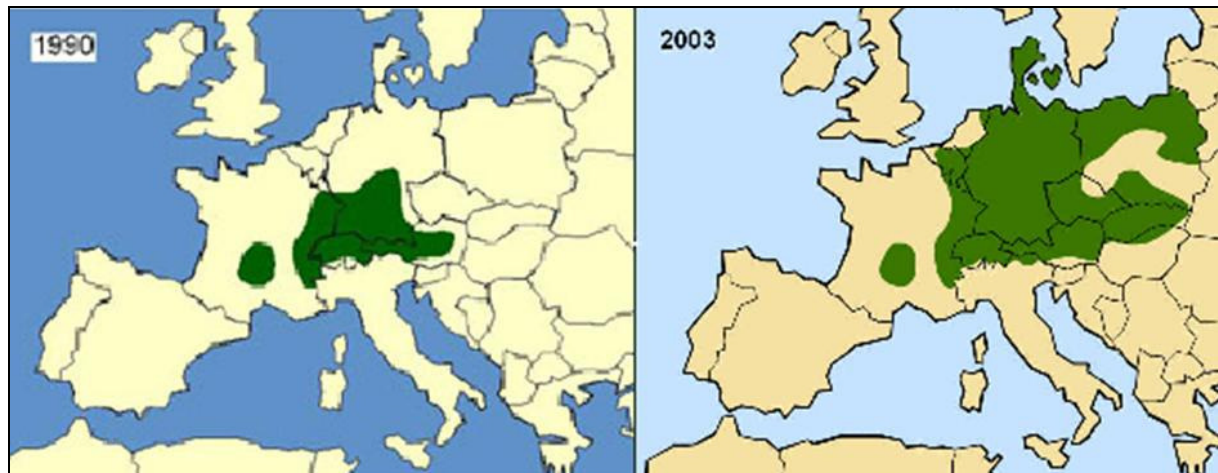


Fig. 4: Prevalence of *E. multilocularis* in foxes in Central Europe. While in 1990, infected foxes were mainly found in Southern Germany, Austria and Switzerland as well as parts of France (left panel), the area of prevalence spreaded further north and east in the following decade. In 2003, infected foxes were found in all areas of Germany, Belgium, Czech Republic, Slovakia, Liechtenstein, Luxembourg and Denmark (From: Bayerisches Landesamt für Arbeitsschutz, Arbeitsmedizin und Sicherheitstechnik LfAS)

2.2 Insulin/ Insulin-like-Growth-Factor I signaling

2.2.1 Hormones of the insulin superfamily

Human insulin is the name giving representative of this family of hormones and was already discovered by Banting and Best in 1921. In vertebrates, insulin regulates the sugar and fatty acid metabolism. It is solely synthesized in the pancreatic β - cells from a prepro-insulin precursor comprising a N-terminal signal peptide which is C-terminally followed by the so-called B-, C- and A- peptides [39, 41]. The removal of the signal peptide in the endoplasmatic reticulum transforms the prepro-insulin into pro-insulin which matures into insulin by the removal of the C-peptide while the A- and B-peptide remain covalently linked via disulfide bonds [39, 40]. Besides insulin, two closely related peptides were identified in vertebrates: insulin-like growth factor (IGF) – I and – II. IGF-I differs from insulin by inducing mitogenic and anti-apoptotic effects and its role in differentiation processes [42]. Unlike insulin, IGF-I is not synthesized in the pancreas but mainly in the liver and to a minor amount in peripheral tissues [43]. Like insulin, IGF-I is synthesized as a prepro-peptide composed of an A-, C- and B-peptide which possesses a N-terminal signal peptide and disulfide bonds which covalently link the A- and B-peptide. In addition, the prepro-IGF-I contains a D- and E-peptide at the C-

terminus of the C-peptide. Since only the E-peptide is proteolytically removed during the maturation steps, mature IGF-I has a higher molecular weight than insulin: 7.6 compared to 5.8 kDa [39]. A schematic structure of insulin and IGF-I are depicted in Fig. 6.

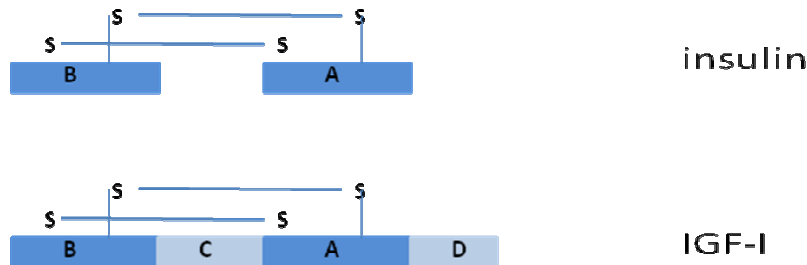


Fig. 6: Schematic structure of insulin and IGF-I. The peptides comprising the mature hormones are indicated by the capitalized letters and the intramolecular disulfide bonds by the solid lines.

Insulin-like proteins (ILPs) or insulin-related proteins (IRPs) are not only identified in vertebrates, but also in invertebrates like mollusks, nematodes and insects with most data obtained from genome sequencing projects [39]. For *Drosophila melanogaster*, 7 genes were annotated to code for *D. melanogaster* insulin-like proteins (DILP1-7) and an EST of the DILP-2 encoding gene could be identified [39]. In the case of *Caenorhabditis elegans*, an *in silico* analysis of its genome identified 37 putative genes (ins-1 – ins 37) encoding insulin-like proteins with the proteins INS-1 and INS-18 being the most similar to human insulin [44, 45]. So far, the direct activation of the *D. melanogaster* and *C. elegans* insulin receptor (DIR and DAF-2; see below) by one of the invertebrate ILPs could not be shown. The known effects of INS-1 on *C. elegans* are based on deletion and overexpression studies [45, 46]. Until very recently, no ILP had been identified in any platyhelminthes. A genome sequencing project of *Schistosoma japonicum* identified a gene (Q5DBU2) encoding an ILP but no EST or the corresponding protein has been detected yet [108].

2.2.2 Insulin/ IGF-I signaling cascade in mammalian (human) cells

The large superfamily of tyrosine kinases can be subdivided into receptor tyrosine kinases (RTK) and non – receptor tyrosine kinases (non-RTK) which are transmembrane and cytoplasmic proteins, respectively. The Insulin/IGF-I signaling cascade in mammalian cells is initiated by the binding of insulin/IGF-I to RTKs which in turn lead to their activation. RTKs generally comprise an extracellular ligand binding domain sensing extracellular signaling molecules, a transmembrane and an intracellular domain. The binding of the ligand to the extracellular domain triggers the dimerization of 2 RTK molecules of the same family and also the activation of the intrinsic tyrosine activity located in the intracellular domain. This kinase domain is the highest conserved domain among RTK and non-RTK characterizing this superfamily [47,49]. Upon dimerization, both intracellular domains become phosphorylated on tyrosine residues by the respective other kinase domain and in turn serve as docking sites for downstream signaling molecules containing phosphotyrosine binding domains (PTB) and Src-homology domains (SH2) [47,48]. The importance of RTKs and their downstream signaling components for proliferation control is demonstrated by the malignant transforming effects of constitutive or enhanced signaling capacities [49]. So far, approximately 20 different RTK families are known [49] and among them are the well characterized platelet-derived growth factor receptor (PDGFR), epidermal-growth factor receptor (EGFR), fibroblast growth factor receptor (FGFR) and the insulin/Insulin-like growth factor-I receptor (Ins/IGF-IR) family. For the latter family, three receptors are known, the insulin receptor (IR), the insulin-like growth factor-I receptor (IGF-IR) and the insulin related receptor (IRR) [47-53]. While for IR and IGF-IR the name giving ligands are known, IRR is an orphan receptor for which no ligand has been yet identified [57]. Among the RTK, the Ins/IGF-IR family differs in some points from the other families. The receptor is synthesized as a proreceptor and becomes, unlike the other RTK families, proteolytically processed into the N-terminal α -subunit and the C-terminal β -subunit at a conserved tetrabasic residue (RKRR) motif by a furin-like protease during the maturation process [66]. These two subunits stay covalently linked via disulfide bonds [188,190]. The α -subunit is located completely extracellular and contains the ligand binding domain, while the β -subunit comprises a short extracellular part, a transmembrane and the intracellular domain (Fig.5) [190]. The receptors of this family form heterodimers even in the unstimulated state and are additionally crosslinked via disulfide bonds [188,190]. The binding of the respective ligand causes a conformational change within the receptor which is believed to activate the intrinsic tyrosine kinase activity leading to the *in*

trans autophosphorylation of three highly conserved tyrosine residues within the kinase domain (human IR: Y¹¹⁵⁸,Y¹¹⁶²,Y¹¹⁶³; human IGF-IR: Y¹¹³¹,Y¹¹³⁵,Y¹¹³⁶) [188-190]. This phosphorylation causes a further increase in the tyrosine kinase activity and in turn the phosphorylation of a further tyrosine residue in the juxtamembrane region and at a non-conserved tyrosine in the C-terminal extension of human IR (Y1316) [110]. The tyrosine residue within in the juxtamembrane region is located within a highly conserved NPXY – motif and the substitution of this tyrosine residue significantly abolishes the binding of downstream effector molecules to the activated receptors [111]. Two important effector molecules are Src homologous and collagen-like (Shc) protein and insulin-receptor substrate-1 (IRS-1) which bind to the phosphorylated NPXY-motif (human IGF-IR: Y⁹⁵⁰; human IR: Y⁹⁶⁰) via their PTB-motif and become in turn phosphorylated by the receptor [60,65,113]. These molecules then recruit the adapter protein Grb2 which binds the mammalian ortholog of the *Drosophila* son of sevenless (mSos). mSos is a guanine nucleotide exchange factor (GEF) which triggers the substitution of GTP for GDP in the membrane bound Ras [60]. Ras-GTP recruits Raf-1 to the membrane, thereby initiating signaling through the Erk1/2 mitogen-activated protein kinase (MAPK) cascade which is known to regulate growth and differentiation in mammalian cells [59]. This cascade transmits external signals by a series of sequential phosphorylation steps starting from a MAPK kinase kinase (MAPKKK) which phosphorylates and activates a MAPK kinase which in turn phosphorylates and activates the MAPK [47]. In this cascade, Raf-1 is the MAPKKK phosphorylating MEK (MAPK Erk kinase) which in turn phosphorylates Erk 1/2 on conserved threonine and tyrosine residues [59]. The double phosphorylated Erk1/2 dimerizes and translocates into the nucleus where it is involved in the regulation of gene transcription [118]. Other known mammalian MAPK cascades are the c-Jun N-terminal kinase (JNK) and p38 MAPK – cascade which are involved in stress response [59]. Erk1/2 regulates not only gene transcription but also protein synthesis by phosphorylating MAPK-integrating kinase -1 (Mnk-1) which then binds to the eukaryotic initiation factor – 4G (eIF-4G) in the eukaryotic translation initiation complex. Phospho-Mnk-1 in turn phosphorylates eIF-4E which has a stimulatory effect on the translation initiation [26]. An overview over the Insulin/IGF-I signaling cascade is given in figure 7.

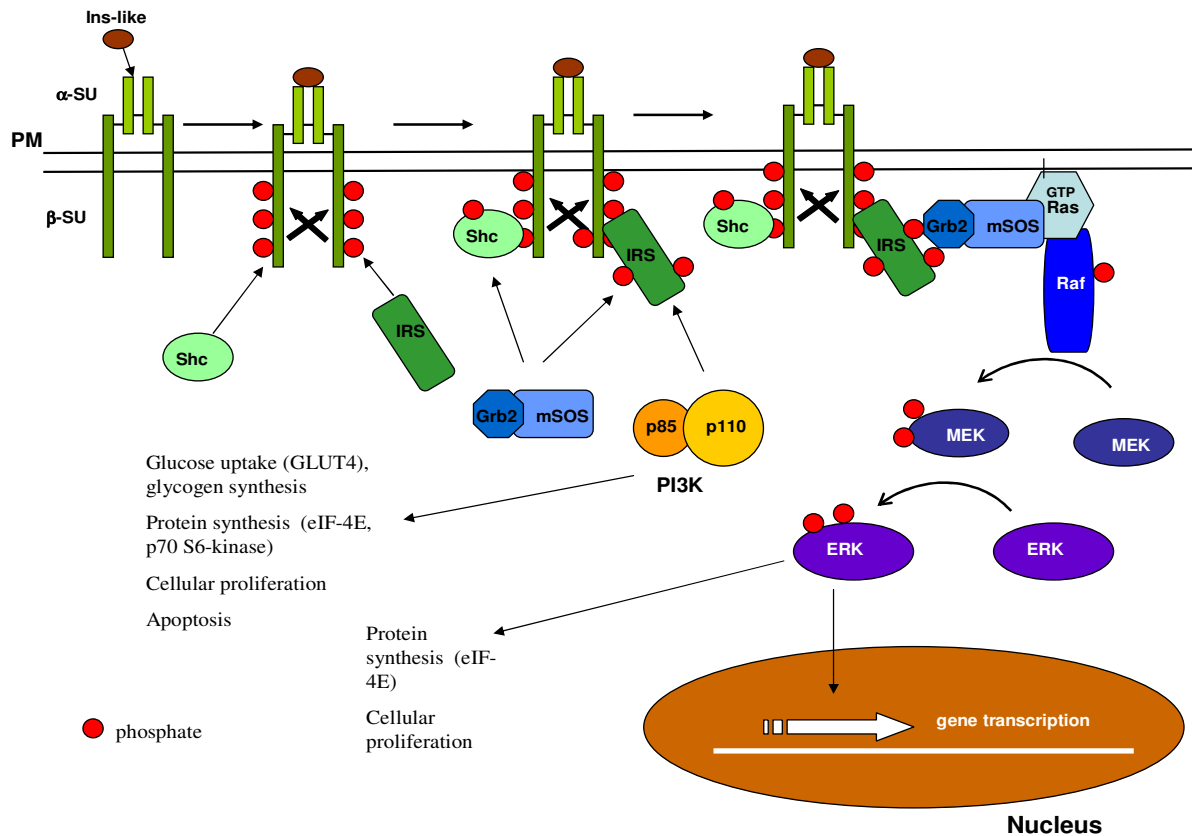


Fig. 7: Simplified schematic view of the Insulin/IGF-I signaling cascade in mammalian cells. The binding of an insulin-like ligand (Ins-like) to its receptor activates the latter's intrinsic kinase activity leading to its autophosphorylation thereby creating docking sites for downstream signaling molecules (Shc, IRS-1). When bound, these molecules are in turn phosphorylated by the activated receptor and serve themselves as docking sites. The two main pathways activated by Ins/IGF-I-RTKs are the PI3K pathway which is initiated when PI3K binds to phosphorylated IRS-1. The Ras/Raf/MEK/ERK MAP kinase pathway is activated when Grb2/mSOS is recruited by either Shc or IRS-1 to the receptor. The binding of mSOS to Ras triggers the GTP for GDP exchange thereby activating Ras and the downstream MAP-kinase cascade.

Another important downstream signaling molecule recruited to the activated IR is the phosphatidylinositol 3 kinase (PI3-K). This kinase is composed of a regulatory (p85) and a catalytic (p110) subunit [194,195]. The p85- subunit contains a SH2 domain through which the protein binds to the tyrosine phosphorylated IRS-1 [194]. But it has also been described that the p110 subunit is activated by the direct interaction with Ras [194]. The activation of PI3-K results in the production of phosphatidylinositol triphosphate (PI(3,4,5)P₃) thereby recruiting protein kinase B (PKB/AktB) to the plasma membrane which triggers a cascade leading to the activation of the glycogen synthase [197]. PI3-K is not only involved in glycogen synthesis but also in the uptake of glucose via the GLUT4 glucose transporter as

well as in protein synthesis [196]. Active PI3-K leads, via FRAP/mTOR, to an increased phosphorylation and inactivation of the eIF-4E inhibitor E4-BP and also to an increased phosphorylation of the S6 protein in the 40S ribosomal subunit by activation of the p70 S6 kinase [195]. In recent times, the FOXO subgroup of the forkhead transcription factors has moved into the focus as downstream targets of the PI3-K pathway. In response to insulin, IGF-I and other growth factors PKB/AktB phosphorylates the FOXO transcription factors on highly conserved residues and causes their export from the nucleus into the cytoplasm [78]. It has been shown that 14-3-3 proteins interact specifically with phosphorylated FOXO proteins and serve as chaperones during the nuclear export [78]. The sequestering of FOXO transcription factors allows the proliferation by preventing the upregulation of cell cycle inhibitors [78] and also promotes cell survival by the inhibition of transcription of apoptosis mediating genes [78].

Although IR and IGF-IR are very similar and initiate similar signaling events, they exert different functions within the cell. While IR regulates mostly the metabolic homeostasis, IGF-IR controls growth, development and differentiation [61]. The different function of the receptors could be revealed by homozygous knockout mice lacking either IR or IGF-IR. The lack of IR leads to the development of diabetes while mice lacking IGF-IR die within minutes after birth [65]. Diabetes also develops when no insulin is released anymore from the pancreas [65]. Quite interestingly, the lack of IGF-I leads also to a reduced embryo body size but the littermates survive and exert only 30% of the body weight of wild type mice after 2 months [65].

It is assumed that the different functions might be in part explained by tissue specific expression. The highest expression of IR is found in the liver and adipose tissue, whereas IGF-IR is rarely expressed in the liver and to a lower rate in adipose tissue [61]. Further, members of downstream signaling cascade were identified which specifically interact with only one of the two receptors [61,62]. The expression of chimeric neurotrophin tyrosine kinase C receptors whose intracellular domain was either replaced by that of IR or IGF-IR revealed that in case of IR the signaling occurs stronger via the IRS-1 and PI3-K pathway, while in case of IGF-IR the signaling via Shc and the MAPK pathway is preferred [61,63,64]

2.2.3 Insulin/ IGF-I signaling cascade in invertebrates

Besides in vertebrates, genes encoding members of the Ins/IGF-IR-family were also identified in invertebrates including molluscs, insects, nematodes and trematodes [72,39] demonstrating the conservation of signal transduction systems throughout animal evolution. The best characterized invertebrate members of the Ins/IGF-IR-family are the *D. melanogaster* insulin receptor (DIR) and *C. elegans* insulin receptor (DAF-2). Like human IR and IGF-IR, DIR is a tetrameric protein composed of two α - and β -subunits which are covalently linked via disulfide bonds [54,55]. The α - and β -subunit are made from a single precursor by proteolytical processing at a conserved tetrabasic motif [54,55] (Fig. 8). Although DIR is approximately 33% identical to human IR and IGF-IR on the amino acid level, it differs by possessing N-terminal and C-terminal extensions [55,56]. Nevertheless, DIR and human IR are closely enough related that human insulin can induce the autophosphorylation of DIR's β -subunit, whereas human IGF-I does not [55]. Presumably due to cell specific post-translational processing, the β -subunit exists as two isoforms with or without a 400 amino acid C-terminal extension which contains potential SH2 – domain binding motifs and seems to play a pivotal role in DIR's downstream signaling capacity [56]. Despite of this difference, the β -subunit possesses all characteristics of a RTK including a NPXY-motif in the juxtamembrane domain [56,68].

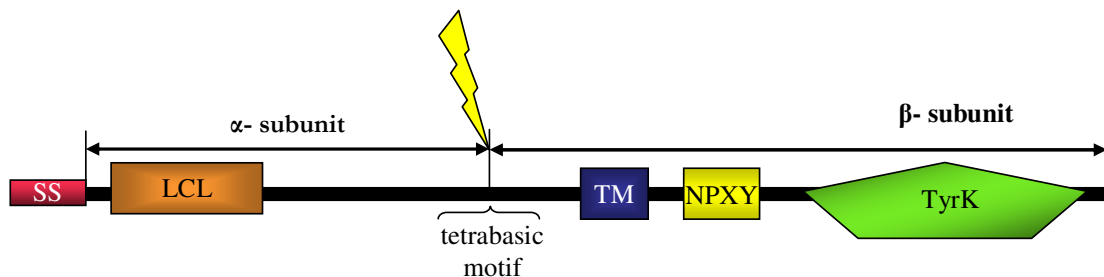


Fig. 8: Subunit-composition of a standardized RTK-precursor of the Ins/IGF-I family.

The rate of conservation is high enough that the signaling capacity of the DIR intracellular domain is indistinguishable from that of IR when expressed in mammalian cells. The expression of chimeric receptors comprising the extracellular domain of human IR and the intracellular domain of DIR leads to phosphorylation and activation of IRS-1 and the MAPK kinase cascade and can stimulate cell proliferation [57, 67]. This again shows the high conservation of the insulin signaling cascade between evolutionary distantly related species. Besides DIR, other genes were identified in *D. melanogaster* which code for orthologs of components of the mammalian Ins/IGF-I intracellular signaling cascade. These include IRS

(CHICO/dIRS), Grb2 (Drk), Sos, Ras (Rheb), MEK (DSORT), ERK (ERK-A), the catalytic subunit of PI3K (Dp110) and Akt/PKB (DAKT/ DPKB) [39,71] as well as p70 S6 kinase (dS6K) [70,71]. The physiological function of the DIR signaling cascade was revealed by the analysis of deletional mutants. Female fruit flies lacking CHICO were sterile, displayed a reduced body size due to a reduction in cell number and cell size and also an increased storage of lipids [39, 9]. A similar phenotype was observed for flies being homozygous for a partial loss-of function-mutation in DIR suggesting that DIR and CHICO act in the same signaling cascade [39,71]. Besides its role in adult flies, DIR is also involved in embryonic differentiation processes [199]. So far, no DILP is reported to activate DIR directly [71], although they appear to be involved in the DIR signaling cascade since the overexpression of *dilp* genes generally results in an increased cell size and cell number of individual organs and therefore in bigger *D. melanogaster* [71]. In addition to the regulation of metabolism and reproduction, the Drosophila insulin signaling pathway also seems to be involved in the regulation of longevity, since mutations in *dir* and *chico* can lead to an increased life span [39].

The effect of mutations in components of the insulin signaling cascade has also been extensively studied in the nematode *C. elegans*. Like in *D. melanogaster*, this pathway regulates metabolism, development and also longevity. The most upstream component of this pathway is DAF (abnormal dauer formation) - 2, the *C. elegans* IR-like protein [39, 46, 73]. DAF-2 exhibits all structural characteristics of a RTK of the Ins/IGF-I family: a signal peptide, a ligand binding domain with a cysteine rich region, a transmembrane domain and a tyrosine kinase domain (from N- to C-terminus). Further, it contains a predicted tetrabasic proteolytical processing site at which the proreceptor is assumed to be cleaved into the α - and β -subunit [73]. With approximately 35% identity to human IR and IGF-IR DAF-2 is as conserved as DIR and it also possess a C-terminal extension which might serve as docking site for downstream signaling molecules [73]. In wildtype *C. elegans*, DAF-2 stimulates reproductive growth while in *daf-2* mutants the larvae arrest in the dauer stage which is normally formed under stress conditions, e.g. food deprivation and overcrowding, and coincides with increased life span and the storage of fat and glycogen [73,75]. The signaling pathway acting downstream of DAF-2 has been partially identified. Among the identified proteins are orthologs of IRS (IST-1), the PI3K catalytic subunit (AGE-1) and regulatory subunit (AAP-1), Akt/ PKB (Akt-1 and Akt-2) and a forkhead transcription factor (DAF-16) which is the major target of the DAF-2 signaling cascade [76]. The mammalian orthologs are FOXO1, FOXO3a and FOXO4 [14]. In both *C. elegans* and mammals the activation of the

insulin-like signaling cascade antagonizes the forkhead transcription factors [76,77]. DAF-16 becomes phosphorylated by AKT-1 preventing its entry into the nucleus. This inhibitory effect is relieved by mutations abolishing the insulin-like signaling cascade. In the current model of longevity, DAF-16/FOXO activates the transcription of genes encoding factors conferring resistance to oxidative stress, protection of protein structure and longevity [76,78]. Dependent on the mutation in the insulin-like signaling cascade, the life cycle of *C. elegans* is differently affected. While a loss-of-function of DAF-2, AGE-1 and AKT-1 causes the larvae to arrest in the dauer stage, a partial-loss-of function (caused by weak mutations in the encoding gene) allows normal reproductive development but extends the adult life span significantly [76,77]. The functional activity of DAF-16 is required for the mutant phenotype, whereas a loss of function mutation in *daf-16* suppresses the *daf-2* and *age-1* mutations [76,77].

2.2.4 Insulin/ IGF-I signaling in *E. multilocularis*

Prior to this work, the single copy gene coding for the *E. multilocularis* ortholog of human IR (EmIR) could be identified and analyzed [79]. The already published results are briefly summarized in this chapter. The *emir* chromosomal locus spans approximately 16.5 kb in which the coding sequence is interrupted by 24 introns. Based on structural comparison, *emir* and mammalian and insect genes coding for insulin receptors are most likely derived from a common ancestor. The mature 5.5 kb mRNA contains an ORF which codes for a protein of 1749 amino acid residues (192 kDa) and RT-PCR analysis revealed that the gene is transcribed in both the metacestode and protoscolex larval stage. Like human IR, EmIR comprises all characteristics of a RTK of the Ins/IGF-I family (Fig.8). First, it possesses a ligand binding domain (LCL), which is composed of two I-lobes, flanking a cysteine rich domain in the putative α -subunit (Fig. 9). This domain is C-terminally followed by three fibronectin domains (Fn3) with the second containing the putative proteolytical processing site. Hence, the putative β -subunit comprises the third Fn3 domain, the transmembrane and the cytoplasmic domain. The latter contains the tyrosine kinase domain which has the conserved residues typical for a RTK, especially the three tyrosine residues (Y¹⁵⁰⁴, Y¹⁵⁰⁸ and Y¹⁵⁰⁹) which are at homologous position to the autophosphorylated tyrosine residues of IR and IGF-IR. Like in IR/IGF-IR, a NPXY motif can be found in the juxtamembrane region (NPEY¹¹⁴⁹) and, like in DIR, an additional NPXY motif in the C-terminal tail (NPSY¹⁷¹²). The

C-terminal tail is the most divergent cytoplasmic region among the RTKs and is involved in mediating downstream metabolic processes regulated by human IR [140].

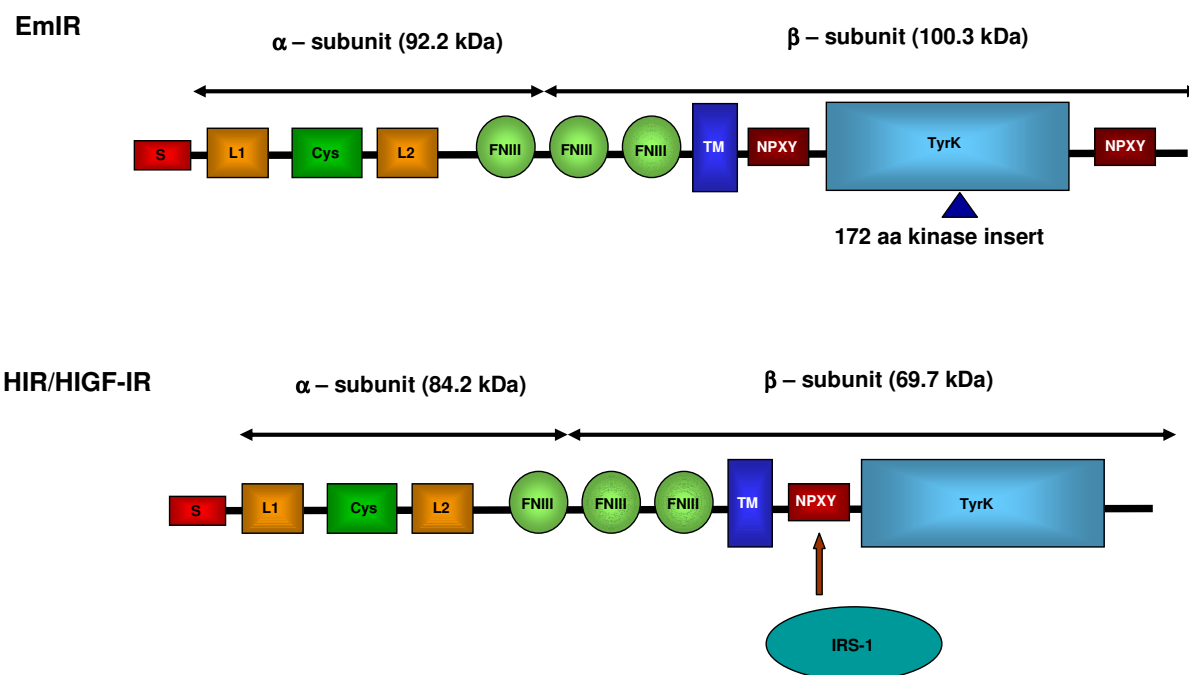


Fig. 9: Comparison of the domain structure of EmIR and human IR/IGF-IR. The *in silico* analysis of the EmIR amino acid sequence predicted all characteristic domains of a member of the family of Ins/IGF-I RTKs: Signal peptide (S); ligand binding lobe 1 and 2 (L1, L2); cysteine rich region (Cys), fibronectin type III domain (FnIII); transmembrane domain (Tm); tyrosine kinase domain (TyrK). Although identical to human IR and IGF-IR regarding the domain structure, EmIR differs in having a second NPXY-motif in its C-terminal tail and a 172 amino acid insert in its kinase domain, counting for most of the larger molecular weight. Further, EmIR lacks the conserved tetrabasic proteolytic processing site, but by sequence comparison, a di-basic motif was predicted to be the processing site.

Despite all homologies, EmIR differs from IR in lacking the conserved tetrabasic proteolytic processing motif, but by sequence comparison a di-lysine (KK⁸³⁴) motif was identified as the putative processing site. In addition, EmIR possesses two non-conserved peptides with one in the region homologous to that part of IR/IGF-IR determining the ligand specificity and the second 172 aa peptide in the kinase domain. The function of both peptides is unknown.

The yeast two hybrid analyses showed that EmIR's ligand binding domain binds human insulin with similar affinities as the ligand binding domain of human IR but not IGF-I. Therefore, EmIR is a potential candidate to play an important role in the development of *E. multilocularis* and its interaction with the host.

2.3 Src-family kinases (non-receptor tyrosine kinases) and GAP-proteins

The large family of non-receptor tyrosine kinases (non-RTK) is involved in the regulation of cellular processes like gene transcription, proliferation and differentiation [122]. The first identified kinase of this family was pp60Src and therefore the members of this family are summarized as Src-family kinases. Today, 10 subfamilies of Src-family kinases are known [122]. The members of this family share a common domain structure with a SH4 and a unique domain at the N-terminus followed by a SH3, SH2, a tyrosine kinase domain and also a short C-terminal tail [128]. A myristoylation of the glycine residue within a conserved Met-Gly-Cys motif located at the N-terminus is described for some subfamilies which recruits the kinases to the plasma membrane [128]. Src-family kinases seem to be directly involved in signaling cascades regulated by receptor tyrosine kinases [122,123]. The activation of IGF-IR in murine 3T3-L1 cells leads to increased Src and Fyn kinase activity and increased DNA synthesis. The addition of PP1, a Src-family tyrosine kinase inhibitor to the cells revealed that Src-family kinases interacted with the IGF-IR downstream signaling cascade. PP1 did not only prevent the *de novo* DNA synthesis but also the tyrosine phosphorylation of Shc and Erk1/2 [122,123]. Further could be shown that Fyn forms a complex with and tyrosine phosphorylates IRS-1 during the stimulation of mammalian cells with insulin [123,129]. With Raf-1, another component of the mammalian MAP Kinase cascade associates with Fyn. This association leads to an increased tyrosine phosphorylation of Raf-1 which in turn stimulates its autophosphorylation activity [130].

The Ras-superfamily is a large group of small GTP binding proteins which is subdivided into at least 5 families based on sequence and functional similarities: Ras, Rab, Arf, Rho and Ran [125]. The interaction with guanine nucleotide exchange factors (GEF) leads to the substitution of GTP for the bound GDP in turn activating the Ras proteins. The interaction with the GTPase-activating proteins (GAP) stimulates the intrinsic GTPase activity leading to the inactivation of the Ras proteins. The members of the Ras superfamily are conserved enough that the GEF and GAP proteins of the Ras subfamily can also regulate the GDP/GTP exchange of other members of the Ras superfamily [125].

The Ras subfamily includes the name-giving Ras, Ral and Rap (Rap1 and Rap2) which are involved in the regulation of intracellular signaling cascades. It could be demonstrated that Rap1 antagonizes the function of Ras in the MAPK cascade [126]. The inhibitory function of Rap1 might be due to the interaction with Raf since the stimulation with insulin leads to the

dissociation of the Raf-Rap1 complex and to an increased association of Raf with Ras [126]. The specific role of Rap2 is unclear [127].

The Rho family of GTP-binding proteins controls actin organization, focal adhesion assembly, cell cycle progression, cytokinesis, transcription, secretion and endocytosis [124]. Like all members of the Ras superfamily, the activity of the members of this subfamily, Rho, Cdc42 and Rac, is determined by the GDP/GTP state which is regulated by the RhoGEFs and RhoGAPs [119,124]. The activity of RhoGAP proteins can be regulated by tyrosine phosphorylation through Src-family kinases. It could be previously demonstrated that mammalian RhoGAP proteins interact with and are tyrosine phosphorylated by Fyn tyrosine kinase and that this phosphorylation is involved in the morphological changes of oligodendrocytes [120,121].

2.4 Molecular biology of *E. multilocularis*

2.4.1 *E. multilocularis* orthologs of mammalian signaling molecules

Besides *emir*, several other *Echinococcus multilocularis* genes encoding proteins which share high identity with vertebrate signal transduction molecules were identified and characterized [80-89]. With EmER, an *Echinococcus* RTK of the epidermal-growth factor receptor family was identified to be 10-fold higher expressed in protoscoleces compared to metacestodes suggesting a role of EmER in the differentiation of the metacestode to the protoscolex [80]. So far, it has not been shown that EmER is activated by host EGF, although it seems possible since SER, the *Schistosoma mansoni* ortholog of the EGF-receptor has been shown to be activated by host EGF [9]. The identification of a gene encoding an EGF-like peptide (*egfd*) raised the possibility that this peptide functions in an autocrine manner via EmER to regulate the parasite's development [88]. In addition to RTK, orthologs of intracellular signaling molecules were found and analyzed. With EmRas, EmRap1, EmRap2 and EmRal small GTP binding proteins and with EmRaf, EmMKK and EmMPK-1 kinases as well as a 14-3-3 ortholog were characterized [82-85] which might comprise the components of an *E. multilocularis* MAPK-cascade regulated by host factors like insulin/IGF-I. Preliminary results obtained during this work indicated that EmMPK is indeed activated by host cytokines [84]. These results were the basis for the analysis of the function of host insulin-like factors and EmIR in the activation of an *E. multilocularis* intracellular signaling cascade.

Very recently, Zavala-Gongora et al. were able to demonstrate that human bone morphogenetic protein 2 (BMP 2) is able to activate *E. multilocularis* TGF (tumor growth factor)- β receptor 1 (EmTR1) and that the activated receptor phosphorylates EmSmadB *in vitro* [86]. In recent times, we also identified and characterized other components of the *E. multilocularis* TGF- β signaling cascade, e.g. EmSmadA and EmSkip [87, 89]. Their role in the parasite's development and hormonal cross-communication with the host is currently under investigation.

2.4.2 *In vitro* cultivation of *E. multilocularis* larval stages

Substantial progress in the analysis of the molecular basis of the interaction of *E. multilocularis* and its host has come from the establishment of an *in vitro* cultivation system for metacestode vesicles. In this system developed by Jura et al. [6], vesicles are incubated in the presence of rat or human hepatocytes embedded between two layers of collagen. This system allows the *in vitro* observation of steps in the development of the metacestode: proliferation, exogenous budding of daughter cysts and development of protoscoleces. In addition to this observation, the effect of specific incubation conditions, e.g. the supplementation with certain peptide hormones, can be analyzed. A similar *in vitro* cultivation system has been developed by Hemphill et al. [187]. Besides the *in vitro* proliferation of the metacestode vesicles, also the development of the oncosphere towards the metacestode can be assessed *in vitro* [186]. Nevertheless, this system does not allow the discrimination between direct and indirect effects. The addition of peptide hormones like insulin might not only affect the metacestode vesicles but also the hepatocytes which could then affect the vesicles indirectly by, e.g. secreting different proteins. This limitation can be circumvented by the cultivation of metacestode vesicles under axenic conditions as developed by Spiliotis et al. [7]. The incubation of vesicles under low oxygen and mild reducing conditions in the presence of medium preconditioned by hepatocytes allows the maintenance of vesicles for several months. This system facilitates the *in vitro* analyses of the effect of host derived factors on the development of *E. multilocularis*.

2.4.3 Trans-splicing in *E. multilocularis*

During the maturation of pre-mRNA, introns are removed and exons on the same pre-mRNA molecule are fused (*in cis*) in the spliceosome. Besides this cis-splicing, an alternative splicing was identified in which exons from different primary transcripts are fused (*in trans*) [6, 7, 99-103]. This event is therefore called trans-splicing. In the predominant form of trans-splicing, a so called spliced leader (SL) is fused to the 5' end of the pre-mRNA. The SL originates from a small nucleolar RNA comprising a so-called mini-exon and outtron [6, 7, 99-103]. Trans-splicing events involving a SL are known for several species but the ratio between cis- and trans-spliced mRNAs might differ among the species. While all mRNAs in kinetoplastid protozoans possess an identical SL [104], two SL were identified in *C. elegans* with SL1 and SL2 found at the 5' end of 60% and 10% of the mRNAs, respectively [6, 7, 99-103]. The functional role of trans-splicing is still widely unclear but in *Trypanosomes* and *C. elegans* trans-splicing is used to resolve polycistronic mRNA into monocistronic mRNA [6, 7, 99-103]. In case of *E. multilocularis*, a 36 nt SL was previously identified in a non-polyadenylated RNA of 104 nt. This SL is spliced *in trans* to the 5' end of approximately 30% of all mRNAs [3]. Trans-splicing was also found for the closely related cestode *Taenia solium* [109]. Since trans-splicing does not occur in the mammalian hosts, the presence of a SL at the 5' end of a transcript clearly discriminates it as a parasitic factor. Recently, trans-spliced genes could be identified which are differentially expressed in the metacestode and protoscolexes by employing a SL-differential display assay [88].

2.4.4 Recombinant antigens

The screening of *E. multilocularis* metacestode cDNA expression libraries identified several different antigens. The first to be identified were EMII/3-10 [91], EM2 [92] and EM4 [93] and shortly thereafter EM13 [94] and ELP (ezrin-radixin-moesin (ERM)-like protein) [95]. The comparison of the amino acid sequences revealed that ELP, EMII/3-10 and EM4 were identical. The chromosomal locus of *elp* was the first *Echinococcus* gene whose coding and promoter region was characterized [96].

2.5 Aims

E. multilocularis and other helminth parasites are able to persist for years or decades within their host without inducing an effective immune response. It is further not known why *E. multilocularis* infects mostly the liver of its intermediate host and how the development of the metacestode vesicles is regulated. It seems very likely that specific host derived signaling molecules are involved in the regulation of development since protoscoleces develop in murines but not in humans. The positive effect of small soluble factors (<15 kDa) secreted by host cells on the development of *E. multilocularis* metacestode vesicles could be demonstrated by *in vitro* cultivation. The mammalian cytokines insulin, IGF-I, EGF, FGF, Bmp2 and TGF- β fall into this class and are known to regulate mitogenic and metabolic as well as differentiation processes in mammalian cells by binding and activating transmembrane receptors which in turn lead to the activation of downstream signaling cascades. With EmIR, an *E. multilocularis* IR/IGF-I-receptor ortholog has been identified. The finding that mammalian insulin enhances the embryonic differentiation of *D. melanogaster* by activation of the *Drosophila* insulin receptor ortholog points out that the Ins/IGF-I signaling cascade is conserved and that hormonal cross-communication between phylogenetically distant species is possible. In contrast to *D. melanogaster*, *E. multilocularis* gets in contact with host derived insulin and IGF-I under *in vivo* conditions, which raised the question if EmIR is involved in the hormonal cross-communication between the host and the parasite.

In this work, the effect of human insulin and IGF-I on the development of *E. multilocularis* has been analyzed using *in vitro* cultivation systems. Further, if these effects were initiated by the binding and activation of EmIR. In addition, a possible initiation of the *E. multilocularis* MAPK-cascade by the activation of EmIR was examined.

3 Results

3.1 Insulin promotes growth and survival of *E. multilocularis* metacystode vesicles *in vitro*

3.1.1 Insulin promotes growth and survival of *E. multilocularis* metacystode vesicles under axenic conditions

The *in vitro* cocultivation of *E. multilocularis* metacystode vesicles with hepatocytes does not allow to discriminate direct effects of substances added to the cocultivation system from indirect ones. By exploiting an axenic cultivation system in which no hepatocytes were present, Spiliotis et al. [2] could demonstrate that exogenously added human insulin promoted both the growth and survival of *E. multilocularis* metacystode vesicles under axenic conditions (Fig. 9). A promoting effect of exogenously added IGF-I was not detected under axenic conditions [2].

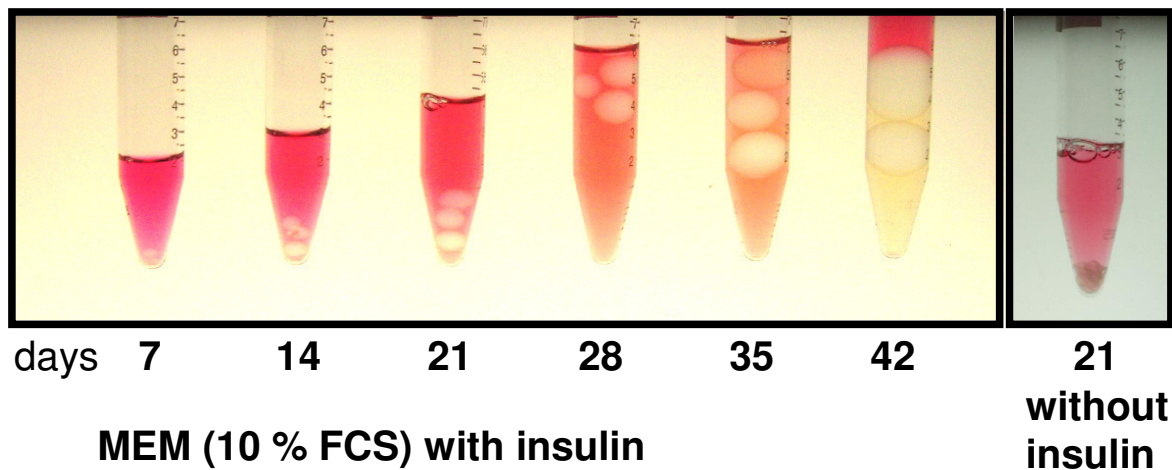


Fig. 9: Cultivation of metacystode vesicles under axenic conditions in the presence and absence of human insulin (courtesy of Spiliotis M.). The supplementation of preconditioned medium (10% FCS) with human insulin increases both the growth and survival of metacystode vesicles under axenic conditions.

3.1.2 Immortal hepatocyte cell lines express insulin

The promoted growth of *E. multilocularis* metacestode vesicles in the presence of exogenously added insulin under axenic conditions brought up the question if insulin is already present in the preconditioned medium used in the axenic cultivation system. One source of insulin could be the serum used in the preparation of the conditioned medium. Since the hepatocytes employed to precondition the medium were carcinoma cells, it was examined if insulin might also be secreted by those cells. Under *in vivo* conditions, insulin is solely synthesized by Langerhans β -cells of the pancreas [149], while hepatocytes are the major site of IGF-I synthesis [148]. The expression of IGF-I and insulin in the human hepatocyte cell line HepG2 was previously shown by RT-PCR using gene specific oligonucleotides (Fig. 10) [5]. The contamination with chromosomal DNA could be excluded because the coding regions of both *ins* and *igf-1* are interrupted by an intron of several kb.

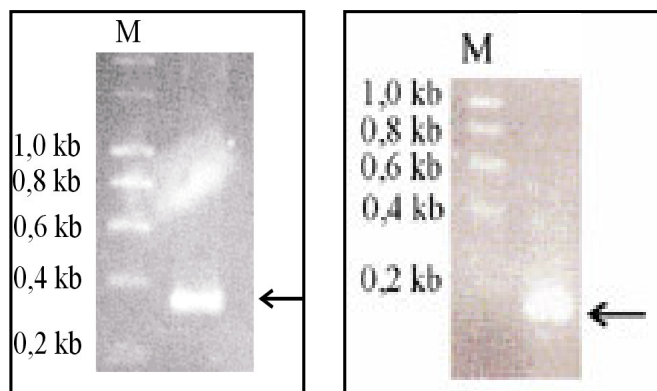


Fig.10: Analysis of the expression of IGF-1 (left) and insulin (right) in the human hepatocyte cell line HepG2. The expression of IGF-1 (left) and insulin (right) in the cell line HepG2 was analyzed via RT-PCR using the gene specific primer CK7 & CK8b for IGF-1 and CK9 & CK88 for insulin. The amplified fragments were separated on a 2% agarose gel and stained with ethidium bromide. The size of the DNA standard (M) is indicated to the left of each panel.

The analysis if the rat hepatocyte cell line RH⁻ also expresses insulin was also carried out by RT-PCR using gene specific oligonucleotides (Fig. 11). A contamination with chromosomal DNA could be excluded because the corresponding chromosomal DNA fragment contains a 501 bp intron.

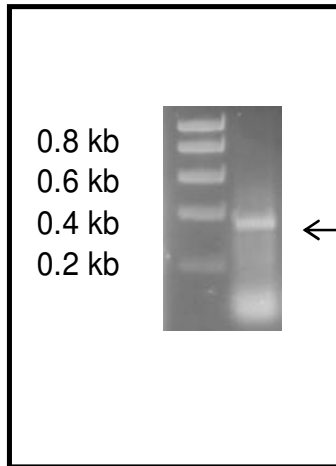


Fig.11: RT-PCR analysis on the expression of insulin in rat hepatocytes. Total RNA from RH- cells was isolated and reversely transcribed. With the oligonucleotides rat ins 1 & rat ins 2, the cDNA encoding rat insulin was amplified. The PCR was analyzed on a 2% agarose gel, followed by ethidium bromide staining. A contamination of the RNA preparation with chromosomal DNA could be excluded, since the coding regions of the gene encoding rat insulin are interrupted by an intron of 501 bp in size.

The finding that the genes encoding human insulin and rat insulin were transcribed in HepG2 and RH- cells, respectively, could indicate that the preconditioned medium contained a higher insulin concentration than serum.

3.1.3 Host albumin promotes survival of *E. multilocularis* metacystode vesicles *in vitro*

Albumin, which is synthesized by hepatocytes, represents the major component of host serum with a final concentration of 3.5 – 4.5% [148,157] and of parasite hydatid fluid [144]. The processes by which host albumin is transported into hydatid fluid are not yet known. Within the host, albumin maintains the colloid osmotic pressure and is the most important carrier molecule in the blood, e.g. for vitamins and cytokines [148]. Therefore, a possible function of albumin as a carrier molecule for insulin in the *in vitro* cultivation system of *E. multilocularis* metacystode vesicles was analyzed (Fig. 12). When the metacystode vesicles were incubated in DMEM alone, only one out of ten was still alive after 16 days, whereas in the presence of 5% bovine serum albumin (BSA) or 100 nM exogenously added insulin, the number of surviving metacystode vesicles was significantly increased. The survival rate was even further increased when metacystode vesicles were incubated in the presence of both 5% BSA and 100 nM insulin, suggesting that BSA serves as an insulin carrier molecule for *E. multilocularis*. Besides the survival rate, the volume of the metacystode vesicles was also measured. But no increase could be determined (data not shown). The finding that killing of the vesicles is only

retarded and not prevented, suggests that both insulin and albumin are necessary but not sufficient for the survival of *E. multilocularis* metacystode vesicles *in vitro*.

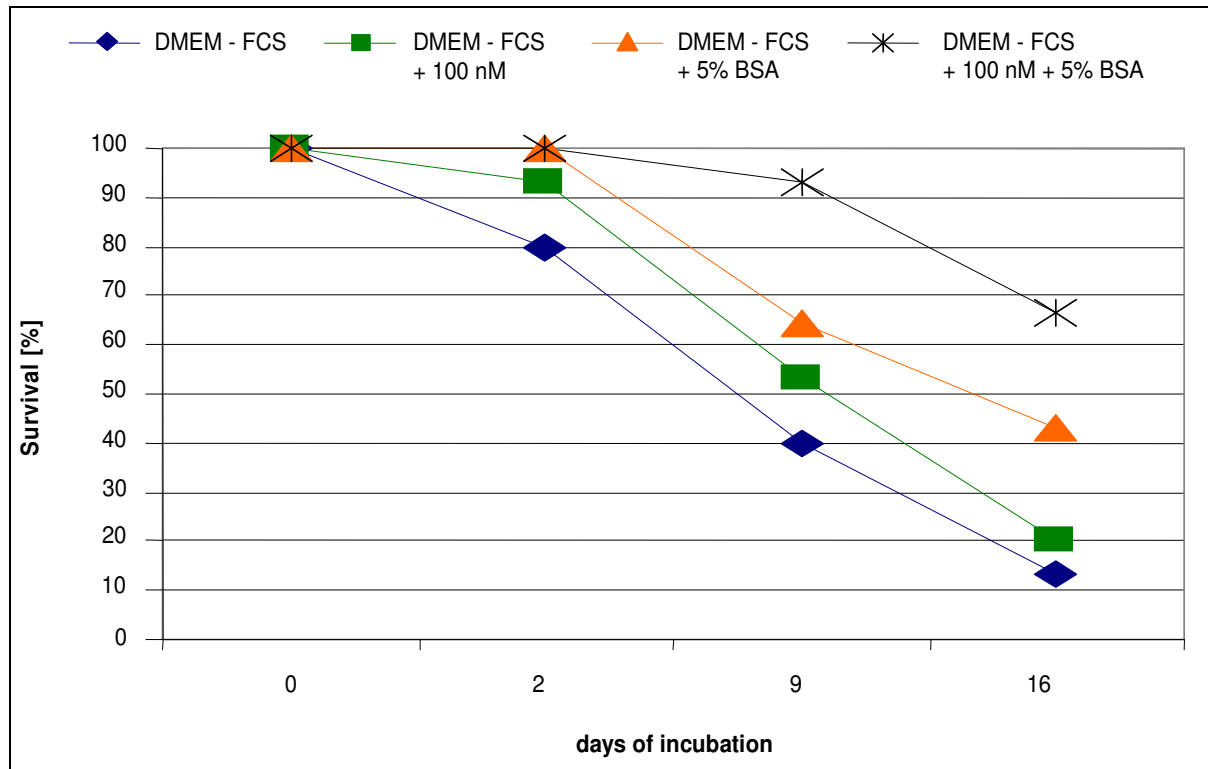


Fig. 12: Survival of axenic cultivated metacystodes in the presence of BSA and human insulin. Axenic cultivated metacystode vesicles were shifted into medium lacking FCS but supplemented with 5% albumin, 100 nM insulin and 5% albumin together with 100 nM insulin under reducing conditions and the exclusion of oxygen. After 2, 9 and 16d, the medium was replaced and the survival rate as well as the volume of the surviving cysts was determined.

3.2 Insulin and IGF-I affect *E. multilocularis* metacestode vesicles on several levels

Based on the promoted growth and survival of *E. multilocularis* metacestode vesicles in the presence of exogenously added insulin *in vitro*, the cellular effects of the addition of insulin should be analyzed by molecular biochemical methods.

3.2.1 Insulin and IGF-I stimulate DNA *de novo* synthesis in *E. multilocularis* metacestode vesicles *in vitro*

Although insulin and IGF-I are closely related, only insulin promoted growth and survival of *E. multilocularis* metacestode vesicles under axenic conditions *in vitro* [2]. For a more precise analysis of the effect of those two hormones, their effect on the DNA *de novo* synthesis in metacestode vesicles *in vitro* was assessed by measuring the incorporation of BrdU during DNA replication [166]. As in the experiments before, the cocultivated metacestode vesicles of isolate H95 were incubated for 2 days in poor medium (0.2% FCS) to remove external stimuli. After the incubation in poor medium supplemented with human insulin or IGF-I for 5 days, the chromosomal DNA was isolated and equal amounts were slot blotted on a nitrocellulose membrane. The incorporated BrdU was detected by chemiluminescence using an anti-BrdU-antibody. A corresponding x-ray film of two experiments is shown in Fig. 13. The signal intensities were determined with the NIH ImageJ software [167] and the DNA replication in the stimulated vesicles relative to the non-stimulated vesicles was determined. In accordance with the results of the axenic cultivation system, the replication of DNA was increased approximately 9 and 7-fold in the presence of 10 and 100 nM human insulin, respectively. Interestingly, IGF-I also stimulated the DNA replication although only at a concentration of 100 nM.

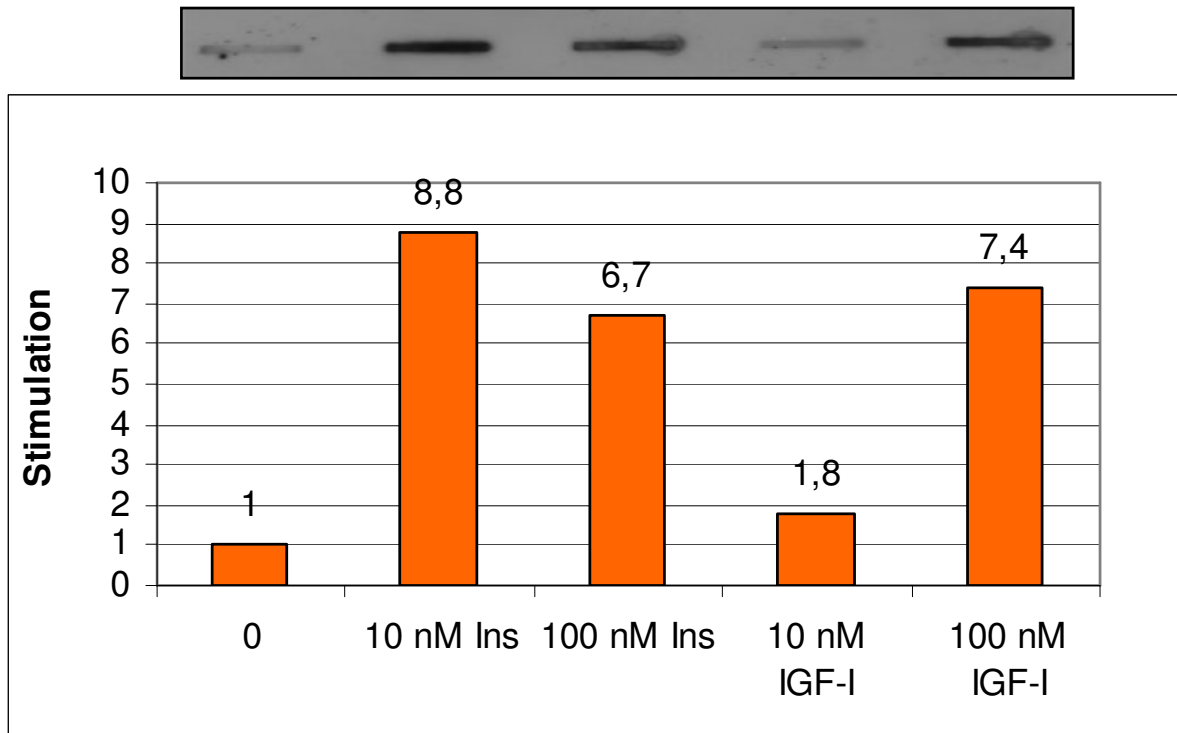


Fig. 13: DNA-Replication in *E. multilocularis* metacystode vesicles is stimulated by human Insulin and IGF-I *in vitro*. 500 ng of chromosomal DNA isolated from metacystode vesicles after 5d incubation in medium 0.2% FCS supplemented with human insulin or IGF-I was transferred onto a nitrocellulose membrane using a slot blotter. The incorporated BrdU was detected with an anti-BrdU-antibody (upper panel) and the intensities of the bands were determined with the NIH ImageJ software. The measured values for stimulated vesicles are given in relation to the value measured for the non-stimulated control (lower panel). The experiment was repeated once with a similar result.

3.2.2 Insulin and IGF-I induce protein phosphorylation in *E. multilocularis* metacystode vesicles *in vitro*

Besides the effect of insulin and IGF-I on proliferation, the immediate effect of these hormones on the phosphorylation of parasitic proteins was analyzed. *E. multilocularis* metacystode vesicles were incubated for 20h in medium lacking phosphate and pyruvate but supplemented with 0.2% FCS and 300 μCi [^{32}P] – phosphoric acid. Following the stimulation with insulin and IGF-I, respectively, the proteins were resolved by SDS-PAGE and the phosphorylation of proteins was detected by autoradiography (Fig.14). While in unstimulated metacystode vesicles only a basal phosphorylation could be detected, the stimulation with insulin and IGF-I resulted in an identical phosphorylation pattern. This result is in contrast to

the finding that insulin is a more potent inducer of DNA *de novo* synthesis than IGF-I (Fig. 13) but might be due to the fact that for the induction of protein phosphorylation the metacystode vesicles were stimulated with 100 nM of insulin and 100 nM IGF-I, respectively, which might reflect the saturation concentration of those two hormones.

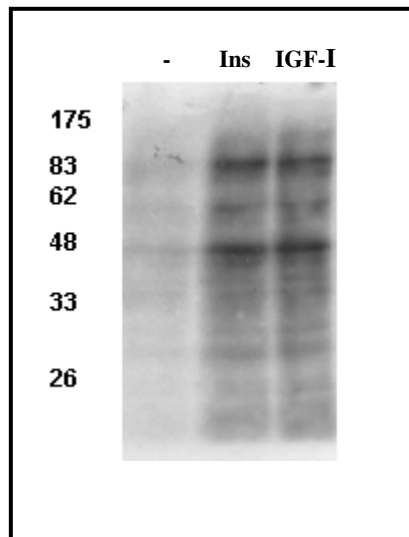


Fig. 14: Insulin and IGF-I trigger the phosphorylation of *E. multilocularis* proteins *in vitro*. Metacystode vesicles of the isolate H95 were incubated under low serum conditions in phosphate – free DMEM, which had been supplemented with 300 $\mu\text{Ci/ml}$ [^{32}P]-phosphoric acid. After 20h incubation at 37°C and 5% CO_2 , the vesicles were stimulated for 10 min with either 100 nM human insulin or 100 nM IGF-I. For the analysis of the phosphorylation, lysates of insulin stimulated (**Ins**), IGF-I stimulated (**IGF-I**) and unstimulated (-) vesicles were subjected to SDS-PAGE (12% PAA) under reducing conditions and subsequently transferred onto a nitrocellulose membrane. The phosphorylation was detected by autoradiography. The x-ray film was exposed over night at – 80°C employing an intensifier screen.

3.2.3 Host derived factors including insulin and IGF-I activate a specific signal transduction pathway in *E. multilocularis* metacystode vesicles *in vitro*

One of the major intracellular signal transduction pathway activated by mammalian RTKs of the Ins/IGF-I family is the well characterized MAP kinase cascade. In this cascade, external stimuli are transmitted within the cell by a series of phosphorylation events initiated by the RTK and lead to the activation of the terminal name giving Erk1/2 MAP kinase [59]. Several orthologs of this mammalian MAP kinase cascade have been identified for *E. multilocularis* larval stages with EmMPK-1A being orthologous to Erk1/2 MAP kinase [2]. It could be further shown that exogenously added human EGF stimulates EmMPK-1A [2]. Therefore, the stimulation of EmMPK-1A in *E. multilocularis* metacystode vesicles under various growth conditions was examined by Western blot analysis. Under permissive growth conditions, EmMPK-1A is expressed and phosphorylated i.e. activated, in metacystode vesicles as well as in protoscolices and activated protoscolices (Fig. 15), indicating a role of EmMPK-1A in the development of these three larval stages. The latter have been exposed to low pH and pepsin

containing medium as well as medium supplemented with bile salts to simulate the activation of the protoscolex after the ingestion by the final host [8].

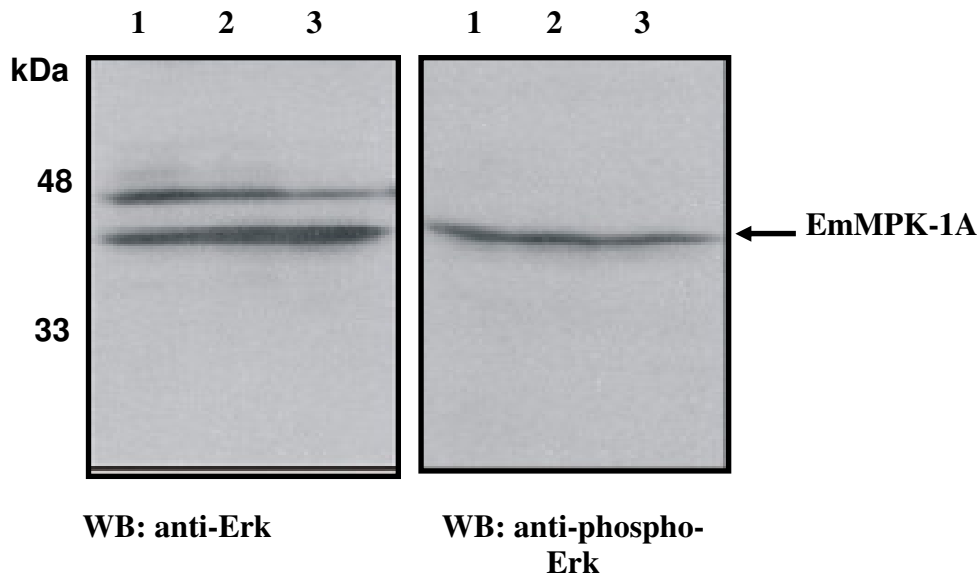


Fig. 15: Expression of EmMPK-1A in *E. multilocularis* larval stages. Lysates of *in vitro* cultivated metacestodes (1), protoscolices (2) and activated protoscolices (3) were separated on a 12% SDS-PAGE, transferred onto a nitrocellulose and analyzed by Western Blotting with antibodies directed against mammalian Erk1/2 and phospho-Erk-1/2 (pT-E-pY) which have been shown to cross react with EmMPK-1A [2]. The position of EmMPK-1A is indicated by the arrow. The anti-Erk1/2 antibody binds also a yet unknown protein of 46 kDa besides the 42 kDa EmMPK-1A.. The size of the protein marker is also indicated.

For the further analysis of the effect of host derived factors on the stimulation of EmMPK-1A in *E. multilocularis* metacestode vesicles, *in vitro* cultivated vesicles were shifted to medium supplemented with only 0.2% FCS. This led to a declined phosphorylation of EmMPK-1A compared to 10% FCS. Already after 2 days of incubation the phosphorylation was significantly reduced, while after 7 days only a marginal phosphorylation could be detected (Fig.16 A, lane 1-3). In the case of physically disrupted metacestode vesicles, i.e. when the hydatid fluid was absent, phosphorylated EmMPK-1A could not be detected already after 2 days of incubation in 0.2 % FCS (Fig.16 A, lane 4).

The vesicles still synthesized proteins under these conditions which is shown by the detection of EmMPK-1A. These findings coincide with the previous observation by Brehm et al., who could induce gene expression in metacestode vesicles which had been maintained for 14 days under reduced serum conditions, demonstrating that the vesicles were still alive [88].

Out of these results arose the question whether the reduced phosphorylation of EmMPK-1A was due to the changes in the serum concentration or mechanical effects. As depicted in Fig.

16 B, this effect was mainly caused by the reduction of serum. When physically damaged metacestode vesicles were incubated for 12 and 24h in the presence of 10% FCS, EmMPK-1A was still phosphorylated (Fig.16 B, lane 1 and 4). By lowering the FCS content to 1% the phosphorylation of EmMPK1A was not significantly reduced (Fig.16 B, lane 2 and 5). A different effect could be seen, when the content of FCS was reduced to 0.2%. The phosphorylation was already massively reduced after 12 h and was undetectable after 24h (Fig.16 B, lane 3 and 6). These findings led to the conclusion that host serum has a stimulatory effect on the metacestode vesicles and that stimulating factors within the hydatid fluid cause an extended phosphorylation of EmMPK-1A under reduced serum conditions. The presence of host proteins like albumin and immunoglobulins as well as free amino acids in the hydatid fluid has already been described [144-146] and the secretion of metacestode proteins into the hydatid fluid could also be shown (see below). With antigen B, a major parasite derived component of the hydatid fluid has been characterized for both *E. granulosus* and *E. multilocularis* [147]. This 160 kDa polymeric lipoprotein dissociates on SDS-PAGE to several subunits [147].

When physically damaged cysts were kept in 0.2% FCS and then transferred back into rich medium, the phosphorylation of EmMPK-1A could not be restored (data not shown). This was only achieved when intact metacestode vesicles were used (Fig.11 C). This and the previous results indicate that the integrity of the metacestode not only prolongs the phosphorylation of EmMPK-1A but is also crucial for its activation. After 4 days in medium containing 0.2 % FCS, the phosphorylation of EmMPK-1A was induced by incubation for 16h with 10% FCS (Fig.16 C, lane 4) or conditioned medium, i.e. medium with 10 % FCS which had been preconditioned with hepatocytes (Fig.16 C, lane 2). The incubation for 16 h in the presence of 10 % FCS and hepatocytes did not only lead to the strongest activation of EmMPK-1A (Fig.11 C, lane 3), but also to the expression of an additional 44 kDa protein (Fig. 16 D, lane 3). This protein was detected with the anti-Erk antibody but not with the phospho-specific anti-Erk antibody. These observations again underline the positive effect of host serum on the phosphorylation of EmMPK-1A and, in addition, demonstrate that the presence of hepatocytes causes a maximal activation of EmMPK-1A. Jura et al. [6] and Spiliotis et al [2,7] demonstrated that these are the conditions under which a maximal proliferation of the metacestodes occurs. With the additional protein being expressed under these conditions a potential candidate for a proliferation marker for *E. multilocularis* was identified.

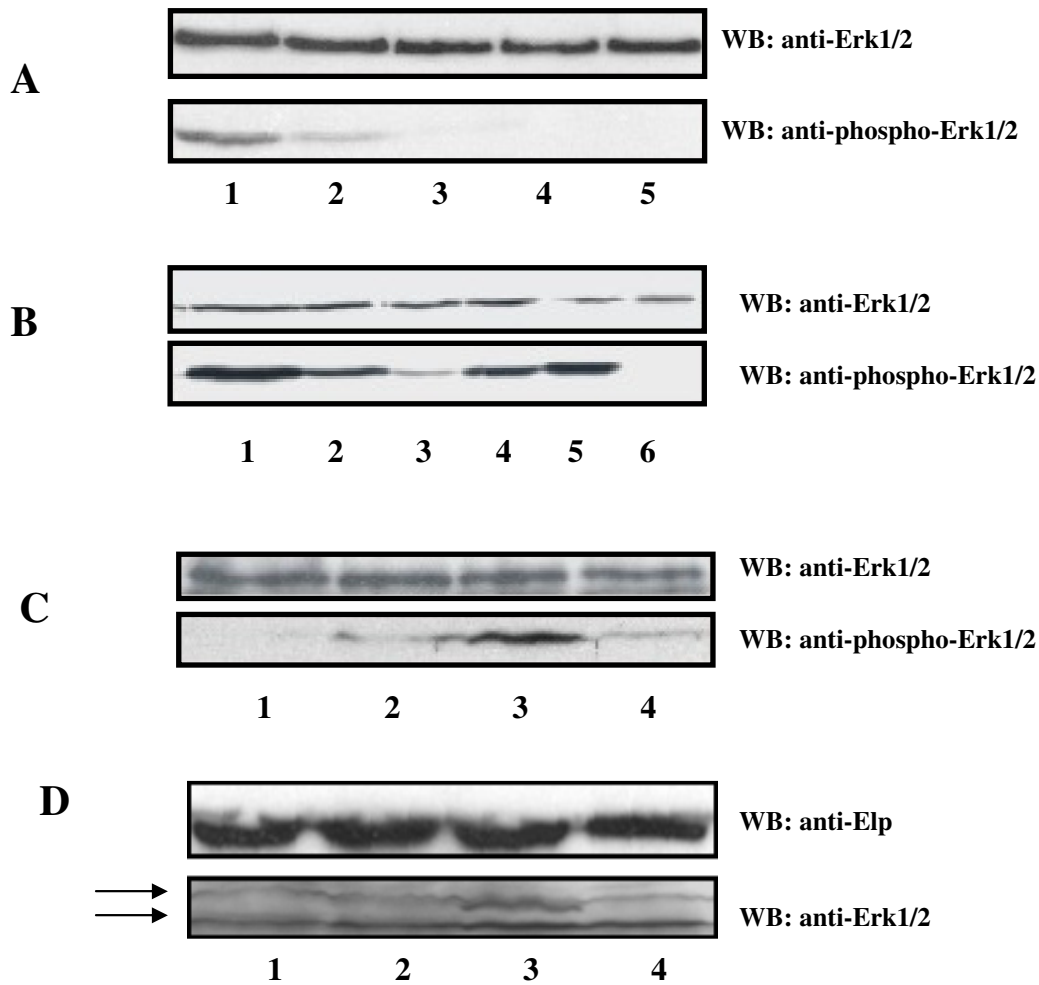


Fig. 16: Phosphorylation of EmMPK-1A under various growth conditions. Metacestode vesicles of *E. multilocularis* (isolate H95) were cultivated *in vitro* under various growth conditions. The vesicles were lysed by adding 2xSDS-sample buffer containing β -mercaptoethanol and crude lysate was analyzed by SDS-PAGE (12% PAA) followed by Western Blotting with the anti-Erk1/2 and anti-phospho-Erk1/2 antibody. **A)** Intact (lane 1-3) or physically disrupted vesicles, i.e. in absence of hydatid fluid (lane 4-5), were incubated in conditioned medium (10% FCS, lane 1) and in 0.2% FCS for 2 and 7d (lane 2, 4 and 3, 5). **B)** Vesicles were physically damaged to remove the hydatid fluid and then incubated for 12h (lane 1-3) and 24h (lane 4-6) with decreasing concentrations of FCS. Lane 1 and 4: 10%; lane 2 and 5: 1%; lane 3 and 6: 0.2%. **C)** Intact vesicles were kept 4d in the medium supplemented with 0.2% FCS and then incubated for 16h in medium containing 0.2% FCS (lane 1), in medium with 10% FCS and preconditioned with hepatocytes (lane 2), medium with 10% FCS and freshly trypsinized hepatocytes (lane 3) and medium with 10% FCS alone (lane 4). **D)** Vesicles were treated as in C), but normalized for Elp. The lower arrow indicates the position of EmMPK-1A while the upper arrow indicated the size of the additional protein.

As shown above (Fig. 16 A), the reduction of serum in the cultivation medium diminished the phosphorylation of EmMPK-1A. It was therefore examined if the effect of the poor medium could be reversed by the stimulation of *E. multilocularis* metacestode vesicles with insulin and IGF-I, respectively, which are shown to be components of the growth medium.

Intact metacestode vesicles were incubated in DMEM containing only 0.2% FCS for 2d and were then stimulated with insulin or IGF-I (Fig.26 A). The stimulation with either 100 nM human insulin (Hoechst) or 100 nM human IGF-I (Immunotools) for 30 min induced the phosphorylation of EmMPK-1A (Fig. 16 A). No induction was detected after stimulation for 60 min (Fig. 16 A), indicating that the phosphorylation of EmMPK-1A is regulated by both kinases and phosphatases in a time dependent manner.

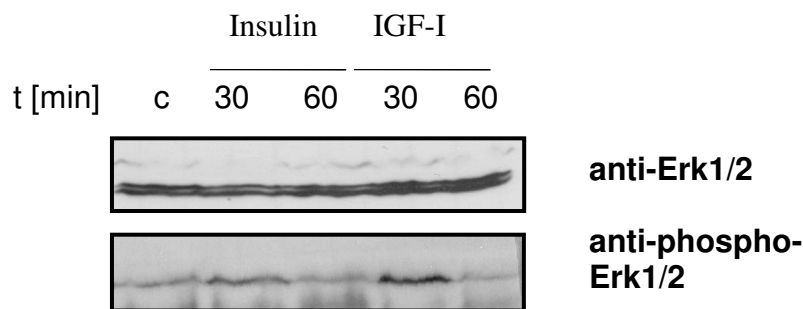


Fig. 17: Effect of human insulin and IGF-I on the phosphorylation of EmMPK-1. Cocultivated metacestode vesicles (isolate H95) were incubated under low serum conditions (0.2% FCS) and then stimulated with 100 nM human insulin or 100 nM human IGF-I for 30 and 60 min or left unstimulated (c). The stimulation was terminated by removing the medium and the addition of 2xSDS sample buffer containing β -mercaptoethanol. Crude protein samples were resolved by SDS-PAGE (12% PAA) and the samples were normalized for EmMPK-1A by Western blotting with the anti-Erk1/2 antibody, while its activation was analyzed by Western blotting with the anti-phospho-Erk1/2 antibody.

3.2.4 Insulin stimulates *egfd* expression in *E. multilocularis* metacestode vesicles *in vitro*

So far, no insulin regulated gene has been identified in *E. multilocularis*. With *emegfd*, Brehm et al. [88] could identify a gene whose expression is upregulated in the presence of host cells *in vitro* and was therefore considered as a good candidate for an insulin regulated gene. The expression of this gene as well as of *emmpk-1* after the stimulation of metacestode vesicles (isolate H95) which had been incubated in medium containing 0.2% FCS supplemented with 100 nM human insulin for 24h was examined by semi-quantitative RT-PCR. The effect of IGF-I was not examined. Although, a stimulatory effect of IGF-I might be possible as it

induces the DNA *de novo* synthesis and protein phosphorylation in metacestode vesicles *in vitro*. Following the stimulation with insulin, total RNA was immediately isolated, DNase I treated and reversely transcribed using a poly-dT oligonucleotide (CD3RT). A dilution series (10-fold in each step) of the synthesized first strand cDNA was made and the expression of the respective gene was analyzed by PCR using gene specific oligonucleotides. The expression of *elp* was used to normalize the samples and subsequently the expression of *emmpk-1* and *emegfd* was analyzed (Fig. 18). While *emmpk-1* was not regulated by insulin, its addition stimulated the expression of *emegfd* about 10-fold in *E. multilocularis* metacestode vesicles. This is within the range Brehm et al. [88] described for the upregulation of *emegfd* in the presence of host cells and further underlines the stimulatory effect of exogenous insulin on *E. multilocularis* metacestode vesicles and points to a potential role of EmEGFD in the development of *E. multilocularis* metacestode vesicles.

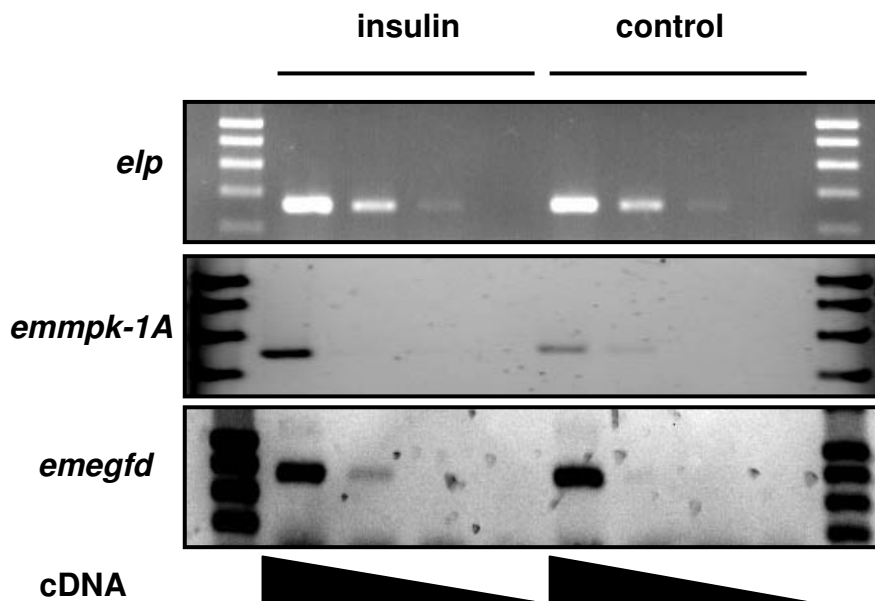


Fig. 18: Effect of human insulin on gene expression in *E. multilocularis* metacestode vesicles *in vitro*. Metacestode vesicles were incubated in medium containing 0.2% FCS for 4d and were then stimulated with 100 nM human insulin for 24h. The isolated and DNase I treated total RNA was reversely transcribed using the Omniscript Kit (QIAGEN) and a poly-dT oligonucleotide (CD3RT). The expression of *emir*, *emmpk-1* and *emegfd* and the housekeeping gene *elp* was analyzed by PCR using gene specific oligonucleotides and serial diluted (10-fold in each step) first strand cDNA as template.

3.3 EmIR - the *E. multilocularis* insulin receptor ortholog as potential transmitter of external signals

It could be clearly shown by the previous experiments, that both exogenously added insulin and IGF-I exert promoting effects on *E. multilocularis* metacystode vesicles with those induced by insulin being more pronounced. Both hormones stimulate the parasite's MAP kinase cascade and induce the *de novo* DNA synthesis, while insulin also stimulates the survival and the gene expression of *E. multilocularis* metacystode vesicles *in vitro*. Konrad et al. previously characterized *emir* cDNA [5]. In the following studies, *emir* was analyzed on the genetic and translational level in more detail.

3.3.1 Southern blot analysis of *E. multilocularis* chromosomal DNA – EmIR is encoded by a single copy gene

Insulin as well as IGF-I clearly affect *E. multilocularis* metacystode vesicles *in vitro*. It might be possible that these effects are induced by the binding to a common receptor or to different receptors. It has been shown for the human system that the effects of insulin and IGF-I are initiated by the binding of the hormones to their cognate receptors [47-53]. Konrad et al. [5,79] characterized the *emir* chromosomal locus. It comprises 16.5 kb and the coding region is interrupted by 24 introns varying in their size from 34 to 1802 bp. The resulting 25 exons range from 51 to 707 bp. A graphic overview of the organization of the chromosomal locus is depicted in Fig. 19.

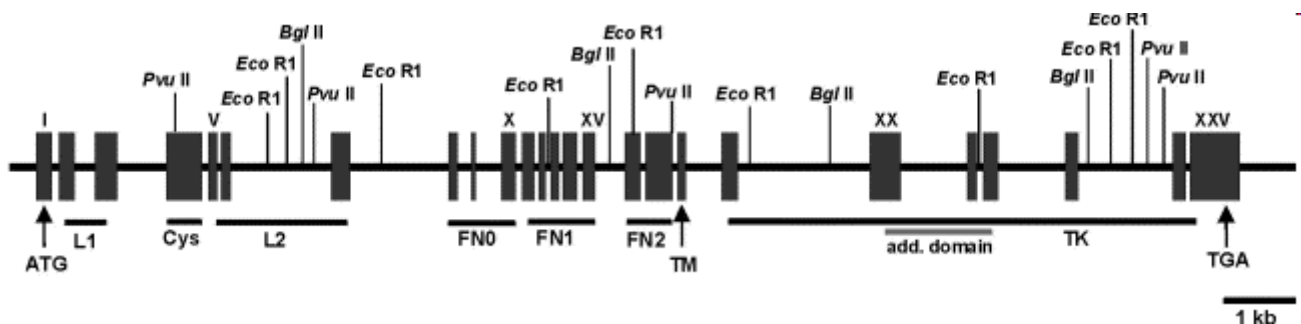


Fig. 19: Exon-intron structure of the *emir* chromosomal locus. The chromosomal locus comprises 25 exons (black bars) which are dispersed over 16.5 kb. The arrows indicate the coding region for the translational start (ATG) and stop (TGA) codons as well as the transmembrane domain (TM). The coding regions for the ligand binding domain (L1-Cys-L2), the three fibronectin III domains (FN0, FN1, FN2) and the tyrosine kinase domain (TK) are marked by black bars, whereas the grey bar marks the coding region for the 172 amino acid insert of the kinase domain (add, domain). Further, restriction sites for *EcoRI*, *PvuII* and *BglIII* are given as well.

The RTKs of the Ins/IGF-I family share the highest identity within the tyrosine kinase domain. For the analysis if more than one receptor of the Ins/IGF-I RTK family is encoded in *E. multilocularis*, a Southern blot analysis of *E. multilocularis* chromosomal DNA was carried out employing a DNA probe spanning exons XXIV and XXV which encode the C-terminal end of Emir's tyrosine kinase domain. For each restriction enzyme used, only a single band was detected by autoradiography suggesting that *emir* is a single copy gene and the only RTK of the Ins/IGF-I family encoded by *E. multilocularis* (Fig.20). The present result might suggest that both exogenous insulin and IGF-I bind to the same receptor but with different affinities as shown by the stimulation of *de novo* DNA synthesis.

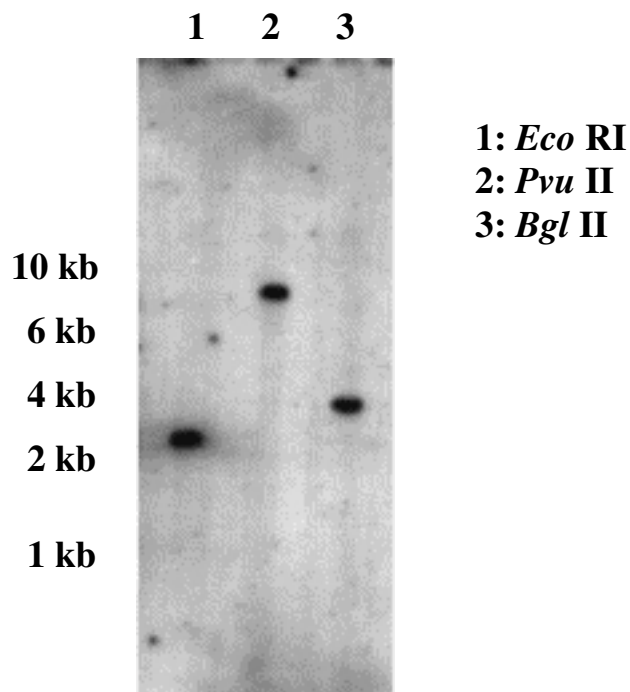


Fig. 20 Southern hybridization of genomic *E. multilocularis* DNA digested with three different restriction enzymes. The DNA fragments were separated on a 0.8% agarose gel, transferred onto a nylon membrane and hybridized with a radioactively labeled DNA fragment spanning exons XXIV and XXV. After 48 h of exposure at -80°C , the x-ray film was developed. The size of the DNA marker and the used restriction enzymes are given in the figure.

3.3.2 Production of polyclonal antibodies directed against EmIR's ligand binding and intracellular domain

For the analysis of the expression of EmIR in different *E. multilocularis* larval stages and its tyrosine phosphorylation antibodies are an essential tool. The receptors of the insulin/IGF-I family are heterotetrameric proteins composed of 2 α – and 2 β -subunits being covalently linked via disulfide bonds. Hence, the ORF encoding the putative ligand binding domain (EmIR_{LCL}, aa 34 - 547) – and putative intracellular domain (EmIR_{intra}, aa 1129 - 1749) of EmIR were cloned into the pBAD/Thio-TOPO® vector for recombinant expression in *E. coli*. A schematic illustration of the encoded fusion proteins EmIR_{LCL} - thio and EmIR_{intra} - thio is depicted in Fig. 21.

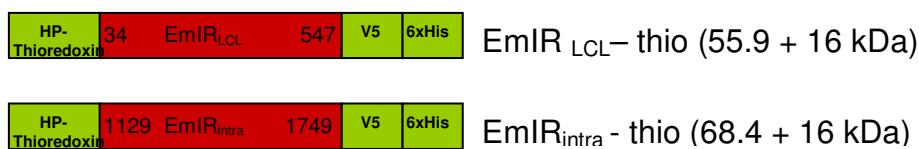


Fig. 21: Schematic view of EmIR ligand binding domain (EmIR_{LCL}) and intracellular domain (EmIR_{intra}) recombinantly expressed in *E. coli* BL21 with the expression plasmid pBAD/Thio-TOPO® vector (Invitrogen). The proteins are expressed with a N-terminally fused HP-thioredoxin epitope, while a V5 epitope and a 6xHis-tag are fused to the C-terminus which allow the detection by Western blotting using an anti-V5 antibody and purification via metal affinity chromatography, respectively. The numbers in the red bars indicate the position of the residue in full length EmIR. Further, the deduced molecular weight of EmIR_{LCL} and EmIR_{intra} as well as the total molecular weight of the additional epitopes are given in parenthesis.

After the induction with 0.2% arabinose (final concentration) for 4h in *E. coli* BL21, which is a commonly used strain to induce eukaryotic proteins, both fusion proteins, EmIR_{LCL} - and EmIR_{intra} – thio, were purified under denaturing conditions (guanidinium HCl method) via the 6xHis – tag. The quality of the protein purifications was validated by both Coomassie staining and Western blotting (Fig. 22) with anti-V5 antibody (Invitrogen).

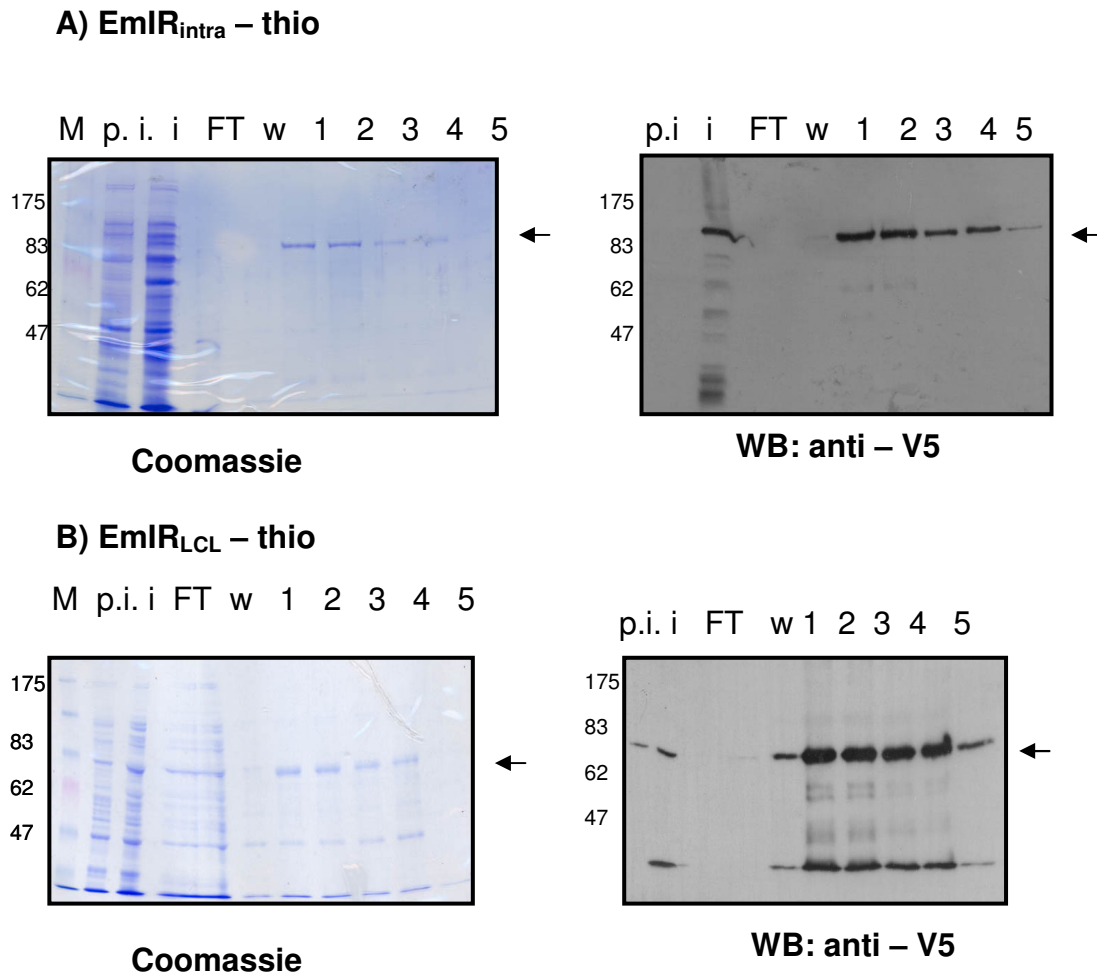


Fig. 22: The expression of the fusion proteins EmIR_{LCL} - and EmIR_{intra} – thio were induced with 0.2% arabinose (final concentration) for 4h in *E. coli* BL21 using the pBAD/Thio-TOPO® vector (Invitrogen) and subsequently purified via the 6xHis-tag under denaturing conditions as described. The induction and purification was analyzed on an 8% PAA –gel followed by Coomassie staining and Western blotting with anti-V5 antibody (Invitrogen) according to the manufacturer’s recommendations. The fragment sizes of the Prestained Protein Marker (M; Invitrogen) are indicated on the left of each picture. The samples separated on the PAA-gel were: *E. coli* lysate prior (p. i.) and after (i.) induction; the protein fraction, which did not bind to the Ni²⁺ column (FT) and the washed out unspecific bound proteins (w); the fusion proteins eluted with denaturing elution buffer (1, 2), imidazole elution buffer (3, 4) and 0.5 M EDTA, pH8.0 (5). The arrow marks the corresponding full length fusion protein, while the smaller fragments detected with the anti – V5 antibody were most likely degradation products.

For the production of polyclonal antibodies against EmIR_{LCL} – and EmIR_{intra} – domain, respectively, (White New Zealand) rabbits, which had previously been examined not to have developed antibodies against the fusion proteins and *Echinococcus* proteins (data not shown), were intravenously immunized with the corresponding purified fusion proteins using the adjuvans ABM-ZK and ABM-N (Linaris, Wertheim-Bettingen). Both rabbits were boosted two to three times before the final bleeding. With each final serum, the corresponding fusion protein which had been used to immunize the rabbit was clearly detected in Western blot assays (data not shown).

Since the recombinant proteins used to immunize the rabbits had an N-terminally fused thioredoxin epitope and a V5/ 6xHis-tag fused to its C-terminus (Fig. 21), it might have been possible that only antibodies directed against the additional epitopes had been induced in the rabbits. Therefore, the coding region for EmIR intracellular domain and the putative α – domain were ligated into the pGEX-3X expression vector. The resulting proteins (Fig. 23) were expressed in *E. coli* BL21 with an N-terminal fused glutathione-S-transferase (GST), which enables the purification of the fusion proteins via affinity chromatography with immobilized glutathione (Fig. 24). In addition, GST was regarded as very unlikely to be detected by the immune sera.



Fig. 23: Schematic view of the EmIR α - domain (EmIR _{α}) and intracellular domain (EmIR_{intra}) recombinantly expressed in *E. coli* BL21 with the pGEX-3X expression vector (Applied Biotech). The proteins are expressed with the N-terminally fused glutathione-S-transferase (GST). The numbers in the red bars indicate the position of the limiting residues in full length EmIR. GST adds 26 kDa to the deduced molecular weight of the recombinantly expressed proteins, which is given in parenthesis.

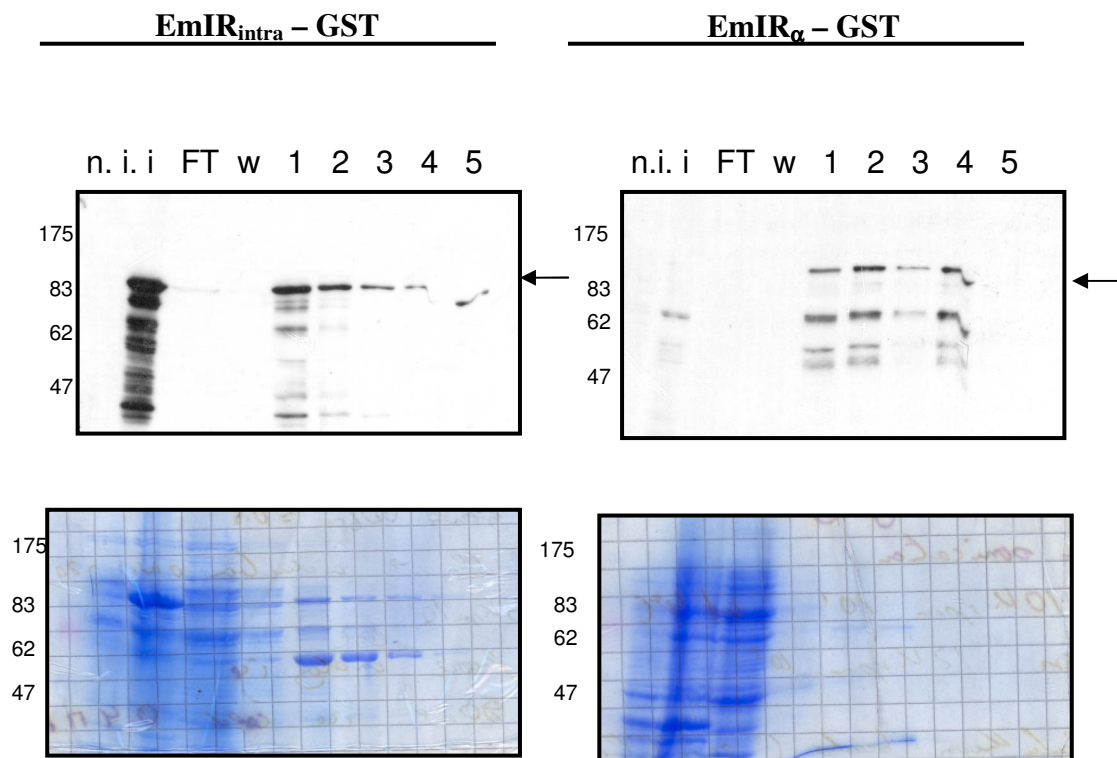


Fig. 24: Expression of the EmIR_{intra} – and EmIR_α – GST fusion proteins in *E. coli* BL21. The expression of the fusion proteins EmIR_α - and EmIR_{intra} – GST were induced with 0.2 mM IPTG in *E. coli* BL21 over night at 20 °C using the pGEX-3X expression vector (Applied Biotech). The fusion proteins were purified via affinity chromatography employing Glutathione Sepharose 4B (Amersham) as described. The induction and purification of both fusion proteins was analyzed via SDS-PAGE (8% PAA) followed by Coomassie staining and Western Blot analysis with anti-GST antibody (Santa Cruz). The samples resolved on the PAA-gel were: *E. coli* lysate prior (**n. i.**) and after (**i.**) induction; the protein fraction, which did not bind to the immobilized glutathione (**FT**) and the washed out unspecific bound proteins (**w**); the GST-fusion proteins eluted with buffer 3 (**1**), buffer 4 (**2**), buffer 5 (**3**), buffer 6 (**4**) and guanidine lysis buffer (**5**). The arrow indicates the corresponding fusion protein. Both fusion proteins are likely to be degraded, since several proteins smaller than the fusion protein are also detected with the antibody. While EmIR_{intra} – GST is expressed well in *E. coli* BL21, EmIR_α – GST is not as well, but sufficiently enough for affinity purification.

By Western blotting (Fig. 25 A) could be demonstrated that the polyclonal serum rose against EmIR_{intra} – thio did not only recognize the recombinantly expressed fusion protein employed in the immunization but also EmIR_{intra} fused to GST. This finding indicates that the serum contains antibodies specific for EmIR_{intra} and not only specific for the thioredoxin and/or V5-His- tag. This was not the case for EmIR_{LCL}-thio. While this polyclonal serum detected the EmIR_{LCL}-thio fusion protein, it barely detected the EmIR_α– GST fusion protein (Fig. 25 B),

indicating that no antibodies against Emir's ligand binding domain were made. A possible explanation might be the high similarity between ligand binding domain of EmIR and that of mammalian RTKs of the Ins/IGF-I family which might prevent the recombinant EmIR_{LCL}-domain to be recognized as antigen by the rabbit's immune system. This could mean that it is difficult to raise antibodies against Emir's ligand binding domain, an assumption that is supported by the failure to detect antibodies against the ligand binding domain in the serum of patients suffering from AE (data not shown). With the additional 172 residues, Emir's intracellular domain differs significantly from the intracellular domain of the other RTKs of the Ins/IGF-I family and might be more antigenic to induce the production of specific antibodies within the rabbit. Since the intracellular domain of RTK contains the kinase domain, which exerts the downstream effects, emphasis was laid on this domain in this work.

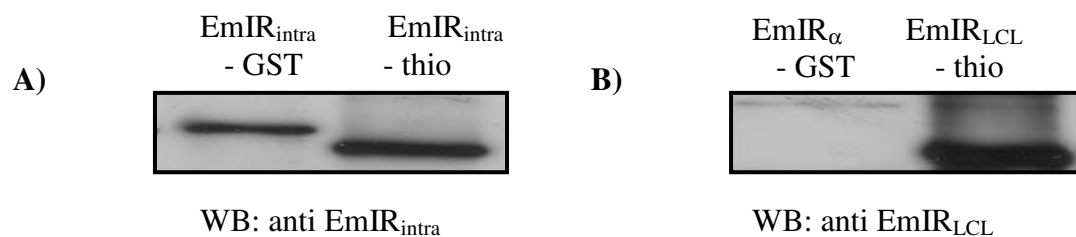


Fig. 25: Western blot analysis of the binding specificity of the immune serum rose against recombinantly expressed EmIR_{intra}-thio and EmIR_{LCL}-thio. 5 µg of the purified fusion proteins EmIR_{intra}-thio, EmIR_{LCL}-thio, EmIR_{intra}-GST and EmIR_{alpha}-GST were loaded on an 8% SDS-PAGE and blotted on a nitrocellulose membrane. For the analysis of the specificity of the corresponding immune serum, EmIR_{intra}-thio and EmIR_{intra}-GST (**A**) as well as EmIR_{LCL}-thio and EmIR_{alpha}-GST (**B**) were blotted on a nitrocellulose membrane and probed with the corresponding serum (1:800 in 1xTBS, 5% skim milk, and 0.05% Tween 20). An anti rabbit-HRP antibody was used as secondary antibody (1:5000 in 1xTBS, 5% skim milk, 0.05% Tween 20) and the blot was developed using Pierce's ECL Kit.

3.3.3 Western blot analysis of *E. multilocularis* metacestode vesicles for the expression of EmIR

In a next step, protein lysates of *in vitro* cultivated *E. multilocularis* metacestode vesicles were examined by Western blotting with the EmIR_{intra} immune serum. As depicted in Fig. 26, the immune serum detected one protein of approximately 140-150 kDa, while the pre-immune serum did not detect any protein, demonstrating the specificity of the induced antibodies. Since the metacestode lysate was analyzed under reducing conditions, the detected protein is presumably the mature β -domain of EmIR. With 140 - 150 kDa, its molecular weight is larger than the deduced molecular weight of 100.3 kDa. For human IR could be shown that the difference between the deduced and the *in vivo* molecular weight of the α - and β -subunit is due to co-translational glycosylation [133]. This protein modification increases the molecular weight of the α - and β -subunit from 84 and 70 kDa to 135 and 95 kDa, respectively [133]. Glycosylation is a likely explanation for the discrepancy observed for the EmIR β -domain as well. This modification has also been proposed to count for the increased molecular weight of the α -subunit of the *S. mansoni* insulin receptor orthologs, SmIR-1 and SmIR-2, compared to the deduced molecular weight [83]. By treating *E. multilocularis* metacestode vesicles with sodium periodate, the glycoproteins should be deglycosylated [222]. But this treatment destructed also the protein moiety of EmIR since no protein could be detected by Western blot analysis using the anti EmIR_{intra} serum (data not shown).

In the next step, the EmIR_{intra} immune serum was used for immunoprecipitations from vesicles' total protein lysate (Fig. 26 B). Besides the immunoglobulins (approx. 48 kDa), a major protein band of 140-150 kDa and a minor protein band of approximately 220 kDa were immunoprecipitated. The major protein corresponds in its size to the protein detected in the Western Blot analysis of crude lysate (Fig. 26 A). The 220 kDa protein is most likely the unprocessed EmIR proreceptor which exerts a larger molecular weight than the deduced 192 kDa [84] most likely due to co-translational glycosylation. Such a glycosylation has been described for the human IR proreceptor [133]. Quite interestingly, the EmIR β -subunit could only be solubilized from metacestode vesicles in the presence of Triton X-100 and sodium deoxycholate suggesting that EmIR is a transmembrane protein. An expression of SmTGF β -RII, a TGF- β receptor homolog identified in *S. mansoni*, in the tegument has been suggested due to its solubility in NP-40 extracts [173].

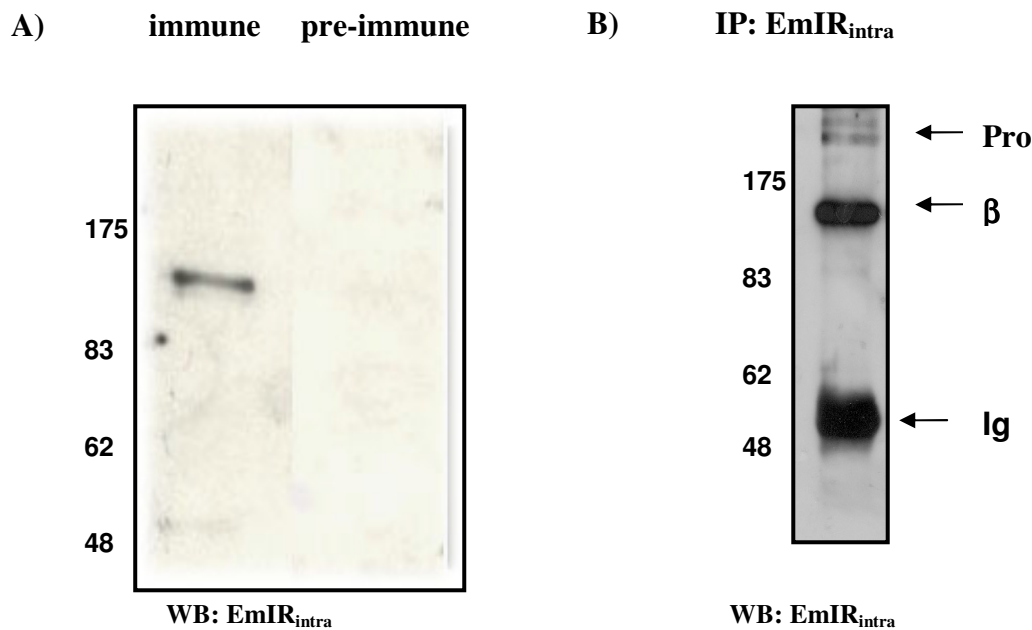


Fig. 26: Western Blotting of crude lysate of metacestode vesicles with EmIR_{intra} immune serum. **A)** *in vitro* cocultivated metacestodes of the isolate H95 (2-5 mm in diameter) were manually picked, intensively washed with 1xPBS, physically disrupted and resuspended in 2xSDS sample buffer containing β -mercaptoethanol and boiled for 5 min. The crude protein lysate was resolved via SDS-PAGE (8% PAA). After the transfer onto a nitrocellulose membrane and blocking with 5% skim milk in 1xTBS 0.05% Tween 20 (1xTBST), the membrane was incubated with the anti EmIR_{intra} immune serum (**immune**) and the pre-immune serum (each 1:800 diluted in blocking buffer) over night at 4°C under gentle agitation. The next day, the membrane was washed 3 times with 1xTBST and then transferred into blocking buffer containing the anti – rabbit – HRP antibody (Jackson ImmunoResearch; 1:5000) and rocked for 1h at room temperature. Following 3 washing steps with 1xTBST, the blot was developed by chemiluminescence (ECL, Pierce). **B)** *in vitro* cocultivated metacestode vesicles were handled as in A) but lysed with TritonX-100/deoxycholate lysis buffer instead of 2xSDS sample buffer. The putative EmIR β -subunit was immunoprecipitated from the soluble proteins by adding the EmIR_{intra} immune serum (1:100) and rocking at 4°C over night. The next day, the antibody-antigen complex was captured by the addition of agarose-G beads (upstate) for 4h at 4°C. For the Western blot analysis of the captured proteins, the bound proteins were eluted by adding 2xSDS sample buffer containing β -mercaptoethanol and boiling for 5 min. The Western blotting was carried out as in A). The position of the EmIR proreceptor (**Pro**) and b-subunit (**β**) as well as the immunoglobulins (**Ig**) are indicated by arrows.

The EmIR_{intra} immune serum detected one protein in the *E. multilocularis* metacestode vesicle crude lysate under reducing conditions in a Western Blot analysis (Fig. 26) and precipitated 2 proteins from a crude lysate. It is known for mature human IR and IGF-IR to be composed of two α – and two β – subunits which are linked via disulfide bonds [188,190]. For the analysis if mature EmIR is also composed of disulfide-linked subunits the crude lysate of metacestode vesicles was analyzed by Western blotting under reducing and non-reducing conditions (Fig. 27). In the presence of 10 % β -mercaptoethanol, the immune serum detected the β -subunit and the non-processed proreceptor as well. The latter was also detected when no reducing agent was present. Under this condition, the β -subunit was also detectable, but not as strong as under reducing conditions. This finding might indicate that the proteolytic processing and the formation of the disulfide bonds do not take place simultaneously during the synthesis of mature EmIR. Nevertheless, like human IR and IGF-IR, mature EmIR is most likely composed of disulfide linked subunits which are derived from a proreceptor by proteolytic processing. Since EmIR does not possess the conserved tetra basic motif at which processing occurs in human IR and IGF-IR [5,133], this processing mechanism differs most likely between mammals and *E. multilocularis*.

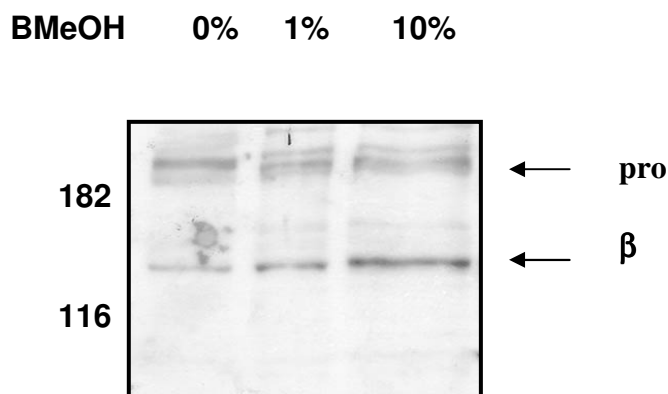


Fig. 27: EmIR is composed of a α - and β -subunit. The lysate was obtained from *in vitro* cultivated metacestodes (isolate H95) of 2 – 5 mm in diameter. On the day of the experiment, the metacestodes were intensively washed with ice cold 1xPBS, physically damaged to enable the hydatid fluid to leak out. The cells were pelletized by centrifugation at 4°C and subsequently resuspended in 2xSDS sample buffer without β -mercaptoethanol. Three identical samples were taken and supplemented with β -mercaptoethanol to a final concentration of 0, 1 and 10%. After boiling for 5 min and removal of the insoluble material by centrifugation, equal volumes were separated on a 7% PAA-Gel. The proteins were then transferred onto a nitrocellulose membrane and the EmIR β -subunit was detected with the EmIR_{intra} immune serum (1:800 in 5% skim milk 1xTBS 0.05% Tween 20) and chemiluminescence. The size of the protein marker is indicated on the left and the position of the β -subunit (**β**) and proreceptor (**pro**) on the right. The concentration of β -mercaptoethanol (**BMeOH**) in the 2xSDS sample buffer is given above each lane.

3.3.4 Expression of EmIR in *E. multilocularis* larval stages under different growth conditions

3.3.4.1 *in vitro* activation of protoscolices affects the expression of EmIR

One essential step in the life cycle of *E. multilocularis* (Fig.3) which coincides with massive morphological changes is the so-called activation of protoscolices in the final host during the passage through the digestive tract [8,174]. This activation is characterized by an evagination of the head structure, the scolex, bearing the suckers and rostellum which enable the parasite to persist in the small intestine of its final host and to develop into the mature worm [17]. It was therefore analyzed by RT-PCR and Western blot analysis if the expression of *emir* is regulated during the protoscolices' activation.

The activation can be mimicked by incubating the protoscolices in acidified medium (pH 2) supplemented with pepsin, followed by an incubation in medium supplemented with sodium taurocholate, a bile salt [8,174]. The non-activated protoscolices were also incubated in pure medium to exclude an effect of the medium itself. The activation, i.e. the evagination of the head structure was verified in a standard light microscope at a 5-10 fold magnification. Prior to the activation, only 10 – 20% of the protoscolices were evaginated, whereas the percentage increased to approximately 70% after the treatment (Fig. 28). In case of the non-activated control, an increase in the number of evaginated protoscolices could not be observed (data not shown). The protoscolices were motile in all samples thereby demonstrating their viability (data not shown).

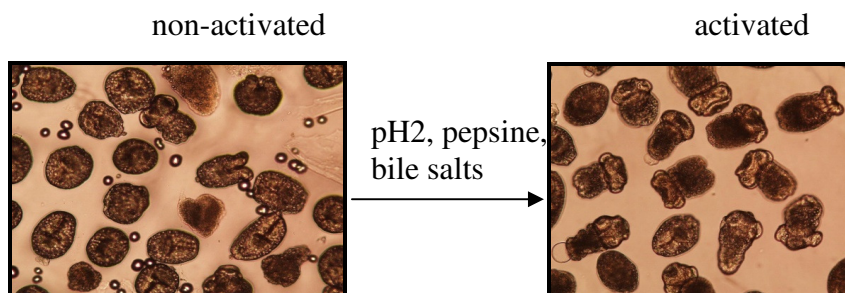


Fig. 28: *in vitro* activation of protoscolices induces the evagination of the scolex. Protoscolices purified from a freshly sacrificed Mongolian jird were incubated in acidified medium supplemented with pepsin, followed by an incubation step in medium supplemented with bile salts to simulate the ingestion by the final host. The activation is characterized by the evagination of the protoscolices' head structures, the scolex, which was examined in the light microscope at 5-10 fold magnification. Representative pictures of non-activated (left) and activated (right) protoscolices are shown.

The expression of *emir* in *E. multilocularis* metacystodes vesicles, protoscoleces and activated protoscoleces were compared to the expression of *elp* [96] by semi-quantitative RT-PCR (Fig. 29 A). Total RNA of activated and non-activated *E. multilocularis* protoscoleces (isolate Java), as well as of cocultivated metacystodes vesicles (isolate H95) was purified. Any contamination with chromosomal DNA was eliminated by DNase I (Roche) treatment prior to the reverse transcription with Omniscript Kit (QIAGEN) and CD3RT oligonucleotide according to the manufacturer's recommendations. A dilution series of the synthesized first strand cDNA (10 – fold diluted in each step) was made and used as template in a standard PCR with Taq polymerase (NEB) and gene specific oligonucleotides (Table 2).

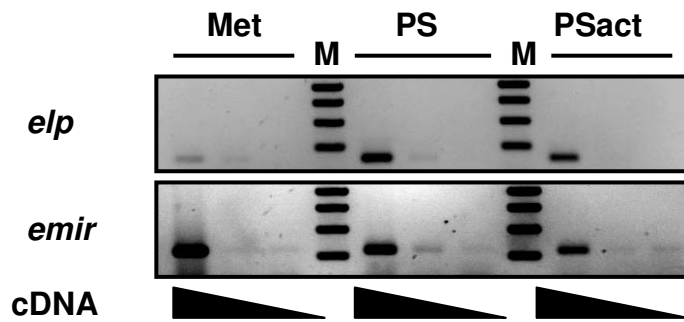
<u>Gene</u>	<u>Oligonucleotides</u>
<i>elp</i>	Em10 up x Em10 dw
<i>emir</i>	CK95 x CK 97

Table 2: Oligonucleotides used in semi-quantitative RT-PCR analysis of gene expression in metacystode vesicles, protoscoleces and activated protoscoleces.
elp: ezrin-like protein; *emir*: *E. multilocularis* insulin receptor

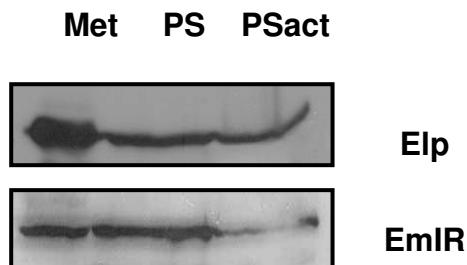
An *elp* specific fragment could be amplified in the identical dilutions for all three larval stages (Fig. 29 A, row 1), indicating that equal amounts of cDNA were present in the samples. The activation of *E. multilocularis* protoscoleces led only to a slightly decrease in the expression of *emir* in activated protoscoleces compared to non-activated protoscoleces (Fig. 29 A, row 2). With the available antibodies against Elp and the EmIR β -subunit the expression was further analyzed on the translational level by Western Blotting (Fig. 29 B). The larval stages were treated as for the isolation of total RNA, except that after the last washing step 2xSDS-sample buffer containing β -mercaptoethanol was added and the samples were immediately boiled. Elp could be detected in all larval stages (Fig. 29 B) and approximately equal amounts of protein were loaded for non-activated and activated protoscoleces, whereas more protein was present in the metacystode lysate (Fig. 29 B). The analysis with the anti EmIRintra-serum verified the result of the RT-PCR that EmIR is expressed in *E. multilocularis* metacystode vesicles and non-activated protoscoleces. Interestingly, the results of the Western blot analysis of activated protoscoleces did not correlate with the results of the RT-PCR analysis. Whereas the RT-PCR clearly showed that *emir* is transcribed in activated protoscoleces the protein was barely detectable, indicating that the expression of *emir* could be regulated on the translational level. In addition, the signal intensities for Elp and EmIR in the Western blot analysis were

determined with the NIH Imaging software [167] and the ratios of the expression of EmIR relative to EIp in the different *E. multilocularis* larval stages were analyzed (Fig. 29 C). Based on this analysis, EmIR is about 2.5 fold stronger expressed in non-activated *E. multilocularis* protoscoleces compared to metacestode vesicles, while in activated protoscoleces the expression is approximately 2 fold lower compared to those in metacestode vesicles. Regarding *E. multilocularis* protoscoleces alone, EmIR is approximately 5 – fold higher expressed in non-activated than in activated protoscoleces. The different expression of *emir* in the different larval stages might reflect the massive morphological change during the development of the protoscolex to the adult worm and might suggest that EmIR plays a role in the development of those *E. multilocularis* larval stages which develop within the intermediate host.

A)



B)



C)

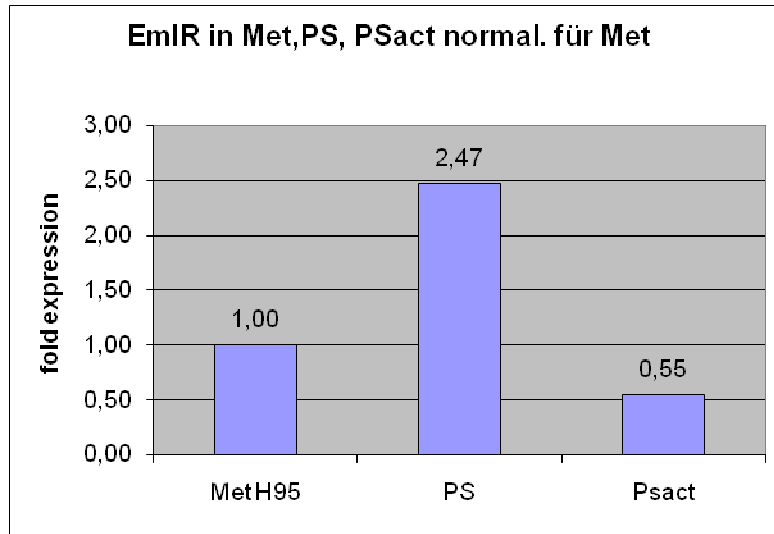
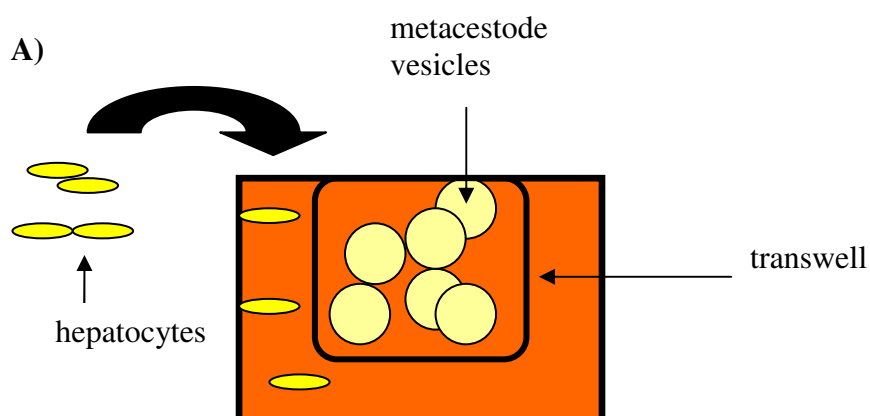


Fig. 29 (next page): Analysis of the expression of *E. multilocularis* genes in co-cultured metacystode vesicles, non-activated and activated protoscoleces. **A)** The expression of *emir*, *emmpk-1* and *emegf* in metacystode vesicles (**Met**; isolate H95), non-activated (**PS**) and activated protoscoleces (**PS**; isolate Java) were analyzed by semi-quantitative RT-PCR. Total RNA was purified, DNase I treated and reversely transcribed using the Omniscript Kit (QIAGEN) and a poly-d(T)-oligonucleotide (CD3RT) according to the manufacturer's recommendations. The first strand cDNA was serially diluted (10-fold in each step) and the expression of the respective genes was assessed by PCR using Taq-DNA polymerase (NEB) and gene specific oligonucleotides. The expression of *elp* was used as normalization. **B)** Western Blot analysis of the expression of EmIR in these samples using the anti-EmIRintra serum. The expression was normalized for the expression of Elp. **C)** The band intensities in the Western blots were measured and the relative expression of EmIR to Elp in each sample was compared to that in the metacystode vesicles.

3.3.4.2 Expression of EmIR in *E. multilocularis* metacystode vesicles is upregulated by host derived factors

The present study clearly shows that host derived factors promote both growth and development of *E. multilocularis* metacystode vesicles *in vitro* and activate intracellular signaling molecules as well as gene expression in *E. multilocularis* metacystode vesicles.

Based on these observations, the expression of EmIR in *E. multilocularis* metacystode vesicles (isolate H95) in the presence of host cells was examined (Fig. 30 B). After the normalization for the cytoskeleton protein Elp [96], Western blotting with the EmIR_{intra} immune serum revealed that the expression of EmIR is upregulated within 36 h of cocultivation. This upregulation could not be observed when host cells were omitted and is not due to the presence of trypsin, which had been added to the growth medium in the control. The measurement of the band intensities with the NIH ImageJ software [167] showed that in the presence of host cells EmIR is about 2.5 fold stronger expressed (Fig. 30 C). The cocultivation was carried out in a transwell system (Fig. 30 A) to exclude a contamination of the *E. multilocularis* metacystode vesicles with host cells which might lead to false Western blotting results. In the transwell system, only soluble factors can pass via the membrane pointing out again the role of soluble factors secreted by the host cells on the growth and development of *E. multilocularis* metacystode vesicles.



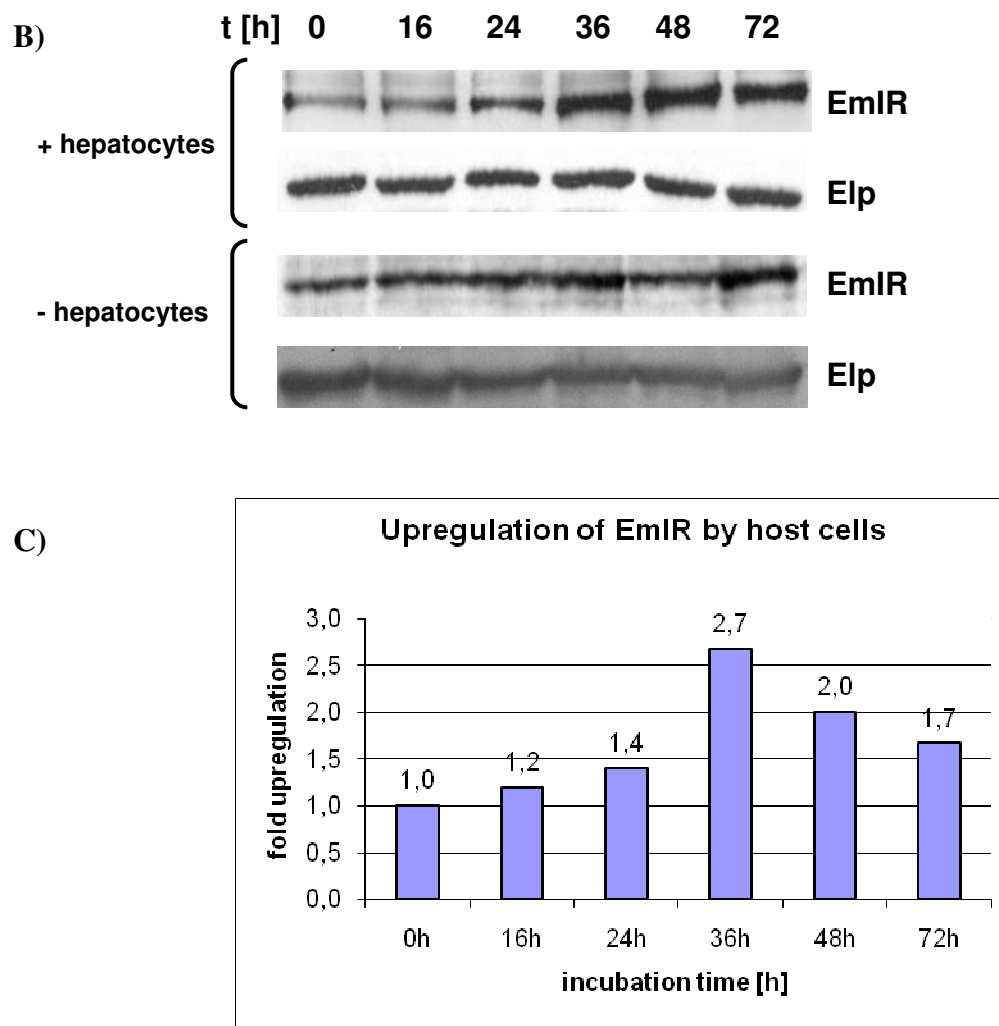


Fig. 30: The expression of EmIR is upregulated in the presence of host cells.

A) Schematic view of a transwell system. **B)** Cocultivated metacystode vesicles (isolate H95) were washed with prewarmed 1xPBS remove the host cells. Vesicles with a total volume of 1.5 ml (8-10 vesicles) were manually picked for each setup and cocultivated with 500,000 freshly trypsinized RH- cells in 2 ml medium (10% FCS) in a 12 well cell culture plate (Nunc) employing a transwell system (Nunc) to avoid direct physical contact (**A**). After 0, 16, 24, 36, 48 and 72h incubation, the vesicles were washed with 1xPBS, physically disrupted and pelleted by centrifugation at room temperature (400xg, 5 min) to remove the hydatid fluid. The pellet was stored at -20° until further use. As a control, the same experiment was carried out in absence of hepatocytes but included the trypsinization step to exclude a trypsin effect. For the analysis of the expression of EmIR, the cells were resuspended in 2xSDS sample buffer containing β -mercaptoethanol and boiled for 5 min. Following SDS-PAGE (8% PAA), the proteins were transferred onto a nitrocellulose membrane and EmIR's β -subunit was detected by immunostaining with the EmIR_{intra} immune serum. The anti-Elp antibody was used to normalize the samples. **C)** The upregulation was quantified by measuring the band intensities of Elp and EmIR with the NIH Image software (ImageJ). The ratio of the expression of EmIR and Elp at a specific time point set in relation to ratio at 0h.

In this work the positive effect of exogenous insulin on the development of *E. multilocularis* metacystode vesicles were shown. It could be further shown that the hepatocytes used in the *in vitro* culture synthesize insulin. Hence, a possible stimulatory effect of exogenously added insulin on the expression of EmIR in *E. multilocularis* metacystode vesicles was analyzed. *E. multilocularis* metacystode vesicles which had been kept under low serum conditions were stimulated with 100 nM human insulin for 24 h and the expression of *emir* compared to *elp* was analyzed by RT-PCR of total RNA (DNase I treated). As depicted in Fig. 31 the stimulation with insulin did not affect the transcription of *emir* in *E. multilocularis* metacystode vesicles.

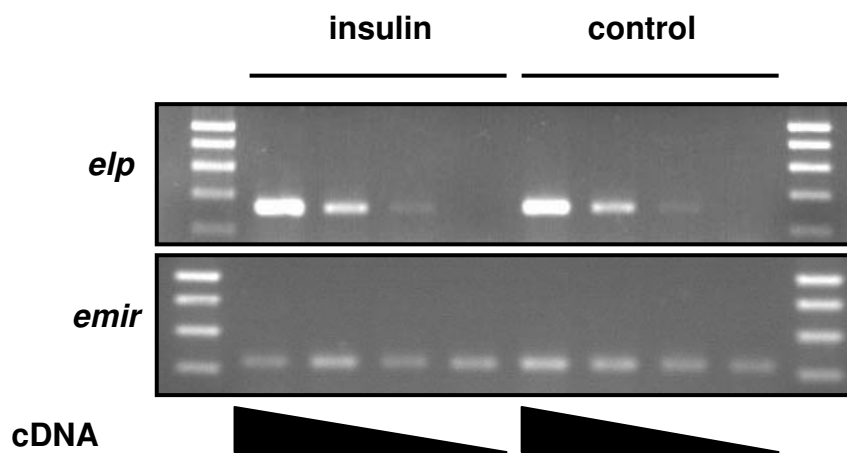


Fig. 31: Effect of human insulin on gene expression in *E. multilocularis* metacystode vesicles *in vitro*. Metacystode vesicles were incubated in medium containing 0.2% FCS for 4d and were then stimulated with 100 nM human insulin for 24h. The isolated and DNase I treated total RNA was reverse transcribed using the Omniscript Kit (QIAGEN) and a poly-d(T)-oligonucleotide (CD3RT). The expression of *emir* and the housekeeping gene *elp* was analyzed by PCR using gene specific oligonucleotides and serially diluted (10-fold in each step) first strand cDNA as template.

With the available antibody the effect of insulin on the expression of *emir* in *E. multilocularis* metacystode vesicles was also analyzed on the translational level. Analogous to the analysis of the transcription rate, the samples were normalized for the expression of Elp. The Western Blot analysis verified the results of the RT-PCR analysis (Fig. 32). The expression of EmIR is not upregulated in the presence of insulin, even after a prolonged stimulation of up to 72h.

This suggests that host derived factors different from insulin are most likely involved in the regulation of *emir* expression in *E. multilocularis* metacystode vesicles.

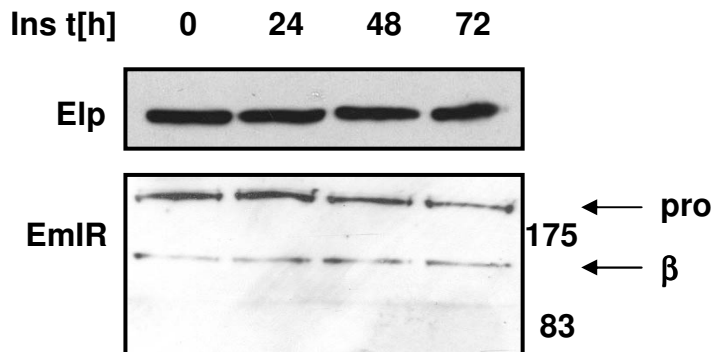


Fig. 32: Western blot analysis of the effect of human insulin on gene expression in *E. multilocularis* metacystode vesicles *in vitro*. *E. multilocularis* metacystode vesicles were incubated in medium supplemented with 0.2% FCS. On day 4, the vesicles were stimulated with 100 nM human insulin for up to 72h. At the indicated time points, the vesicles were lysed by removing the medium and resuspending in 2xSDS sample buffer containing β -mercaptoethanol. The crude protein lysates were subjected to SDS-PAGE (8% PAA in case of Eip and EmIR) followed by Western blotting on a nitrocellulose. The samples were normalized by probing with the anti-Eip antibody. The expression of EmIR was analyzed with the anti-EmIRintra antiserum.

3.3.5 Immunohistochemical and electron microscopical analysis of the expression of EmIR in *E. multilocularis* larval stages

For a more precise analysis of the expression of EmIR in *E. multilocularis* larval stages immunohistochemical and electronmicroscopical experiments were carried out. Sections of the liver of secondary infected *M. unguiculatus* were prepared and the expression of EmIR was determined by immunostaining employing the anti-EmIRintra – immune serum. This work was done in cooperation with Dr. Dennis Tappe and Prof. Dr. Andrew Hemphill. In accordance with the previously exerted RT-PCR and Western blot analyses, EmIR is expressed in both the *E. multilocularis* metacystode vesicles and protoscoleces (Fig. 33). In case of the metacystodes, the receptor is located in the germinal layer and seems to face both the laminated layer, i.e. the surrounding tissue, as well as the hydatid fluid making it accessible for insulin from the surrounding host tissue and the hydatid fluid. The hematoxylin counterstaining shows that the metacystode vesicles are surrounded by host cells but that the

laminated layer separates them from the germinal layer (Fig. 33A). The immunofluorescence verified this observation and reveals that EmIR is expressed in the germinal layer, especially in the glycogen storage cells of *E. multilocularis* metacystode vesicles (Fig. 33 B) suggesting also a metabolic function for EmIR.

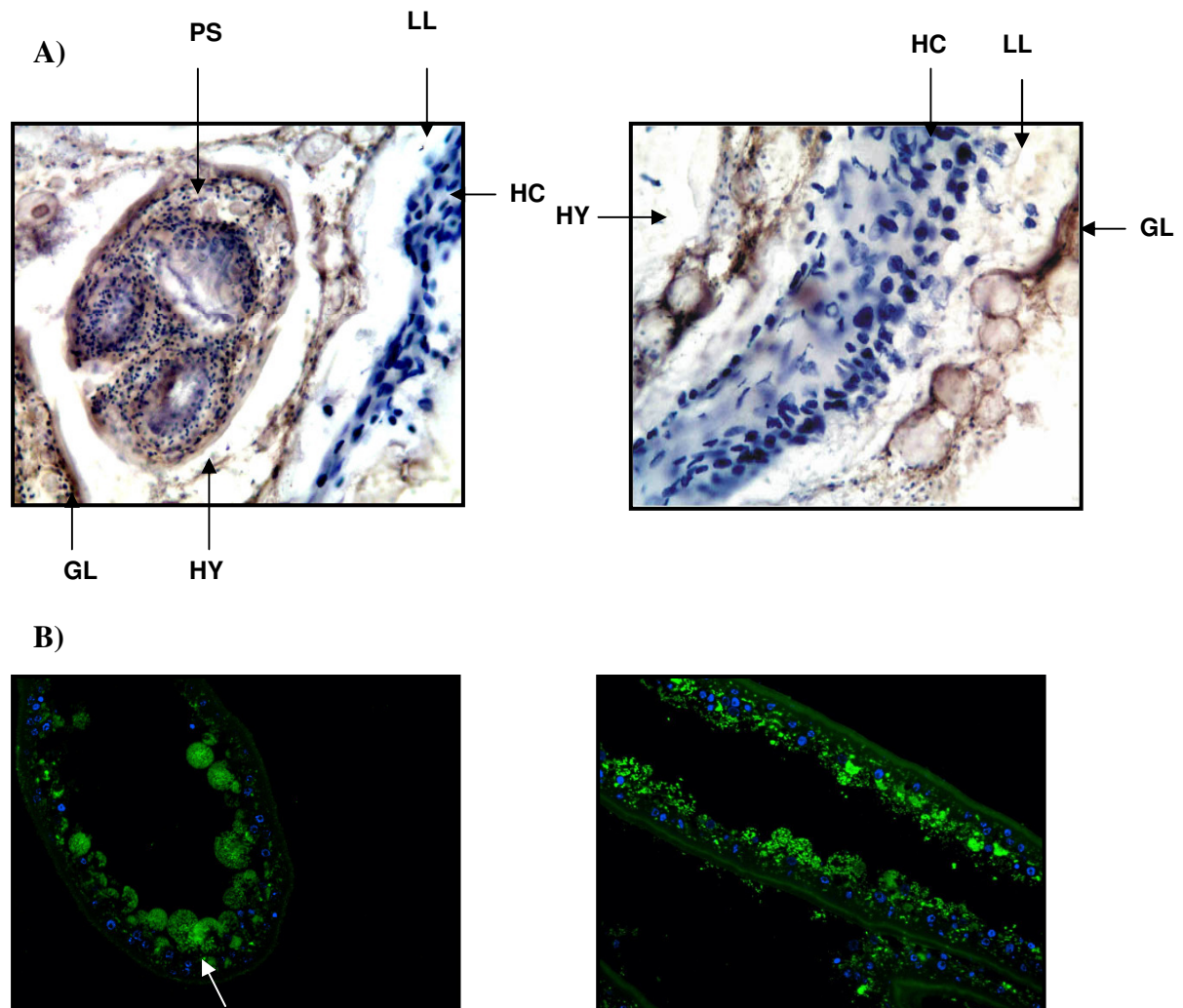


Fig. 33: Immunohistochemical analysis of the expression of EmIR in metacystode vesicles *in vivo*.

A) The liver of secondary infected *M. unguiculatus* was isolated and 5 μm cryosections were made. The expression of EmIR was assessed by probing with the anti-EmIR_{intra} serum and an anti-rabbit-antibody coupled to peroxidase. The samples were developed using diaminobenzidine reagent, followed by a counterstaining with hematoxylin. **B)** Cryosections of *in vitro* cultivated metacystode vesicles were made and probed with anti-EmIR_{intra} serum and an FITC-coupled anti-rabbit-antibody and nuclei were DAPI stained. The arrow marks a glycogen storage cell. **GL:** germinal layer; **LL:** laminated layer; **HC:** host cells; **Hy:** lumen of the vesicle filled with hydatid fluid; **PS:** invaginated protoscolex.

A further expression analysis of EmIR in *E. multilocularis* metacystode vesicles was done by Andrew Hemphill (University of Bern, Switzerland). Immunostaining of cryosections of *in vitro* cultivated metacystode vesicles using the anti-EmIRintra serum and gold coupled secondary anti-rabbit antibodies for an electronmicroscopical (Fig. 34) analysis verified the observation of the immunohistochemistry. EmIR is expressed in the germinal layer of *E. multilocularis* metacystode vesicles and also in the glycogen storage cells.

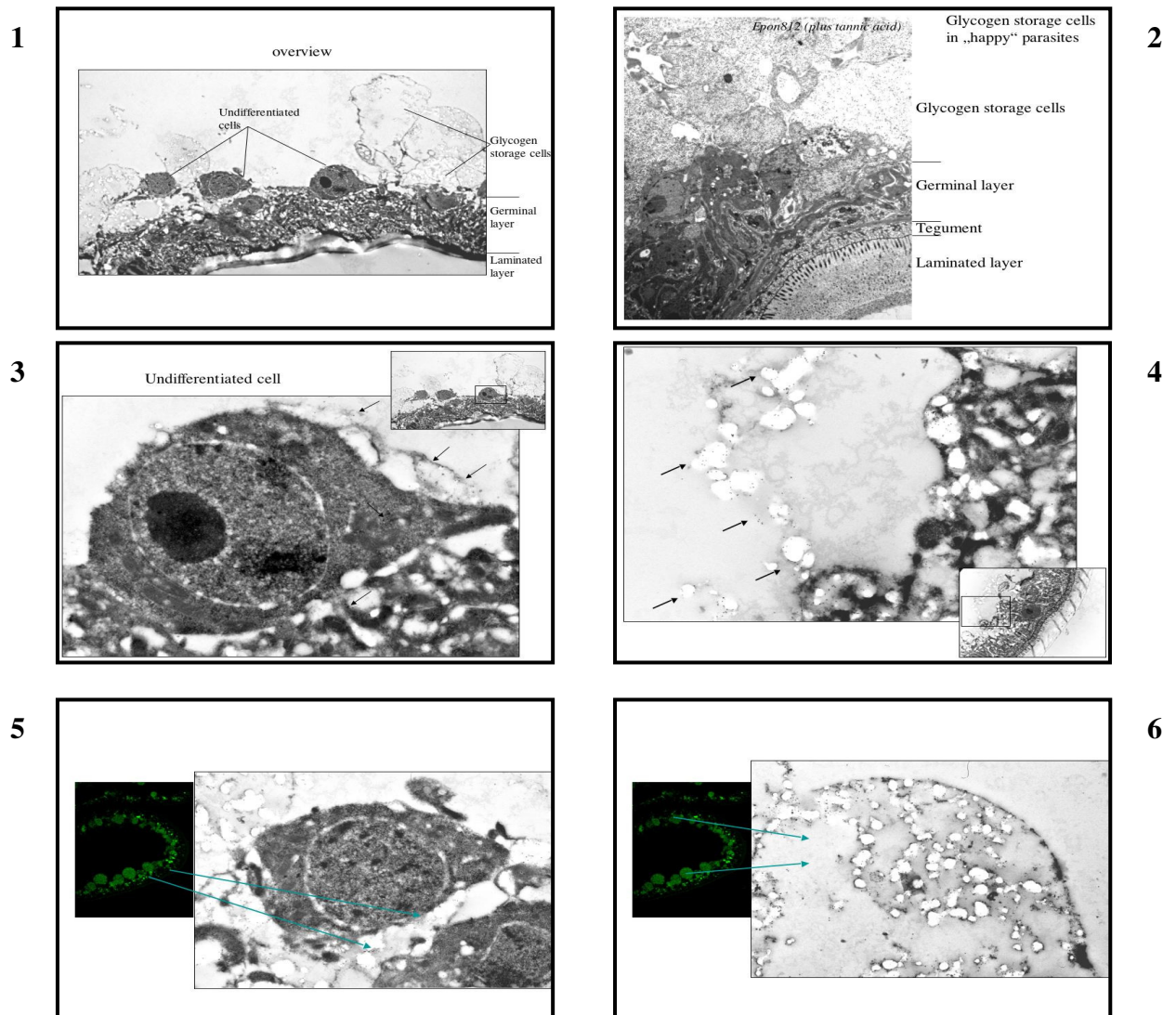


Fig. 34: Electronmicroscopical analysis of EmIR expression in metacystode vesicles. The cryosections were fixed and the expression of EmIR was analyzed with the anti-EmIRintra serum and gold-coupled anti-rabbit antibodies. **1)** Overview of the germinal layer and the outer laminated layer. The glycogen storage cells are empty due to the fixing method; **2)** Overview of the germinal layer and the outer laminated layer with filled glycogen storage cells; **3,6)** undifferentiated cell expressing EmIR (arrow); **4,6)** Glycogen storage cells which were empty due to the fixation. The expressed EmIR is indicated by the arrow.

The present study clearly demonstrated the stimulatory effect of exogenous insulin and IGF-I on the *E. multilocularis* metacystode vesicles. With a polyclonal anti-serum raised against EmIR's intracellular domain, it could be also shown that it is expressed in those *E. multilocularis* larval stages in which the stimulatory effects could be detected. An immunohistochemical analysis also revealed that EmIR is exposed in those tissues of *E. multilocularis* metacystode vesicle which have access to exogenous hormones. It should be examined in the following if EmIR represents an insulin and/or an IGF-I receptor of *E. multilocularis*.

3.3.6 Expression of EmIR in a heterologous system

The human embryonal kidney (HEK293) cell line was chosen for the heterologous expression of EmIR because the expression in the initially chosen *Drosophila* cell line (S2) had not been successful. While a transcript could be detected by RT-PCR analysis using *emir* specific oligonucleotides, a translation product has not been detectable by Western blotting (data not shown). As shown above, mature EmIR is composed of α - and β - subunit which are covalently linked via at least one disulfide bond. Since EmIR lacks a tetrabasic motif which constitutes the proteolytic processing site in human IR and IGF-IR proreceptor [5,133], the proteolytic processing of EmIR in Human Embryonal Kidney (HEK293) cells was analyzed. Unfortunately, the pSecTag2/Hygro expression system (Invitrogen) allows only the expression of proteins with a C-terminally fused Myc- and His - tag. In case of a correct proteolytic processing of EmIR, only the β - subunit and the unprocessed proreceptor but not the α -subunit would have been detected. Therefore, EmIR was expressed with an additional N-terminally fused Flag tag. Although this Flag tag is composed of highly charged residues which might affect the expression, it has the advantage of being very short compared to other tags, e.g. V5. For human Epidermal Growth Factor Receptor (EGFR) could be shown that an N-terminally fused Flag tag did not affect EGFR's capability to be activated by EGF [176]. In Western blot analysis of crude protein lysates of transiently transfected HEK 293, both the anti-Flag and anti-Myc antibody detected only one protein of approximately 210 kDa starting from 24h post-transfection which is absent in non-transfected cells. With 210 kDa, this protein exerts a higher molecular weight than the 192 kDa deduced for EmIR, indicating that the heterologously expressed EmIR is glycosylated. But even a prolonged post-transfectional incubation time did not lead to a proteolytic processing of this protein (Fig. 35), suggesting

that the lack of the tetrabasic processing motif did not lead to a correct processing of EmIR by the expressing cells.

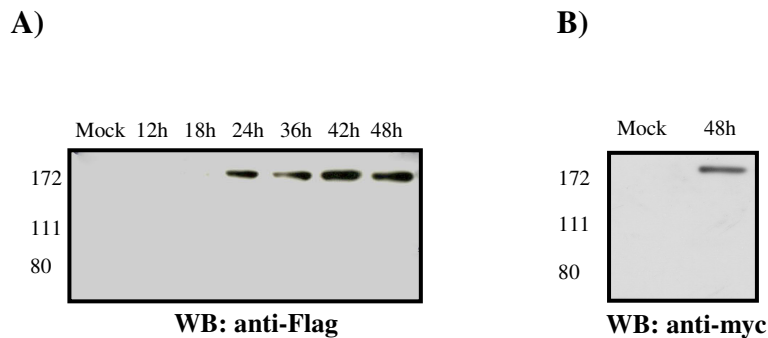


Fig. 35: Heterologous Expression of EmIR in human embryonal kidney (HEK293) cells. 1.3×10^6 cells were transiently transfected with $10\mu\text{g}$ of pSec – *emir* Flag and incubated for up to 48h. After this incubation period, the cells were lysed in 2xSDS sample buffer containing β -mercaptoethanol and boiled. The crude lysate was resolved via SDS-PAGE (8% PAA), followed by Western blot analysis with an anti-Flag (A) and anti-Myc (B) antibody.

For the determination of the ligand specificity determining region within the ligand binding domain of human IR and human IGF-IR, chimeric receptors have been used [177]. In addition, chimeric receptors composed of human IR's extracellular domain and DIR's intracellular domain have been used to study the latter's intracellular signaling capacities [57,67]. It is not only possible to create chimeras out of receptors of the same family but also out of receptors of different families. Riedel et al. [178] could demonstrate that the extracellular domain of human IR is still able to bind insulin and to trigger autophosphorylation when the transmembrane and cytoplasmic domains are replaced by the corresponding domains of EGFR. These results demonstrated that the signal transduction mechanisms between receptor tyrosine kinases are highly conserved. Therefore, a chimera was constructed to circumvent the incorrect processing of EmIR when expressed in a heterologous system (HEK293 cells). In the pSec – *emir*LCL – *hir* – chimera expression plasmid the coding region of the residues 33 – 729 representing the putative LCL and part of the Fn1 domain of EmIR was fused via PCR to the ORF encoding the residues 675 – 1382 of human IR. This *hir* fragment codes for the proteolytic processing site, the transmembrane domain and the cytoplasmic domain of human IR (Fig. 36). Hence, the chimeric insulin

proreceptor should be proteolytically processed to yield the mature chimeric receptor and its β -subunit should be indistinguishable from the β -subunit of human IR.

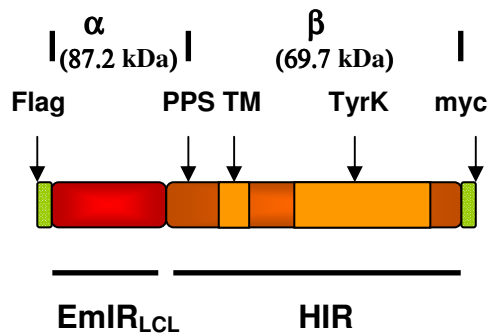


Fig. 36: Schematic view of the EmIR_{LCL} - HIR - chimera. The coding region of the residues 33 – 729 of EmIR were fused to the region coding for the residues 675 – 1382 of the human insulin receptor (HIR) by PCR. The chimeric protein possesses the EmIR putative ligand binding domain (LCL) and the tyrosine kinase domain (Tyrk) of human IR. The proteolytic processing site (PPS) and the transmembrane domain (TM) are also derived from human IR. For the improved detection of the α - and β - subunit, the expressed protein possesses an N-terminal Flag - tag (**Flag**) and a C-terminal Myc - tag (**myc**). The deduced molecular weights of the corresponding subunits are given in parenthesis.

This chimera was transiently expressed in HEK293 cells and its processing was analyzed by Western Blotting. Using an anti-Flag-HRP and anti-Myc antibody, the proteolytically unprocessed proreceptor could be detected (Fig. 37 A, B). With approximately 190 - 200 KDa, this proreceptor has a molecular weight larger than the 156.9 kDa deduced from the amino acid sequence. The same discrepancy in the molecular weight could be observed when *hir* was expressed as control in the HEK293 cells. The expressed human IR proreceptor was also larger than the deduced molecular weight (Fig. 37 B). Instead of the deduced 153.9 KDa this proreceptor also had a molecular weight of about 190 - 200 kDa. In the case of human IR the apparent discrepancy in the molecular weight is due posttranslational N - and O - linked glycosylation in both the α - and β - domain [132,133] and for EmIR several potential glycosylation sites could be identified *in silico* [181,182], suggesting that the higher molecular weight of the chimeric protein might also be due to glycosylation. Proteolytic cleavage and further glycolytic modification of the human IR proreceptor lead to the mature human IR consisting of 2 α - and 2 β - subunits, each α - and β - subunit having a molecular weight of approximately 135 and 85-95 kDa compared to the deduced molecular of approximately 84 and 70 kDa, respectively [132,133].

When *hir* was expressed in HEK293 cells, a 95 kDa protein was detected by the anti-Myc antibody in the Western blot analysis which represents the mature β -subunit (Fig. 37 B). Although the chimera is proteolytically processed, it does not occur as well as for the human IR

(Fig. 37 B). While approximately equal amounts of the EmIR_{LCL}- HIR – chimera and HIR proreceptor are synthesized within HEK293 cells, the amount of mature β - subunits differs. Additionally, slightly differently modified isoforms of the chimeric 95 kDa β -subunit were detected by Western blotting with the anti-Myc antibody (Fig. 37 B). Besides this finding, the proteolytic processing of the chimera could also be demonstrated by detection of the α – subunit (Fig. 37 A) in a Western blot with the anti-Flag antibody. It possessed a molecular weight of approximately 120 kDa compared to the deduced molecular weight of 92.2 kDa indicating that also this domain was glycosylated, but most likely not like the α -subunit of human IR which exerts a molecular weight of 135 kDa *in vivo* compared to the deduced 84 kDa. Besides the already described proteins, a further protein of approximately 160 kDa and 120 kDa was detected by the anti – Myc antibody when the chimeric receptor and the human IR, respectively, were transiently expressed in the HEK293 cells (Fig. 37 B). In case of the human IR, a 120 kDa isoform of the β -subunit has been described for recombinantly expressed receptors [183]. The deduced molecular weight of the non-processed chimeric proreceptor was 156.9 kDa. Since a protein of identical size was also detected by the anti – Flag antibody (Fig. 37 A), it is likely that this protein was the non-processed and non-glycosylated chimeric proreceptor. This finding might indicate that the chimeric receptor is synthesized in the HEK293 cells but less well post-translationally processed compared to human IR.

Nevertheless, a possible activation of the EmIR_{LCL} – HIR – chimera by human insulin and IGF-I was examined (Fig. 37 B). 48h post-transfection, HEK293 cells expressing either human IR or the EmIR_{LCL} – HIR – chimera were rendered quiescent for external stimuli by incubation for 5h under low serum conditions. After the stimulation with 100 nM human insulin or 100 nM human IGF-I for 10 min, the cells were lysed and the myc-tagged wildtyp and chimeric insulin receptors were immunoprecipitated via their C-terminal myc-tag. The immunoprecipitated proteins were analyzed for tyrosine phosphorylation by Western blotting with an anti-phospho-tyrosine antibody (Cell Signal, YP-100) (Fig. 37 B). The addition of insulin to the medium did not only induce the tyrosine phosphorylation of the β -subunit of human IR, demonstrating the suitability of this experimental setup, but also the β -subunit of EmIR_{LCL} – HIR – chimera (Fig. 37 B). The weaker activation compared to human IR might be due to the low rate of proteolytic processing and differences in the glycosylation. A negative effect of an altered glycosylation on the activity and processing of human IR has been described [133]. The weaker activation might also be explained by a lower affinity of EmIR's ligand binding domain towards insulin. This is the first demonstration that a ligand

binding domain of a parasitic RTK of the Ins/ IGF-I family can bind externally administered human insulin *in vitro*. The tyrosine phosphorylation of the proreceptor suggests a functional kinase domain in the chimeric receptor (Fig. 37 B), supporting the assumption that the increased tyrosine phosphorylation is due to autophosphorylation and not due to phosphorylation through the endogenous insulin receptor. It has been described for human IR that the proreceptor is already tyrosine phosphorylated independent of external stimuli (Fig.41 B) thereby revealing a functional kinase domain [66]. Interestingly, IGF-I did not activate the chimera supporting previous results that EmIR binds insulin and not IGF-I [79], although this is in contrast to the IGF-I induced effects in *E. multilocularis* metacystode vesicles presented in this study. This discrepancy might be explained by a low affinity of EmIR's ligand binding domain towards IGF-I which could not be detected with this experimental setup.

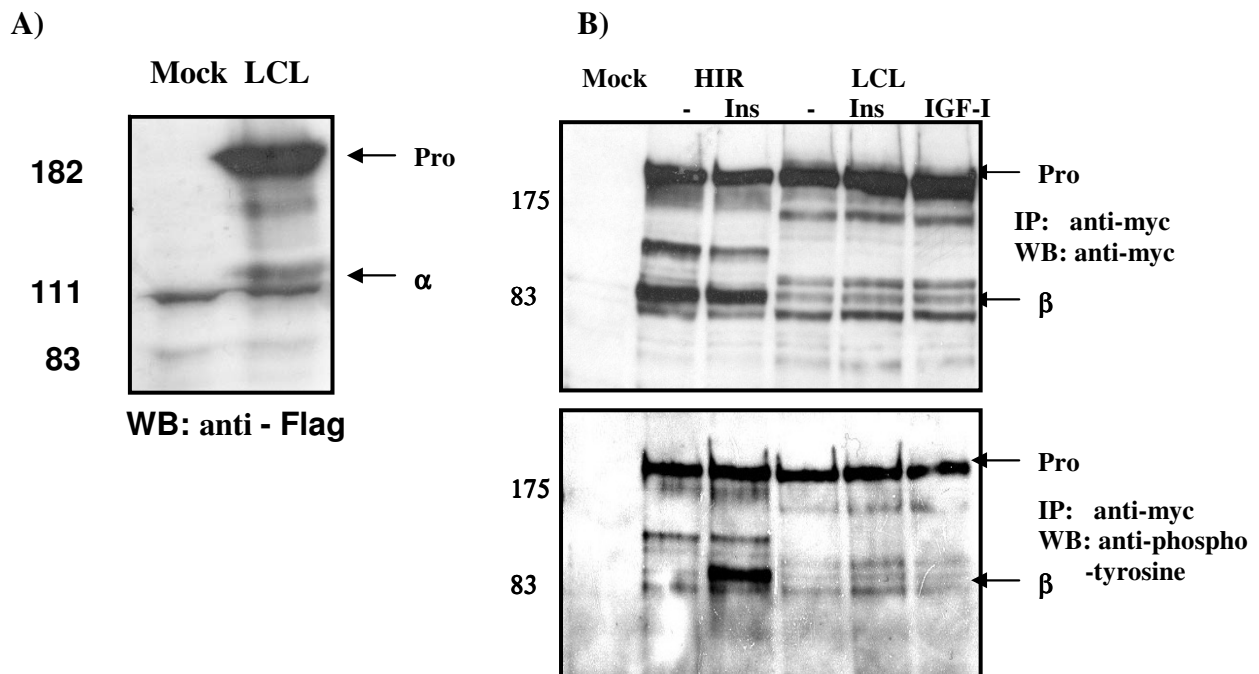


Fig. 37: Expression of EmIR_{LCL} - HIR - chimera in HEK293 cells and activation by human insulin. A chimeric receptor in which human IR ligand binding domain is replaced by that of the EmIR (EmIR: aa 33 – 729; HIR: aa 675 – 1382, LCL)) and full length human IR (HIR) are transiently expressed in HEK293 cells. 48h post-transfection, cells were incubated in medium 0.2% FCS for 5h and then stimulated with 100 nM human insulin or 100 nM human IGF-I for 10 min. **A)** Detection of the chimeric proreceptor (**Pro**) and α -subunit (α) in crude cell lysates by Western blotting using the anti-Flag antibody. **B) Upper panel:** Detection of the human IR and chimeric proreceptor as well as the β -subunits immunoprecipitated from crude cell lysate with anti-Myc antibody by Western blotting with anti-Myc antibody. **Lower panel:** Detection of tyrosine phosphorylation in immunoprecipitated proteins by Western blot analysis using an anti-phospho-tyrosine antibody.

3.3.7 *in vitro* autophosphorylation of Insulin stimulated EmIR

The RTKs of the Ins/IGF-I family are autophosphorylated on tyrosine residues within their β -subunit upon the stimulation with their cognate ligands. This phosphorylation is the initial event which leads to the transmission of external signals within the cells leading to the activation of specific intracellular signaling cascades [50,51]. The stimulation and autophosphorylation of RTK can also be examined *in vitro* with (partially) purified RTKs under selective conditions, i.e. inhibitors can be added to the reaction and tested for their specificity [169]. In a first experimental setup the activation of EmIR, partially purified from *E. multilocularis* metacystode vesicles, by insulin and IGF-I was analyzed *in vitro* (Fig. 38). The presence of EmIR in the membrane preparation of *in vitro* cultivated *E. multilocularis* metacystode vesicles was demonstrated by Western blotting with the anti-EmIR_{intra} immune serum (Fig. 38 A). The antiserum detected a protein in the membrane fraction corresponding in its size the β -subunit in the total protein lysate of *E. multilocularis* metacystode vesicles. Together with the previous finding that the β -subunit can only be solubilized in the presence of Triton-X 100 and sodium deoxycholate, this further supports that EmIR is a membrane-bound protein. The relatively low amount of EmIR β -subunit in the membrane preparation compared to total vesicle protein lysate might reflect the loss of protein during the preparation step. When the membrane fraction was stimulated with insulin and incubated in the presence of [³²P]- γ -ATP, a phosphorylated protein of the size of the EmIR β -subunit could be immunoprecipitated with the anti-EmIR_{intra} immune serum, indicating the activation of EmIR's tyrosine kinase domain by host insulin (Fig. 38 B). The other phosphorylated proteins which co-immunoprecipitated with the β -subunit are most likely components of the downstream signaling cascade binding the β -subunit, because proteins of these sizes were not detected by the immune serum in Western blot analysis of *E. multilocularis* metacystode vesicles' total protein lysate nor were among the proteins immunoprecipitated from this lysate (Fig. 26,38 A). It could be shown for human IR that downstream intracellular signaling molecules co-immunoprecipitate with the receptor [134-137]. The absence of phosphorylation after the stimulation with IGF-I is in accordance with the result presented in this work that a chimeric IR containing EmIR's ligand binding domain is only activated by insulin and not by IGF-I (Fig. 37). When an inhibitor of human IR tyrosine kinase, HNMPA-(AM)₃ [169], was added to the kinase buffer, the phosphorylation was completely abolished, indicating that this inhibitor also inhibits EmIR's tyrosine kinase. This inhibitor competes with the substrate tyrosine without competing with ATP to bind to the insulin receptor's kinase domain [169].

Although this inhibitor is highly selective for tyrosine kinases versus serine kinases, it is less selective within the tyrosine kinases. But it could be shown that HNMPA-(AM)₃ is an over two-fold stronger inhibitor of human IR tyrosine kinase compared to human EGFR tyrosine kinase [169].

A)

B)

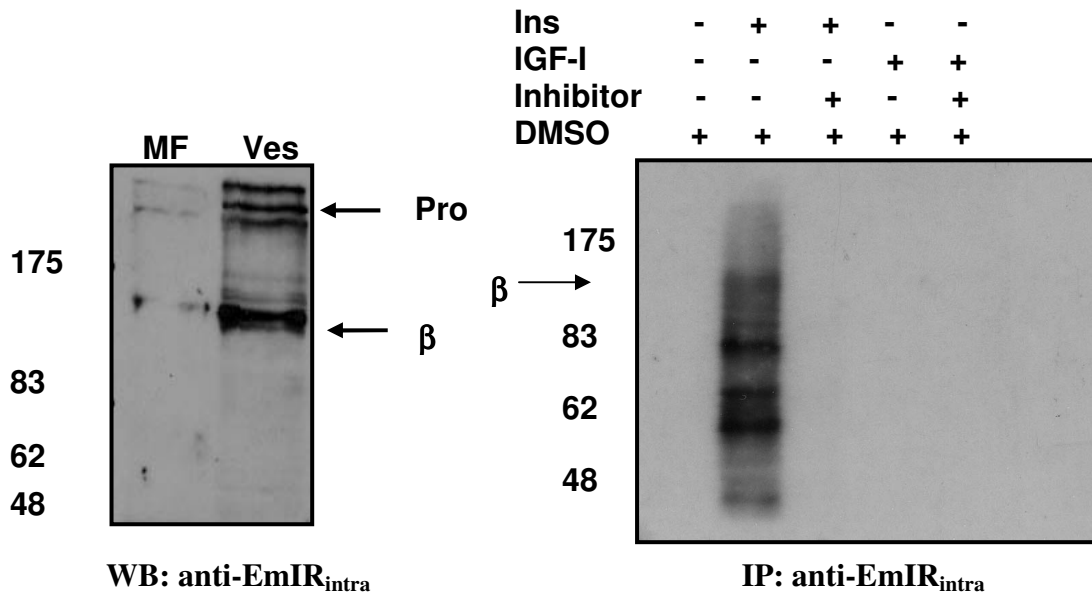


Fig. 38: *in vitro* phosphorylation of EmIR. A) The membrane fraction (MF) of *in vitro* cultivated metacestode vesicles was isolated. The presence of EmIR in this fraction was analyzed by Western blotting using the anti-EmIR_{intra} serum and compared to the presence in total vesicle lysate (Ves). B) The proteins in the membrane fraction were stimulated with 100 nM insulin (Ins) or IGF-I. The phosphorylation reaction was initiated by resuspending the membrane fraction in kinase buffer supplemented with [³²P]γ-ATP and allowed to proceed for 30 min in the presence or absence of 250 μM HNMPA-(AM)₃, an inhibitor shown to inhibit the autophosphorylation of human IR's β- subunit. The proteins in the membrane fraction were then solubilized and the EmIR β-subunit was immunoprecipitated with the anti-EmIR_{intra} serum. The immunoprecipitated proteins were resolved by SDS-PAGE (8% PAA) and the phosphorylation was detected by autoradiography. The X-ray film was exposed over night at -80°C using an intensifier screen. The phosphorylation reaction was repeated three times and one representative experiment is shown.

3.3.8 Activation of EmIR in *E. multilocularis* metacystode vesicles by insulin

It was further examined if the activation of EmIR can also be induced by stimulating intact *E. multilocularis* metacystode vesicles with insulin. Hence, intact vesicles were incubated under low serum conditions (0.2% FCS) and then stimulated for 10 min with 100 nM human insulin. After the solubilization, EmIR was immunoprecipitated with the anti-EmIR_{intra} serum. The analysis of the tyrosine phosphorylation with an anti-phospho-tyrosine specific antibody revealed that the stimulation with insulin induced the tyrosine phosphorylation of EmIR's β -subunit (Fig. 39), thereby verifying the results of the *in vitro* kinase assay that exogenous insulin directly stimulates EmIR's kinase domain.

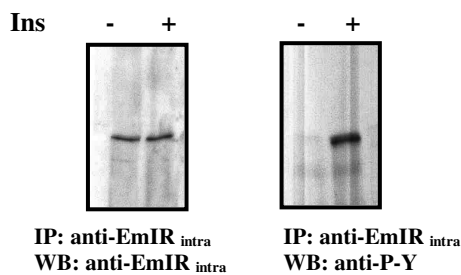


Fig. 39: The tyrosine phosphorylation of EmIR in intact metacystode vesicles is induced by human insulin *in vitro*.

Metacystode vesicles were incubated in medium with 0.2% FCS for 16h and then stimulated with 100 nM insulin for 10 min. Following the solubilization, the EmIR β -subunit was immunoprecipitated with the anti-EmIR_{intra} serum. The immunoprecipitates of non-stimulated (-) and stimulated (+) vesicles were normalized by Western blotting with the anti-EmIR_{intra} serum (left panel) and the tyrosine phosphorylation was assessed by Western blotting with an anti-phospho tyrosine antibody (P-Y 100; cell signal) (right panel).

3.3.9 An inhibitor of human IR tyrosine kinase affects *E. multilocularis* metacystode vesicles *in vitro*

The present study identified that exogenous insulin, and to some way also exogenous IGF-I, promote *E. multilocularis* metacystode vesicles in several ways. In addition, exogenous insulin activated EmIR *in vitro* which was reversed by the addition of an inhibitor of human IR tyrosine kinase. In the following, the effect of this inhibitor on intact *E. multilocularis* metacystode vesicles was analyzed by incubation in medium supplemented with 10% FCS and 250 μ M HNMPA-(AM)₃. On day 4 of incubation in medium 10% FCS supplemented

with 250 μM inhibitor or the dissolvent DMSO, the metacystode vesicles were inspected visually (Fig. 40). No abnormality could be observed in case of the control. The cultivation medium had also slightly changed its color indicating a decrease of the pH due to metabolic products, while in the presence of the inhibitor this color change could not be observed. In addition, the hydatid fluid of some of the vesicles incubated with the inhibitor became slightly turbid and the vesicles started to lose their round shape. On day 7, the experiment was terminated because all metacystode vesicles incubated with the inhibitor were killed (Fig. 40). The germinal layer was detached from the laminated layer and the medium still possessed the same color as at the start of the incubation, indicating that HNMPA-(AM)₃ inhibited a metabolic signaling pathway. No effect of DMSO was detected, showing that the observed effects were due to the inhibitor and not due to the solvent (Fig. 40). The human IR inhibitor exerted an identical effect on axenic cultivated *E. multilocularis* metacystode vesicles. While in the control, all vesicles remained intact, the vesicles incubated in the presence of 250 μM HNMPA-(AM)₃ were dead within 4 to 7 days (data not shown). This finding again supports the assumption that the inhibitor affects an important *E. multilocularis* signaling cascade.

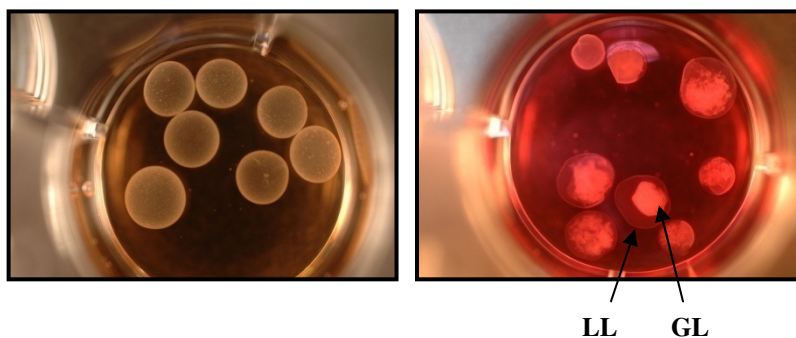
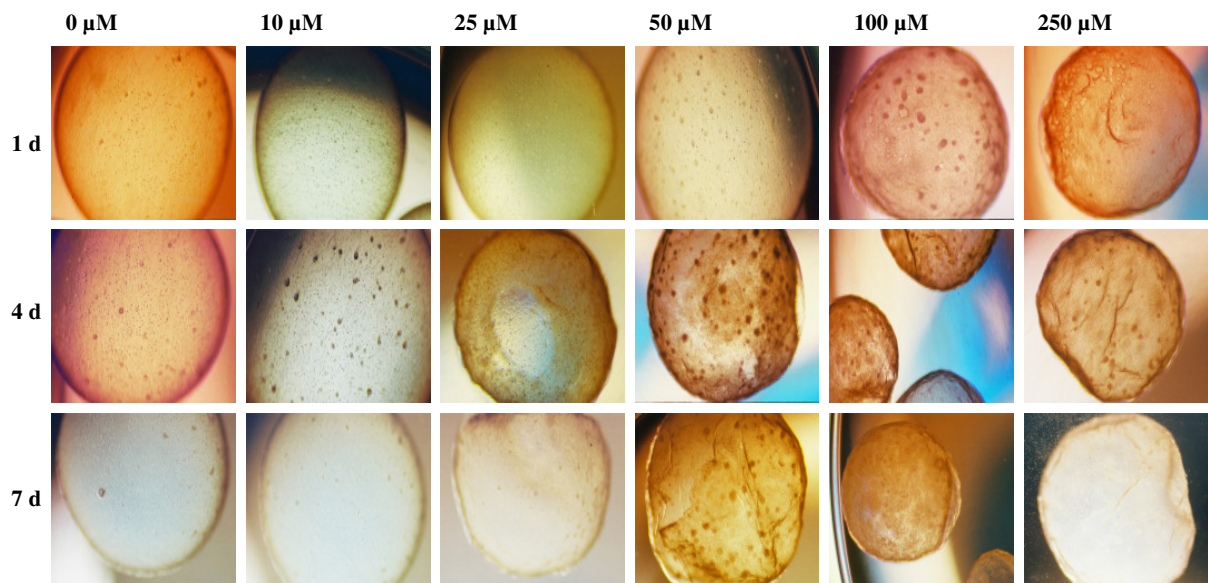


Fig. 40: HNMPA-(AM)₃ has a detrimental effect on *in vitro* cultivated metacystode vesicles. *E. multilocularis* metacystode vesicles were incubated in DMEM 10%FCS supplemented with 250 μM HNMPA-(AM)₃ (right picture) or DMSO alone (left picture). The vesicles were photographed on day 7 of incubation with a 5-fold magnification objective using an inverse light microscope. While the supplementation with DMSO had no effect on the metacystode vesicles, the inhibitor led to the detaching of the germinal layer (GL) from the laminated layer (LL). The medium of the control changed its color due to the decreased pH most likely caused by the metabolic products. However, the red color observed in the presence of the inhibitor indicated that the inhibitor also affected a metabolic pathway.

In the next step, the critical concentration of HNMPA-(AM)₃ for its effect on *E. multilocularis* metacystode vesicles was determined. Therefore, vesicles were incubated in medium supplemented with 10% FCS and an increasing concentration of the inhibitor (1 – 250 μM). Stettler et al. [10,171] recently described that the alkaline phosphatase activity in the supernatant of *in vitro* cultured *E. multilocularis* metacystode vesicles correlates indirectly with their viability. The results of the light microscopy analysis and the alkaline phosphatase assay are shown in Fig.41, revealing that the effect of the inhibitor depends on the one hand on the incubation time and on the other hand on the concentration. After 24h, a loss of cells from the germinal layer could be observed at a concentration as low as 100 μM (Fig. 41 A). This deleterious effect was also seen in the presence of 25 μM inhibitor, but after 4 days of incubation (Fig. 41 A). Three days later, no difference to the effects after 4 days could be seen, that means the presence of 1 – 10 μM inhibitor had no visible effect, while 25 μM were sufficient to exert a visible inhibitory effect (Fig. 41 A).

A)



B)

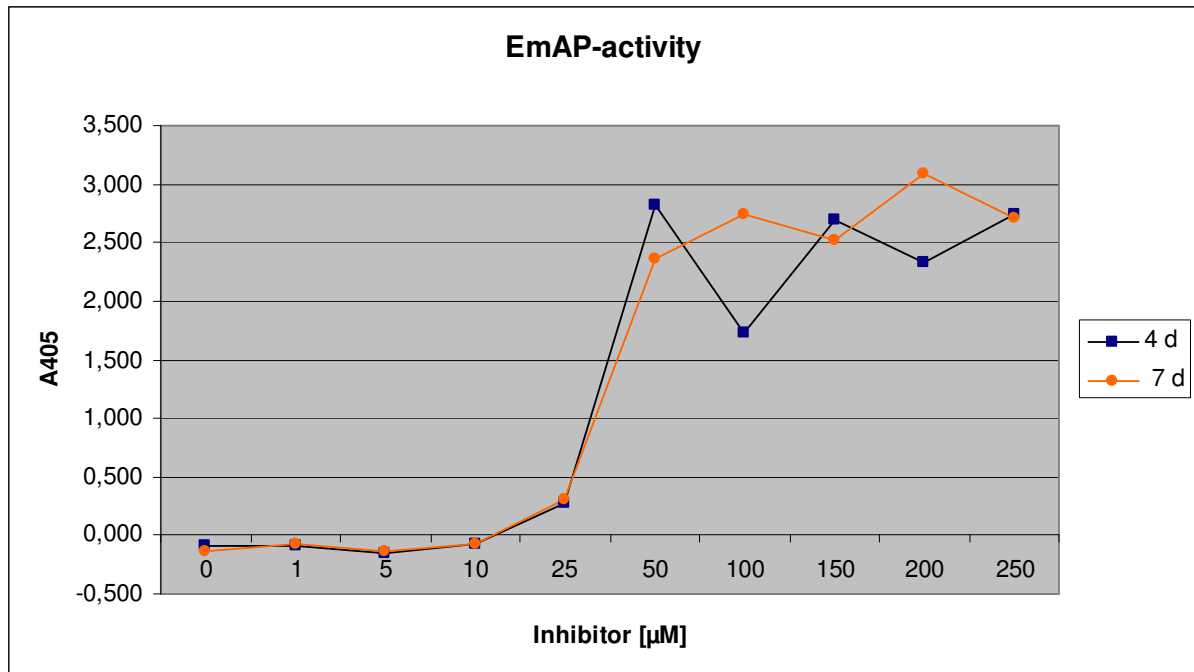


Fig. 41: The effect of HIR-inhibitor HNMPA-(AM)₃ on metacestodes depends on both the concentration and time. Cocultivated metacestodes of the isolate H95 were transferred into DMEM 10% FCS supplemented with increasing concentration of HNMPA-(AM)₃ and incubated at 37°C and 5% CO₂. **A)** At the indicated time points, the metacestodes were analyzed using an inverse light microscope and pictures were taken. **B)** After 4 and 7d, the alkaline phosphatase activity in the medium was determined, which is inversely proportional to the metacestodes' viability.

The measured alkaline phosphatase (AP) activity supported the observations in the light microscope (Fig. 41 B). An increased AP activity, although slightly, could be already observed in the supernatant of cultivated *E. multilocularis* metacestode vesicles in the presence of 25 μM inhibitor, while starting from 50 μM the activity was strongly induced. This is in accordance with the light microscopical observations. The finding that the inhibitor of human IR tyrosine kinase, HNMPA-(AM)₃, exerted such detrimental effect on the *E. multilocularis* metacestode vesicles leading to their death in a both concentration and time dependent manner supports the previous results that an insulin/IGF-I signaling cascade affects the growth and survival of the parasite *in vitro*. With EmMPK-1A, an *E. multilocularis* protein which is stimulated by host derived factors including insulin and IGF-I has been identified in the present work. As demonstrated above, *E. multilocularis* metacestode vesicles were viable for at least 24h in medium supplemented with 10% FCS and 25μM inhibitor. In addition, lower and higher concentrations were included in the experimental setup. After 1d

incubation in the presence of inhibitor (Fig. 42, lane 2-3), no difference in the phosphorylation state of EmMPK-1A compared to the control could be detected (Fig. 42, lane 1), whereas the phosphorylation decreased after 2d in the presence of 10 and 25 μM inhibitor (Fig. 42, lane 6 and 7) and was barely detectable when the medium was supplemented with 50 μM inhibitor (Fig. 42, lane 8).

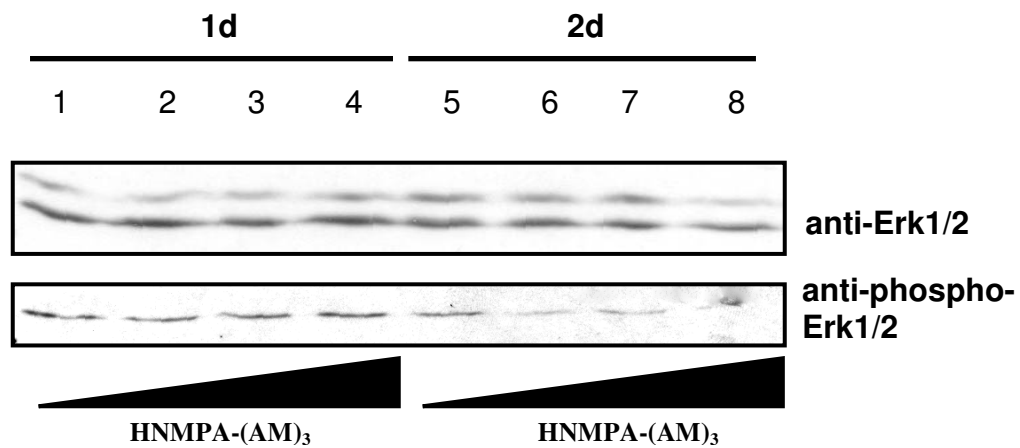


Fig. 42: Effect of HNMPA-(AM)₃ on the phosphorylation of EmMPK-1A in metacostode vesicles *in vitro*. Cocultivated *E. multilocularis* metacostode vesicles were transferred into medium (10% FCS) and supplemented with 0 (lane 1, 5), 10 (lane 2, 6), 25 (lane 3, 7) and 50 μM inhibitor of human IR (lane 4, 8) and incubated for 1d (lane 1-4) and 2d (lane 5-8). At the indicated time points, the metacostode vesicles were lysed by adding 2xSDS sample buffer containing β -mercaptoethanol. The proteins were resolved via SDS-PAGE (12% PAA) and subsequently transferred onto a nitrocellulose membrane. The samples were normalized for EmMPK-1A (upper panel) by probing with the anti-Erk1/2 antibody. The activation of EmMPK-1A was determined by probing with the anti-phospho-Erk1/2 antibody.

The finding that HNMPA-(AM)₃ caused a decrease in the phosphorylation of EmMPK-1A supports the finding that insulin stimulates its phosphorylation. Although it could be shown that the inhibitor inhibits human IR tyrosine kinase [169] and EmIR's tyrosine kinase *in vitro*, it can not be excluded that it also inhibits the tyrosine kinase of RTKs different from the Ins/IGF-I family. An inhibitory effect of the tyrosine kinase domain of human EGFR has been described, although with lower affinity than to the tyrosine kinase domain of human IR [169]. It has been demonstrated that EmMPK-1A is also stimulated by exogenous EGF and that *E. multilocularis* metacostode larval stages express an EGFR ortholog, EmER, which might transmit this stimulus [2]. Hence, it could be possible that the decrease in the phosphorylation of EmMPK-1A in the presence of HNMPA-(AM)₃ was not due to the inhibition of EmIR's but of EmER's tyrosine kinase domain.

The results of two independent experiments are shown in table 3. With 4.7 and 5.1 $\mu\text{IU} / \text{ml}$, the insulin concentration is clearly higher than the lower detection threshold (2 $\mu\text{IU} / \text{ml}$) of the employed Immulite[®]-systems. By multiplication with the conversion factor 6.945, the measured values were converted into SI units [158], i.e. the insulin concentration in the hydatid fluid was 32.95 and 35.42 pM, respectively. In addition, the insulin concentration in the hydatid fluid of *E. multilocularis* metacestode vesicles isolated from a freshly sacrificed gerbil was also determined. With 9.9 $\mu\text{IU}/\text{ml}$ (68.76 pM), the concentration was nearly twice as high as for the *in vitro* metacestode vesicles. Despite the identities between mammalian insulin, the difference in the measured insulin concentrations could be due to the preference of the antibodies used in the ELISA for murine insulin over bovine insulin. Therefore, the insulin concentration in the hydatid fluid of *E. multilocularis* metacestode vesicles cultivated *in vitro* under humanized conditions, i.e. in the presence of human serum and the human hepatocyte cell line HepG2. Besides the differences in the cell line and the serum, the metacestode vesicles were treated like those in the coculture with FCS and rat hepatocytes [2,6]. The hydatid fluid was isolated in two independent experiments and the insulin concentration was determined. The measured concentrations were 5.1 and 9.1 $\mu\text{IU}/\text{ml}$ (35.42 and 63.20 pM), respectively. The large difference between the two concentrations might be explained by the different human serum pools used to supplement the medium and could indicate that the feast state of the host, i.e. its serum insulin concentration, might affect the concentration of insulin in the hydatid fluid. Further, insulin could be measured in the hydatid fluid of *E. granulosus* cysts removed by surgery in Italy and Ulm, Germany. For the former 3.35 $\mu\text{IU}/\text{ml}$ (23.27 pM) and for the latter 6.15 $\mu\text{IU}/\text{ml}$ (42.71 pM) were determined (Tab. 3). This shows that insulin is present not only in the hydatid fluid of *E. multilocularis* metacestode vesicles but also of *E. granulosus* suggesting a promoting effect of insulin from the inside on the parasites not only during AE but also during cystic echinococcosis. Very interestingly, in none of those samples the IGF-I concentration was above the detection threshold of 25 ng/ μl which might indicate that it is not present in the hydatid fluid.

hydatid fluid	Ins [μ U/ ml]	Ins [pM] (μ U/ml*6,945)	IGF-I [ng/ μ l]
1)			
<i>E. granulosus</i> patient 1 (Italy)	3,35	23,27	< 25
<i>E. granulosus</i> patient 2 (Ulm)	6,15	42,71	< 25
2)			
<i>E. multilocularis</i> H95 (in vitro; FCS; RH-) 1	4,7	32,64	< 25
<i>E. multilocularis</i> H95 (in vitro; FCS; RH-) 2	5,1	35,42	< 25
3)			
<i>E. multilocularis</i> H95 (in vitro; HS; HepG2) 1	5,1	35,42	< 25
<i>E. multilocularis</i> H95 (in vitro; HS; HepG2) 2	9,1	63,20	< 25
4)			
<i>E. multilocularis</i> Töle (in vivo; gerbil)	9,9	68,76	< 25

Tab. 3: Insulin but not IGF-I can be detected in metacestodes' hydatid fluid *in vitro* and *in vivo*. For the measurement of insulin and IGF-I in the hydatid fluid of *in vivo* (1,4) and *in vitro* (2,3) grown metacestodes, the hydatid fluid was removed with a thin needle (0.4 gauge). The samples used were from **1)** patients with primary cystic echinococcosis from whom the cysts were removed by surgery, **2)** *E. multilocularis* metacestode vesicles incubated in medium supplemented with 10% FCS and rat hepatocytes (RH-), **3)** *E. multilocularis* metacestode vesicles incubated in medium supplemented with 10% human serum and human hepatocytes (HepG2), **4)** *Mongolian jirds* with a secondary alveolar echinococcosis.

Although the uptake of exogenous insulin into the hydatid fluid (by an yet unknown mechanism) seems to be the most likely explanation for the measurement of insulin in the hydatid fluid, it can not be completely ruled out that the detected insulin is of endogenous origin. But it appears to be very unlikely that the antibodies of the Immulite[®]-system cross reacted with invertebrate insulin-like peptides which share only low identity with mammalian insulin (Fig. 43). This assumption is supported that until today no insulin-like peptide has been identified for any platyhelminthes. In case of *S. japonicum* only an ORF coding for a putative insulin-like peptide with low identity to mammalian insulin has been described [108]. A direct demonstration for the uptake of exogenous insulin would be the detection of labeled insulin in the hydatid fluid after the addition to the cultivation medium of *E. multilocularis* metacestode vesicles. Hence, *in vitro* cultivated metacestode vesicles were incubated in

preconditioned medium (10% FCS) supplemented with 100 nM biotinylated insulin (insulin-biotin, Sigma) and incubated up to 48h. At various time points, both medium (Fig. 44) and hydatid fluid were isolated and analyzed by Western blotting for the presence of insulin-biotin using an anti-biotin antibody. While the amount of biotinylated insulin decreased with the time indicating an uptake by the *E. multilocularis* metacestode vesicles, the labeled insulin could not be detected in the corresponding hydatid fluid (data not shown). This could be due to the low sensitivity of the Western blot analysis and/or the low amount of biotinylated insulin taken up. As presented in this study, the positive effect of insulin on the survival of *E. multilocularis* metacestode vesicles *in vitro* is promoted by albumin. A potential promoting effect of albumin on the uptake of insulin needs to be further analyzed.

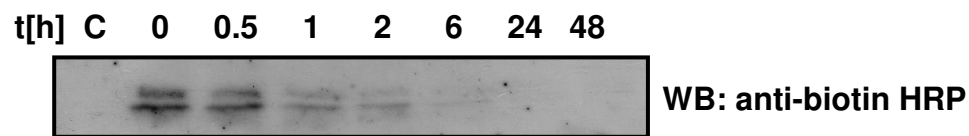


Fig. 44: Detection of insulin-biotin in the medium of metacestode vesicle culture. *E. multilocularis* metacestodes were incubated in preconditioned medium (cMEMA1) supplemented with 100 nM insulin-biotin. At the indicated time point, the supernatant was mixed with an equal volume of 2xSDS without β -mercaptoethanol and the proteins were resolved via SDS-PAGE (18% PAA, 7M urea). After blotting on nitrocellulose membrane, insulin-biotin was detected with an anti-biotin-HRP antibody and chemiluminescence. The antibody binds specific to insulin- biotin since no protein is detected in pure cMEMA1 (c).The double band are most likely due to different biotinylated insulin molecules. With 244 Da, biotin increases significantly the mass of insulin (5.6 kDa).

3.5 Protein *de novo* synthesis in *E. multilocularis* metacestode vesicles is upregulated by host derived factors different from insulin

One effect of insulin on *E. multilocularis* metacestode vesicles presented in this study was the induction of DNA *de novo* synthesis. In the following, the effect of insulin on the protein *de novo* synthesis was analyzed [143,195]. *E. multilocularis* metacestode vesicles were incubated over night under low serum conditions to bring the translation rate to a basal level. In the next step, these vesicles were transferred into cMEM, DMEM 10% FCS and 1% FCS containing 0, 10, 100 nM and 1 μ M human insulin, respectively, and incubated for 24h. Samples of medium containing the secreted proteins, the cellular fraction and the hydatid fluid were isolated and the incorporation of [³⁵S]-Met-label was determined in the scintillation counter. The highest *de novo* protein synthesis, higher than in the presence of 10% FCS alone, was detected for *E. multilocularis* metacestode vesicles cultivated in preconditioned medium in all taken samples, indicating again that secreted factors by the host cells are crucial for the development of the parasite *in vitro* (Fig. 45). The reduction of FCS in the cultivation medium from 10 to 1% led only to a slight decrease in the detected *de novo* synthesized proteins in the cellular fraction and the hydatid fluid, whereas the secretion into the medium dropped dramatically. This finding is a further support that host cells and their secreted proteins different from insulin exert a stimulatory effect on *E. multilocularis* metacestode vesicles. The basal level of protein synthesis under low serum conditions demonstrated that the metacestode vesicles were still viable under these conditions and that the reduced *de novo* protein synthesis was not due to their death.

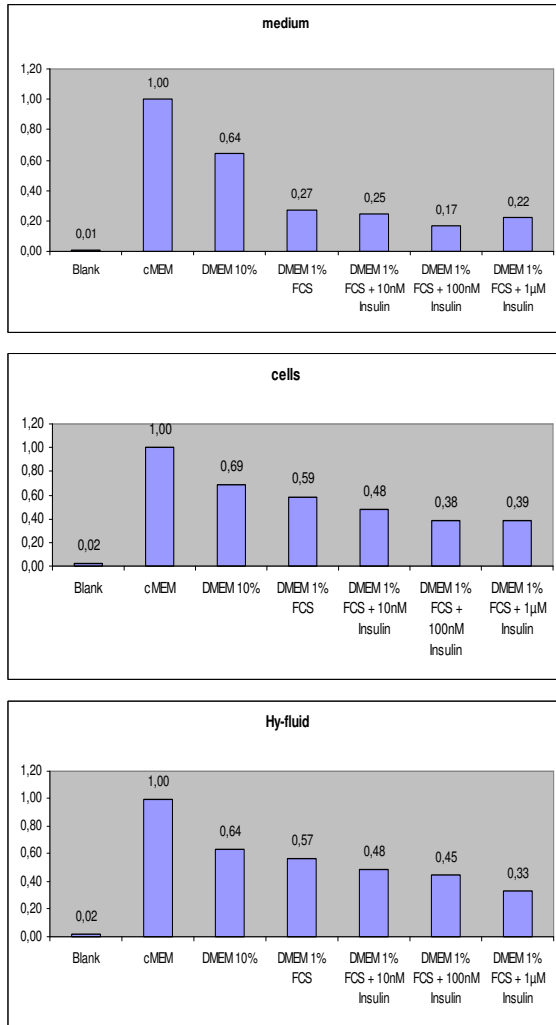


Fig. 45: Effect of various growth conditions on the protein *de novo* synthesis of *in vitro* cultivated *E. multilocularis* metacystode vesicles of the isolate H95. *E. multilocularis* metacystode vesicles which had been cocultivated in the presence of hepatocytes were kept over night under reduced serum conditions (DMEM 0.2% FCS) and were then transferred into medium supplemented with 10% FCS but preconditioned by hepatocytes (cMEM), medium with 10% FCS (DMEM 10%) and medium with 1% FCS and supplemented with 0 (DMEM 1%), 10 nM (DMEM 1% 10 nM), 100 nM (DMEM 1% 100 nM) or 1 µM human insulin (DMEM 1% 1 µM). After 48h incubation at 37°C, the incorporation of [³⁵S]-methionine and [³⁵S]-cysteine was measured in a scintillation counter for the secreted proteins into the medium (**medium**) and hydatid fluid (**Hy-fluid**), as well as for the synthesized proteins in the cellular fraction (**cells**). In case of the medium and the hydatid fluid, the proteins were TCA-precipitated to remove non-incorporated labeled amino acids. The absolute values are given in the ratio to values measured for cMEM for a better comparison.

3.6 Downstream signaling of EmIR in *E. multilocularis* larval stages

3.6.1 Expression of EmIR tyrosine kinase domain in a heterologous system

For the identification of signaling molecules acting downstream of EmIR its tyrosine kinase was expressed in a heterologous system. Since it has been demonstrated in the present work that EmIR is not correctly processed when expressed in a heterologous system, EmIR's tyrosine kinase domain was expressed in a chimeric protein (Fig. 46). This chimeric protein comprised the residues 28 – 979 from human IR and the residues 1133 – 1749 from EmIR, giving rise to a protein with a deduced molecular weight of 176.3 kDa. The deduced molecular weight of the α – and β – subunit is 84.2 and 92.1 kDa, respectively.

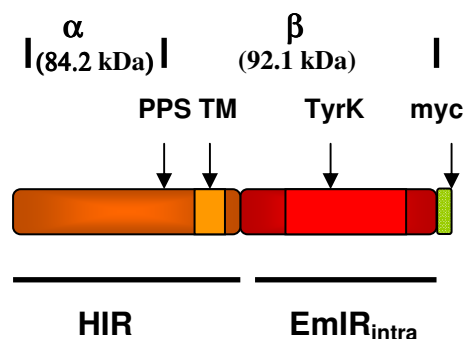


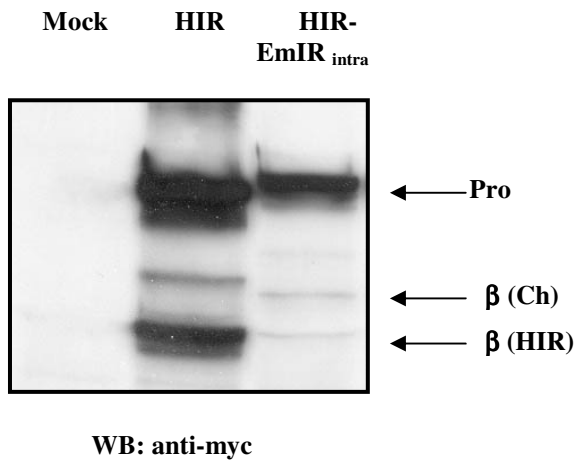
Fig. 46: Schematic view of the HIR - EmIR_{intra} – chimera. The coding region of the residues 28 – 979 of the human insulin receptor (**HIR**) were fused to the residues 1133 – 1749 of the *Echinococcus multilocularis* Insulin Receptor (**EmIR_{intra}**). The chimeric protein comprises the ligand binding domain, the proteolytic processing site (**PPS**), the transmembrane domain (**TM**) and residues of the juxtamembrane region of HIR which are C-terminally fused with the putative cytoplasmic domain of EmIR which contains the kinase domain. The expressed protein possesses a C-terminal myc – tag (**myc**) and the deduced molecular weights of the corresponding α – and β - subunit are given in parenthesis.

The transient expression of the HIR -EmIR_{intra} chimera in HEK293 cells was executed analogously to the expression of the EmIR_{LCL} – HIR – chimera. 48h post-transfection, the expression was analyzed by Western blotting of the crude cell lysate with the anti-Myc antibody (Fig. 47 A). In case of the HIR -EmIR_{intra} chimera the antibody detected a protein which is slightly larger but less strong expressed than the human IR proreceptor (Fig. 47 A)

representing the glycosylated chimeric proreceptor. While the two isoforms of the β - subunit of human IR could be clearly identified, the β - subunit of the chimera was barely detectable in the cell lysate (Fig. 47 A). The transient expression of the HIR – EmIR_{intra} chimera was repeated with the same and a different plasmid preparation to exclude the possibility of a failure during the handling. But in all experimental setups, a similar result was observed suggesting that this chimeric protein is less efficiently expressed and processed in HEK293 cells. Nevertheless, human IR and the HIR – EmIR_{intra} chimera were immunoprecipitated from the cell lysate with the anti – Myc antibody to examine the tyrosine phosphorylation of the corresponding β – subunits in response to the stimulation with human insulin (Fig. 47 B). 48 h post- transfection, the cells were incubated for 5 h in medium supplemented with 0.2% FCS, followed by the stimulation with 100 nM human insulin for 10 min. In case of the chimera, the proreceptor as well as two additional 115 and 160 kDa proteins could be immunoprecipitated from the cell lysate (Fig. 47 B). The 115 kDa protein was most likely the chimeric β -subunit whereas the 160 kDa protein represented most likely a smaller form of the proreceptor. For a better detection, the x-ray film had to be exposed for 30 min, explaining the strong signal for the immunoprecipitated human IR. An identical Western blot was done in parallel and probed with an anti – phospho tyrosine antibody (Fig. 47 B). The addition of insulin to the medium activated human IR, while in case of the HIR – EmIR_{intra} chimera no tyrosine phosphorylation could be detected (Fig. 47 B). In contrast to human IR and the EmIR_{LCL}-HIR-chimera, even the proreceptor was not tyrosine phosphorylated indicating that the HIR-EmIR_{intra} chimera is kinase inactive in HEK293 cells [66].

The present finding raised the question why EmIR's tyrosine kinase domain is non-functional when expressed in a heterologous, albeit Konrad et al. showed that this domain shared over 60% identity with the tyrosine kinase domain of human IR [5]. The most striking difference between EmIR and the other known RTKs of the Ins/IGF-I family is the presence of an additional 172 residue peptide within the tyrosine kinase domain which does not possess any homology [5]. It might be possible that an additional *Echinococcus* factor needs to be bound to this additional peptide for EmIR's tyrosine kinase domain to be active and that the lack of this factor inactivates EmIR's tyrosine kinase domain. I planned to express a HIR-EmIR_{intra} chimeric receptor lacking the additional peptide, but this experimental setup has not been finished during the present work.

A)



B)

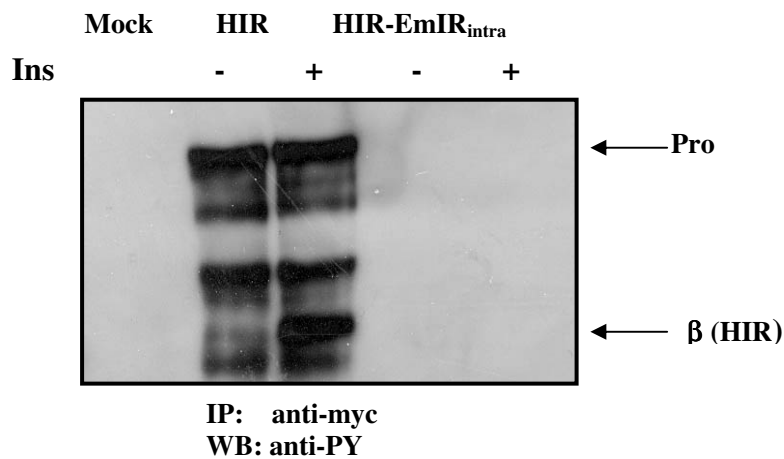
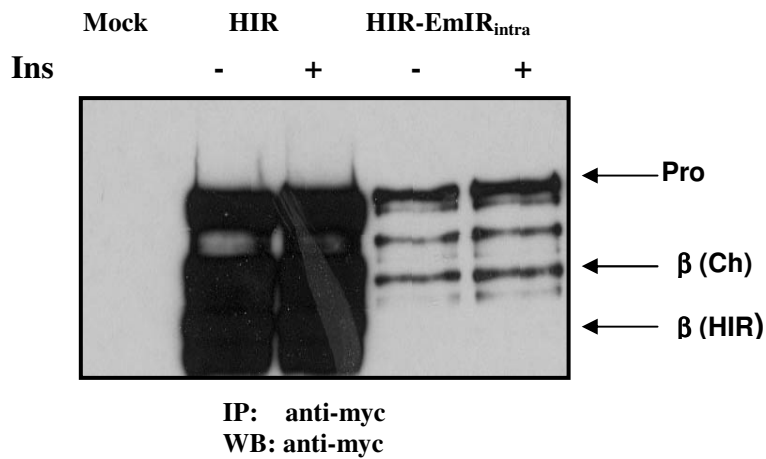


Fig. 47: Expression of HIR-EmIR_{intra} in HEK293 cells. The cytoplasmic domain of EmIR (aa 1133-1749) was transiently expressed with the N-terminally fused extracellular and transmembrane domain of HIR (aa 28 – 979) in HEK293 cells. As a control, HIR was also transiently expressed. **A)** 48h post-transfection, the expression of the chimeric protein and HIR was analyzed by Western blotting using the anti-Myc antibody. **B)** HEK293 cells transiently expressing HIR or the HIR-EmIR_{intra} chimera were incubated under low serum conditions (0.2) and were then stimulated with 100 nM human insulin for 10 min. The cells were solubilized and the recombinantly expressed proteins were immunoprecipitated with the anti-Myc antibody. The immunoprecipitated proteins were subjected to Western blot analysis using the anti-myc antibody (upper panel) and an anti-phospho-tyrosine antibody (lower panel).

3.6.2 Identification of IR orthologs in other cestodes

As described in the above section, a HIR-EmIR_{intra} chimeric receptor is not active when expressed in a heterologous system and that the inactivity might be due to the presence of an additional 172 residue peptide in the tyrosine kinase domain of EmIR. Besides the insert within its tyrosine kinase domain, Konrad et al. could show that EmIR differs from the other known RTKs of the Ins/IGF-I family by possessing an additional insert of unknown function in a region of its cysteine rich domain which is homologous to that region in human IR and human IGF-IR determining their ligand specificity [5,79,177]. For both human IR and human IGF-IR this specificity determining region has been narrowed to the ligand binding domain 1 and cysteine rich domain [97,98]. The comparison of the crystal structure of IR and IGF-IR revealed that the 4 additional residues within the cysteine rich domain of IR protrude into the insulin binding pocket and it is assumed that these residues inhibit the binding of IGF-I for sterical reasons (Fig. 66). As for the insert in EmIR's kinase domain, the function of the insert in EmIR's ligand binding domain is not known and a possible involvement in determining the ligand specificity needs to be demonstrated.

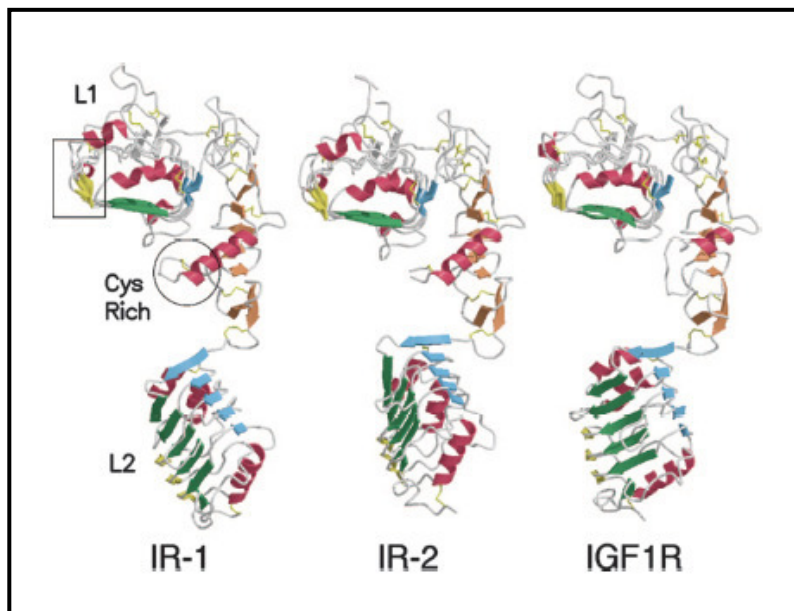


Fig. 66 (from [97]): Comparison of the structures of the L1-Cys Rich-L2 domain fragments of human IR and human IGF-IR. Helices are indicated by curled red ribbons and β -strands are indicated by broad arrows. The side chains of disulfide-linked cysteine residues are depicted as yellow sticks. Two notable regions of difference between IR and IGF-1R in the L1 (box) and the loop of the cysteine rich (Cys Rich; circle) domain are indicated. The Cys Rich domain of EmIR contains additional 26 residues in the domain which is homologous to the loop forming domain of IR.

The analysis of IR from closely related species which might differ in these unique features could help to reveal their function. So far, only EmIR has been identified as an IR ortholog in a cestode. For the analysis if these unique features of EmIR are conserved among cestodes, the IR of *E. granulosus*, *T. solium* and *T. crassiceps* were identified and partially characterized. The focus of this analysis was laid on the ligand and tyrosine kinase domain which are most important for a functional RTK.

3.6.2.1 Characterization of cDNAs from distinct cestodes encoding ligand binding and tyrosine kinase domain of IR orthologs

In a first step, total RNA of *E. granulosus* was isolated from frozen parasitic material with the RNeasy Kit (QIAGEN), DNase I treated and reversely transcribed employing the Omniscript Kit (QIAGEN) and the a poly-d(T)- oligonucleotide (CD3RT). This cDNA pool was prepared and kindly provided by Cécilia Fernandez. The same procedure was carried out to synthesize a *T. crassiceps* cDNA pool, except that total RNA was isolated from *in vitro* cultivated metacestodes using the procedure described for *E. multilocularis* metacestode vesicles. In case of *T. solium*, a phage cDNA-library served as template in the PCR. This library was kindly provided by Prof. Brehm. In an initial attempt to isolate cDNAs with ORFs coding for IR orthologs, these cDNAs served as templates in a PCR with oligonucleotides specific for 3' and 5' UTR of *emir*, respectively, under low stringency conditions. But even with nested oligonucleotides, no cDNA fragment could be amplified. Therefore, oligonucleotides directed against the coding region of *emir* were used in the PCR to amplify cDNA fragments. The oligonucleotide pairs CK35 and CK36 as well as CK37 and CK38 had been used to amplify the cDNA fragment coding for EmIR's extracellular and intracellular domain, respectively, and the subsequent ligation into pGEX-3X. Since no cDNA fragment was amplified under low stringency conditions, nested PCRs were carried out with oligonucleotides directed against the coding region of the LCL and TyrK domain which share the highest homology among all members of the Ins/IGF-IR family. For the amplification of the LCL domain (C³² - Y⁷⁴⁴ in EmIR) encoding cDNA fragment, two oligonucleotide pairs were used: i) EmIGFRdw and EmIGFRup spanning nt 141 – 1265 on *emir* cDNA (amplicon 1125 bp); ii) CK49 and CK50 spanning nt 1047– 2279 on *emir* cDNA (amplicon 1233 bp). With EmIGFRdw and EmIGFRup as nested oligonucleotides, an 1125 bp fragment could be amplified for both *E.*

granulosus and *T. solium*. When CK49 and CK50 were used as nested oligonucleotides, another fragment of 1233 bp could be amplified for both *E. granulosus* and *T. solium*. After cloning into pCR2.1 TOPO TA vector, the amplified fragments were sequenced using vector and gene specific oligonucleotides. For both, *E. granulosus* and *T. solium*, the 3' end of the fragment amplified with EmIGFRdw and EmIGFRup overlapped with the 5' end of the amplicon obtained with CK49 and CK50. The cDNA sequences were fused *in silico*. For both *E. granulosus* and *T. solium*, the corresponding 2139 bp fragment (*egLCL* and *tsLCL*, respectively) contained an ORF coding for 713 residues (Fig. 48A, B). A BlastP analysis [184] revealed 93% and 94% identity to EmIR for EgLCL and TsLCL, respectively. The ORF coding for the ligand binding domain of *T. crassiceps* could not be isolated with this experimental setup and was therefore not further pursued.

A nested PCR with the oligonucleotides CK93 and CK96 spanning the 1335 bp fragment (nt 3549 – 4883) of *emir ORF* coding for the 445 residues of the kinase domain led to the amplification of a cDNA fragment for all three species. These amplicons were also cloned into the pCR2.1 TOPO TA vector and sequenced. The ORF of the *E. granulosus* fragment (1350 bp; *egTyrk*) encoded 450 residues (Fig. 48 C) sharing 87% with EmIR. In case of *T. crassiceps*, the 1335 bp cDNA fragment (*tcTyrk*) contained an ORF coding for 445 residues (Fig.50 E) being 86% identical to EmIR. The amplicon of *T. solium* (*tsTyrk*) comprised only 819 bp and the ORF therein encoded for only 273 residues (Fig. 48 D). The BlastP analysis determined 79% identity to EmIR for the residues 1 – 110, which increased up to 98% for the residues 84 – 273.

A) *egLCL*

		EmIGFRdw															
		→															
1		TGT	CGG	GTC	TTC	GGT	GGA	AAT	CAT	ACA	TAT	CTG	CAG	CAG	AAC	GAA	45
1		C	R	V	F	G	G	N	H	T	Y	L	Q	Q	N	E	15
46		ATG	CTG	TGT	GGG	GAC	TTT	GAC	GTT	CGG	CGA	CCT	TCC	GCT	TTG	TCA	90
16		M	L	C	G	D	F	D	V	R	R	P	S	A	L	S	30
91		CGC	ATC	AAA	TCA	TGC	ACT	GTT	ATC	GAA	GGA	AAC	CTT	CTA	ATC	GTG	135
31		R	I	K	S	C	T	V	I	E	G	N	L	L	I	V	45
136		ATG	ACG	AGG	CTC	CCC	GTA	AAT	GCC	TCG	ATA	CCA	AAT	CTC	CGG	GAA	180
46		M	T	R	L	P	V	N	A	S	I	P	N	L	R	E	60

181	ATA	ACG	GGA	TTT	CTA	GTA	ATC	TAT	GAC	CTT	ATG	GGT	TTG	GAT	GGG	225
61	I	T	G	F	L	V	I	Y	D	L	M	G	L	D	G	75
226	CTG	GCC	ACT	CTT	TTT	CCT	AAC	CTA	ACT	GTC	ATC	CGT	GGA	CGC	TCA	270
76	L	A	T	L	F	P	N	L	T	V	I	R	G	R	S	90
271	TTG	ATT	TCT	AAT	TTT	GCT	CTT	GTC	ATT	CGC	AGT	ACC	TCT	CTG	AAG	315
91	L	I	S	N	F	A	L	V	I	R	S	T	S	L	K	105
316	ACA	ATC	GGT	CTA	CCC	TCG	CTC	CGC	GTG	ATT	CAG	CGT	GGT	GGA	GTG	360
106	T	I	G	L	P	S	L	R	V	I	Q	R	G	G	V	120
361	CGT	GTT	GAC	TTG	AAC	ACA	AAC	CTG	TGC	TAC	GTG	CGG	ACT	GTG	AAT	405
121	R	V	D	L	N	T	N	L	C	Y	V	R	T	V	N	135
406	TGG	TCC	TAC	ATT	CTG	GGC	GAT	CGG	ACA	GCG	GCG	GCT	GCC	CCA	GTT	450
136	W	S	Y	I	L	G	D	R	T	A	A	A	A	P	V	150
451	CGC	TTG	TTG	ACA	AAT	CGT	CTC	ATC	TGC	CCA	GAC	ACC	TGT	CAA	CCC	495
151	R	L	L	T	N	R	L	I	C	P	D	T	C	Q	P	165
496	GAG	TGT	GCG	GCC	TCC	ACG	CCG	GAG	GCA	ATA	AGT	TCA	ACT	GAA	CTG	540
166	E	C	A	A	S	T	P	E	A	I	S	S	T	E	L	180
541	GAA	GGC	ACT	TCT	CGT	GAA	AAG	GAT	GCC	AAA	CTG	GGC	CAC	TGC	TGG	585
181	E	G	T	S	R	E	K	D	A	K	L	G	H	C	W	195
586	TCG	TTG	TCT	TAC	TGT	CAA	TCC	ATC	TGC	TCT	GCA	AAC	TGC	ACA	AGT	630
196	S	L	S	Y	C	Q	S	I	C	S	A	N	C	T	S	210
631	CGT	GGC	ATC	GCA	TGC	CGA	ATG	GAC	AAT	ACC	CAA	CTT	TGT	TGC	CAT	675
211	R	G	I	A	C	R	M	D	N	T	Q	L	C	C	H	225
676	AAA	GAG	TGC	CTT	GCC	GGC	TGT	TAC	GGC	CCT	GGT	CCA	GAG	GCA	TGT	720
226	K	E	C	L	A	G	C	Y	G	P	G	P	E	A	C	240
721	GTG	GCT	TGT	AAG	GGG	GCT	CTG	CAC	CGT	GGA	GTT	TGC	GTT	TCC	CAA	765
241	V	A	C	K	G	A	L	H	R	G	V	C	V	S	Q	255
766	TGC	CCT	CCA	TCC	ACC	TAT	CTC	TTC	CAT	GGA	CGT	CGG	TGC	GTG	ACC	810
256	C	P	P	S	T	Y	L	F	H	G	R	R	C	V	T	270
811	GCG	GCA	GAG	TGC	TTC	AAT	ATG	AGC	AGT	ACC	TAC	CGT	CTT	CCT	CAT	855
271	A	A	E	C	F	N	M	S	S	T	Y	R	L	P	H	285

856 GTC GCA GGC AGC AGC GGA AGC AGC TCT ATC GGT TTT GCC GCC TCA 900
 286 V A G S S G S S S I G F A A S 300

CK49

901 GTG ATA GTC AAC ACC ACG GCA GCT → GTA GCC ACC ACC GCT ATT CGC 945
 301 V I V N T T A A V A T T A I R 315

946 CAG TTC GCT ATC CAT CAG GGT CGC TGC GTT CCC GAC TGC CCC TCA 990
 316 Q F A I H Q G R C V P D C P S 330

991 GGT CAT CAG CGC GAC GAA GTC AGT GGG CAG TGT GTG CCA TGT GGC 1035
 331 G H Q R D E V S G Q C V P C G 345

1036 GAC GAG TGT CCG AGG ATT CGA TGC CAT CAT ATG CTA ATA AGC AGC 1080
 346 D E C P R I R C H H M L I S S 360

EmIGFRup

1081 CTT AAG TCA CTG TCC AAA CTG AAG GAC TGC TTC TCT GTC ACC GAT 1125
 361 L K S L S K L K D C F S V T D 375

1126 CTC TAC ATC TCC ATT CAT GAG GGC GAC ACG GTT CTG ATA CAG CAG 1170
 376 L Y I S I H E G D T V L I Q Q 390

1171 CAA TTC GAT GAG GCT TTT TCG AGT CTG CGG GGG GTT GAG AGC ATC 1215
 391 Q F D E A F S S L R G V E S I 405

1216 AAG GTT GTT CGG GCA ACA GCT CTC ACT TCC CTT GCC TTC CTC CGC 1260
 406 K V V R A T A L T S L A F L R 420

1261 CAC GTC AAA CGC ATA AAC ACC ATT CCT AAT TCC TCG CCC AAC GTG 1305
 421 H V K R I N T I P N S S P N V 435

1306 ACA GTG ATA GAG ATA AGA GGC AAC GAT AAC CTG CTG GAA TTG TGG 1350
 436 T V I E I R G N D N L L E L W 450

1351 CCT CCG CCA ACG AGG AAC CAG ACA GGC GGA CTT CAG GTG GTG TCA 1395
 451 P P P T R N Q T G G L Q V V S 465

1396 GAA GGG CTT GTA CAT TTC ATC CTC AAT CGC TAC CTT TGC CCC AAG 1440
 466 E G L V H F I L N R Y L C P K 480

1441 AAG ATC ACG GAC TTG GTG AGG ACA GGC GCT CTG ACG CTG CCC GGT 1485
 481 K I T D L V R T G A L T L P G 495

1486 GGG CGC AAC TTT CGT ATA GAG GAG CTT GAA CTC GCT GAG GCT ACC 1530

496 G R N F R I E E L E L A E A T 510

1531 AAT GGC AAA CTC GGC TTC TGT GAG ACT ACA CAA ATC TCG CTT GAA 1575
511 N G K L G F C E T T Q I S L E 525

1576 TTG AAG GAT GTC TTT TCC TCA ACT GCT GCC ATC CAA TGG CCA CGT 1620
526 L K D V F S S T A A I Q W P R 540

1621 TCC TTT GAC AAC CGC ACA ACT GGC CAA GCA GCT TCC ACT CTG GTG 1665
541 S F D N R T T G Q A A S T L V 555

1666 TTG GTC TTC TTT CAG GCT ACA ACA AAA AAT TTG ACA GTC TAC ACG 1710
556 L V F F Q A T T K N L T V Y T 570

1711 AAT CGA CTC TCC TGC GGC GAT GAT TCA TGG AGG ATG ATT CCT TCG 1755
571 N R L S C G D D S W R M I P S 585

1756 ATC TGC AAC ACC TCT ACG ATA CGT GAA GAG AAA GGA GAG AAT GTT 1800
586 I C N T S T I R E E K G E N V 600

1801 GCC TTT TGC AGC AAA ATA CTC ACT GGC CTC CAA CCA GCT ACT CGC 1845
601 A F C S K I L T G L Q P A T R 615

1846 TAT GCC GTC TAT GTT GAG TCT AAA ACG CTT TTT AGT CAG CGT GGG 1890
616 Y A V Y V E S K T L F S Q R G 630

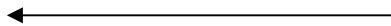
1891 GCG ATT AGC AAC ATC GTC TAC TTC ACC ACA AAT CCT AGT AAA CCG 1935
631 A I S N I V Y F T T N P S K P 645

1936 TCG CAT CCG CGT ATG GAG AGG TTG CAG GCG TTA AAT GAT TCA AGG 1980
646 S H P R M E R L Q A L N D S R 660

1981 ATT TCT GTT AGG TGG TCA CCG CCT CAA TAC AAC AAT GGC CTC TTG 2025
661 I S V R W S P P Q Y N N G L L 675

2026 GCC GTG TAC CTT CTC TGG TTC CGT TCT ATT CAC ATC GAT CCG GAG 2070
676 A V Y L L W F R S I H I D P E 690

2071 CCC TAT CTT TAC CGA GAC TTC TGT TTT TTG GCA CCT GAT TGG CTT 2115
691 P Y L Y R D F C F L A P D W L 705

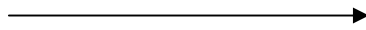
CK50

2116 TCT TCC GCG ATC ACG CCC TCT TAC 2139
706 S S A I T P S Y

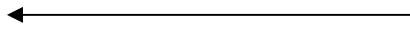
B) *tsLCL***EmIGFRdw**

	→															
1	TGT	CGG	GTC	TTC	GGT	GGA	AAT	CAT	ACA	TAT	CTG	CAG	CAG	AAC	GAA	45
1	C	R	V	F	G	G	N	H	T	Y	L	Q	Q	N	E	15
46	ATG	CTG	TGT	GGG	GAC	TTT	GAC	GTT	CGG	CGA	CCT	TCC	GCT	TTG	TCA	90
16	M	L	C	G	D	F	D	V	R	R	P	S	A	L	S	30
91	CGC	ATC	AAA	TCA	TGC	ACT	GTT	ATC	GAA	GGA	AAC	CTT	CTA	ATC	GTG	135
31	R	I	K	S	C	T	V	I	E	G	N	L	L	I	V	45
136	ATG	ACG	AGG	CTC	CCC	GTA	AAT	GCC	TCG	ATA	CCA	AAT	CTC	CGG	GAA	180
46	M	T	R	L	P	V	N	A	S	I	P	N	L	R	E	60
181	ATA	ACG	GGA	TTT	CTA	GTA	ATC	TAT	GAC	CTT	ATG	GGT	TTG	GAT	GGG	225
61	I	T	G	F	L	V	I	Y	D	L	M	G	L	D	G	75
226	CTG	GCC	ACT	CTT	TTT	CCT	AAC	CTA	ACT	GTC	ATC	CGT	GGA	CGA	TCA	270
76	L	A	T	L	F	P	N	L	T	V	I	R	G	R	S	90
271	TTG	ATT	TCT	AAT	TTT	GCT	CTT	GTC	ATT	CGC	AGT	ACC	TCT	CTG	AAG	315
91	L	I	S	N	F	A	L	V	I	R	S	T	S	L	K	105
316	ACA	ATC	GGT	CTA	CCC	TCG	CTC	CGC	GTG	ATT	CAG	CGT	GGT	GGA	GTG	360
106	T	I	G	L	P	S	L	R	V	I	Q	R	G	G	V	120
361	CGT	GTT	GAC	TTG	AAC	ACA	AAC	CTG	TGC	TAC	GTG	CGG	ACT	GTG	AAT	405
121	R	V	D	L	N	T	N	L	C	Y	V	R	T	V	N	135
406	TGG	TCC	TAC	ATT	CTG	GGC	GAT	CAG	ACA	GCG	GCG	GCT	GCC	CCA	GTT	450
136	W	S	Y	I	L	G	D	Q	T	A	A	A	A	P	V	150
451	CGC	TTG	TTG	ACA	AAT	CGT	CTC	ATC	TGC	CCA	GAC	ACC	TGT	CAA	CCC	495
151	R	L	L	T	N	R	L	I	C	P	D	T	C	Q	P	165
496	GAG	TGT	GCG	GCC	TCC	ACG	CCG	GAG	GCA	ATA	AGT	TTA	ACT	GAA	CTG	540
166	E	C	A	A	S	T	P	E	A	I	S	L	T	E	L	180
541	GAA	GGC	ACT	TCT	CGT	GAA	AAG	GAT	GCC	AAA	CTG	GGT	CAC	TGC	TGG	585
181	E	G	T	S	R	E	K	D	A	K	L	G	H	C	W	195
586	TCG	TTG	TCT	TAC	TGT	CAA	TCC	ATC	TGC	TCT	GCA	AAC	TGC	ACA	AGT	630
196	S	L	S	Y	C	Q	S	I	C	S	A	N	C	T	S	210

631	CGT	GGC	ATC	GCA	TGC	CGA	ATG	GAC	AAT	ACC	CAA	CTT	TGT	TGC	CAT	675
211	R	G	I	A	C	R	M	D	N	T	Q	L	C	C	H	225
676	AAA	GAG	TGC	CTT	GCC	GGC	TGT	TAC	GGC	CCT	GGT	CCA	GAG	GCA	TGT	720
226	K	E	C	L	A	G	C	Y	G	P	G	P	E	A	C	240
721	GTG	GCC	TGT	AAG	GGG	GCT	CTG	CAC	CGT	GGA	GTT	TGC	GTT	TCC	CAA	765
241	V	A	C	K	G	A	L	H	R	G	V	C	V	S	Q	255
766	TGC	CCT	CCA	TCC	ACC	TAT	CTC	TTC	CAT	GGA	CGT	CGG	TGC	GTG	ACC	810
256	C	P	P	S	T	Y	L	F	H	G	R	R	C	V	T	270
811	GCG	GCA	GAG	TGC	TTC	AAT	ATG	AGC	AGT	ACC	TAC	CGT	CTT	CCT	CAT	855
271	A	A	E	C	F	N	M	S	S	T	Y	R	L	P	H	285
856	GTC	GCA	GGC	AGC	AGC	GGA	AGC	AGC	TCT	ATC	GGT	TTT	GCC	GCC	TCA	900
286	V	A	G	S	S	G	S	S	S	I	G	F	A	A	S	300

CK49

901	GTG	ATA	GTC	AAC	ACC	ACG	GCA	GCT	GTA	GCC	ACC	ACC	GCT	ATT	CGC	945
301	V	I	V	N	T	T	A	A	V	A	T	T	A	I	R	315
946	CAG	TTC	GCT	ATC	CAT	CAG	GGT	CGC	TGC	GTT	CCC	GAC	TGC	CCC	TCA	990
316	Q	F	A	I	H	Q	G	R	C	V	P	D	C	P	S	330
991	GGT	CAT	CAG	CGC	GAC	GAA	GTC	AGT	GGG	CAG	TGT	GTG	CCA	TGT	GGC	1035
331	G	H	Q	R	D	E	V	S	G	Q	C	V	P	C	G	345
1036	GAC	GAG	TGT	CCG	AGG	ATT	CGA	TGC	CAT	CAT	ATG	CTA	ATA	AGC	AGC	1080
346	D	E	C	P	R	I	R	C	H	H	M	L	I	S	S	360

EmIGFRup

1081	CTT	AAG	TCA	CTG	TCC	AAA	CTG	AAG	GAC	TGC	TTC	TCT	GTC	ACC	GAT	1125
361	L	K	S	L	S	K	L	K	D	C	F	S	V	T	D	375
1126	CTC	TAC	ATC	TCC	ATT	CAT	GAG	GGC	GAC	ACG	GTT	CTG	ATA	CAG	CAG	1170
376	L	Y	I	S	I	H	E	G	D	T	V	L	I	Q	Q	390
1171	CAA	TTC	GAT	GAG	GCT	TTT	TCG	AGT	CTG	CGG	GAG	GTT	GAG	AGC	ATC	1215
391	Q	F	D	E	A	F	S	S	L	R	E	V	E	S	I	405
1216	AAG	GTT	GTT	CGG	GCA	ACA	GCT	CTC	ACT	TCC	CTT	GCC	TTC	CTC	CGC	1260
406	K	V	V	R	A	T	A	L	T	S	L	A	F	L	R	420
1261	CAC	GTC	AAA	CGC	ATA	AAC	ACC	ATT	CCT	AAT	TCC	TCG	CCC	AAC	GTG	1305
421	H	V	K	R	I	N	T	I	P	N	S	S	P	N	V	435

1306	ACA GTG ATA GAG ATA AGA GGC AAC GAT AAC CTG CTG GAA TTG TGG	1350
436	T V I E I R G N D N L L E L W	450
1351	CCT CCG CCA ACG AGG AAC CAG ACA GGC GGA CTT CAG GTG GTG TCA	1395
451	P P P T R N Q T G G L Q V V S	465
1396	GAA GGG CTT GTA CAT TTC ATC CTC AAT CGC TAC CTT TGC CCC AAG	1440
466	E G L V H F I L N R Y L C P K	480
1441	AAG ATC ACG GAC TTG GTG AGG ACA GGC GCT CTG ACG CTG CCC GGT	1485
481	K I T D L V R T G A L T L P G	495
1486	GGG CGC AAC TTT CGT ATA GAG GAG CTT GAA CTC GCT GAG GCT ACC	1530
496	G R N F R I E E L E L A E A T	510
1531	AAT GGC AAA CTC GGC TTC TGT GAG ACT ACA CAA ATC TCG CTT GAA	1575
511	N G K L G F C E T T Q I S L E	525
1576	TTG AAG GAT GTC TTT TCC TCA ACT GCT GCC ATC CAA TGG CCA CGT	1620
526	L K D V F S S T A A I Q W P R	540
1621	TTC TTT GAC AAC CGC ACA ACT GGC CAA GCA GCT TCC ACT CTG GTG	1665
541	F F D N R T T G Q A A S T L V	555
1666	TTG GTC TTC TTT CAG GCT ACA ACA AAA AAT TTG ACT GTC TAC ACG	1710
556	L V F F Q A T T K N L T V Y T	570
1711	AAT GGA CTC TCC TGC GGC GAT GAT TCA TGG AGG ATG ATT CCT TCG	1755
571	N G L S C G D D S W R M I P S	585
1756	ATT TGC AAC ACC TCT ACG ATA CGT GAA GAG AAA GGA GAG AAT GTT	1800
586	I C N T S T I R E E K G E N V	600
1801	GCC TTT TGC AGC AAA ATA CTC ACT GGC CTC CAA CCA GCT ACT CGC	1845
601	A F C S K I L T G L Q P A T R	615
1846	TAT GCC GTC TAT GTT GAG TCT AAA ACG CTT TTT AGT CAG CGT GGG	1890
616	Y A V Y V E S K T L F S Q R G	630
1891	GCG ATT AGC AAC ATC GTC TAC TTC ACC ACA AAT CCT AGT AAA CCG	1935
631	A I S N I V Y F T T N P S K P	645
1936	TCG CAT CCG CGT ATG GAG AGG TTG CAG GCG TTA AAT GAT TCA AGG	1980
646	S H P R M E R L Q A L N D S R	660

1981	ATT	TCT	GTT	AGG	TGG	TCA	CCG	CCT	CAA	TAC	AAC	AAT	GGC	CTC	TTG	2025
661	I	S	V	R	W	S	P	P	Q	Y	N	N	G	L	L	675
2026	GCC	GTG	TAC	CTT	CTC	TGG	TTC	CGT	TCT	ATT	CAC	ATC	GAT	CCG	GAG	2070
676	A	V	Y	L	L	W	F	R	S	I	H	I	D	P	E	690
2071	CCC	TAT	CTT	TAC	CGA	GAC	TTC	TGT	TTT	TTG	ACA	CCT	GAT	TGG	CTT	2115
691	P	Y	L	Y	R	D	F	C	F	L	T	P	D	W	L	705
CK50																
←—————																
2116	TCT	TCC	GCG	ATC	ACG	CCC	TCT	TAC								2139
706	S	S	A	I	T	P	S	Y								

C) *egTyrk*

CK93																
—————→																
1	CTG	AAT	TTC	CGT	CAT	CCT	CTT	GGG	CGC	GGA	AAC	TTT	GGC	ATG	GTG	45
1	L	N	F	R	H	P	L	G	R	G	N	F	G	M	V	15
46	TAT	CGG	GGA	TTT	GTG	AAA	TCG	CTT	CGC	ACT	CCC	GCC	CAT	TGC	TTC	90
16	Y	R	G	F	V	K	S	L	R	T	P	A	H	C	F	30
91	TAT	ACC	GAA	CCC	CAT	AAT	ATT	CCT	GCT	GCC	ATC	GCG	ACG	CTT	TCT	135
31	Y	T	E	P	H	N	I	P	A	A	I	A	T	L	S	45
136	TCT	GCT	TGT	ACT	GTA	TTC	GAC	CGT	CGC	GAT	TTT	ATC	ACG	GAG	GCC	180
46	S	A	C	T	V	F	D	R	R	D	F	I	T	E	A	60
181	TGC	TAC	ATG	AAG	CAA	TTT	CAG	AGT	TTC	CAC	ATT	GTG	AGA	CTC	TTT	225
61	C	Y	M	K	Q	F	Q	S	F	H	I	V	R	L	F	75
226	GGC	ATC	GTG	AGC	GAG	TGC	TCC	CCA	TCC	TCT	GCA	GTC	CCT	GCT	GCT	270
76	G	I	V	S	E	C	S	P	S	S	A	V	P	A	A	90
271	GCC	AGA	ACC	TTT	CTC	AGT	GGT	GGA	AGT	GGA	AGT	GGC	AGC	GGT	GAT	315
91	A	R	T	F	L	S	G	G	S	G	S	G	S	G	D	105
316	GGC	GGT	GGT	GGT	TTC	AGT	TCG	GCG	CAG	ACG	AAG	TTC	CGC	TTC	AGT	360
106	G	G	G	G	F	S	S	A	Q	T	K	F	R	F	S	120
361	TTG	TTT	CGT	CTC	TTT	GGT	GGT	GGA	GGC	TTC	TGG	AGA	CGA	CAT	CGG	405
121	L	F	R	L	F	G	G	G	G	F	W	R	R	H	R	135

406	CCC AAG CGC CAG GCC GTG CCC GTG CCC ATC AAG AAG AAG CTC TTC	450
136	P K R Q A V P V P I K K K L F	150
451	AGT TTA TCC GCT GAG GAA GCC ATG ACC GGT AAC ACT GGC AAC GGA	495
151	S L S A E E A M T G N T G N G	165
496	GGT TCT CTC ACG CGC ACT GCT AGA ACA CCC TCT AAC GAA GGG TTC	540
166	G S L T R T A R T P S N E G F	180
541	AAC ACC TCA AGG GGA CCT GAC GGT TCC AAC GGA ACG ACA GAT GCC	585
181	N T S R G P D G S N G T T D A	195
586	TCT CCA ACG AAA AGA GTT TGG ACG GGG AGT GGA CGC CTT GGT CGG	630
196	S P T K R V W T G S G R L G R	210
631	GGC TCG TTT TCC CGC CTC TTG ATG AAG AAC CAA AAG GAT TTT AGG	675
211	G S F S R L L M K N Q K D F R	225
676	TCT ACC CTA ACG ACA CAA GAT GAG ACT GGT GTT GCG ACT GTG CAG	720
226	S T L T T Q D E T G V A T V Q	240
721	CGC TTG ACT GTG CAG CGC TGC TCC AGC TCC GAC TCT ATC CGA CCC	765
241	R L T V Q R C S S S D S I R P	255
766	TTC TCC CAG TAC GGT CTG TTC GTG GTG ATG GAG CTG ATG GAG AGC	810
256	F S Q Y G L F V V M E L M E S	270
811	GGG GAT TTG GCC TCG TAT TTA CGC AAG CTT GGT GAC AGT GGT ATT	855
271	G D L A S Y L R K L G D S G I	285
856	GGC TTT GTG AAG CCC GCG CAA GCT TAC CTC TGG GCC GTT CAA ATA	900
286	G F V K P A Q A Y L W A V Q I	300
901	GCT GAT GGA ATG GCT TAT TTG GAA AGA AAA AAA TAC GTC CAT CGT	945
301	A D G M A Y L E R K K Y V H R	315
946	GAC TTG GCG GCC CGA AAT TGC CTG GTG GAT GGG CGA GGC GTG GTA	990
316	D L A A R N C L V D G R G V V	330
991	AAG GTG GGT GAT TTC GGC CTG TGT CGG GAC ATT TAC GAG AGG AAT	1035
331	K V G D F G L C R D I Y E R N	345
1036	TAC TAT CAC AAG GTG GGC GCG GGC AAG CTA CCT GTG CGG TGG ATG	1080
346	Y Y H K V G A G K L P V R W M	360
1081	GCG CCG GAG TCA CTT CAG TCT GCA TAC TTT ACC TCC CGC TCT GAC	1125

361	A	P	E	S	L	Q	S	A	Y	F	T	S	R	S	D	375
1126	GTG	TGG	TCA	TTC	GGT	GTG	GTT	TTG	TGG	GAG	ATC	GCA	ACA	ATG	GCG	1170
376	V	W	S	F	G	V	V	L	W	E	I	A	T	M	A	390
1171	TGT	TTG	CCC	TAC	CAG	GGC	ATG	TCG	CAC	AAT	GAA	GCG	ATC	TCC	TAC	1215
391	C	L	P	Y	Q	G	M	S	H	N	E	A	I	S	Y	405
1216	GTC	CTT	GAC	GGC	AAC	ACC	CTC	GTC	TCC	GGT	GGT	GCT	CCA	ATC	AAC	1260
406	V	L	D	G	N	T	L	V	S	G	G	A	P	I	N	420
1261	TGC	CCT	CCC	CTA	CTA	CAA	TCG	GTG	ATG	CTC	TAC	TGC	TGG	TCC	TAC	1305
421	C	P	P	L	L	Q	S	V	M	L	Y	C	W	S	Y	435
CK96																
←—————																
1306	CGT	CCC	GCT	CAG	CGG	CCC	ACC	TTT	CTG	CAC	CTC	CTC	TAT	CTC	CTT	1350
436	R	P	A	Q	R	P	T	F	L	H	L	L	Y	L	L	

D) *tsTyrk*

CK93																
—————→																
1	CTG	AAT	TTC	CGT	CAT	CCT	CTT	GGG	CGC	GGA	AAC	TTT	GGC	ATG	GTG	45
1	L	N	F	R	H	P	L	G	R	G	N	F	G	M	V	15
46	TAT	CGG	GGA	TTT	GTG	AAA	TCG	CTT	CGC	GCT	CCC	GCC	CAT	TGC	TTC	90
16	Y	R	G	F	V	K	S	L	R	A	P	A	H	C	F	30
91	TAT	ACC	GAA	CCC	CAC	AAT	ATT	CCT	GCT	GCC	ATC	GCG	ACG	CTT	TCT	135
31	Y	T	E	P	H	N	I	P	A	A	I	A	T	L	S	45
136	TCT	GCT	TGT	ACT	GTA	TTC	GAC	CGT	CGC	GAT	TTT	ATC	ACG	GAG	GCC	180
46	S	A	C	T	V	F	D	R	R	D	F	I	T	E	A	60
181	TGC	TAC	ATG	AAG	CAA	TTT	CAG	AGT	TTC	CAC	ATT	GTG	AGA	CTC	TTT	225
61	C	Y	M	K	Q	F	Q	S	F	H	I	V	R	L	F	75
226	GGC	ATC	GTG	AGC	AAG	TGC	TCC	CCA	CTG	TTC	GTG	GTG	ATG	GAG	CTG	270
76	G	I	V	S	K	C	S	P	L	F	V	V	M	E	L	90
271	ATG	GAG	AGC	GGG	GAT	TTG	GCC	TCG	TAT	TTA	CGC	AAG	CTT	GGT	GAC	315
91	M	E	S	G	D	L	A	S	Y	L	R	K	L	G	D	105

E) *tcTyrk***CK93**

		→															
1	CTG AAT TTC CGT CAT CCT CTT GGG CGC GGA AAC TTT GGC ATG GTG	45															
1	L N F R H P L G R G N F G M V	15															
46	TAT CGG GGA TTT GTG AAA TCG CCT CGC ACT CCC GCC CAT TGC TTC	90															
16	Y R G F V K S P R T P A H C F	30															
91	TAT ACC GAA CCC CAT AAT ATT CCT GCT GCC ATC AAG ACG CTT TCT	135															
31	Y T E P H N I P A A I K T L S	45															
136	TCT GCT TGT ACT GTA TTC GAC CGT CGC GAT TTT ATC ACG GAG GCC	180															
46	S A C T V F D R R D F I T E A	60															
181	TGC TAC ATG AAG CAA TTT CAG AGT TTC CAC ATT GTG AGA CTC TTT	225															
61	C Y M K Q F Q S F H I V R L F	75															
226	GGC ATC GTG AGC AAG TGC TCC CCA TCC TCT GCA GTC CCT GCT GCT	270															
76	G I V S K C S P S S A V P A A	90															
271	GCC AGA ACC TTT CTC AGT GGT GGA AGT GGA AGT GGC AGC GGT GAT	315															
91	A R T F L S G G S G S G S G D	105															
316	GGC GGT GGT GGT TTC AGT TCG GCG CAG ACG AAG TTC CGC TTC AGT	360															
106	G G G G F S S A Q T K F R F S	120															
361	TTG TTT CGT CTC TTT GGT GGT GGA GGC TTC TGG AGA CGA CAT CGG	405															
121	L F R L F G G G G F W R R H R	135															
406	CCC AAG CGC CAG GCC GTG CCC GTG CCC ATC GAG AAG AAG CTC TTC	450															
136	P K R Q A V P V P I E K K L F	150															
451	AGT TTA TCC GCT GAG GAA GCC ATG ACC GGT AAC ACT GGC AAC GGA	495															
151	S L S A E E A M T G N T G N G	165															
496	GGT TCT CTC ACG CGC ACT GCT AGA ACA CCC TCT AAC GAA GGG TTC	540															
166	G S L T R T A R T P S N E G F	180															
541	AAC ACC TCA AGG GGA CCT GAC GGT TCC AAC GGA ACA ACA GAT GCC	585															
181	N T S R G P D G S N G T T D A	195															
586	TCT CCA ACG AAA AGA GTT TGG ACG GGG AGT GGA CGC CTT GGT CGG	630															
196	S P T K R V W T G S G R L G R	210															

631	GGC TCG TTT TCC CGC CTC TTG ATG AGG AAC CAA AAG GAT TTT AGG	675
211	G S F S R L L M R N Q K D F R	225
676	TCT ACT CTA ACG ACA CAA GAT GAG ATT GGT GTT GCG ACT GTG CAG	720
226	S T L T T Q D E I G V A T V Q	240
721	CGC TGC TCC AGC TCC GAC TCT ATT CGA CCC TTC TCC CAG TAC GGT	765
241	R C S S S D S I R P F S Q Y G	255
766	CTG TTC GTG GTG ATG GAG CAG ATG GAG AGC GGG GAT TTG GCC TCG	810
256	L F V V M E Q M E S G D L A S	270
811	TAT TTA CGC AAG CTT GGT GAC AGT GGT ATT GGC TTT GTG AAG CCC	855
271	Y L R K L G D S G I G F V K P	285
856	GCG CAA GCT TAC CTC TGG GCC GTT CAA ATA GCT GAT GGA ATG GCT	900
286	A Q A Y L W A V Q I A D G M A	300
901	TAT TTG GAA AGA AAA AAA TAC GTC CAT CGT GAC TTG GCG GCC CGA	945
301	Y L E R K K Y V H R D L A A R	315
946	AAT TGC CTG GTG GAT GGG CGA GGC GTG GTA AAG GTG GGT GAT TTC	990
316	N C L V D G R G V V K V G D F	330
991	GGC CTG TGT CGG GAC ATT TAC GAG AGG AAT TAC TAT CAC AAG GTG	1035
331	G L C R D I Y E R N Y Y H K V	345
1036	GGC GCG GGC AAG CTA TCT GTG CGG TGG ATG GCG CCG GAG TCA CTT	1080
346	G A G K L S V R W M A P E S L	360
1081	CAG TCT GCA TAC TTT ACC TCC CGC CCT GAC GTG TGG TCA TTC GGT	1125
361	Q S A Y F T S R P D V W S F G	375
1126	GTG GTT TTG TGG GAG ATC GCA ACA ATG GCG TGT TTG CCC TAC CAG	1170
376	V V L W E I A T M A C L P Y Q	390
1171	GGC ATG TCC CAC AAT GAA GTG ATC TCC TAC GTC CTT GAC GGC AAC	1215
391	G M S H N E V I S Y V L D G N	405
1216	ACC CTC GTC TCC GGT GGT GCT CCA ATC AAC TGC CCT CCC CTA CTA	1260
406	T L V S G G A P I N C P P L L	420
1261	CAA TCG GTG ATG CTC TAC TGC TGG CCC TAC CGT CCC GCT CAG CGG	1305
421	Q S V M L Y C W P Y R P A Q R	435

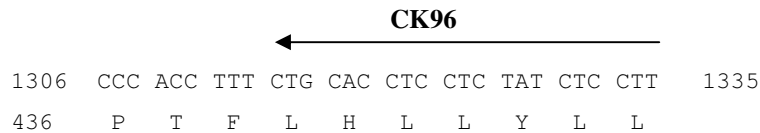


Fig. 48: Nucleotide sequences of cDNA fragments amplified in a PCR using *emir* specific oligonucleotides.

The sequence of the cDNA fragment and the deduced amino acid sequence encoded in the longest ORF are shown. The positions of the *emir* specific oligonucleotides are also indicated. **A)** *E. granulosus* LCL domain: *egLCL*; **B)** *T. solium* LCL domain: *tsLCL*; **C)** *E. granulosus* tyrosine kinase domain: *egTyrk*; **D)** *T. solium* tyrosine kinase domain: *egTyrk*; **E)** *T. crassiceps* tyrosine kinase domain: *egTyrk*;

3.6.2.2 Amino acid sequence comparison of the ligand binding and tyrosine kinase domain of cestode IR orthologs

For a more detailed analysis, the deduced amino acid sequences were aligned with the corresponding domain of EmIR (Fig. 49,50). A ClustalW analysis [185] of EgLCL and TsLCL with the ligand binding domain of EmIR and human IR again visualized the high identity between these proteins (Fig.49). The ligand binding domain of the IR/IGF-I receptor family is characterized by a highly conserved cysteine rich domain which contributes to the conformation of the mature receptor and is involved in the determination of the ligand specificity [177,188]. Such a domain is also found in EgLCL and TsLCL having over 20 cysteine residues at homologous positions with human IR and EmIR (Fig. 49 A). For human IR and human IGF-IR, a peptide of 56 (HIR: N²³⁰-I²⁸⁵) and 52 (HIGF-IR: H²²³-M²⁷⁴) residues could be identified as the receptors primary ligand specificity determining region, respectively [97,98]. In this publication, the signal peptide was not included in the numbering of the human IR residues but was done in this work. Therefore, the 56 residue peptide comprises N²⁵² – I³¹² in Fig. 49. The amino acid alignment of EmIR with human IR and human IGF-IR revealed that EmIR possesses an additional 26 residue insert in its homologous region (G²⁷⁶-V³⁵⁶) [5,79]. This insert could also be identified for EgLCL and TSLCL suggesting a platyhelminthes specific function. Further, cysteine residues could be found in ortholog positions to those cysteine residues of EmIR which are potentially be involved in the formation of the disulfide bond between the two α – subunits and the α – and β - subunit (Fig. 49 A) [79,202,203]. The high identity between the ligand binding domains of IR from

distinct cestodes with that of EmIR suggests that also these receptors could be activated by insulin.

```

.....|.....|.....|.....|.....|.....|.....|.....|.....|.....|.....|.....|.....|.....|.....|.....|
      10      20      30      40      50      60
HIR LCL  1  -----MGTGRRGAAAAPLLVAVAAALLGAAGHLYPGEVCPGMDIRNNLTRL 47
EmIR LCL 1  MPKSSSYSVMCIGSYVFCLFFFQLPVFVPSYCRVFGGNHTYLQONEMLCGDFDVRPVSAL 60
Eg LCL   1  -----CRVFGGNHTYLQONEMLCGDFDVRPVSAL 29
Ts LCL   1  -----CRVFGGNHTYLQONEMLCGDFDVRPVSAL 29
    
```

```

.....|.....|.....|.....|.....|.....|.....|.....|.....|.....|.....|.....|.....|.....|.....|.....|
      70      80      90      100     110     120
HIR LCL  48  HELENC+SVIEGH+IQILLMFKTRPEDFRDL+SFK+LIMITDYL+LLFRVY+GLES+LKDL+LPNLT 107
EmIR LCL  61  SRIKS+CTVIEGNLLIVMTRLP-----VNASIPNLR+EITGFLVIYDL+MGLDGLATL+FPNLT 115
Eg LCL   30  SRIKS+CTVIEGNLLIVMTRLP-----VNASIPNLR+EITGFLVIYDL+MGLDGLATL+FPNLT 84
Ts LCL   30  SRIKS+CTVIEGNLLIVMTRLP-----VNASIPNLR+EITGFLVIYDL+MGLDGLATL+FPNLT 84
    
```

```

.....|.....|.....|.....|.....|.....|.....|.....|.....|.....|.....|.....|.....|.....|.....|.....|
      130     140     150     160     170     180
HIR LCL  108  VIRGRSLFFN+YALVIFEMVHL+LKEL+GLYNLMN+ITRGS+VRIEK+NNEL+CYLATIDWS+RIL+DS- 166
EmIR LCL  116  VIRGRSLISNFALVIRSTS-LKTIGLPSLRVIQ+GGVRVDLNTNL+CYVRTVNWSY+ILGDQ 174
Eg LCL   85  VIRGRSLISNFALVIRSTS-LKTIGLPSLRVIQ+GGVRVDLNTNL+CYVRTVNWSY+ILGDR 143
Ts LCL   85  VIRGRSLISNFALVIRSTS-LKTIGLPSLRVIQ+GGVRVDLNTNL+CYVRTVNWSY+ILGDQ 143
    
```

```

.....|.....|.....|.....|.....|.....|.....|.....|.....|.....|.....|.....|.....|.....|.....|.....|
      190     200     210     220     230     240
HIR LCL  166  -----VEDN+HIVL+NKDDNE+ECGDIC+PGTAKGKTNCPAT+VINGQF+VERCW+THSH+CC+KV 218
EmIR LCL  175  TAAAAPVRL+LTNRLI+CPDTC+QPE+CAASTPEAISL+TELEGTSREKDAKL+GHCWSLSY+CQSI 234
Eg LCL   144  TAAAAPVRL+LTNRLI+CPDTC+QPE+CAASTPEAISL+TELEGTSREKDAKL+GHCWSLSY+CQSI 203
Ts LCL   144  TAAAAPVRL+LTNRLI+CPDTC+QPE+CAASTPEAISL+TELEGTSREKDAKL+GHCWSLSY+CQSI 203
    
```

```

.....|.....|.....|.....|.....|.....|.....|.....|.....|.....|.....|.....|.....|.....|.....|.....|
      250     260     270     280     290     300
HIR LCL  219  CPTI+CKSHG+--CTAEG--LCCH+SE+CLGN+CSQ+PDD+TKCVAC+RNFYLD+GRC+VET+CP+PY+YH 274
EmIR LCL  235  CSAN+CTSRGIA+CRMDNTQL+CC+HKE+CLAGCYGPG+-PEACVAC+KGALHRGV+CVSQC+PPSTYL 293
Eg LCL   204  CSAN+CTSRGIA+CRMDNTQL+CC+HKE+CLAGCYGPG+-PEACVAC+KGALHRGV+CVSQC+PPSTYL 262
Ts LCL   204  CSAN+CTSRGIA+CRMDNTQL+CC+HKE+CLAGCYGPG+-PEACVAC+KGALHRGV+CVSQC+PPSTYL 262
    
```

```

.....|.....|.....|.....|.....|.....|.....|.....|.....|.....|.....|.....|
      310      320      330      340      350      360
HIR LCL  275  EQDWRCVNFSECDLHHKCKNSRRQG-----CHQYVTHNN 309
EmIR LCL  294  FHGRRCVTAAECFNMSSTYRLPHVAGSSGSSSIGFAASVIVNTTAAVATTAIRQFAIHQG 353
E.g. LCL  263  FHGRRCVTAAECFNMSSTYRLPHVAGSSGSSSIGFAASVIVNTTAAVATTAIRQFAIHQG 322
T.s. LCL  263  FHGRRCVTAAECFNMSSTYRLPHVAGSSGSSSIGFAASVIVNTTAAVATTAIRQFAIHQG 322

```

```

.....|.....|.....|.....|.....|.....|.....|.....|.....|.....|.....|.....|
      370      380      390      400      410      420
>
HIR LCL  310  KCIPECPSGYTMNSSNLLCTPCLGFCPKVCHLLEGEKTIIDSVTSAQELRGCTVINGSLHI 369
EmIR LCL  354  RCVPCPSGHQRDEVSGQCVP CGDECP RIRCHH--MLISSLKSLSKLKD CFSVTDLYIS 410
Eg LCL  323  RCVPCPSGHQRDEVSGQCVP CGDECP RIRCHH--MLISSLKSLSKLKD CFSVTDLYIS 379
Ts LCL  323  RCVPCPSGHQRDEVSGQCVP CGDECP RIRCHH--MLISSLKSLSKLKD CFSVTDLYIS 379

```

```

.....|.....|.....|.....|.....|.....|.....|.....|.....|.....|.....|.....|
      430      440      450      460      470      480
HIR LCL  370  NIRGGNNLAABLEANLGLIEEISGYLKIIRRSYALVSLSFRRKLRLLRGETLEIGNYSFYA 429
EmIR LCL  411  THEGDTVLIQQQFDEAFSSLREVESIKVVRATALTSLAFLRHVKRINTIPNSSPNVTIVIE 470
Eg LCL  380  THEGDTVLIQQQFDEAFSSLRGEVESIKVVRATALTSLAFLRHVKRINTIPNSSPNVTIVIE 439
Ts LCL  380  THEGDTVLIQQQFDEAFSSLREVESIKVVRATALTSLAFLRHVKRINTIPNSSPNVTIVIE 439

```

```

.....|.....|.....|.....|.....|.....|.....|.....|.....|.....|.....|.....|
      490      500      510      520      530      540
HIR LCL  430  LD-NQNLROLWDWSKHNLIT-----TTOGKLFHYNPKLCLSETHKMEEVSGTKG----- 477
EmIR LCL  471  IRGNDNLELWPPPTRNQTGGLQVVSEGLVHFILNRYLCPKKITDLVRTGALTLPGGRNF 530
Eg LCL  440  IRGNDNLELWPPPTRNQTGGLQVVSEGLVHFILNRYLCPKKITDLVRTGALTLPGGRNF 499
Ts LCL  440  IRGNDNLELWPPPTRNQTGGLQVVSEGLVHFILNRYLCPKKITDLVRTGALTLPGGRNF 499

```

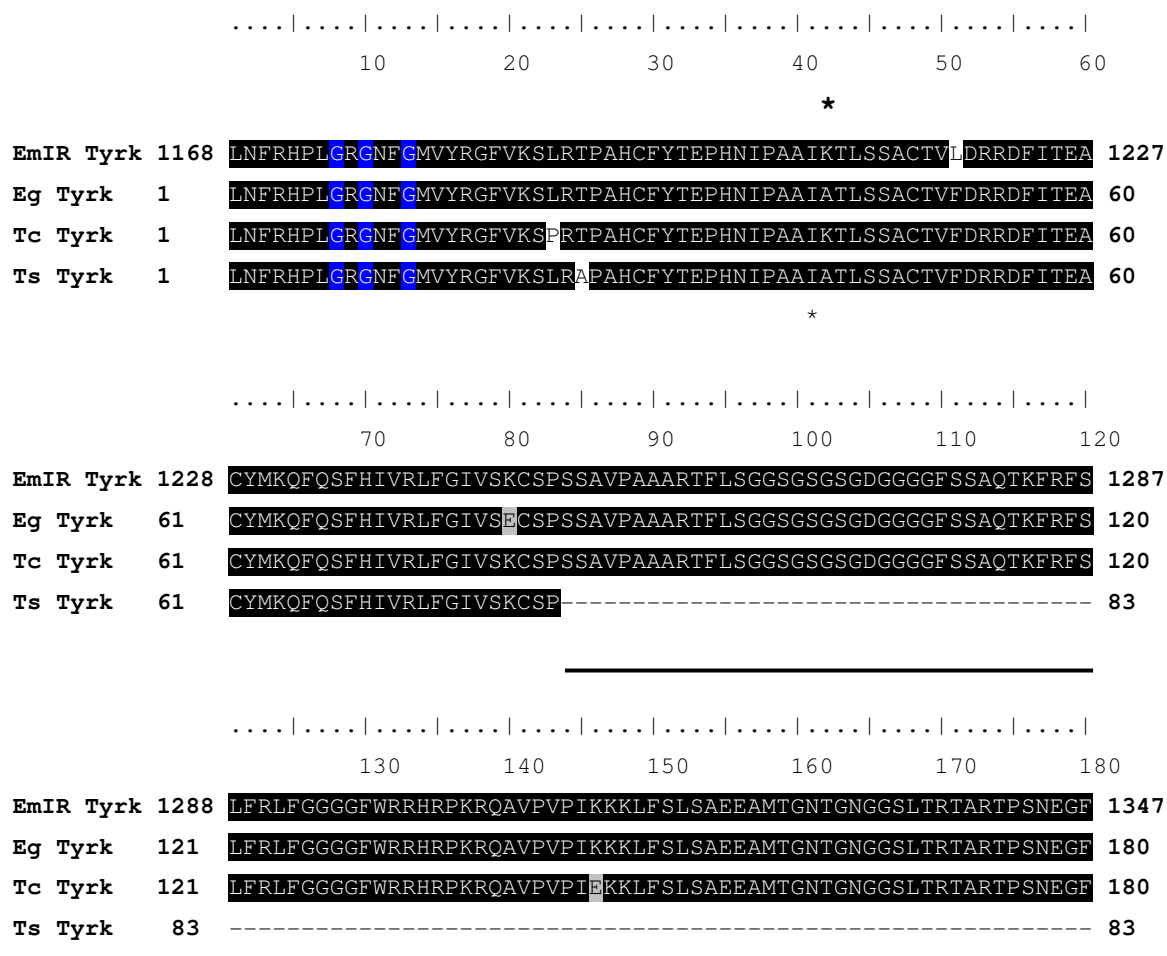
```

.....|.....|.....|.....|.....|.....|.....|.....|.....|.....|.....|.....|
      550      560      570      580      590      600
HIR LCL  478  RQERNDIALKTNGDKASCENELLKFSYIRTSFDKILLRWEPYWPDPFRDLLG--FMLEFYK 535
EmIR LCL  531  RIEELELAEATNGKLGFCETTQISLELKDVFSSATAIQWPRFFDNRTTGQAASTLVLVVF 590
Eg LCL  500  RIEELELAEATNGKLGFCETTQISLELKDVFSSATAIQWPRSF DNRTTGQAASTLVLVVF 559
Ts LCL  500  RIEELELAEATNGKLGFCETTQISLELKDVFSSATAIQWPRFFDNRTTGQAASTLVLVVF 559

```


in EmIR [79] and with K⁴² a lysine residue at a homologous position can also be found in the tyrosine kinase domain of *T. crassiceps* (TcTyrk; Fig. 50). According to the ClustalW alignment [185], the tyrosine kinase domains of *E. granulosus* (EgTyrk) and *T. solium* (TsTyrk) possess an alanine instead of a lysine residue at position 42 (Fig. 50). This might indicate that K¹²⁰⁹ in EmIR does not have the crucial role as K¹⁰³⁰ in human IR.

The finding that *T. solium* IR kinase domain lacks the additional 172 residue peptide while it has been identified in the kinase domain of *E. multilocularis*, *E. granulosus* and *T. crassiceps* indicates a specific function of this peptide. In the following, the cDNA coding for the complete EgIR, TsIR and TcIR needs to be identified and characterized. It would be of special interest if the kinase domain of TsIR is functional when expressed in a heterologous system and if the deletion of the 172 residue peptide leads to a functional HIR-EmIRintra chimera. The deletion of this peptide has been initiated but could not be completed during the present study.



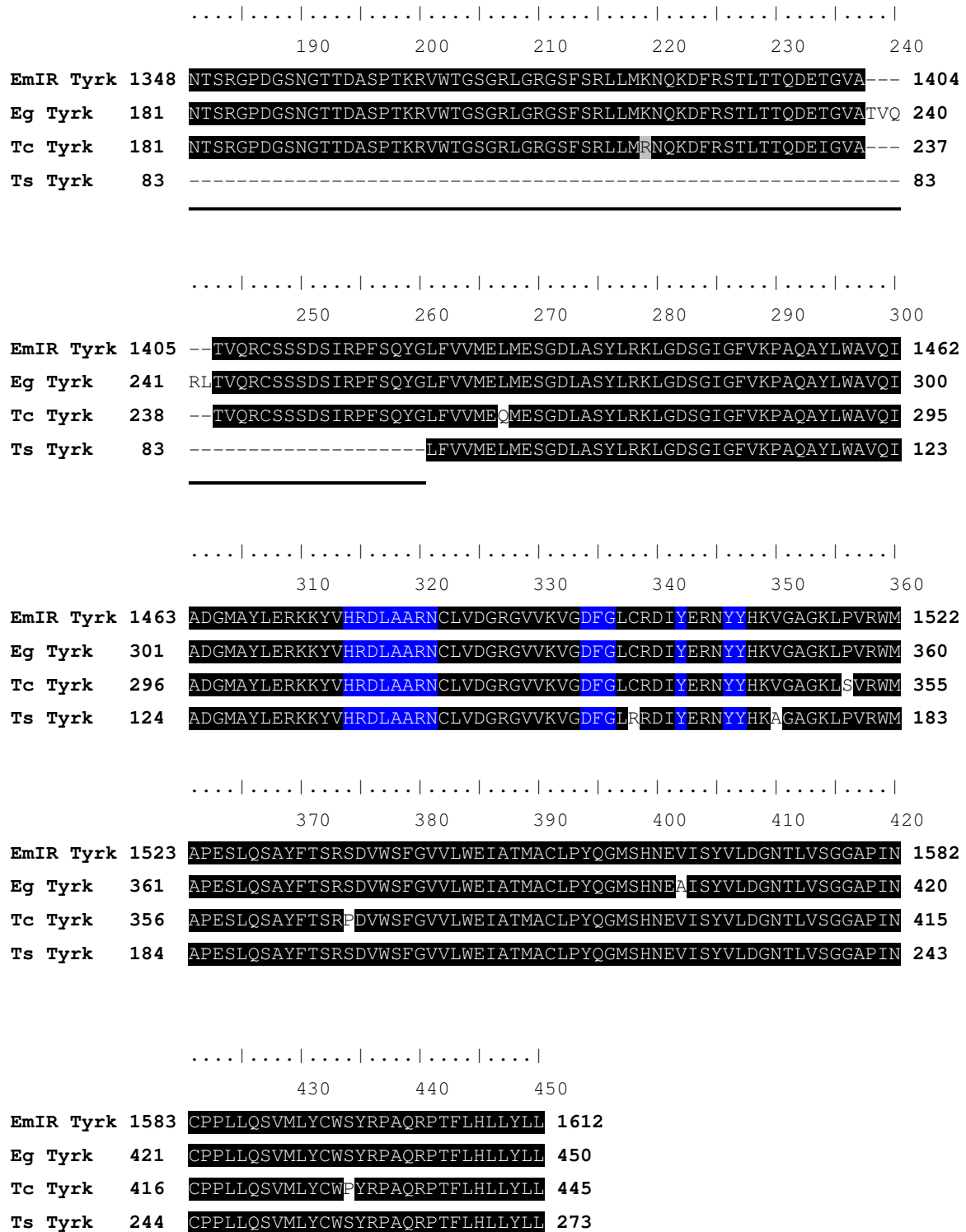


Fig. 50: Amino acid alignment of the tyrosine kinase domain. The deduced amino acid sequences of the ORF coding for the putative tyrosine kinase domain of *E. granulosus* (EgTyrk), *T. solium* (TsTyrk) and *T. crassiceps* (TcTyrk) insulin receptor orthologs were compared with the corresponding domain of *E. multilocularis* (EmIRTyrk) insulin receptor. Identical residues are shaded in black and similar residues in grey. Critical residues and motifs conserved among tyrosine kinase domains are shaded in blue. The insert in the kinase domain is underlined and K¹²⁰⁹ is marked by the asterisk. The numbering indicates the position of the residue in the amino acid sequence.

3.6.3 Identification of a possible EmIR downstream signaling cascade in *E. multilocularis* larval stages

The characterization of the EmIR downstream signaling cascade within *E. multilocularis* larval stages was another aim of the present study. With the MAP kinase cascade leading to the activation of EmMPK-1A after the stimulation with insulin, an EmIR downstream signaling cascade has been identified in the present study. Another family of proteins involved in the downstream signaling of IR RTKs is the family of Src-kinases [122,123]. This family includes Fyn-kinase which forms a complex with and tyrosine phosphorylates IRS-1 during the stimulation of mammalian cells with insulin [123,129]. With Raf-1, another component of the mammalian MAP Kinase cascade associates with Fyn. This association leads to an increased tyrosine phosphorylation of Raf-1 which in turn stimulates Raf-1's autophosphorylation activity thereby activating the MAP kinase cascade [130]. Besides the MAP kinase cascade, Src-family kinases also regulate RhoGAPs by tyrosine phosphorylation. It could be previously demonstrated that mammalian RhoGAP proteins interact with and are tyrosine phosphorylated by Fyn and that this phosphorylation is involved in the morphological changes of oligodendrocytes [120,121]. RhoGAP proteins regulate the activity of the Rho family of GTP-binding proteins which control actin organization, focal adhesion assembly, cell cycle progression, cytokinesis, transcription, secretion and endocytosis [124]. During an expressed sequence – tag (EST) analysis of trans-spliced cDNAs of *E. multilocularis*, two cDNAs were isolated and identified. A computational analysis revealed that one cDNA coded for a protein with homology to the family of RhoGAPs with the highest identity to Arhgap8 from *Rattus norvegicus* (39% identical/ 56% similar), Arhgap1 from *Mus musculus* (36% identical/ 56% similar) and ARHGAP1/p50RhoGAP from *Homo sapiens* (37% identical/ 57% similar). This cDNA was therefore named *emrhogap* and the encoded protein EmRhoGAP.

The other cDNA encoded a protein being homologous to the family of Src tyrosine kinases which comprises 9 subfamilies in mammalian cells (Src, Lck, Hck, Fyn, Blk, Lyn, Fgr, Yes, and Yrk). All members share a conserved domain structure (see below for details) but contain a unique domain in their N-terminal region which is divergent among family members [128]. The database search [184] identified p59Fyn of the teleost fish *Xiphophorus helleri* (48% identity/ 63% similarity) and cfyn-a protein of *Xenopus laevis* (48% identity/ 63% similarity) as the proteins with the highest identity to this *Echinococcus multilocularis* Src-like protein. Therefore this protein was named EmFyn and the corresponding gene *emfyn*.

In the present study, EmFyn and EmRhoGAP were characterized on the genetic level and their involvement in the downstream signaling of EmIR was analyzed.

3.6.3.1 Analysis of *emrhogap* cDNA

The *emrhogap* cDNA comprises a total of 1909 bp (including poly-A-tail). Although no stop codon can be found upstream of the first start codon (Fig.53), the assumption that the complete 5' end of this cDNA was isolated is supported by the initial isolation of *emrhogap* from a pool of *trans* spliced mRNA. Approximately 30% of all *E. multilocularis* mRNAs possess a spliced-leader which is spliced in *trans* to the 5' end of the cDNA thereby indicating its 5' end [3]. Within the longest ORF (Fig. 51), two potential start codons are located (TTTTGT²⁰ATG²³T; AAGGCG¹⁰¹ATG¹⁰⁴G) of whom the second corresponds better to the Kozak – consensus sequence (GCCRCCATGG; R = A or G) for the translation initiation site [204]. Hence, the second ATG was assumed as the start codon of a 1500 bp ORF coding for a 500 residue protein, EmRhoGAP, which is limited at its 3' end by a TAA¹⁶⁰⁴ stop codon. Further downstream of the putative stop codon and 20 nt upstream of the poly-A-tail, a hexanucleotide is found that is identical to the consensus sequence for a polyadenylation signal (Fig.53) [205].

```

1      TCCTTACCTT GCAGTTTTGT ATGTCTCTTC AAGTGGATTC GTCACGGGAT 50

51     AGCCTTCCGG TGAAGAAAGT CGCCTATAAT CATTACCGGA AGGCTAAGGC 100

101    G      ATG GAA TCT GAC CCT GCG GTT ACC AGT ACA GTC AAT   137
1      M     E     S     D     P     A     V     T     S     T     V     N     12


138    GAG TCA GAC CTG AGT TAT TCC AGT TCC CCC AGT GAA AAG ACA GAG   182
13     E     S     D     L     S     Y     S     S     S     P     S     E     K     T     E   27


183    GTT CCC ATT TCA GCA AAG CCT CAT TGG ATA TTT TGT TCA GTA CAA   227
28     V     P     I     S     A     K     P     H     W     I     F     C     S     V     Q     42

228    ACG GCA AAT CCA CCC CCC TTT TCC GAA GGT GAA ACT CCT CCA ACA   272
43     T     A     N     P     P     P     F     S     E     G     E     T     P     P     T     57

273    TCT GTA CAT GAA TTC GAA ATT CCA GAA CTT GAG TTT GAC GAC GAA   317
58     S     V     H     E     F     E     I     P     E     L     E     F     D     D     E     72

```

318	ATA CCA GAT CTT GAA GGA GAT CTA GAT GAT GAC GAA TTC GAT GTA	362
73	I P D L E G D L D D D E F D V	87
363	CCG ATG ACT CCC AAT GGA TTA ATT GAC GAA GAC TTT GAA CGC GAA	407
88	P M T P N G L I D E D F E R E	102
408	CTG GGT TGG TAT GAA AAG GAA CTT TCT ATT CAA GAA GTG ATA GAC	452
103	L G W Y E K E L S I Q E V I D	117
Z2-123--1		
		
453	TCA GAA TTT CGC GAT ATC TCT CGA CTG GGT ATT ATC CAG GTT GGC	497
118	S E F R D I S R L G I I Q V G	132
498	GTC TCC GAT CAC GAT GGA CGA AGT GTC TTC GCC TTT TTC GCT TGC	542
133	V S D H D G R S V F A F F A C	147
543	CGC CTC CCC CAC ACC GAA CTC ATC GAT CAT GAT CGG TTG TTG CAA	587
148	R L P H T E L I D H D R L L Q	162
588	TAC GTG ACA AAG ACT CTT GAG CAG TAC GCG TCC TCG AAC TAC ACT	632
163	Y V T K T L E Q Y A S S N Y T	177
633	CTG GTC TAC TTC CAC TGG GGT CTG ACG AGT CGA AAT AAG CCT AGC	677
178	L V Y F H W G L T S R N K P S	192
678	TTT TCC TGG CTC GCA CGG GCT TTT CAA ACC TTT GAT CGA AGC TTC	722
193	F S W L A R A F Q T F D R S F	207
723	AAG AAG AAC CTT AAA TCG CTC ATC ATC GTC TAT CCA ACT CGA ACT	767
208	K K N L K S L I I V Y P T R T	222
768	GTT CGT GTA CTC TGG AAC TTA TTC AAT GCT TTC ATC AGC GCC AAA	812
223	V R V L W N L F N A F I S A K	237
813	ATG AAG AAG AAA CTG CAC TAC GTT CAA AAC CTT CAG GAA TTG GAG	857
238	M K K K L H Y V Q N L Q E L E	252
858	AAT CAC ATC CCG GTT TGC CAG TTG AAT CTT CCT CTA CGG ATT CGT	902
253	N H I P V C Q L N L P L R I R	267
903	GAC TAC GAC AGA AAG ATC GGT CTC TCC GAC GTA CCC CTG CCC ATC	947
268	D Y D R K I G L S D V P L P I	282
948	GAT TCC ACA GCT GTC TCC GTG ATT GAA GAC CAC GAT GTT GAT GAC	992
283	D S T A V S V I E D H D V D D	297

993	ACC CGG TAC AAT GTT TAC CAA CAA TTT GGC GTA TCC CTG GAG CAT	1037
298	T R Y N V Y Q Q F G V S L E H	312
1038	ATT AAG GCC AAC AAT GGC GGA CGC AAG CTA CCC ATT GTT GTT GAA	1082
313	I K A N N G G R K L P I V V E	327
<p>Z2-123-2</p> 		
1083	GAT ACT ATA ACC TAC CTT CGA GGT CAT GGT CTC GAC ACC GTC GGT	1127
328	D T I T Y L R G H G L D T V G	342
1128	CTT TTT ATC AAA CCG GTC CAT TTA ATG ACT CTA CGC GAT GTT CAA	1172
343	L F I K P V H L M T L R D V Q	357
1173	TCC ATG TAC AAT CGG GGT GAA TAC GTT GAT CTG TGC GAA ATA AGT	1217
358	S M Y N R G E Y V D L C E I S	372
1218	GAC CCT CAC CTA GCT GCC CAC TTG TTA AAA TCC TTC CTC TCC GAA	1262
373	D P H L A A H L L K S F L S E	387
1263	TTG AAA GAG CCC CTC CTA ACC TTC GAT CTC TAC GAG AGC ATT CTC	1307
388	L K E P L L T F D L Y E S I L	402
1308	AAG TCG TGT AGC CAA ACA CCC TGG CAA CGA GTG ATT TCC ATT CGA	1352
403	K S C S Q T P W Q R V I S I R	417
1353	CGA CTC CTC ACC GTT CAT CTT CCG CAT GAG AAC TAT GAC ATT TTG	1397
418	R L L T V H L P H E N Y D I L	432
1398	CAT TAT ATC TTC AAG TTC CTT ACT GAG GTG CTT GAA CAC TCG GCA	1442
433	H Y I F K F L T E V L E H S A	447
1443	AAG AAC ATG GTG ACA GCG GTG AAT CTC TCC ATT GCG ATG TCT CCG	1487
448	K N M V T A V N L S I A M S P	462
1488	AGT CTC ATT CGA TCG CGC CAG GAT TTT GTG ATG CCC TCG CGG CGC	1532
463	S L I R S R Q D F V M P S R R	477
1533	GTA CAG CGT CTC ATT ACC TCC TTC ACC CAA CTC TGC ATC ACC CAT	1577
478	V Q R L I T S F T Q L C I T H	492
1578	TTT GAG AGC GTA TTT GTT CGC ACC TAA CAG ACC TCG CCC CCT GTC	1622
493	F E S V F V R T *	500
1623	TTT GCT TTT TAA CTG TCA TTT TTG TGA CTT TTT TCC CCT AGA TTG	1667

```

1668  GAT ATT TTC TTT TTT AAC AAT ATG ATG TTT GTG TGA TGG GCG CAC 1712
1713  TGT TTA GCA CCT TAG CTT CTA GCG TTG CAT TCG TCA TGA CGT CTC 1757
1758  GTT ACT TTC TTG TAT GCG TCT GAA TAT TGT GTC TTA CAT GAC ATG 1802
1803  ACT TCT TTA TTA ATT GCA CTT AAT GTG CGT TGC AAA CTA ATT TGC 1847
1848  TGA GAT ATT CGT GGC CTG GGA ATA AAC ACG TTT TTC TCG GAA AAA 1892
1893  AAA AAA AAA AAA AAA 1907

```

Fig. 51: Nucleotide sequence of *emrhogap* and deduced aa sequence. The two possible ATG start codons are given in bold letters, the stop codon is marked by the asterisks and the putative polyadenylation signal sequence (AATAAA) is underlined, while the spliced leader is indicated by the solid bar.

3.6.3.2 Structural features of EmRhoGAP

The deduced amino acid sequences of EmRhoGAP and EmFyn (see below) were further analyzed. The 500 residues of EmRhoGAP have a predicted molecular weight of 57.7 kDa and a pI of 5.3 [206]. The analysis of the domain structure with the SMART program [198] identified a long N-terminal region without any predicted domain (aa 1 -119), a Sec14p/CalTrio domain (aa 120 – 271) and a RhoGAP domain (aa 320 – 494), the name giving domain of the family of RhoGAPs. An overview of the domain structure and the residues comprising the single domains are given in Fig. 52. This domain structure clearly identifies EmRhoGAP as a member of the ARHGAP subfamily of RhoGAPs. With a predicted molecular weight of 57.7 kDa, EmRhoGAP possesses a similar size as human ARHGAP8 (53.5 kDa) and human ARHGAP1 (50.5 kDa) [207]. While the human homologs are identical in their subunit composition, ARHGAP1 differs from ARHGAP8 in having a 50 amino acid extension N-terminal of the Sec14p domain instead of a 44 amino acid extension C-terminal of the RhoGAP domain [207]. With 119 residues, the N-terminal extension of EmRhoGAP is even longer than in ARHGAP1 and reveals that it is the *Echinococcus* ortholog of human ARHGAP1.

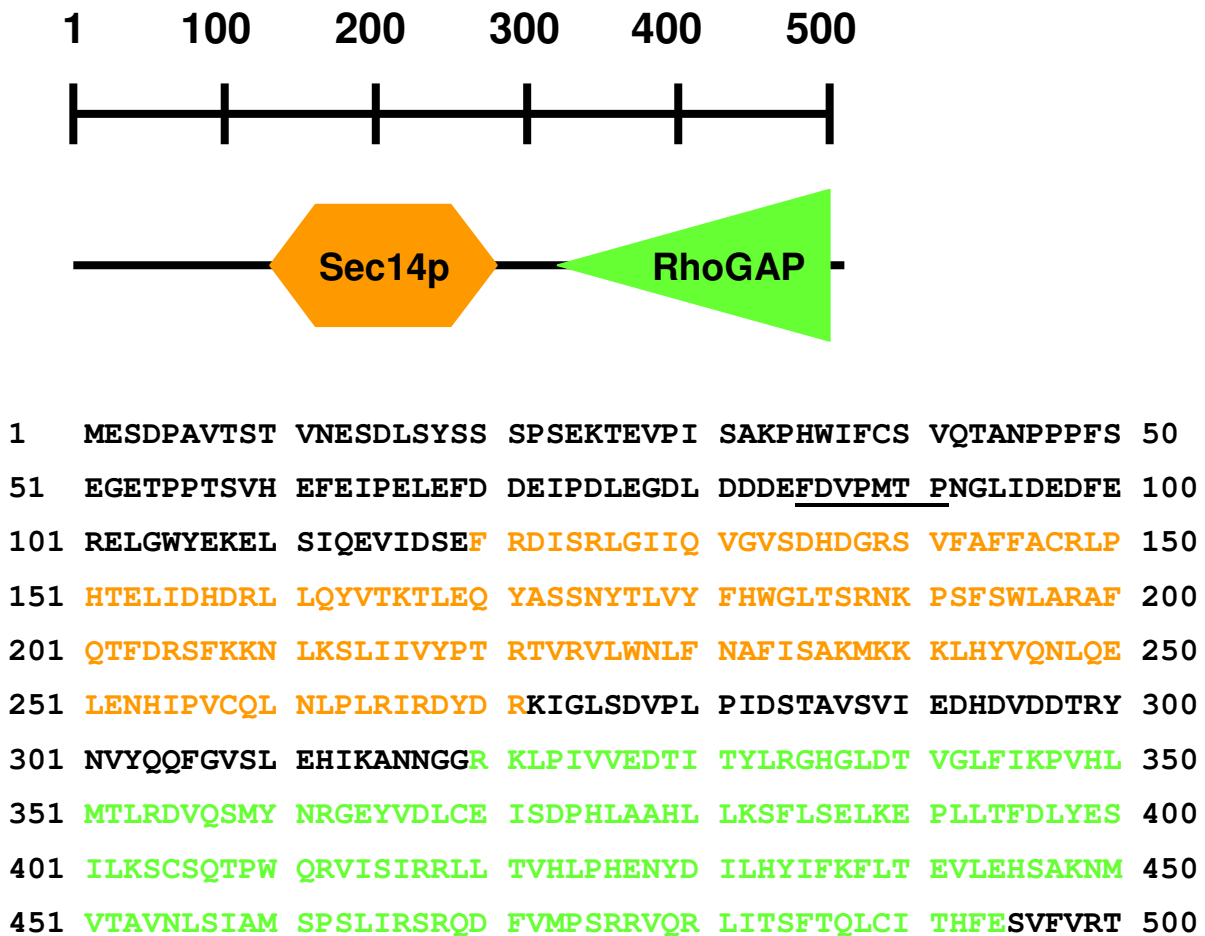


Fig. 52: Domain structure of EmRhoGAP and corresponding amino acid sequence. The predicted non-canonical SH3 binding motif in the N-terminal extension is underlined. The residues comprising the Sec14 domain are kept in orange while those comprising the RhoGAP domain are kept in green. The numbers indicate the relative position of the residue in the amino acid sequence.

A ClustalW [185] amino acid sequence alignment of EmRhoGAP with ARHGAP1 and ARHGAP8 from both human and murine origin as well as non-mammalian and invertebrate orthologs was carried out (Fig. 53). The most conserved domain in EmRhoGAP is the Sec14p/CalTrio domain with approximately 47% identical and 66% similar residues, while the similarity of the RhoGAP domain is in the range of the complete protein (35% identical and 59% similar residues). By *in vitro* binding studies could be shown, that the SH3 domains of Src and p85 α (PI3K adapter subunit) bind to a proline rich stretch in p50RhoGAP (K²²⁹PMPPRP²³⁵) located immediately N-terminal of the RhoGAP domain [208]. This motif corresponds to the consensus sequence for SH3 binding motifs (R/KxxPxxP) recognized by class I SH3 domains [209,210]. Very interestingly, this motif can only be found at a

homologous position in the vertebrate RhoGAPs used for the alignment. Although the homologous region of *C. elegans* RhoGAP, Rga-1, is rich in prolines this motif does not correspond to the consensus sequence of the SH3 binding motif. A computational analysis identified this region of Rga-1 as a potential motif for those SH3 domains with a non-canonical class I recognition specificity (Fig. 53) [210]. The *in silico* analysis of EmRhoGAP identified a single putative non-canonical SH3 binding motif in the N-terminal extension making EmRhoGAP a potential binding partner for SH3 domain containing proteins. Quite interestingly, this predicted SH3 binding motif is located in that region of the N-terminal extension which does not show any homology to the other RhoGAPs employed in the alignment (Fig. 52,53) [210]. Another point of interest was the identification of potential crucial residues. Although numerous proteins containing a RhoGAP domain are known which also exert overlapping substrate specificity *in vivo* as well as *in vitro*, they share a common activation mechanism by employing a so-called “arginine finger” motif to stabilize *in trans* the transition state of the GTP hydrolysis in the target protein [211-213]. For human ARHGAP1/p50RhoGAP this residue was identified and the recently described human ARHGAP8 as well as the other RhoGAPs used for the alignment possess an arginine residue at a homologous position [207,212]. In some way surprising, the alignment did not identify a homologous arginine residue for EmRhoGAP (Fig. 53). In contrast, for *D. melanogaster* and *C. elegans* a conserved arginine residue could be identified. While for the latter, the amino acid context is also well conserved, it is not in the case of *E. multilocularis* (Fig. 53). This may be due to a different mechanism by which EmRhoGAP stabilizes the transition state of GTP binding proteins. This assumption is supported by recent publications showing that human RanGAP and RapGAP use an arginine finger independent motif to stabilize the transition state of Ran-GTP and Rap-GTP, respectively [214,215].

	
	10 20 30 40 50 60	
EmRhoGAP	----MESDPAVTSITVNESDLSYSSSPSEKTEVPIISAKPHWIFCSVQTANPPPFSEGETEP	56
Rga-1 Ce	-MDTKHPPDFSGSPDPNINLGEFEDFVDGYADDDLTPDDL SVSVTGMPTRSRSFLETEEF	59
RhoGAP68F Dm	MDAHSRFAPRLPGPAINPIVDNSDEPQPSLSDLHDFEPKLEFDDETELLAPSPLEKDVMMVG	60
Rhogap68f Xl	-----MASDPLSDLNDDLDKDETNO-LDQLKSLASLDDKNWPSDDVQDYFNANNYSKPSPE	54
p50RhoGAP Hs	-----MDPLSELQDDLTLDLDTSEALNQLKSLASLDEKNWPSDEMPDFPKSDDSKSSSPE	53
Arhgap1 Mm	-----MDPLSELQDDLTLDLDTSQALNQLKSLASLDEKNWPSDEMPDFPKSDDSKSSSPE	53
ARHGAP8 Hs	-----MVIIRDKIRFYEEELQRDKAAAAAVLG-----AVRKRFSVVPMAQODE	42
Arhgap8 Rn	-----MAQLDF	6
Arhgap9 Mm	-----MAQLDF	6

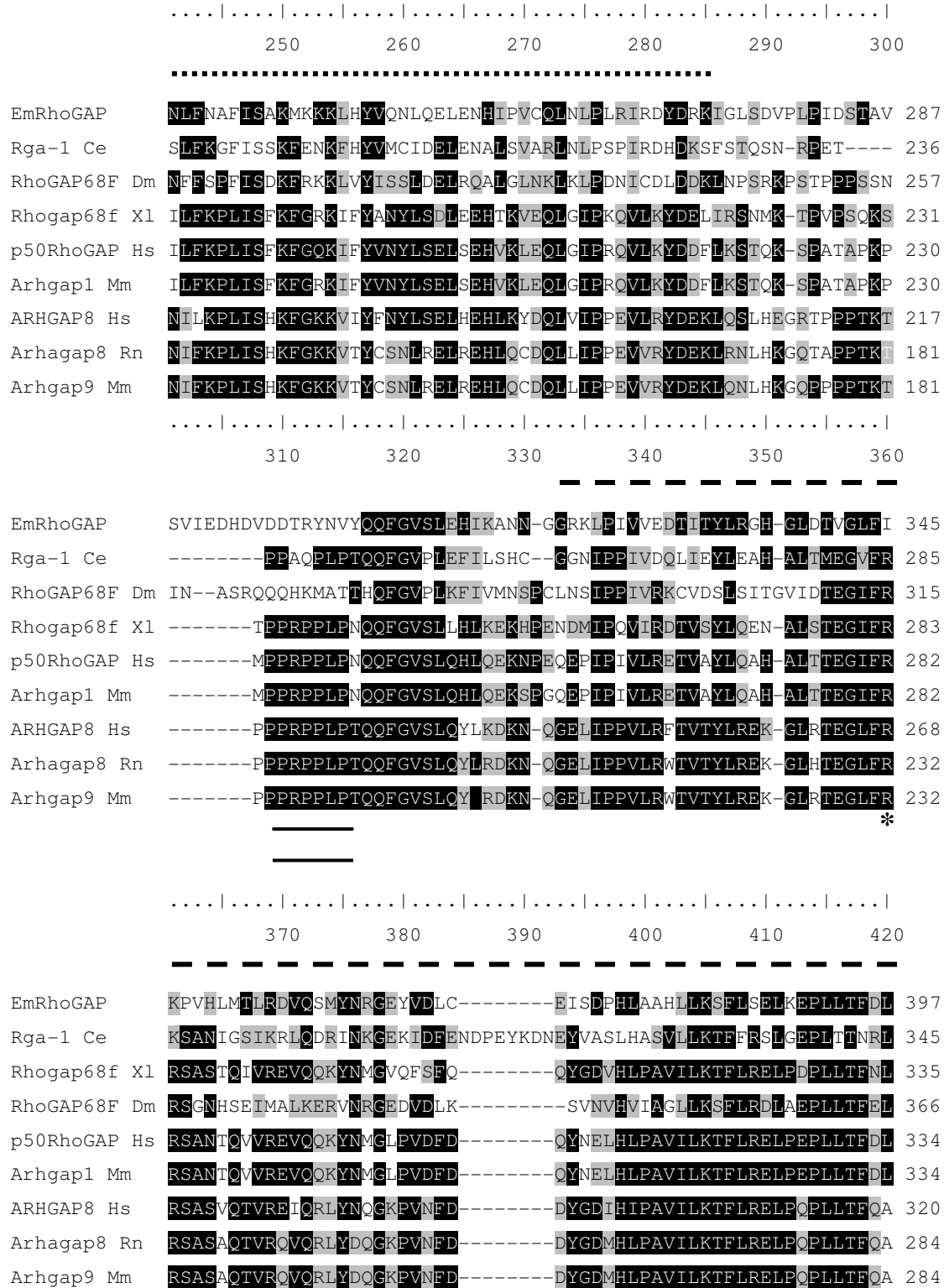
```

.....|.....|.....|.....|.....|.....|.....|.....|.....|.....|.....|
          70          80          90          100          110          120
          ───────────
EmRhoGAP      TSVHEFEIPELEFDDEIPDLEGLDLDDEDFVPMTPNGLIDEDFERELGWYEKELSIQEV 116
Rga-1 Ce      ETELG-----GVEPF 69
RhoGAP68F Dm  DFVLAEDPE-----LEPEEDVNPL 79
Rhogap68f Xl  P-----VTHLRW 61
p50RhoGAP Hs  L-----VTHLKW 60
Arhgap1 Mm    P-----VTHLKW 60
ARHGAP8 Hs    -----ALST 46
Arhgap8 Rn    -----TLST 10
Arhgap9 Mm    -----TLST 10

.....|.....|.....|.....|.....|.....|.....|.....|.....|.....|.....|
          130          140          150          160          170          180
          .....
EmRhoGAP      DSEFRDISRLGIIOVGVS-----DHDGRSVEAFFACRLPHTELIDHDRLLOYVTKT 167
Rga-1 Ce      EDLENDISAEHIIQVIADG-----DRVGRPIVVVYAYRLPSKEIDHARLLOYLVQI 121
RhoGAP68F Dm  EDDFEDQLREQSENFQTPRNKCDFLGTDKQGRHIFGIYASRFPEKSOLEG--FVRETIKE 137
Rhogap68f Xl  DDPFYDIARHQIVEVAGD-----DKYGRKTIIVFSACRLPACHEIDHVKLLQYLKHT 112
p50RhoGAP Hs  DDPFYDIARHQIVEVAGD-----DKYGRKTIIVFSACRMPPSHOLDHSKLLGYLKHT 111
Arhgap1 Mm    DDPFYDIARHQIVEVAGD-----DKYGRKTIIVFSACRMPPSHOLDHSKLLGYLKHT 111
ARHGAP8 Hs    SHPFYDVARHGILQVAGD-----DRFGRRVTFSCCRMPPSHEL DHQRLLLEYLKYT 97
Arhgap8 Rn    SHPFYDVARHGILQVAGD-----DRQGRRIE TFSCCRLPPLHQLNHQRLLLEYLKYT 61
Arhgap9 Mm    SHPFYDVARHGILQVAGD-----DRQGRRIE TFSCCRLPPLHQLNHQRLLLEYLKYT 61

.....|.....|.....|.....|.....|.....|.....|.....|.....|.....|.....|
          190          200          210          220          230          240
          .....
EmRhoGAP      LEQYASSNYTLVYFHWGLTSRNKPSFSWLRARAFQTFDRSFKKNLKSIIIVYPTRTVRVLW 227
Rga-1 Ce      IDKIIVDQDYTIVYFHYGLRSNKPVPVWLFQAYKQLDRRFKKNLKALYVVHPTRFIRIIF 181
RhoGAP68F Dm  IEPFVENDYILVYFHQGLKEDNKPSAQFLWNSYKELDRNFRKNLKTLYVVHPTWFRVIW 197
RhoGAP68f Xl  LDQYVESDYTLVYLLHHGLTSDNKPSLGWLRDAYREFDRKYKKNIKALYIVHPTMFIKTL 172
p50RhoGAP Hs  LDQYVESDYTLVYLLHHGLTSDNKPSLSWLRDAYREFDRKYKKNIKALYIVHPTMFIKTL 171
Arhgap1 Mm    LDQYVESDYTLVYLLHHGLTSDNKPSLSWLRDAYREFDRKYKKNIKALYIVHPTMFIKTL 171
ARHGAP8 Hs    LDQYVENDYTIVYFHYGLNSRNKPSLGWLSAYKEFDRKYKKNLKALYVVHPTSFIKVLW 157
Arhgap8 Rn    LDQYVENDYTIVYFHYGLSSQNKPSLGWLQAYKEFDRKYKKNLKALYVVHPTSLIKALW 121
Arhgap9 Mm    LDQYVENDYTIVYFHYGLSSQNKPSLGWLQNTYKEFDRKYKKNLKALYVVHPTSLIKALW 121

```



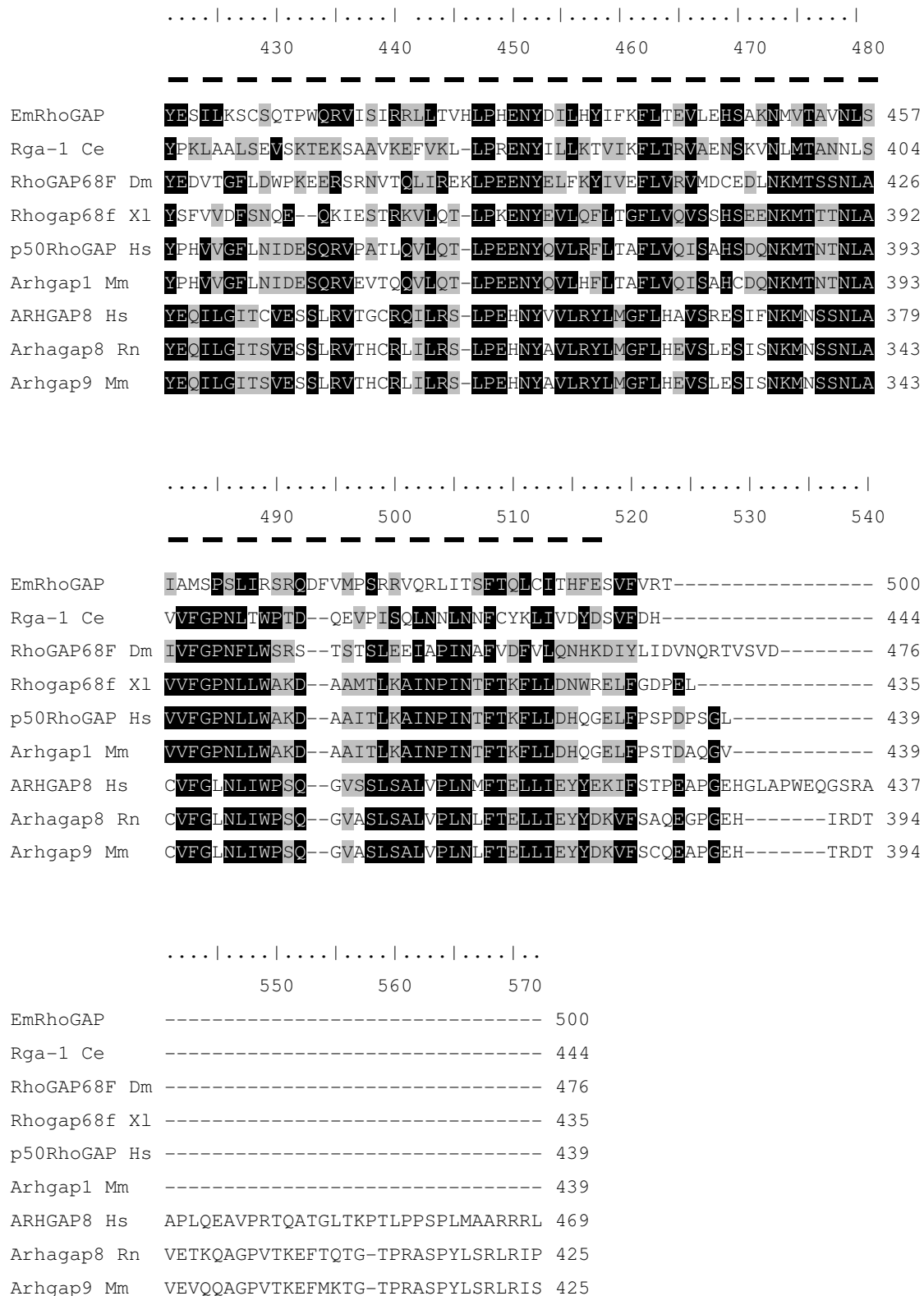


Fig. 53: Amino acid sequence alignment of EmRhoGAP with RhoGAPs originating from various species. Identical residues are shaded in black while similar residues are shaded in grey. This subclass of RhoGAPs is characterized by two conserved domains: an N-terminal Sec14p/CalTrio domain and a C-terminal RhoGAP domain. The predicted position the of the Sec14p/CalTrio domain RhoGAP domain in EmRhoGAP are indicated

by the dotted and dashed lines, respectively, and these domains share the highest identity with the orthologs from *Homo sapiens* (Hm), *Rattus norvegicus* (Rn), *Mus musculus* (Mm), *Xenopus laevis* (Xl), *Caenorhabditis elegans* (Ce) and *Drosophila melanogaster* (Dm). The conserved SH3 binding motif (PPRPPLP) among this family of vertebrate RhoGAPs is indicated by the double line while the conserved R residue within the RhoGAP domain is marked by the asterisk. The non-canonical SH3 binding motif in the EmRhoGAPs N-terminal extension is (FDVPMTP⁹¹) indicated by the solid line.

3.6.3.3 Analysis of *emfyn* cDNA

The identified cDNA containing the ORF coding for EmFyn was 2006 bp in total (including the poly-A-tail; Fig. 54). As for *emrhogap*, the spliced leader sequence could be identified at the cDNA's 5' end indicating that the complete cDNA was isolated. Among the 4 possible start codons identified in the 5' region (Fig.56) ATG²³ and ATG³⁹ would lead to the translation of peptides comprising only 8 and 58 residues, respectively, and are therefore not considered as the start codon. Although two in frame start codons are present in the longest ORF, the residues flanking ATG⁶⁴ correspond better to the Kozak consensus sequence (GCCRCCATGG; R = A or G) for translational initiation than for ATG⁴⁶ [204]. Therefore, ATG⁶⁴ was considered as the most likely start codon of a 1710 bp ORF coding for 570 aa which is limited by a TGA stop codon at position 1772 (Fig.56). No canonical polyadenylation signal is located within the 3' UTR, but with ATTAAC¹⁹⁷⁵ a hexamer almost corresponding to the consensus sequence could be found [205].

```

1 TCCTTACCTT GCAGTTTTGT ATGTTCCAG CCATTCATGC TTTATGAACT 50
51 CAAGTTGCAC A ATG GGG AAT TGT TTT ACT TGC CAC GAC CAC 91
1 M G N C F T C H D H 10

92 AAA GAA AAT CTT CAG TGC CAT GGA GAC AAT GGC ATG ACG CCG 133
11 K E N L Q C H G D N G M T P 24

134 ATG GGT GCA AAT TCC CAA GGG GGT GGC CAG GGA CTA GGG CAA 175
25 M G A N S Q G G G Q G L G Q 38

176 GCC CCA TTC GGT CGT CAC TAT GGT CCT TCA GGT GAC GCT GCA 217
39 A P F G R H Y G P S G D A A 52

218 TCG GTC GGT GCC AAT CAG TCC GCC ATT GTG CCT GCT TCG CGT 259
53 S V G A N Q S A I V P A S R 66

```

260 GGT GCA CAT CAA CCC TCC CAA CAG TAC TCC GTG AAT CTT TAC 301
 67 G A H Q P S Q Q Y S V N L Y 80

302 GGC ATG CAG AAT GGA CCA CAA CAG AGT GCA TCC TAC GCC TAC 343
 81 G M Q N G P Q Q S A S Y A Y 94

344 AGT CTC GCC CAA CCT CCC GCG ACT CTT GGC CAG CAG CTG GCA 385
 95 S L A Q P P A T L G Q Q L A 108

386 GAG CAG TCA CCT CGA GTT GTC CGT GTT CAC GCT TTA TAC ACT 427
 109 E Q S P R V V R V H A L Y T 122

428 TAC GTT GCG CAA AAC GCT GAT GAT CTG AGC TTC CAG AAG GGT 469
 123 Y V A Q N A D D L S F Q K G 136

470 GAT GTC ATG CTA GTC GAG TCG GGC TTA TCC GAA GCC TGG TGG 511
 137 D V M L V E S G L S E A W W 150

Z3-159N



512 TTG GCG CGT CAC TTG AGG ACC GGG CAA CAG GGC TAC ATA CCC 553
 151 L A R H L R T G Q Q G Y I P 164

554 AGT AAC TAT GTG ACT GTA GAA AAT GGT CTC TCT ACA CAA ATG 595
 165 S N Y V T V E N G L S T Q M 178

596 GAA GCC TGG TAT GAC ATT ACA CGT AAA GAT GCC GAG AGA ATG 637
 179 E A W Y D I T R K D A E R M 192

638 CTT TTG ATG CCC GGG TTG CCT CAA GGG ACT TAC ATT TTA CGC 679
 193 L L M P G L P Q G T Y I L R 206

680 CCC TGT TCC GAT TCC CGA AGT TAT GCT CTC TCC ATC CGG TTC 721
 207 P C S D S R S Y A L S I R F 220

722 GAA ATT GAG AGG AAT ATG TAT GCA ATA AAG CAC TAC AAG ATC 763
 221 E I E R N M Y A I K H Y K I 234

764 CGA ACT CGC GAT AAC GGT GCC GGC TTC TAC ATC ACC AAT CGA 805
 235 R T R D N G A G F Y I T N R 248

806 ACC AAC TTT GCT TCT GTC GCC GAT CTC ATC TCT CAC TAT CAG 847
 249 T N F A S V A D L I S H Y Q 262

848 TCC ACT AGC GAT GGG CTG TGC TGT CGC CTA TCG CAG CCG TGT 889
 263 S T S D G L C C R L S Q P C 276

890 CCG CGG AAG TAT ACC CCG CCG GTG CAG TTC CGT GAC ATC GAG 931
277 P R K Y T P P V Q F R D I E 290

932 GCA AAT CGG CGG AGC CTG GAA TTC ATC TGC GAG CTA GGC AAC 973
291 A N R R S L E F I C E L G N 304

974 GGC AGC TTC GGC ATG GTT TAC CGG GCT CGG TGG AAC AAG ACC 1015
305 G S F G M V Y R A R W N K T 318

1016 TTC GAC GTG GCG GTG AAG AAG CGC CTC GCT ACC ACG GAC CGC 1057
319 F D V A V K K R L A T T D R 332

1058 GCA CTT TTC ATT GAG GAA GCG AAA GTG ATG CAC AAA TTG CAT 1099
333 A L F I E E A K V M H K L H 346

1100 CAC CGC CGT ATC GTT CGC CTC CTC GGT GTC TGC ACC GAG CCG 1141
347 H R R I V R L L G V C T E P 360

1142 GCT GAT GAG CCT GTT TTC ATC ATC ACA GAG TTG CTA GAG AAG 1183
361 A D E P V F I I T E L L E K 374

1184 GGT GCT CTG CGC AAC TTC CTC AGC AGC GAA GAG GGC CGC CAA 1225
375 G A L R N F L S S E E G R Q 388

1226 CTC TTC CTC AGT GAC CTT ATC GAT ATG ATT GCT CAG ATT GCC 1267
389 L F L S D L I D M I A Q I A 402

1268 GAA GGA ATG GCA TAC CTG GAG GAG ATG AAT TTC GTC CAC CGA 1309
403 E G M A Y L E E M N F V H R 416

1310 GAC CTT CGA GCC GCC AAC ATC CTT GTG GAT CGC GAC AAC TCC 1351
417 D L R A A N I L V D R D N S 430

1352 GTC AAG GTA GCT GAT TTC GGA CTT GCA AAA ATG CTT GAT TCG 1393
431 V K V A D F G L A K M L D S 444

1394 GAT GTT CAA AAT GAT GGC GTC ATT AAA TTC CCC ATC AAG TGG 1435
445 D V Q N D G V I K F P I K W 458

1436 ACC GCG CCA GAG GCG GCT CTT CCC GAC CAC CAT TTC AGT ATA 1477
459 T A P E A A L P D H H F S I 472

1478 AAG TCG GAC GTC TGG TCC TTC GGT GTG CTC ATG TAC GAA ATC 1519
473 K S D V W S F G V L M Y E I 486

1520 GTC ACT TAC GGT GGC ACT CCC TAC CCC CGC TTC ACT AAT CGG 1561

```

487 V T Y G G T P Y P R F T N R 500

1562 GAG ACG GTA CAG CAG GTA GAG CGC GGC TAT CGA ATG CCA AAT 1603
501 E T V Q Q V E R G Y R M P N 514

1604 CCG AAT ACA CCG ACA CAG CCG TGT CCG GAC GAC CTC TAC GAC 1645
515 P N T P T Q P C P D D L Y D 528

                                Z3-159C
                                ←—————
1646 ATC ATG ATG CAG TGT TGG TCA GCA CGA CCC GAG GAT CGA CCT 1687
529 I M M Q C W S A R P E D R P 542

1688 ACC TTC CAC AAC CTC TAC GAC ATC TTT GAG AAC TGG GCC GTC 1729
543 T F H N L Y D I F E N W A V 556

1730 CAG ACG GAG GGT CAG TAC ATC TCG GAT GGA GCG CAA AAC ACT 1771
557 Q T E G Q Y I S D G A Q N T 570

1772 TGA ATCAGTCACC GCAGCCGCCG CCACCTCTAC AAAGACCGCG 1814
*

1815 TGTGATTGTC GTTTATCCAT CCACCCGATC TCTCCGCGCT GCATTTGACT 1864
1865 TCATCAATTC AATCCACCCT ATCCCCTTTC CCTCCTCTCA ACTGACTCCT 1914
1915 TCATGTCGAT TTTTTGACGC CTTGGCTTTC TCTTCTCTCA TGTTCTTTTG 1964
1965 CTAAGATTAA CACCGTCCCA ATAAGAAAAA AAAAAAAAAA AA 2006

```

Fig. 54: Nucleotide sequence of the cDNA containing the ORF coding for EmFyn. The spliced leader is marked by the solid bar. The possible start codons are indicated by bold letters while the stop codon is indicated by the asterisk. The putative polyadenylation signal is underlined.

3.6.3.4 Structural features of EmFyn

The 570 aa of EmFyn have a deduced isoelectric point of 6.1 and a molecular weight of 64.2 kDa [206] which is only slightly larger than the average 60.5 kDa calculated for the orthologous proteins. Members of the family Src tyrosine kinases are characterized by 4 domains: a SH4, SH3, SH2 and tyrosine kinase domain (from the N- to the C-terminus) [128, 139]. Employing the SMART program [198] and amino acid sequence comparison [185], these domains could also be identified in EmFyn (Fig. 55). For a better understanding, it should be noted that by convention, the numbering of the amino acid residues in chicken Src is used to describe essential residues in vertebrate Src-family kinases [128]. Therefore, the position number of a conserved residue may vary for a single Src-family kinase. The first 6

residues comprise the SH4 domain and in nearly all Src family kinases, including mammalian Fyn kinase, this domain contains the Met-Gly-Cys consensus sequence in which the Gly is co-translationally myristoylated, whereas the Cys is palmitoylated. This modification promotes plasma membrane targeting and membrane binding in general. In addition, Src-family kinases contain a stretch of basic residues immediately C-terminal to the SH4 domain supporting membrane binding by electrostatic interactions with acidic phospholipids [128,139,216]. Recently, Liang et al. identified that methylation of K⁷ and K⁹ in mammalian Fyn (Fig. 56) as important for the enzymatic function [216]. With Met-Gly-Asn-Cys, EmFyn has an amino acid sequence almost identical to the Met-Gly-Cys motif (Fig.55).

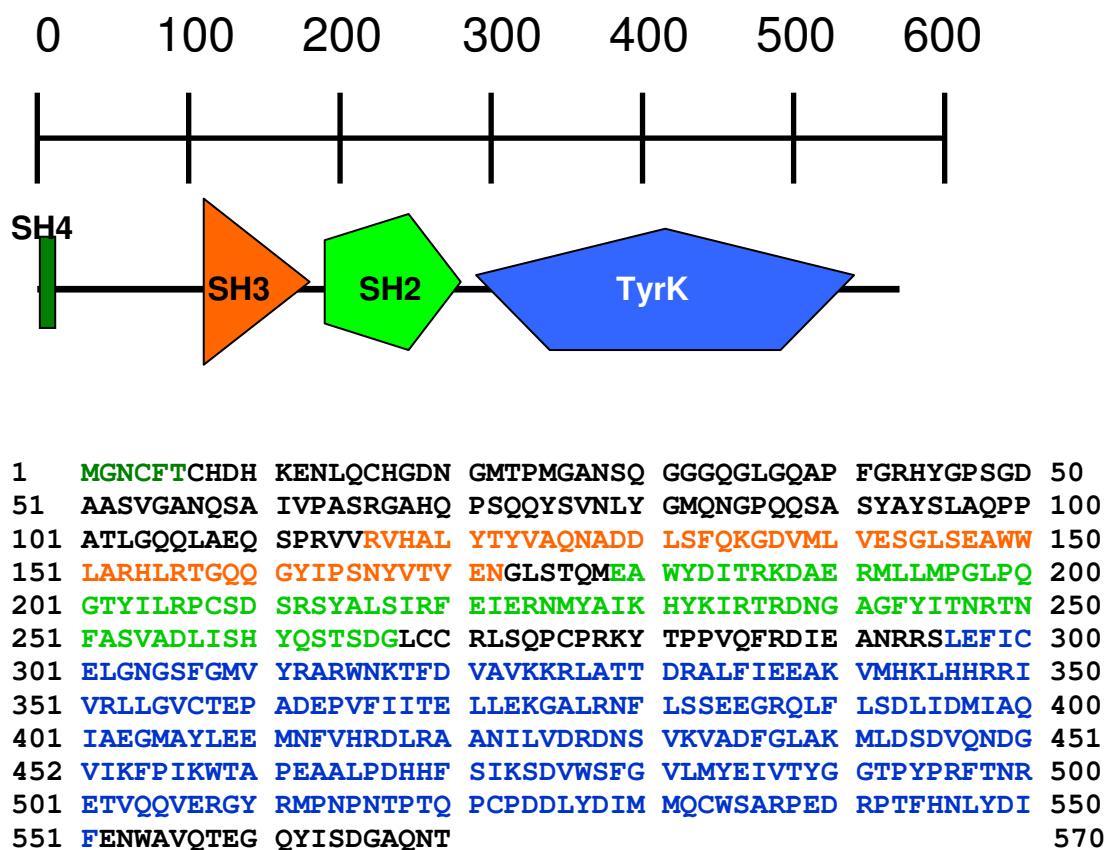


Fig. 55: Domain structure of EmFyn and corresponding amino acid sequence. The residues comprising the different domains of EmFyn are indicated by the different colors: SH4 - dark green; SH3 - orange; SH2 - green; tyrosine kinase (Tyrk) domain - blue.

The alignment of EmFyn with its homologs revealed that Met-Gly-Cys motif is present even in the Src family kinase identified in the sponge *Suberitus domuncula* as well as the teleost fish *Xiphophorus helleri*, but that in the Src-family kinases identified in platyhelminthes this motif is interrupted by the insertion of an Asn residue, as it is the case for the *S. mansoni* tyrosine kinase 5 (SmTK5) [141] and EmFyn, or reduced to Met-Gly in case of the planarian *Dugesia tigrina* Src-like protein kinase 1 (Spk-1) [217] (Fig. 56). Although the basic stretch is not well conserved comparing the amino acid sequence between the vertebrates and invertebrates Src-like kinases, the peptide comprising the first 20 residues of EmFyn contains four basic amino acids like human Fyn. In case of EmFyn 4 amino acids with an amide group in their side chain can additionally be found (Fig. 55,56), suggesting that this domain might also be involved in the location of EmFyn to the plasma membrane. The EmFyn SH4 and SH3 domain are connected via a stretch of approximately 100 residues without any homology to the other Src-family kinases used in the amino acid sequence alignment (Fig. 56). Although the corresponding stretch in SmTK5 [141] shares a similar length with EmFyn, it is highly divergent. The peptide connecting the SH4 and SH3 represents EmFyn's and SmTK5's "unique" domain and is significantly longer than the 50-70 residues comprising the highly divergent "unique" domain among the Src family members [128]. The SH3 domain in EmFyn limiting the "unique" domain stretch is predicted to comprise the residues 115 – 172 (Fig. 55) [198]. SH3 domains are generally known to bind to Pro-rich motifs thereby mediating protein-protein interactions [128]. With Tyr¹³⁶ within the SH3 domain of Src, a target site for PDGFR activity was identified. It was shown that the phosphorylation of this residue by PDGFR diminished the SH3 domain's ability to bind to its ligand [141,142]. With Y¹⁶⁷, a homologous tyrosine residue can be found in EmFyn (Fig. 56). The domain following C-terminally to the SH3 domain is the SH2 domain. It was found that Src-family SH2 domains bind preferentially to the pY-E-E-I motif but the residues at position +1 and +2 may vary [128]. For the phosphotyrosyl recognition pocket within the SH2 domain a highly conserved arginine residue could be identified which interacts electrostatically with the phosphorylated tyrosine [128]. With R²⁰⁶, EmFyn contains a residue homologous to R¹⁷⁵ in Src and R¹⁷⁶ in human Fyn (Fig. 56). It was also found that this domain is crucial for the autoregulation of Src's enzymatic activity [128]. In its inactive state, a conserved tyrosine residue within the C-terminal tail is phosphorylated by the cytoplasmic C-terminal Src kinase (Csk) thereby creating a binding site for the SH2 domain. This intramolecular binding inhibits Src's intrinsic kinase activity. Besides Src, the tyrosine residue is highly conserved among Src-family kinases [128,139,218] and with Tyr⁵⁶² the C-terminal tail of EmFyn contains a

tyrosine residue at a homologous position which indicates that the activity of EmFyn might also be regulated by an intramolecular interaction between its SH2 domain and the tyrosine phosphorylated C-terminal tail (Fig. 56). A further tyrosine (Tyr²¹³) residue at the C-terminal end of Src's SH2 domain was found to be phosphorylated in response to PDGF-stimulated cells which resulted in the reactivation of the kinase without the dephosphorylation of the regulatory tyrosine residue in the C-terminal tail. Since this tyrosine residue in the SH2 domain is highly conserved, Stovert et al. [218] suggested that a phosphorylation at this site might be a regulatory mechanism of all Src-like kinases. The comparison of the EmFyn amino acid sequence with those of other Src-like kinases (Fig. 56) did identify a tyrosine at position 244 which corresponds to position 213 in chicken Src and position 214 in human Fyn. A homologous tyrosine is also found in SmTK5 and Dt SPK-1 (Fig. 58) [141,217] which might indicate that this tyrosine residue is also crucial for the regulation of the enzymatic activity of Src-like kinases in platyhelminthes. Interestingly, a homologous tyrosine residue is not found in the sponge Src-like kinase (Fig. 56), indicating that this potential regulatory mechanism might have evolved later in evolution.

The most conserved domain among Src-like kinases is the tyrosine kinase (Tyrk) domain which was predicted to comprise the residues 296 – 551 in EmFyn (Fig. 55) [198]. A computational analysis [184] with this domain revealed a slightly higher similarity (52% identical, 68% similar residues) with the other Src-like kinases than for full length EmFyn. Further, several sequence motifs were identified which are characteristic for tyrosine kinases (Fig. 55,56). Among those are a canonical GxGxxG³⁰⁸ motif and further C-terminal an AxK³²⁴ motif as well as a critical E³³⁸ which have been shown to be involved in ATP binding, the catalytic loop with the HRDLRAAN⁴²² and DFG⁴³⁷- motif and other conserved residues (Fig. 56) [47,128]. Another regulatory tyrosine phosphorylation occurs in the activation loop of Src. The dephosphorylation of the inhibitory tyrosine residue in the C-terminal tail leads to the autophosphorylation of tyrosine 416 which in turn triggers Src into its active state [128]. This activatory tyrosine residue is found in the vertebrate Src-family kinases as well as in SdSrc-1 [141]. In case of the platyhelminthes, a homologous tyrosine residue is only found for SmTK5 [141].

		
		190 200 210 220 230 240	
EmFyn	181	WYD--ITRKDAERMLLMPGLPQGTYYILRPCSDSR-SYALSIRFEIERNMY---ATIKHYKI	234
SmTK5	179	WEMPMLSRKDSERLLLEGNAGVFLVRESETSQGSLLTSVRDEERGLSGIMNTVKHYRI	238
Dt SPK-1	100	EAWREIQRWEAEKSLMKIGLQKGTYYIIRPS-RKENSYALSVRDFDEKKK--ICIVKHFQI	156
Sd Src 1	127	WYYGDVTRAEAEKWLFLFPGNPSCGTFLVRTSSQKSGVSLSVRDGE-----SIKHYRI	178
Xh p59 Fyn	149	WYFGKLGKDAERQLLSTGNPRGTYYLIRESETTKGAFSLSIRDWDEKGG---DHVKHYKI	205
Xl cfyn-a	149	WYFGKLGKDAERQLLSTGNPRGTYYLIRESETTKGAYSLSIRDWDDMKG---DHVKHYKI	205
Hs Fyn	149	WYFGKLGKDAERQLLSTGNPRGTFLIRESETTKGAYSLSIRDWDDMKG---DHVKHYKI	205
Mm Fyn	149	WYFGKLGKDAERQLLSTGNPRGTFLIRESETTKGAYSLSIRDWDDMKG---DHVKHYKI	205
Rn Fyn	149	WYFGKLGKDAERQLLSTGNPRGTFLIRESETTKGAYSLSIRDWDDMKG---DHVKHYKI	205
		
		250 260 270 280 290 300	
EmFyn	235	RIR-DNGAGFYITNRTNFASVADLISHYQSTSDGLCCRLSQPCPR---KYTPPVQFRD-	288
SmTK5	239	KHP-DYRY-YYITTKCSFSSLQELIQFYISDHSGLCCCKLTRACLCPPIITSDLVSKTKDH	296
Dt SPK-1	157	KTLDQDEKGISYVSNIRNFPNILLTIQFYEKNGIG--NTHIPLTDFMPDNYQPPVHFQD-	212
Sd Src 1	179	RRL-DDGG-YFIASRATFRDLSDLIEHYSRDSGLAQRLTLPCPR-ADLPQTGGLSYRDE	235
Xh p59 Fyn	206	RKL-DSGG-YYITTRAQFDTLQQLVQHYSDRAAGLCCRLVVPCHKGMPRLADLSVTKDVK	263
Xl cfyn-a	206	RKL-DNGG-YYITTRAQFEALQQLVQHYSERAAAGLCCRLVVPCHKGMPRLTDLVSKTKDV	263
Hs Fyn	206	RKL-DNGG-YYITTRAQFETLQQLVQHYSERAAAGLCCRLVVPCHKGMPRLTDLVSKTKDV	263
Mm Fyn	206	RKL-DNGG-YYITTRAQFETLQQLVQHYSERAAAGLCCRLVVPCHKGMPRLTDLVSKTKDV	263
Rn Fyn	206	RKL-DNGG-YYITTRAQFETLQQLVQHYSERAAAGLCCRLVVPCHKGMPRLTDLVSKTKDV	263
		
		310 320 330 340 350 360	
EmFyn	289	IEANRRSLEFICELGNGSFGMVYRARWNKTFDVAVK-KRLATIDRALFIEEAKVMHKLHH	347
SmTK5	297	WEISKSSIVLIEKLGAGQFGEVWVKTWNGTTEVAVKTLKQGTMTKEDFLKEARIMRAAQH	356
Dt SPK-1	213	IEINRENIEILNEIGRGFFGSVHRAKWGRSYEVAAKMLQSSKAEREKFFVLEAKIMHKLIRH	272
Sd Src 1	236	WEIDRSTLVFQKKLGGQGNFGEVWVSGVWNGTTPVAIKTLKTGTMEVKDFVAEAQVMKKIHH	295
Xh p59 Fyn	264	WEIPRESLQLIKRLGNGQFGEVWVWGTWNGTTPVAIKTLKPGTMSPEFLEEAQIMKKLIRH	323
Xl cfyn-a	264	WEIPRESLQLIKRLGNGQFGEVWVWGTWNGTTPVAIKTLKPGTMSPEFLEEAQIMKKLKH	323
Hs Fyn	264	WEIPRESLQLIKRLGNGQFGEVWVWGTWNGTTPVAIKTLKPGTMSPEFLEEAQIMKKLKH	323
Mm Fyn	264	WEIPRESLQLIKRLGNGQFGEVWVWGTWNGTTPVAIKTLKPGTMSPEFLEEAQIMKKLKH	323
Rn Fyn	264	WEIPRESLQLIKRLGNGQFGEVWVWGTWNGTTPVAIKTLKPGTMSPEFLEEAQIMKKLKH	323
		* * * * * * *	

		
		370 380 390 400 410 420	
EmFyn	348	RRI V RLLG V CT E PA D E P V F I I T E L L E K G A L R N F L S S E E G R O L F L S D L I D M I A Q I A E G M A Y	407
SmTK5	357	P K L V R L Y A V C T --- E D P I Y I V T E L M C N G S L L O Y L R D G P G K N L L I N Q L V D M M A Q I A N G M A Y	413
Dt SPK-1	273	R K I V E L L G V C T E P D M P M L I I V E Y M K N G S L K E Y L K T P D G K K T N L N Q M V H M M A E I S E G M A Y	332
Sd Src 1	296	P N L L Q L Y A V C T L ---E E P I Y I V T E L M K H G S L L E Y L R H C D G R S I S I H Q A I D M I A Q I T S G M A Y	353
Xh p59 Fyn	324	D K L V Q L Y A V S ---E E P I Y I V T E Y M S K G S L L D F L K D G E G R A L K L P N L V D M A A Q V A A G M A Y	380
Xl cfyn-a	324	D K L V Q L Y A V S ---E E P I Y I V T E Y M S K G S L L D F L K D G E G R A L K L P N L V D M A A Q V A A G M A Y	380
Hs Fyn	324	D K L V Q L Y A V S ---E E P I Y I V T E Y M N K G S L L D F L K D G E G R A L K L P N L V D M A A Q V A A G M A Y	380
Mm Fyn	324	D K L V Q L Y A V S ---E E P I Y I V T E Y M S K G S L L D F L K D G E G R A L K L P N L V D M A A Q V A A G M A Y	380
Rn Fyn	324	D K L V Q L Y A V S ---E E P I Y I V T E Y M N K G S L L D F L K D G E G R A L K L P N L V D M A A Q V A A G M A Y	380
		
		430 440 450 460 470 480	
EmFyn	408	L E E M N F V H R D L R A A N I L V D R D N S V K V A D F L G L A K M L D S D --- V Q N D G V I K F P I K W T A P E A A	464
SmTK5	414	L E K E H Y I H R D L A A R N I L V G E N N C V K V A D F L G L A R M V E D H Y C T Y M A Q K S T K F P I K W T A P E A A	473
Dt SPK-1	333	SE K V V H R D L R A D N I L V A N D L T R K V A D F L G L T E L T D G S -L G D Q E K K T L R F P Y K W T A P E A A	391
Sd Src 1	354	L E E H N Y L H R D L A A R N I L V G E N V C K V A D F L G L A R L I K E D ---I Y N P R E G T K F P I K W T A P E A A	411
Xh p59 Fyn	381	I E R M N Y I H R D L R S A N I L V G D N L V C K I A D F L G L A R L I E D N --- E Y T A R Q A K F P I K W T A P E A A	438
Xl cfyn-a	381	I E R M N Y I H R D L R S A N I L V G N L I C K I A D F L G L A R L I E D N ---E Y T A R Q A K F P I K W T A P E A A	438
Hs Fyn	381	I E R M N Y I H R D L R S A N I L V G N L I C K I A D F L G L A R L I E D N ---E Y T A R Q A K F P I K W T A P E A A	438
Mm Fyn	381	I E R M N Y I H R D L R S A N I L V G N L I C K I A D F L G L A R L I E D N ---E Y T A R Q A K F P I K W T A P E A A	438
Rn Fyn	381	I E R M N Y I H R D L R S A N I L V G N L I C K I A D F L G L A R L I E D N ---E Y T A R Q A K F P I K W T A P E A A	438
		**** *	***
		
		490 500 510 520 530 540	
EmFyn	465	L P D H H F S I K S D V S F G V L M Y E I V T Y G G T P Y P R F T N R E T V Q Q V E R G Y R M P N P N --- T P T Q P C	522
SmTK5	478	L M G --- R F T I K S D V S F G I V I Y E L I T L G O V P Y P S M N T E T L H Q V S T G Y R M P R F ----- V N C	526
Dt SPK-1	392	K S K --- V F T S K S D V S Y G I V M F E L L T W A S S P Y P D I P A K E V I E K V S K G Y R M P N P E K F I T G V C C	450
Sd Src 1	412	L Y N --- R F S I K S D V S F G V V I S E V V T K G A M P Y P G M N R Q V L E A V D R G Y R M P R F ----- E S A	464
Xh p59 Fyn	439	L Y G --- R F T I K S D V S F G I L L T E L V T K G R V P Y P G M N R E V L E Q V E R G Y R M P C P ----- Q D C	491
Xl cfyn-a	439	L Y G --- R F T I K S D V S F G I L L T E L V T K G R V P Y P G M N R E V L E Q V E R G Y R M P C P ----- Q D C	491
Hs Fyn	439	L Y G --- R F T I K S D V S F G I L L T E L V T K G R V P Y P G M N R E V L E Q V E R G Y R M P C P ----- Q D C	491
Mm Fyn	439	L Y G --- R F T I K S D V S F G I L L T E L V T K G R V P Y P G M N R E V L E Q V E R G Y R M P C P ----- Q D C	491
Rn Fyn	439	L Y G --- R F T I K S D V S F G I L L T E L V T K G R V P Y P G M N R E V L E Q V E R G Y R M P C P ----- Q D C	491

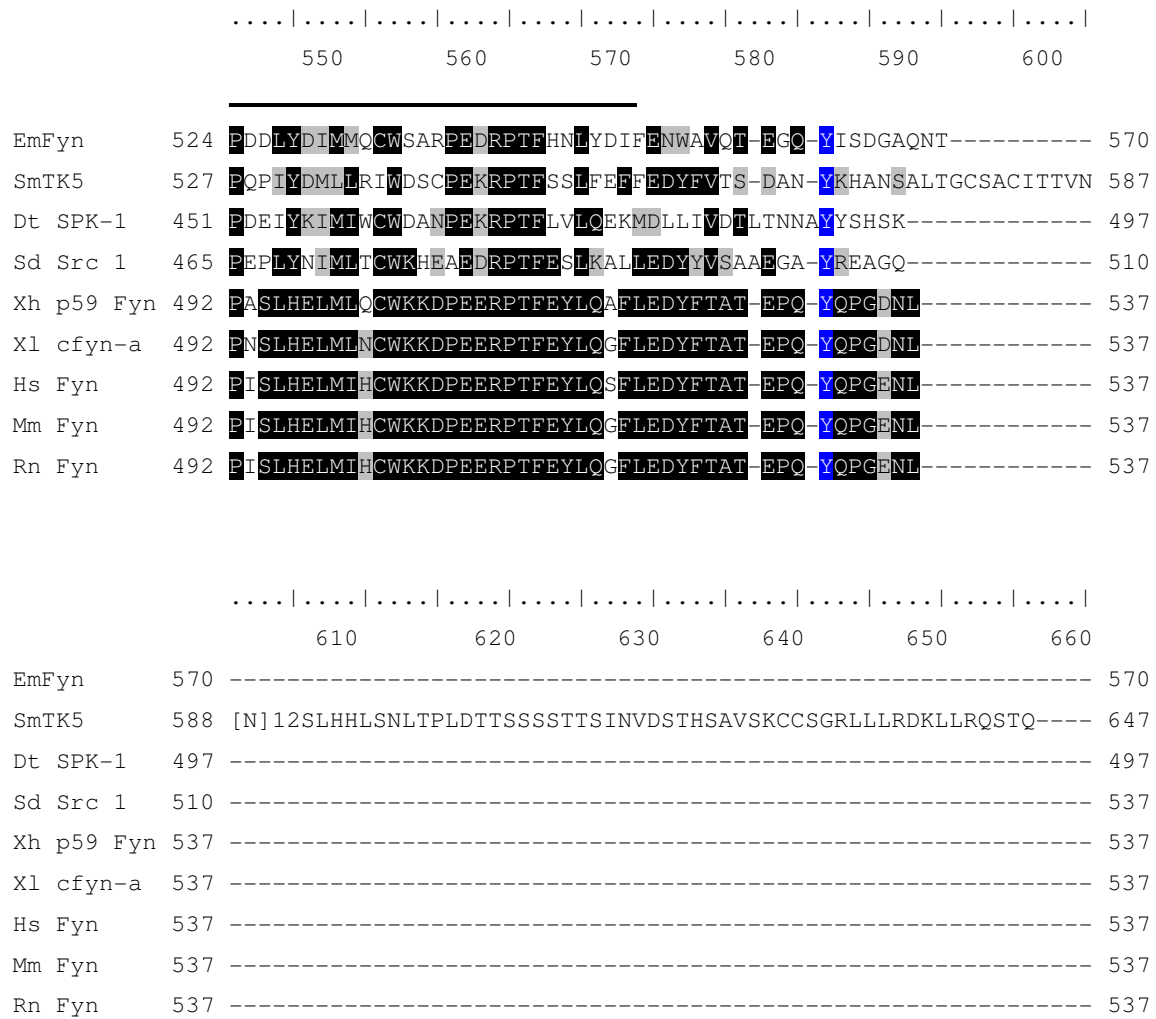


Fig. 56: Amino acid sequence alignment of EmFyn with Fyn-like kinases from distantly related species.

Identical residues are highlighted by black boxes, while similar residues are highlighted by grey boxes. Conserved residues most likely to be involved the regulation of EmFyn are shaded in blue, while conserved residues between tyrosine kinases are marked by asterisks. The alignment was carried out using the CLUSTALW method but was manually modified at the N- and C-terminus to improve the quality of the alignment. The Fyn-like kinases are characterized by 4 domains and the position of these domains in EmFyn predicted by the SMART program are indicated: SH4 (aa 1-6), dashed line; SH3 (aa 115-172), dotted line; SH2 (aa 179-267), dashed/dotted line; tyrosine kinase domain (aa 296-551), solid line. The putative regulatory tyrosine residues in the tyrosine kinase domain of Hs Fyn (Y³²⁰) and the conserved tyrosine residue in the other Fyn-like kinases are indicated. For EmFyn, no tyrosine residue could be identified which was homologous to the regulatory tyrosine residue in the kinase domain. In contrast, the other regulatory tyrosine residue in the short C-terminal region is conserved (Hs Fyn: Y⁵³¹; EmFyn: Y⁵⁶²) and is also indicated. EmFyn: *Echinococcus multilocularis* Fyn ; SmTK5: *Schistosoma mansoni* tyrosine kinase 5, Dt SPK-1: *Dugesia tigrina* Sd Src-1; Sd Src 1: *Suberitus domuncula* Src kinase 1 Xh p59Fyn: *Xiphophorus helleri* p59Fyn ; Xl cfyn-a: *Xenopus laevis* cfyn-a ; Hs Fyn: *Homo sapiens* Fyn; Mm Fyn: *Mus musculus* Fyn; Rn Fyn: *Rattus norvegicus* Fyn.

3.6.3.5 Analysis of the expression of *emfyn* and *emrhogap* in *E. multilocularis* larval stages

The expression of *emfyn* and *emrhogap* in *E. multilocularis* metacystode vesicles (isolate H95) *in vitro* as well as in inactivated (PS) and activated protoscoleces (PSact) (isolate Java) were analyzed by RT-PCR using gene specific oligonucleotides (Tab. 5). *emfyn* and *emrhogap* were approximately equally expressed in the metacystode larval stage, but the expression in PS and PSact was lower and different (Fig. 57). While *emfyn* was not expressed in PS but in PSact, it was vice versa for *emrhogap*. Since *emfyn* and *emrhogap* are both expressed in *E. multilocularis* metacystode vesicles together with *emir*, it might be possible that the encoded proteins are members of an EmIR downstream signalling cascade.

<u>Gene</u>	<u>Oligonucleotides</u>
<i>emfyn</i>	Z3-159N x Z3-159C
<i>emrhogap</i>	Z2-123-1 x Z2-123-2

Tab. 5: Oligonucleotides used in the RT-PCR analysis of the expression of *emfyn* and *emrhogap* in different *E. multilocularis* larval stages.

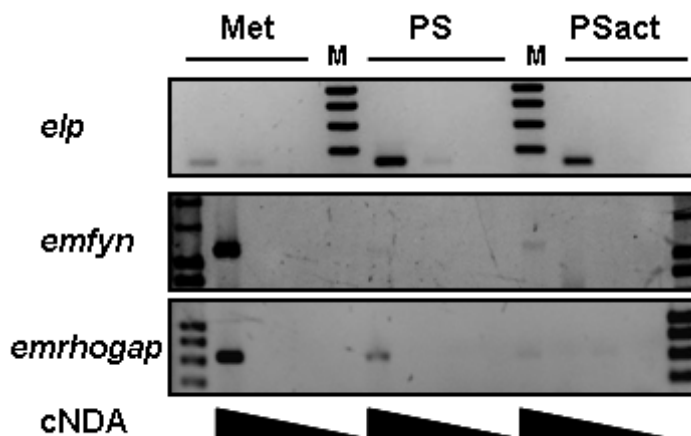


Fig. 57: Expression of *emfyn* and *emrhogap* in different *E. multilocularis* larval stages. Total RNA isolated from *in vitro* cultivated metacystode vesicles (Met) as well as from non-activated (PS) and activated protoscoleces (PSact), was DNase I treated and reversely transcribed with the Omniscript (QIAGEN) and a poly-d(T) oligonucleotide (CD3RT). The first strand cDNA was serially diluted (10-fold in each step) and the expression of *emfyn* and *emrhogap* were analyzed by PCR using gene specific oligonucleotides. The samples were normalized for the expression of *elp*.

3.6.3. 6 Analysis of the expression of *emfyn* and *emrhogap* in insulin stimulated *E. multilocularis* metacystode vesicles

The data presented in this study clearly revealed that insulin exerts a proliferative effect on *E. multilocularis* metacystode vesicles *in vitro*. The induction of *de novo* DNA synthesis suggests that the proliferation coincides with an increased cell division which is characterized by a massive rearrangement of the cytoskeleton. It has been described that RhoGTPases are involved in this rearrangement [223]. With EmFyn and EmRhoGAP, two proteins have been identified in *E. multilocularis* metacystode vesicles which could be involved in cytoskeleton rearrangement events. Therefore, the effect of exogenous insulin on the expression of *emfyn* and *emrhogap* was analyzed. The stimulation of metacystode vesicles which had been kept under low serum (0.2% FCS) conditions for 4 days with 100 nM human insulin for 24h slightly upregulated the expression of *emfyn*, while the expression of *emrhogap* was not affected (Fig. 58), identifying *emfyn* as a further *Echinococcus* gene probably regulated by insulin. .

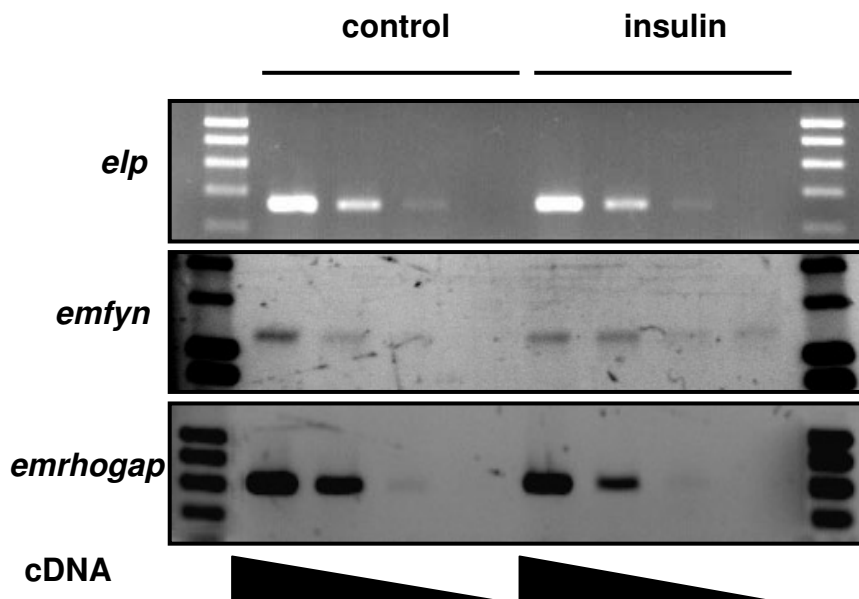


Fig. 58: Expression of *emfyn* and *emrhogap* in metacystode vesicles after the stimulation with human insulin. *in vitro* cocultivated metacystode vesicles were incubated for 4d in medium 0.2% FCS and were then stimulated for 24h with 100 nM insulin. Total RNA (DNase I) treated was reversely transcribed with the Omniscript (QIAGEN) and the poly-d(T) oligonucleotide CD3RT. The expression of *emfyn* and *emrhogap* in relation to *elp* was analyzed by PCR using gene specific oligonucleotides and serially diluted (10-fold in each step) first strand cDNA.

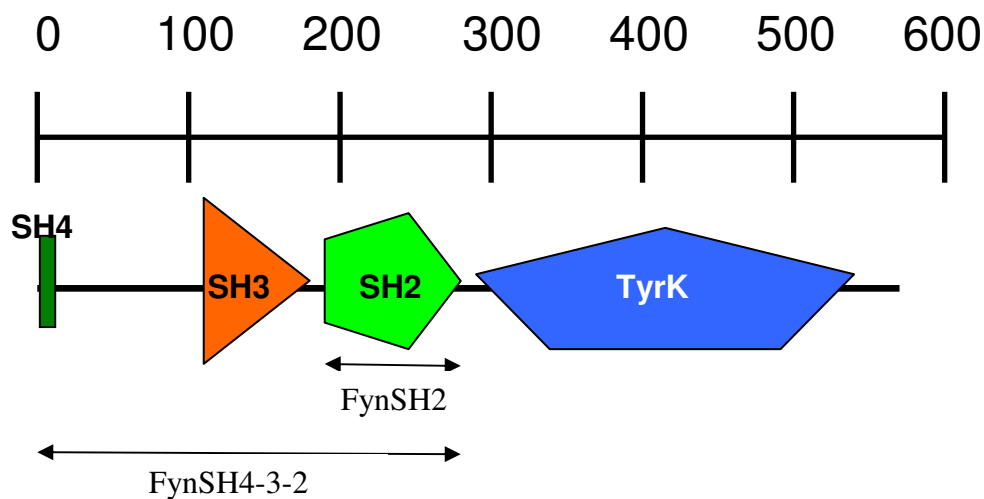
3.6.3.7 Interaction between EmFyn and EmIR *in vitro*

It has been demonstrated that in mammalian cells Fyn – kinase is recruited to the insulin receptor by binding to IRS-1 after the stimulation with insulin and that this interaction depended on the SH2 domain of Fyn. The authors could further show that Fyn phosphorylated specific tyrosine residues of IRS-1 [129]. EmFyn possesses a predicted SH2 domain and SH2 domains in general are known to bind to phosphorylated tyrosines located in conserved motifs. The intracellular domain of EmIR contains a conserved NPXY – motif in juxtamembrane region (NPEY¹¹⁴⁹) and in the C-terminal extension (NPSY¹⁷¹¹) [79]. Since no IRS ortholog has been identified yet in *E. multilocularis*, the question arose if EmFyn could interact with EmIR. The Yeast Two Hybrid System was used to identify downstream binding partners of both mammalian IR and IGF-IR and to reveal that the receptors intrinsic kinase activity was required for this interaction [112,193,201,219]. Therefore, the complete putative intracellular domain of EmIR was expressed with the N-terminal fused GAL4-BD domain both as WT and also with a K1209A substitution (BD-EmIR_{intra} WT, BD-EmIR_{intra} K1209A). This lysine residue is in a homologous position to the critical lysine in the ATP binding site (K¹⁰¹⁸ in HIR, K¹⁰⁰³ in HIGF-IR) whose substitution for an alanine residue abolishes the HIR's kinase activity *in vitro* [192]. When EmFynSH4-3-2 fused to the AD - domain (AD- EmFynSH4-3-2) was co-expressed with BD-EmIR_{intra} in AH109, it interacted with both the wildtype and the K1209A mutant under high stringency conditions, while the SH2 domain was not sufficient for an interaction (Fig. 59, lane 6 and 9). As a control, the intracellular domain of HIR fused to the BD-domain (BD-HIR) was also coexpressed with the EmFyn-constructs. Quite surprisingly, *S. cerevisiae* AH109 co-expressing BD-HIR and AD-FynSH4-3-2 grew already after 4d of incubation (Fig. 59, lane 3) as did the positive control (Fig. 59, lane 18). Since the yeast cells coexpressing AD-FynSH4-3-2 and BD-EmIR_{intra} had to be incubated for 7d to be grown almost as well as the positive control, the interaction of AD-EmFyn SH4-3-2 with BD-HIR_{intra} seemed to stronger than with BD-EmIR_{intra}. It was even more surprising, that in contrast to EmIR, the SH2 domain of EmFyn fused to the AD-domain (AD-EmFynSH2) alone was sufficient for an interaction with HIR (Fig. 59, lane 2), suggesting that EmIR in contrast to HIR is not tyrosine phosphorylated *in vitro*. Although the intracellular domain of EmIR exerts all characteristics of a RTK of the insulin/IGF-I family it differs in having a of 172 residue insert within the kinase domain which is absent in HIR and suggested to play a role in the regulation of downstream signalling cascades emanating from EmIR [79]. Therefore, EmIR_{intra} lacking this peptide (BD-EmIR_{intra}Δ172) was co-expressed

with the AD-fusion proteins. But EmFynSH2 did not interact with BD-EmIR Δ 172 (Fig. 59, lane 5 and 14). In contrast to full length EmIR_{intra}, the cells expressing the truncated intracellular domain as BD-fusion and AD-EmFynSH4-3-2 (Fig. 59, lane 12 and 15) grew as fast as those cells expressing BD-HIR_{intra} and AD-EmFynSH4-3-2 (Fig. 59, lane 3).

A)

Number	BD	AD	selection for plasmids	4 days high stringency	7 days high stringency
1	HIR _{intra}	AD	++++	-	-
2	HIR _{intra}	Fyn SH2	++++	++++	++++
3	HIR _{intra}	Fyn SH4-3-2	++++	++++	++++
4	EmIR _{intra} WT	AD	++++	-	-
5	EmIR _{intra} WT	Fyn SH2	++++	-	-
6	EmIR _{intra} WT	Fyn SH4-3-2	++++	-	+++
7	EmIR _{intra} mut	AD	++++	-	-
8	EmIR _{intra} mut	Fyn SH2	++++	-	-
9	EmIR _{intra} mut	Fyn SH4-3-2	++++	-	+++
10	EmIR _{intra} Δ 172 WT	AD	++++	-	-
11	EmIR _{intra} Δ 172 WT	Fyn SH2	++++	-	-
12	EmIR _{intra} Δ 172 WT	Fyn SH4-3-2	++++	++++	++++
13	EmIR _{intra} Δ 172 mut	AD	++++	-	-
14	EmIR _{intra} Δ 172 mut	Fyn SH2	++++	-	-
15	EmIR _{intra} Δ 172 mut	Fyn SH4-3-2	++++	++++	++++
16	BD	Fyn SH2	++++	-	-
17	BD	Fyn SH4-3-2	++++	-	-
18	p53	SV T40- antigen	++++	++++	++++
19	p53	lamin C	++++	-	-



B)

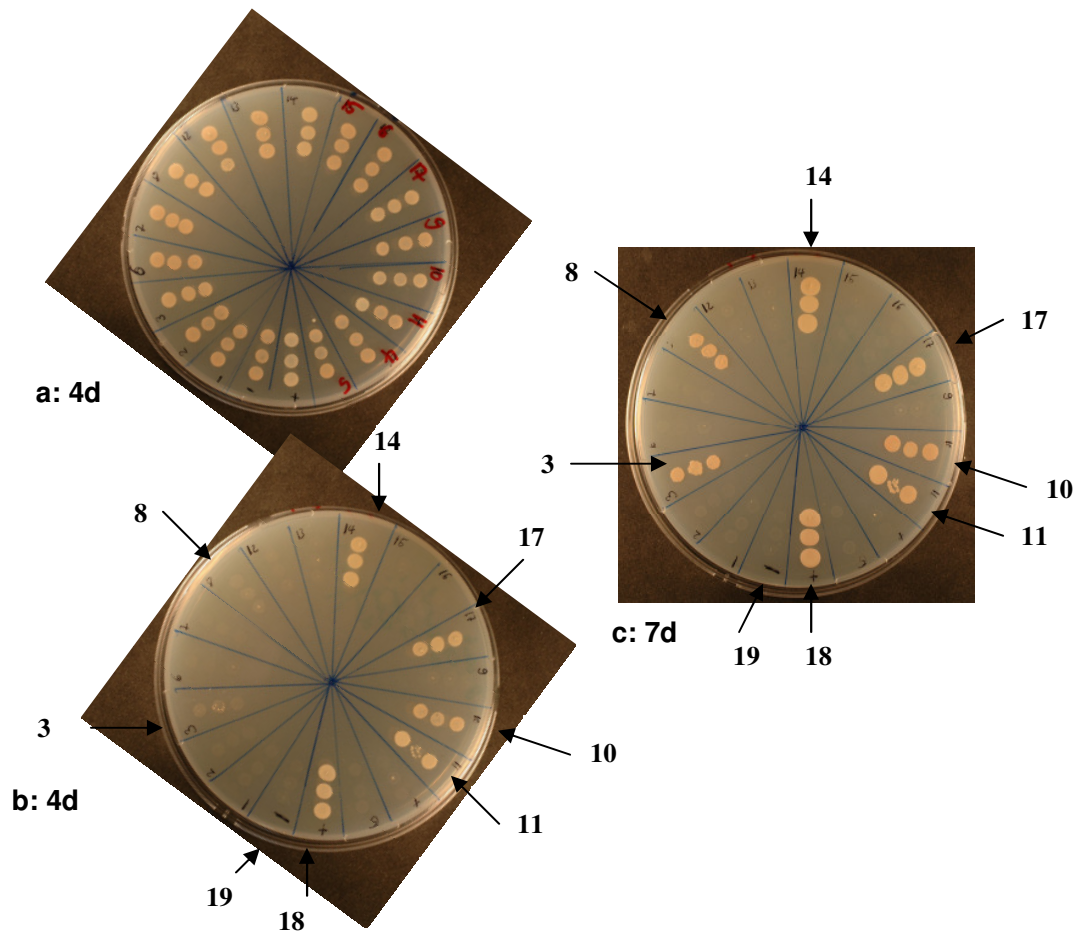


Fig. 59: Yeast Two Hybrid analysis of the interaction of EmIR intracellular domain with EmFyn. The intracellular domain of EmIR (EmIR_{intra}) and the intracellular domain in which the 172 aa insert had been deleted (EmIR_{intra}Δ172) were expressed fused to the GAL4-DNA binding domain (BD) and expressed in *S. cerevisiae* AH109. In both constructs a K1209A substitution was introduced to abolish kinase activity (EmIR_{intra} K1209A; EmIR_{intra}Δ172 K1209A). These constructs were coexpressed with the SH2 domain of EmFyn (EmFynSH2) and EmFyn lacking the kinase domain and the short C-terminal tail (EmFynSH4-3-2) fused to the GAL4 activation domain (AD). As controls, the constructs were coexpressed with BD and AD alone, respectively. The growth of the cotransformants was compared to the growth of the positive and negative controls included in the Yeast Two Hybrid System. Positive control: BD-p53 x AD-T; Negative control: BD-p53 x AD-lamin C; -: no growth; +, ++, +++, +++++: growth. **A)** Summarized results of the yeast two hybrid interaction studies. **B)** Pictures of the yeast clones growing on the respective selection plates: growth under plasmid selective conditions after 4d (a) and growth of under high stringency conditions after 4 (b) and 7d (c).

Taken together, the presented data suggest that EmFyn interacts with EmIR *in vivo* and suggest again that the additional 172 residue peptide within EmIR's tyrosine kinase domain is involved in the regulation of downstream signaling cascades.

3.6.3.8 EmFyn and EmRhoGAP interact in the Yeast Two Hybrid

Since *emfyn* and *emrhogap* are both expressed in *E. multilocularis* metacystode vesicles *in vitro* and the former codes for a SH3 domain containing protein and the latter for a protein with putative non-canonical SH3 binding motif, a possible interaction of EmFyn and EmRhoGAP was analyzed. Until the identification of EmRhoGAP no GAP protein has been characterized for cestodes and no Rho protein has been either. But with EmRas [82], EmRap1 and EmRap2 [2] orthologs of the other subfamilies of the Ras-superfamily of small GTP binding proteins [125] have been characterized for *E. multilocularis*. It has been described that a certain GAP protein could bind to small GTP binding proteins from different families [125]. Therefore, a possible interaction between EmRhoGAP and EmRap2 was also analyzed in an initial experiment. The analysis of the interaction of EmRhoGAP with EmRas and EmRap1 is currently under progress and no results are available yet.

The analysis of interaction was carried out using a yeast two hybrid (Y2H) system which has been shown to be feasible to examine the interaction of Src-family kinases with their binding partners [120,121]. A summary of the examined interactions is shown in Fig. 60. When AD-EmRhoGAP was co-expressed with a truncated EmFyn (BD-EmFynSH4-3-2) which lacks all residues C-terminal the SH2 domain, an interaction could be observed under high stringency conditions (Fig. 60, lane 1). But similar growth was seen when BD-EmFynSH4-3-2 was expressed together with empty pGADT7 (Fig. 60, lane 10), indicating that BD-EmFynSH4-3-2 autoactivated the expression of the reporter genes. The further deletion of EmFyn – domains, i.e. the expression of the SH2 domain alone fused to BD (BD-EmFynSH2) could eliminate the strong autoactivation of the reporter genes (Fig. 60, lane 10). Nevertheless, the SH2 domain alone did not interact with EmRhoGAP under high stringency conditions (Fig. 60, lane 11). In the next step, the interaction of EmRhoGAP and EmFyn was analyzed by co-expressing EmRhoGAP fused to the BD-domain (BD-EmRhoGAP) together with either EmFynSH4-3-2 or EmFynSH2 fused to the AD-domain (AD-EmFynSH4-3-2, AD-EmFynSH2). The growth of the transformants on high stringency plates indicated a strong interaction between EmRhoGAP and the two truncated EmFyn BD-fusion proteins (Fig. 60, lane 8 and 9), while no autoactivation was seen under these conditions (Fig. 60, lane 12, 16 and 17). The finding that the SH2 domain is sufficient for an interaction with EmRhoGAP might suggest that the latter is tyrosine phosphorylated in *S. cerevisiae* or that this domain also interacts with other than phosphorylated tyrosine motifs.

While it is known that Rho family proteins like Cdc42, Rac and RhoA form reversible homodimers [220], it is not known for their respective RhoGAP proteins. Therefore, it was also examined if EmRhoGAP forms homodimers *in vitro*. The homodimerization of EmRhoGAP under high stringency conditions could be detected (Fig. 60; lane 3), but the possible function of this homodimerization still needs to be analyzed.

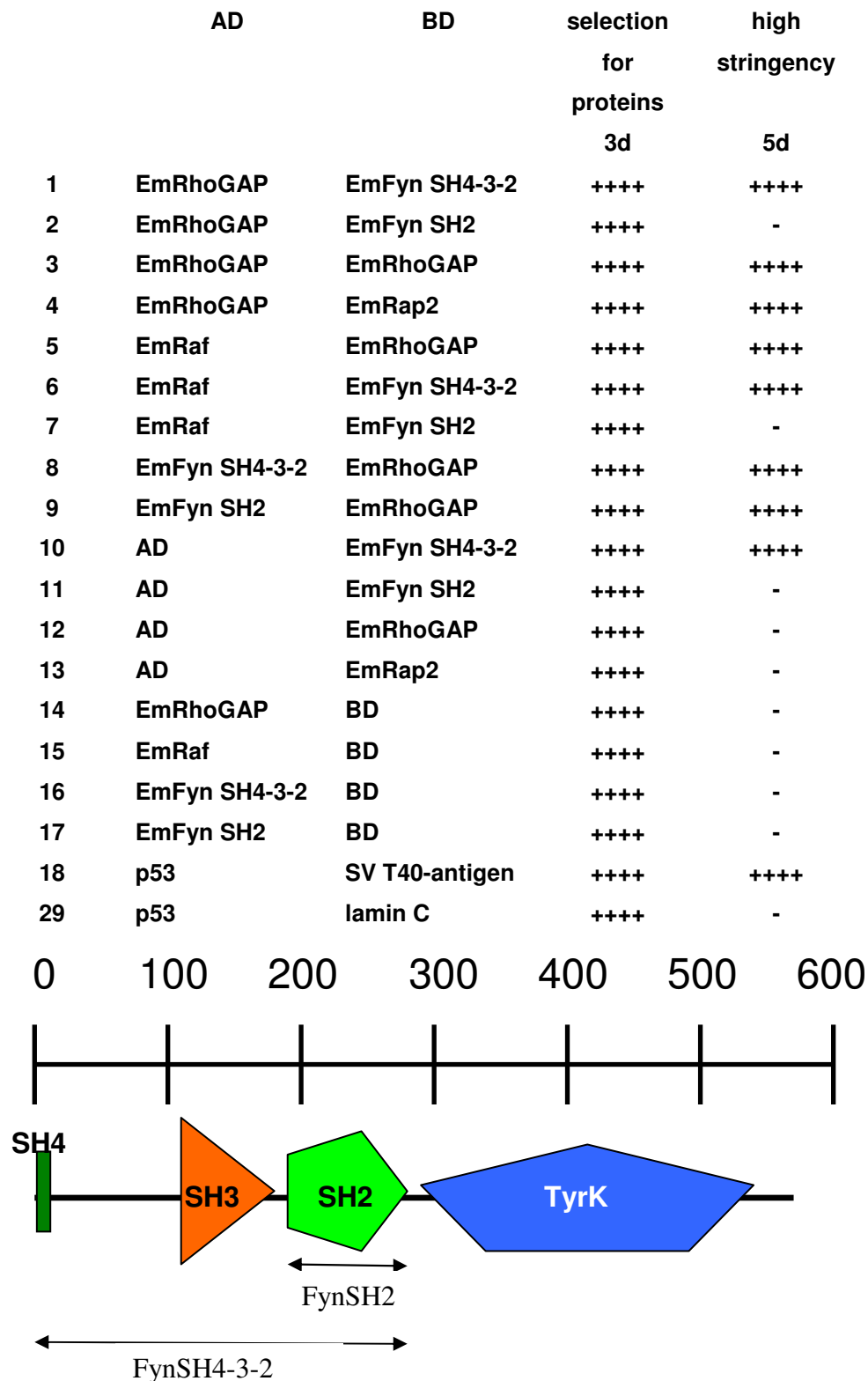


Fig. 60: Yeast Two Hybrid analysis. Co-transformants expressing proteins fused to the GAL4 DNA binding domain (BD) and activation domain (AD) were transferred onto defined agar plated selecting for the expression of the fusion proteins and also for protein-protein interactions under high stringency conditions. As controls, the constructs were coexpressed with BD and AD alone, respectively. After 3 and 5 days the growth on the plates were analyzed. The growth of the co-transformants was compared to the growth of the positive (BD-p53 x AD-T) and negative control (BD-p53 x AD-lamin C). +,+,+,+,+,+,+,+ indicate growth, while – indicated no growth. The following constructs were expressed: the SH2 domain of EmFyn (EmFynSH2) and EmFyn lacking the kinase domain and the short C-terminal tail (EmFynSH4-SH3-SH2) fused to the GAL4 activation domain (AD);

3.6.3.9 EmRhoGAP interacts with EmRap2 and EmRaf in the Yeast Two Hybrid

With EmRap2 [2], EmRaf and EmRas [82] putative components of the *E. multilocularis* MAP kinase cascade were identified. So far, their position in the signal cascade is not known. It has been recently published that the Ras/Raf/MEK/ERK MAP Kinase pathway regulates the Rho-GTPase-activating protein activity of p190RhoGAP [221] and therefore a possible interaction of EmRaf with EmRhoGAP was examined in the Yeast Two Hybrid. As it is depicted in Fig. 60 lane 5, the interaction of those proteins were strong enough to enable the yeast cells to grow under high stringency conditions, while the yeast cells transformed with the controls did not grow (Fig. 60, lane 12 and 15). As already mentioned, GAP proteins exert some degree of promiscuity toward their GTP binding proteins [125] which brought up the question if EmRhoGAP could interact with EmRap proteins. In an initial screen, the interaction between EmRhoGAP and EmRap2 was analyzed in the Yeast Two Hybrid. These two proteins interacted under high stringency conditions (Fig. 60, lane 4) while the controls did not (Fig. 60, lane 13 and 14). Very recently, Myagmar et al. [127] identified that the *C. elegans* ortholog of Rap2 interacted with ZK669.1a, an ortholog of human RhoGAP protein PARG1, in the Yeast Two Hybrid. This finding again supports the assumption that the interaction of EmRhoGAP with EmRaf and EmRap2 might also occur in *E. multilocularis* metacystode vesicles *in vivo*. A possible role could be that EmRaf regulates the RhoGTPase activating protein activity of EmRhoGAP towards EmRap2 and thereby the further downstream signaling.

Based on the identified protein-protein interactions, the following working scheme of the EmIR intracellular signaling cascade is proposed (Fig. 61). The activation of EmIR might lead to the recruiting of EmFyn and in turn to its activation by the phosphorylation through EmIR.

The recruiting of human Fyn to the human IR signaling complex via IRS-1 and the tyrosine phosphorylation of human Fyn by the PDGFR has already been described [129,141,142].

Activated Fyn might then interact with and phosphorylate EmRhoGAP, as shown by Yeast Two Hybrid and co-expression studies, and might thereby regulating its activity towards small GTP binding proteins. Such a regulatory effect could be shown for Fyn kinase and RhoGAPs in human oligodendrocytes [120,121]. With EmRas, EmRap1 and EmRap2 small GTP binding proteins have been identified for *E. multilocularis* which are homologous to human Ras, Rap1 and Rap2. Although the function of Rap2 is unclear [127], Rap1 is an antagonist of Ras [126]. It is assumed that this antagonism is exerted by the interaction with mammalian Raf1 and it could further be shown that the stimulation of mammalian cells with insulin releases the antagonistic effect of Rap1 [126]. EmRap2 might play a similar role in the

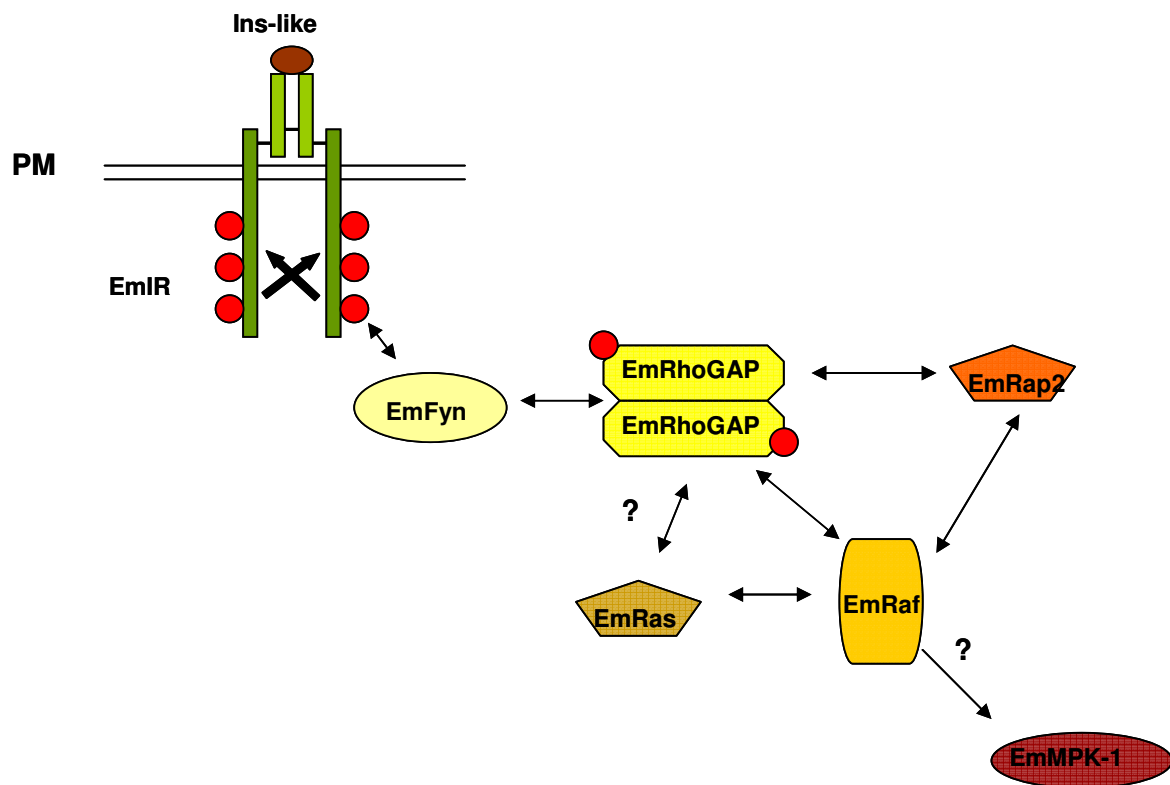


Fig. 61: Working scheme of EmIR intracellular signaling cascade based on previously results [2] and data presented in the present work.

insulin signaling cascade of *E. multilocularis*. Binding studies carried out by Markus Spiliotis demonstrated that EmRaf interacted in vitro with EmRap2 and EmRas [2,82]. EmRap2 belongs to the Ras superfamily whose members are active in the GTP bound state and inactive in the GDP bound state [125]. The activation of EmRhoGAP could promote EmRap2's

intrinsic GTPase activity thereby leading to its inactivation and the release of EmRaf. The interaction of EmRaf with EmRhoGAP might promote the recruitment to the EmRaf-EmRap2 complex. In general, GAP proteins stimulate the GTPase activity by stabilizing the transition state via a conserved arginine finger motif [211-213]. A homologous motif could not be found in EmRhoGAP but it has been recently shown that RapGAP activates the GTPase activity of Rap without the arginine finger motif [214]. Therefore, it might be possible that EmRhoGAP is the GAP of EmRap2 although exerting the highest homology to ARHGAP1 and p50RhoGAP. Since it has been shown that the GAP proteins of one Ras subfamily can regulate the GDP/GTP exchange of other members of the Ras superfamily [125], it might be possible that EmRhoGAP also interacts with EmRas and a yet unknown EmRho protein. The release of the EmRaf inhibition could then lead to the activation of EmMPK-1 and in turn to the observed insulin induced effects in *E. multilocularis*. This proposed *E. multilocularis* intracellular signaling cascade could serve as basis for a more detailed molecular analysis

3.6.3.10 Src-family kinase inhibitors affect *E. multilocularis* metacestode vesicles *in vitro*

For the analysis of the role of Src-family kinases in the development of *E. multilocularis*, metacestode vesicles were incubated in medium (10%FCS) supplemented with Src-family kinase inhibitors. The following inhibitors were used: PP2 (Calbiochem) is an inhibitor which preferentially inhibits the mammalian Src-family kinases p56Lck, p59Fyn and Hck at low nanomolar concentrations ($IC_{50} \cong 5$ nm) compared to EGF-receptor ($IC_{50} \cong 480$ nm), JAK2 ($IC_{50} > 50$ μ M) and ZAP-70 ($IC_{50} > 100$ μ M) [189]. The other inhibitor, Leflunomide (Sigma), inhibited the downstream effects of p59Fyn at concentrations as low as 20 μ M and also its autophosphorylation at 125 μ M [74]. Despite all homologies of EmFyn to mammalian Src-family kinases which clearly identified it as a member of this family, though, it differs in its amino acid composition. Therefore, higher inhibitor concentrations than reported for the mammalian Src-family kinases were used. In one experimental setup, metacestode vesicles were incubated in medium preconditioned by hepatocytes and supplemented with 250 μ M Leflunomide. In a second independent experimental setup, the medium was supplemented with 50 nM PP2. In both cases, an equal volume of the inhibitor's solvent DMSO was added to the control. After 1, 2, 4 and 7 days, the alkaline phosphatase (AP) activity was determined as described for human IR inhibitor. A slightly increased AP activity for both inhibitors could

only be detected after 7days (data not shown). Analogously to the human IR inhibitor, the effect of the Src-family kinase inhibitors on the phosphorylation of EmMPK-1A and in addition of Elp was analyzed (Fig. 62). The supplementation of the medium with either Leflunomide or PP2 caused the dephosphorylation of Elp (Fig. 62 A and C), which supports the assumption that Src-family kinases are involved in the regulation of the cytoskeleton not only in mammalian cells [120,121] but also in *E. multilocularis* metacystode vesicles. Interestingly, the phosphorylation of EmMPK-1A was slightly stimulated by the presence of Leflunomide (Fig. 62 B), whereas it was dephosphorylated in the presence of PP2 compared to the control (Fig. 62 D). This could suggest that the inhibitors effect different Src-family kinases whose signaling activity might converge at EmMPK-1A, again underlining the pivotal role of EmMPK-1A in the development of *E. multilocularis* metacystode vesicles. But it still needs to be analyzed if these inhibitors inhibit EmFyn or a different Src-family kinase.

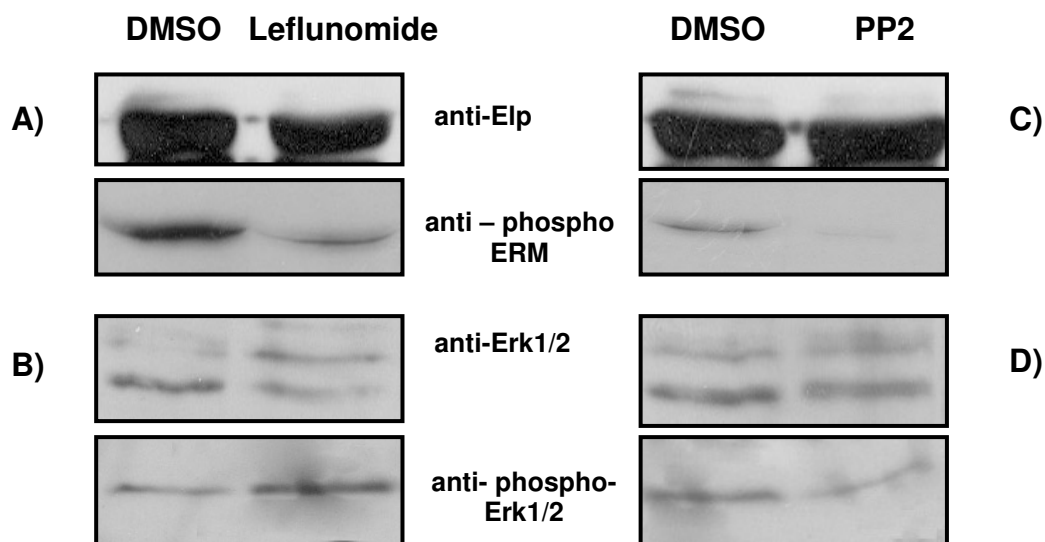


Fig. 62: Effect of the Src-family kinase inhibitors Leflunomide and PP2 on in vitro cultivated metacystodes. Metacystode vesicles of the *E. multilocularis* isolate H95 were incubated in conditioned medium in the presence of the Src-family kinase inhibitors Leflunomide and PP2, respectively. As control, the metacystodes were incubated in the presence of DMSO, the inhibitors' solvent. The effect on the metacystodes was analyzed by Western blotting of whole cell lysate using specific phospho and non-phospho antibodies. The phosphorylation of the cytoskeleton protein Elp was analyzed with anti-Elp and anti-P-ERM antibody (A and C), while the phosphorylation of EmMPK-1A was analyzed by using anti-Erk1/2 and anti-phospho-Erk1/2.

4 Discussion

Among the diverse groups of infectious agents (e.g. bacteria, fungi, viruses, protozoa), parasitic helminths are in so far unique as they rely on developmental pathways and mechanisms which have arisen early in metazoan evolution and are, therefore, also present in their various metazoan hosts (vertebrates and invertebrates). In the case of systemic helminths which develop in close contact to the host's endocrine and paracrine systems, this has led to the interesting concept of host-helminth cross-communication via evolutionary conserved signaling molecules [90,225-227]. In this hypothesis it is assumed that host cytokines such as insulin, TGF- β or EGF bind to corresponding members of the insulin-, TGF- β - or EGF-receptor families on the surface of parasitic helminths, thus regulating parasite development during an infection. Likewise, evolutionary conserved cytokines of parasitic helminths could be secreted and, via binding to corresponding receptors of the host, be involved in mechanisms such as immune evasion or the induction of apoptosis [108,226,228]. Particularly during recent years, examples of such cytokines and surface receptors have been reported in all three major groups of parasitic helminths (nematodes, trematodes and cestodes) and their interaction with the host counterparts has been investigated to a certain degree at the biochemical level. Respective studies on the parasitic flatworms *E. multilocularis* and *S. mansoni* revealed that at least two major developmental pathways are relevant for host-parasite interactions. One of these is receptor tyrosine kinase signaling which involves surface receptors of the insulin- and the EGF-receptor family and which usually transmits signals to the MAP kinase cascade as a central control point of cellular signaling [9,79,80,84]. The second is TGF- β /BMP signaling which utilizes surface serine threonine kinases and intracellular signal transducers of the Smad family [86,173,229]. However, despite increasing evidence that hormonal cross-communication can occur during helminth infections, no clear-cut evidence for an *in vivo* role of these interactions has been obtained. Furthermore, although biochemical interactions between host hormones and TGF- β or EGF receptor kinases were observed, no data were so far available for one of the most important human cytokines/hormones, insulin, and insulin-receptor-like kinases of parasitic helminths.

In the present study, it has been demonstrated for the first time that hormonal cross-communication between the Ins/IGF-I systems of a helminth and its host can occur and that human insulin regulates the development and signal transduction pathways of *E. multilocularis* metacystode vesicles *in vitro*. Evidence has been presented that the addition of insulin to *E. multilocularis* metacystode vesicles promotes *in vitro* survival and growth and stimulates DNA *de novo* synthesis. Furthermore, exogenous insulin also affected parasite

gene expression and overall phosphorylation of cellular proteins. The well known MAP kinase cascade is one of the major intracellular signaling transduction pathways transmitting the signals from activated RTK of the Ins/IGF-I family [190]. It could be demonstrated in the present study that exogenous insulin activates a MAP kinase cascade in *E. multilocularis* metacystode vesicles *in vitro* which clearly supports the assumption that metacystode vesicles express a surface receptor which detects exogenous insulin. With EmIR, Konrad et al. identified and characterized a potential receptor molecule in *E. multilocularis* sharing all structural features of a receptor of the Ins/IGF-I family of RTK and which is significantly homologous to human IR [5]. Using specific antibodies, generated in the present work, and RT-PCR methods, it could be revealed that EmIR is expressed in those *E. multilocularis* larval stages which develop within the intermediate host. Immunohistochemical studies showed that EmIR is expressed in the metacystode's germinal layer thereby having access to insulin from the outside and the metacystode's hydatid fluid. Like human IR [188,190], endogenously expressed EmIR is synthesized as a proreceptor that becomes proteolytically processed into a α - and β -subunit. This procession did not occur when EmIR was heterologously expressed in a mammalian cell line. In contrast to human IR, EmIR does not possess the tetrabasic residues motif at which the processing of human IR occurs, suggesting that the processing mechanism of human IR and EmIR differ. For the biochemical analysis of EmIR in a heterologous system, a chimeric human IR receptor was constructed in which its ligand binding domain has been replaced by the corresponding domain of EmIR. Upon the heterologous expression in a mammalian cell line, the exogenous addition of human insulin stimulated the tyrosine phosphorylation of the chimeric receptor suggesting that EmIR's ligand binding domain is functional in the heterologous system and binds human insulin. The stimulation of *E. multilocularis* metacystode vesicles with exogenous insulin *in vitro* led to an increased phosphorylation of EmIR. This phosphorylation could be prevented by an inhibitor originally designed for human IR tyrosine kinase supporting that the promoting effects of exogenous insulin on *E. multilocularis* metacystode vesicles are transmitted by the activation of EmIR as the most upstream component of *E. multilocularis* insulin signaling cascade. The prolonged administration of this IR tyrosine kinase inhibitor led to the degradation of *E. multilocularis* metacystode vesicles *in vitro* as monitored by the analysis in the light microscope and the activity of *Echinococcus* alkaline phosphatase [10]. These results could provide the basis for the synthesis of EmIR tyrosine kinase specific inhibitors as new drugs for the therapy of AE.

All the data presented herein clearly indicate that the activation of EmIR by exogenous insulin is the initial step of the promoting effect of exogenous insulin in *E. multilocularis* metacystode vesicles. These data further support the hypothesis that *E. multilocularis* and its host are able to cross-communicate via phylogenetically conserved hormonal signal transduction pathways.

The analysis of the effect of exogenous IGF-I on *E. multilocularis* metacystode vesicles led to different results. IGF-I activated the metacystode's MAP kinase cascade and stimulated the *de novo* DNA synthesis, although the latter effect was approximately 10-fold lower compared to the stimulatory effect of insulin. This difference in the stimulation of *de novo* DNA synthesis might be due to different binding affinities of EmIR towards insulin and IGF-I. It has been demonstrated that both insulin and IGF-I are bound by human IR, albeit with different affinities [61]. The comparable activation of the *E. multilocularis* MAP kinase cascade by both insulin and IGF-I questions that EmIR binds both hormones with different affinities. Thus it cannot be excluded that *E. multilocularis* codes for more than one RTK of the Ins/IGF-I family with one being activated by insulin and the other by IGF-I. The finding that EmIR is only activated by insulin and not by IGF-I speaks in favor of this hypothesis. The spatial separation of insulin and IGF-I binding to different receptors has been described only for vertebrates, while invertebrates like *C. elegans* and *D. melanogaster* possess only one receptor of the Ins/IGF-I family of RTKs [39,54]. Very recently, Khayath et al. [83] identified two members of the Ins/IGF-I family of RTKs in *S. mansoni* making it possible that platyhelminthes express two RTKs of the Ins/IGF-I family. The Southern blot analysis of *E. multilocularis* identified *emir* as a single copy gene. But it can not be excluded that the chosen probe and hybridization conditions biased the result of the Southern blot analysis. The discrepancy in the effects of insulin and IGF-I, especially in the activation of EmIR needs to be further analyzed and the ongoing EST and genomic sequencing projects might reveal if *E. multilocularis* codes for two RTKs of the Ins/IGF-I family.

Previous studies revealed that *egfd* is upregulated in *E. multilocularis* metacystode vesicles in the presence of host cells [88]. The encoded protein belongs to the family of EGF-like cytokines which are known to regulate differentiation and developmental processes [230]. It has been suggested that the induction of *egfd* expression in *E. multilocularis* metacystode vesicles by host derived factors triggers the activation of an EGFD-specific RTK which in turn activates the MAP kinase cascade. The present study identified insulin as one of those potential host derived factors since it clearly upregulates *egfd* expression and is expressed in cell lines whose supernatant induces *egfd* transcription.. The upregulation of *egfd* expression

by insulin could also mean that insulin activates the *E. multilocularis* MAP kinase cascade indirectly due to the activation of EmER by EGFD. It has, for example, been recently shown that exogenous EGF activates the MAP kinase cascade in *E. multilocularis* [84] and the parasite's EGF-receptor ortholog, EmER [Gelmedin V, Spiliotis M, Dissous C, Brehm K. Personal communication]. Although this possibility cannot be completely excluded, the indirect activation of the MAP kinase cascade in *E. multilocularis* metacystode vesicles by insulin seems to be very unlikely. A direct activation of the cascade through the activation of EmIR is supported by the observed activation of the MAP kinase cascade by exogenous insulin within 10 – 30 min and also by the finding that insulin and EGF activate distinguishable signaling pathways. An increased survival of *E. multilocularis* metacystode vesicles *in vitro* could only be observed in the presence of exogenous insulin and not of exogenous EGF [2]. Based on the presented data, the activation of *E. multilocularis* MAP kinase cascade appears to be a primary effect and the upregulation of *egfd* a secondary effect of host insulin on *E. multilocularis* metacystode vesicles.

The finding that PI3K is not only present in vertebrates but also in *C. elegans* and *D. melanogaster* [39,76], suggests that this is also the case for *E. multilocularis* although no PI3K ortholog has been identified so far. In vertebrates, the PI3K pathway is also activated by insulin but in invertebrates this pathway is only poorly characterized and a direct activation by insulin is still to be shown. The ongoing EST sequencing projects could identify a PI3K ortholog in *E. multilocularis* and the analysis of the activation in response to insulin might lead to the activation of a further signal transduction pathway regulated by exogenous insulin. An important question raised on the basis of the presented results is whether the effects induced by exogenous insulin *in vitro* affect the tropism of the *E. multilocularis* metacystode to the intermediate host's liver. In over 95% of all cases of AE as well as in the natural intermediate host, the liver is infected [69]. Like *E. multilocularis*, *E. granulosus* also infects primarily the liver of the *Fehlwirtl* intermediate host but also lung, kidneys and the brain [231]. Although *T. solium* enters the host similarly to *E. multilocularis* and *E. granulosus* (the oncosphere penetrates the intestinal epithelium and is transported with the blood in the portal vein leading to the liver) the *T. solium* metacystode does not develop within the liver but in muscles and the brain [232]. In mammals, insulin is released after feeding by the pancreas into the portal vein which leads to the liver (Fig. 64). Therefore, the highest insulin concentrations within the mammalian body are measured at the transition of the portal vein and liver parenchyma. At the liver, 60% of the released insulin is removed and only 40% are transported to the body periphery via the serum. Interestingly, the site of the highest insulin

concentrations is also the site where the oncosphere gets in contact with the liver. It could be possible that a high insulin concentration at the liver is one of the first host derived stimuli targeting the oncosphere after the penetration of the intestinal epithelium. Although the expression of EmIR in the oncosphere still needs to be shown, it seems likely that insulin stimulates EmIR expressed in the oncosphere and its downstream signaling cascade which promotes the preferential development of the oncosphere to the metacestode larval stage within the liver. The uptake of oncospheres with the food is discussed as one source of infection for the intermediate host. Since insulin is released from the pancreas in response to high glucose concentrations after eating [39,41], the uptake of oncospheres with food would ensure a stimulus with high concentrations of insulin which could promote the transformation of the oncosphere into the metacestode.

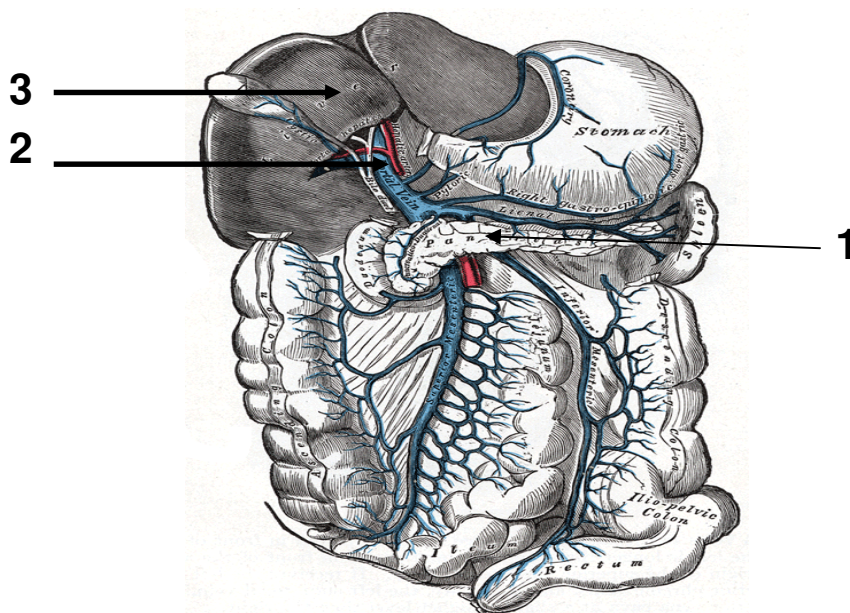


Fig. 64: Insulin is released from the pancreas (1) into the portal vein (2) leading to the highest concentrations of insulin in the liver (3). (Figure from Gray's Anatomy of the Human Body, Twentieth Edition, Philadelphia: Lea & Febiger, 1918; New York: Bartleby.com, 2000)

The possible correlation between an uptake of insulin-inducing nutrients and *Echinococcus* organotropism towards the intermediate host's liver requires further investigation (i.e. *in vivo* infection experiments) and has not been addressed in the present study. Nevertheless, the expression of EmIR in *E. multilocularis* oncospheres and its involvement in establishing the infection is very likely. In addition to a possible stimulatory role of insulin on the parasite's oncosphere, the direct effects on the metacestode which were observed in the present study could also contribute to liver organ tropism. To address these questions, *in vivo* infection studies of wild-type and diabetes (streptozotocin-treated) mice with oncospheres under insulin and non-insulin inducing conditions are required. If insulin exerts its promoting effects also *in vivo*, the strongest infection should be found in non-diabetes mice under insulin inducing conditions. In this case, at least a pivotal role of insulin on the spreading of *E. multilocularis* metacestode vesicles in the liver would be proven. A similar effect of insulin on the infection with *E. granulosus* and *T. crassiceps* can be assumed because the data presented in this work suggest that insulin signaling in these parasites is similar to that in *E. multilocularis*. In case of *T. solium*, insulin signaling seems to differ from *E. multilocularis* since the *T. solium* IR ortholog lacks the additional 172 residue peptide identified in the tyrosine kinase domain of EmIR. This peptide seems to be involved in the regulation of downstream signaling as demonstrated by yeast two hybrid interaction studies in which EmFyn only interacted with the intracellular domain of EmIR comparable to the intracellular domain of human IR when its tyrosine kinase domain lacked the 172 residue peptide. The high homology between the tyrosine kinase of TsIR and EmIR except the peptide insert supports the assumption that the EmFyn ortholog of *T. solium* would interact with the intracellular domain of TsIR. The finding that EmFyn did not interact with EmIR's intracellular domain in the yeast two hybrid in the presence of the insert might indicate that this interaction does not occur *in vivo* after the stimulation of *E. multilocularis* metacestode vesicles with insulin. A different intracellular signaling mechanism might be involved in the transmission of signals emanating from activated EmIR and in the regulation of development. The differences in insulin signaling between *T. solium* and *E. multilocularis* could provide a basis to reveal species specific insulin signaling cascades. In a first step, full length TsIR and TsFyn need to be identified to analyze the overall identity between TsIR and EmIR and TsFyn and EmFyn, respectively, and in a second step, the interaction between TsIR and TsFyn needs to be analyzed, e.g. by using the yeast two-hybrid technology.

In the present work, an inhibitor (HNMPA-(AM)₃) could be identified which obviously affects EmIR activity and which has deleterious effects on *in vitro* cultivated metacestode

vesicles. Although the respective molecule was originally designed to inactivate the human insulin receptor, an activity towards the parasite ortholog was expected due to the considerable sequence homologies between EmIR and human IR in the tyrosine kinase domain (which serves as target site for HNMPA-(AM)₃) [169]. Based on the strong anti-parasitic effect of HNMPA-(AM)₃, insulin signaling seems to play an important role for parasite survival, at least *in vitro* and most probably also *in vivo*. This renders EmIR and its downstream signaling factors promising targets for the development of novel anti-*Echinococcus* drugs. One obvious starting point for drug development would be HNMPA-(AM)₃ itself which, through chemical modification, could be altered in order to obtain drugs that have a higher activity towards EmIR than to the human ortholog IR.

As second possibility to utilize *Echinococcus* insulin signaling as a target for drug development are antibodies which specifically inhibit EmIR's signaling activity. Ideally, these antibodies would act against the extracellular EmIR domain since this allows facilitated access. It is, on the other hand, questionable whether such antibodies can be generated since, in the present work, no antibody production using the recombinantly expressed EmIR ligand binding domain was obtained in immunized rabbits. As a possible alternative, native EmIR, immunoprecipitated from parasite material could be used which should contain sugar modifications that are necessary for effective antibody production.

Another way to inhibit the activation of EmIR could be blocking of its insulin binding sites by insulin-analogs which do not per se activate EmIR. So far, no inhibitory insulin has been identified but the finding that in *C. elegans* more than 30 ORFs (*ins1-ins37*) are present coding for insulin-like peptides suggested that also inhibitory insulin-like peptides are encoded in invertebrates. Interestingly, the over-expression of *ins-1* in *C. elegans* leads to the formation of the *dauer* stage similar to mutations which abrogate signaling through DAF-2, the *C. elegans* IR ortholog [46].

The hydatid fluid of *E. multilocularis* metacestode vesicles plays a pivotal role in their development. The removal of the hydatid fluid by physical disruption of vesicles caused a rapid dephosphorylation of EmMPK-1A compared to intact vesicles. Intriguingly, EmMPK-1A's phosphorylation could only be restored in intact vesicles when reincubated under permissive conditions and also the stimulation by insulin was only observed with intact vesicles. These findings raised the question whether exogenous insulin is taken up into the hydatid fluid. Although, only the uptake of albumin into the hydatid fluid could be shown in the present work (data not shown), three points were found supporting the uptake of insulin. First, the amount of a biotinylated insulin added to the medium decreased in time and second, insulin but not IGF-I could be measured in the hydatid fluid isolated from *in vivo* and *in vitro* (either with FCS or human serum) cultivated *E. multilocularis* metacestode vesicles. Insulin could also be

measured in the hydatid fluid of *E. granulosus* cysts surgically removed from human patients, suggesting that insulin can also be found in the hydatid fluid of *E. multilocularis in vivo*. The failure to detect labeled insulin in the hydatid fluid might be due to the limited sensitivity of the Western blot, while the Insulin-Immulite[®] System employs a solid phase sandwich ELISA to detect insulin in the pM range. The decrease of insulin-biotin in the medium might be explained by degradation through a secreted protease or by the sequestration from the medium and/or hydatid fluid after having bound to the receptor. Insulin degradation after the internalization of activated receptors which have still bound insulin is an integral part of the insulin signaling cascade [159]. Insulin degrading enzymes are evolutionary conserved and were identified in mammals as well as in *D. melanogaster* [160-162] suggesting that such a protein is also expressed in *E. multilocularis*. Third, it seems possible that the detected insulin is of parasite origin since genes encoding insulin-like proteins have been identified in *D. melanogaster* and *C. elegans* although a direct activation of the corresponding IR has not been shown [46,71]. Very recently, an ORF was identified encoding an insulin-like protein in *S. japonicum* [108] suggesting that insulin-like proteins might also be encoded by *E. multilocularis* and *E. granulosus*. But it is questionable if this insulin would be detected by the antibodies used for the ELISA due limited sequence homologies between vertebrate insulin and invertebrate insulin-like molecules on the amino acid sequence level. In support of this, no cross-reacting bands were observed in Western blot analyses when *E. multilocularis* lysate (without hydatid fluid) was probed with an anti-insulin antibody that recognizes mammalian insulin under non-reducing conditions (data not shown). Hence, the presented results indicate that an interaction between EmIR and exogenous insulin is not only possible *in vitro* but also *in vivo*.

In summary, this work demonstrates for the first time that development and differentiation of a parasitic helminth is regulated by host derived insulin via the activation of a phylogenetically conserved signaling cascade in the parasite. This finding provides fundamental data on growth and organ tropism of *E. multilocularis*. So far, the regulation of the growth of *E. multilocularis* metacystode and the preference of the liver as the major site of infection is only poorly understood. The highest concentrations of insulin *in vivo* are found in the liver which might explain the parasite's preferential growth in the liver. The present study also provided fundamental data on *E. multilocularis* IR ortholog, EmIR, and its involvement in insulin signaling. The inhibition of EmIR's tyrosine kinase activity with an inhibitor originally designed for human IR led to the death of the parasite *in vitro* identifying the receptor and its downstream signaling cascade as good candidates for the development of new drugs for the treatment of AE.

5 Materials and Methods

5.1 Equipment

Incubators (Heraeus, Hanau)

DNA – Gel Electrophoresis Chamber (BioRad, München)

Gel-Documentation System MidiDOC (Herolab, Wiesloch)

Heating Block, DB-3 (Techne, Cambridge, UK)

Protein Separation Chambers, Minigel-Twin (Biometra, Göttingen)

Agitation Incubators, G25 (New Brunswick Scientific, Edison, NJ, USA)

Sequencing Apparatus, ABI Prism™ Sequencer 377 (Perkin Elmer, Weiterstadt)

Power Supplies: Power Pack P25 und P24 (Biometra, Göttingen)

Spectrophotometer U-2000 (Hitachi, NY, USA)

Thermocycler: Trio-Thermoblock™ (Biometra, Göttingen)

Overhead Agitation Wheel (Renner GmbH, Dannstadt)

Ultrasonication Apparatus: Sonifier® II Desintegrator Modell 250 (Branson, Danburg)

Ultra-Turrax T25 (Janke&Kunkel/IKA Labortechnik)

Cooling Centrifuge RC-5B (Heraeus, Hanau)

5.2 Consuming articles

Blotting-Paper (Schleicher&Schüll, Dassel)

positively charged nylon membrane *porablot NY plus* (Macherey&Nagel, Düren)

0,5 – 2,0 ml reaction tubes (Sarstedt, Nümbrecht)

15 ml sterile tubes (Greiner, Nürtingen)

50 ml centrifugation tubes (Falcon, Heidelberg)

X-Ray film (Fuji)

Syringes and Needles, sterile (Braun Melsungen AG, Melsungen)

Sterile Filters, 150 ml Bottle Top Filter, 0.45 µm (Nalgene, NY)

5.3 Enzymes, commercial kits, chemicals and oligonucleotides

Agarose NEO (Roth)

Amino Acids, Antibiotica (Sigma, Deisenhofen)

Benchmark™ Prestained Protein Ladder (Life Technologies)

Broadrange Prestained Protein Marker (NEB, Schwalbach)

dNTPs lyophilized (Roth, Heidelberg)

ECL Chemiluminescence Kit (Amersham Buchler, Braunschweig; Pierce)

Phusion Proof Reading DNA Polymerase (Finnzymes)

Matchmaker Two Hybrid System 3 (Clontech, Heidelberg)

Agar-Agar, Bacto-Peptone, Yeast Extract, Glucose, Yeast Nitrogen Base Without Amino Acids (Difco Laboratories, Augsburg)

PBS Dulbecco without $\text{Ca}^{2+}/\text{Mg}^{2+}$

Pfu Turbo Polymerase (Stratagene)

Pierce BCA Protein Assay

Qiagen Plasmid Midi Kit, QIAprep Spin Miniprep Kit, QIAquick PCR Purification Kit, QIAgen Gelextraction Kit

Restriction Enzymes, DNA Modifying Enzymes and T4 DNA Ligase (New England Biolabs (NEB, Schwalbach)

TOPO-TA Cloning® KIT, Original TA Cloning Kit, pBAD/Thio expression Kit (Invitrogen, Groningen, Netherlands)

Protease Inhibitors (Applichem)

Protease Inhibitor Complete (Roche)

RNase Inhibitor (NEB, Schwalbach)

DNase I, RNase free (Roche)

Insulin (H-Insulin, Hoechst)

IGF-I (rh-IGF-I, ImmunoTools)

All buffers and solutions have been made with previously distilled water, autoclaved and sterile filtrated, respectively. For all enzymatic reactions, except for those in which RNA was handled, double distilled and autoclaved water has been used. In all reactions dealing with RNA, either DEPC-treated or commercially available RNase-free water has been used.

All oligonucleotides were ordered from Sigma-Aldrich/Sigma-Genosys in lyophilized form and were reconstituted with PCR grade water at a final concentration of 50 μ M.

5.4 Working with RNA

Besides RNase-free solutions, only disposable sterile or two times autoclaved materials, e.g. PCR reaction tubes, were used when dealing with RNA.

5.4.1 Isolating total RNA from mammalian cells

To isolate the total RNA from the immortal rat hepatocyte cell line (Reuber cells, RH⁻) and human hepatocyte cell line HepG2, confluent grown cells were washed with 10 ml prewarmed 1x PBS, detached from the bottom of the flask with Trypsine/ EDTA (2ml, 10 min 37°C) and then resuspended in 8 ml DMEM containing 10% FCS and Penicillin/ Streptomycin. The number of viable cells were determined with a Neubauer Chamber and 1 x 10⁶ cells were transferred into a fresh 75 cm² cell culture flask containing 20 ml DMEM (10% FCS , Pen/ Strep) and cultivated at 37°C 5% CO₂ for 2 days until the cells were approximately 80% confluent grown. At this time point, the medium was removed and the cells were washed once with 10 ml prewarmed PBS and then treated with 2 ml Trypsine/ EDTA for 10 min at 37°C 5% CO₂. To stop the trypsinization reaction, the cells were resuspended in 4 ml DMEM (10% FCS, Pen/ Strep). In the following step, the cells were pelletized by centrifugation at 4°C (300 x g, 5 min). The supernatant was discarded and the cells lyzed with 600 μ l RLT buffer containing β -mercaptoethanol. All following steps were executed according to the manual of the RNeasy Kit (Qiagen).

5.4.2 Isolating total RNA from metacystode vesicles and protoscolices

The same protocol as mentioned in 5.4.1 was used to isolate the total RNA from both *in vitro* cultivated metacystode vesicles and protoscolices freshly isolated from a sacrificed *Mongolian jird* (*M. unguiculatus*) The starting material was an *in vitro* cultivated metacystode of 0.5-1 cm in diameter and approximately 20 protoscolices, respectively. Prior to the isolation of RNA, the parasite material was washed several times with 1xPBS to remove any remaining debris or hepatocytes.

5.4.3 DNase I treatment of isolated total RNA

The isolated RNA was digested with RNase-free DNase I (Roche) to remove co-purified chromosomal DNA according to the manufacturer's instructions.

5.4.4 Synthesis of first strand cDNA

The synthesis of the first strand cDNA was done in all cases with the Qiagen Omniscript™ Reverse Transcriptase Kit according to the manufacturer's instructions with some minor modifications. Briefly, up to 2 µg of total RNA (in 12 µl RNase – free water) and 2 µl of CD3RT oligonucleotide (stock 10 µM) were pre-heated at 65°C for 10 min to eliminate the RNAs' secondary structures. After the solution had cooled to room temperature, all other components were added and the reverse transcription was executed for 90 min at 37°C.

CD3RT: ATCTCTTGAAAGGATCCTGCAGGACTTTTTTTTTTTTTTTTTTTTTTTTTTTTTT
(V = G+A+C)

5.5 Working with DNA

5.5.1 Isolation of chromosomal DNA from *E. multilocularis* larval stages

lysis buffer: 100 mM NaCl
10 mM Tris-HCl, pH 8.0
50 mM EDTA, pH 8.0
0.5 % SDS
20 µg/ml RNase A
0.1 mg/ml Proteinase K

The chromosomal DNA of the larval stages of *E. multilocularis* was isolated according to the following manual and not with a commercially available kit, because the yields with the latter were insufficient for downstream applications.

Metacestode vesicles were washed with 1xPBS and carefully physically disrupted. The pellet was resuspended in lysis buffer (1.2 ml per 100 mg) and incubation at 50°C in a water bath until the tissue was completely digested (in general, the incubation took place over night). In the next step, an equal volume of a Phenol: Chloroform: Isoamylalcohol (25: 24: 1; Applichem) solution was added to the lysate and the sample was mixed by inverting the tube several times. After a centrifugation step (15 min; 2,000 rpm) at room temperature, the aqueous phase (top phase) was removed and transferred into a new tube, while the organic phase (lower phase) was discarded. The Phenol: Chloroform: Isoamylalcohol – extraction step was repeated and the DNA was pelletized from the aqueous phase by adding 0.1 volumes 5 M LiCl and 2 volumes 96% ethanol. The precipitation was completed by incubating the tube at –20°C over night followed by centrifugation for 15 min at 14,000 rpm at 4°C. The supernatant was discarded and the air-dried pellet resuspended in 1xTE (10 mM Tris, 1mM EDTA, pH 7.5). The concentration of the DNA was determined in a photo spectrometer.

5.5.2 Isolation of plasmid DNA from bacteria

The isolation of plasmid DNA from bacteria was done with Qiagen's QIAprep® Spin Miniprep Kit and QIAGEN® Plasmid Midi Kit.

5.5.3 Determination of DNA concentration

The concentration of DNA was photometrically determined at a wave length of 260 nm with appropriate dilutions with the Gene Quant Pro. An optical density (OD) of 1 corresponds to 50 µg/ml double stranded and 40 µg/ml single stranded DNA [1]. In a less precise way, the DNA was separated in an agarose gel (see 5.4.4) and the intensity of the bands was compared to the intensity of the size marker bands of known concentrations. The utilized size marker was Eurogentec's SMARTLADDER.

5.5.4 Agarose - gelelectrophoresis

1xTAE: 40 mM Tris
 1 mM EDTA, pH8.0
 0.11% glacial acetic acid
 ad 1000 ml
 pH 8.5

6xDNA-Puffer: 0.25% bromo phenol blue
 0.25% xylene cyanol
 40% succrose
 30% glycerol

size marker: SMARTLADDER (Eurogentec): 0.2 – 10 kb

With this method DNA – fragments can be resolved according to their size which also determines the percentage of the agarose gel. While fragments ranging from 0.5 to 7 kilo bases (kb) can easily be resolved in 1% gels, gels containing 1.5% agarose are the better choice to resolved 0.2 to 3 kb fragments. Even smaller fragments are resolved in a 2% gel.


For the preparation of the gel, the appropriate amount of agarose was dissolved in 1xTAE by heating. When the agarose/ TAE solution has cooled down to approximately 50 – 60°C, the agarose/TAE solution was poured into a horizontal gel-sleigh and the loading wells are made by the usage of a comb. For the loading into the wells, the samples are mixed with 6x DNA-loading buffer and then resolved at 100V and room temperature. The resolving of the DNA can be observed with the dyes bromo phenol blue and xylene cyanol. While the former runs in 1% gel like a 300 bp fragment the latter runs like a 3 kb fragment. To visualize the resolved DNA fragments, the gel is stained in an ethidium bromide solution (2 mg/l in 1xTAE) and then exposed to ultraviolet light (302 nm). By comparing the run of the unknown fragments with that of the defined size marker fragments, the size and concentration of the unknown fragment can be determined.

5.5.8 Polymerase Chain Reaction (PCR)

The PCR method has been established by Saiki et al in 1988. With this method it is possible to amplify defined DNA fragments by employing sequence specific oligonucleotides. These provide the crucial 3'-OH for the heat stable DNA-Polymerase to initiate the synthesis of DNA. The other components of the reaction mixture are the enzyme specific buffer and dNTPs. The first used thermostable DNA-Polymerase was isolated from *Thermus aquaticus*. This Polymerase does not possess proof reading activity. In the last years, more and more proof reading polymerases were commercially available which decreased the likelihood of misincorporated nucleotides within the amplified DNA-fragments. Nethertheless, non-proofreading polymerases are still widely used due to their lower price and higher amplification rate compared to proofreading polymerases. As a rule of thumb for both kinds of polymerases, the incorporation rate is 1000 nucleotides per minute. For this work, the Taq DNA-Polymerase from New England Biolabs (NEB) and the proof reading polymerases Pfu Turbo from Stratagene and Phusion from Finnzymes were used.

A standard PCR setup is given. Depending on each PCR being done, the reaction conditions need to be adjusted.

0.5 – 2 μ l template
2.5 μ l 10x Buffer
0.25 μ l dNTP-mix (10 mM)
0.25 μ l oligonucleotide 1 (50 μ M)
0.25 μ l oligonucleotide 2 (50 μ M)
0.2 μ l Taq DNA-Polymerase (2.5 U/ μ l)
ad 25 μ l ddH₂O

Initial denaturation:	60 s	94°C	
Denaturation:	20 s	94°C	
Annealing:	30 s	T _{anneal}	
Elongation:	60 s/1000 nt	72°C	
Terminal elongation:	10 – 30 min	72°C	

25 – 30x

The primer's annealing temperature (T_{anneal}) depends on the percentage of G and C nucleotides and should be approximately 2-5°C lower than the melting temperature (T_m). The latter is the temperature at which 50% of the primer is hybridized with its complementary sequence and can be roughly calculated with the following equation although other calculation methods are also eligible:

$$T_m = 4x (G+C) + 2x (A+T)$$

At the correct T_{anneal} , mishybridisation of the primer and hence the amplification of unspecific DNA-fragments shall be prevented. By repeating the cycle of denaturation, annealing and elongation for 25 – 30 times, the DNA-fragment is exponentially amplified. During the terminal elongation, yet unfinished DNA-fragments are completed and, in case of the Taq-Polymerase, an additional 3' - adenylated is added which is exploited for cloning into the pCR 2.1 TOPO-TA vector or Original TA cloning vector (both Invitrogen)

The PCR products are either directly purified with the QIAquick® PCR Purification Kit or the QIAquick® Gel Extraction Kit when cut from an agarose gel and then purified.

5.5.9 Restriction digest of DNA

All restriction digests are done with enzymes from NEB according the recommendations. When digested fragments are to be ligated into an expression vector, an additional dephosphorylation step is carried out using the Antarctic Phosphatase (NEB) which can be heat inactivated.

5.5.10 Ligation of DNA fragments

The T4-DNA-Ligase (NEB) is used for ligations with the Ligation reaction taking place for 1 h at room temperature or over night at 16°C.

5.5.11 TOPO-TA and TA-cloning

DNA fragments amplified in a PCR with Taq DNA-Polymerase have an additional 3' A added by the DNA-Polymerase. This overhang is used to ligate the amplified fragment either into the pCR2.1 TOP-TA vector (Invitrogen) or the Original TA Cloning Vector (Invitrogen). In the former vector Topoisomerase II is used for the ligation reaction, while in the latter a classical ligation with the T4-DNA-ligase takes place. DNA fragments amplified with proof reading DNA polymerases lack this additional 3' A. But it can easily be added by incubating the purified DNA fragment in a standard Taq DNA-Polymerase PCR setup for 1h at 72°C.

pCR2.1[®] TOPO/ Original TA – Cloning:

M13 (forward): GTAAAACGACGGCCAGT

M13 (reverse). CAGGAAACAGCTATGACC

5.5.12 Southern blot hybridization

The chromosomal DNA of *E. multilocularis* was isolated from parasite material obtained from an infected *Meriones unguiculatus* as previously described [2, 3]. 20 µg DNA were then digested over night with either *Eco* RI, *Pvu* II or *Bgl* II according to the manufacturer's instructions (NEB). The next day, the DNA fragments were separated on a 0.8% agarose gel and the gel was then incubated in 0.25 M HCl for 15 min. To neutralize the acidic buffer, the gel was washed twice with a solution containing 0.5 M NaOH and 1.5 M NaCl for 15 min, followed by two wash steps with a solution containing 0.5 M Tris-HCl pH 7.0 and 1.5 M NaCl for 30 min. All washing steps were carried out at room temperature.

After capillary transfer onto a nylon membrane (Machery –Nagel) by using 20xSSC (1xSSC: 150 mM NaCl, 15 mM sodium citrate, pH 7.0), the fragments were fixed on the membrane by UV-cross linking. Then, the membrane was incubated for 30 min with blocking buffer (0.5 M NaH₂PO₄ pH7.2, 7% sodium dodecyl sulfate, 1 mM EDTA). Hybridization was carried out with a PCR – fragment amplified from the cloned emir cDNA using the oligonucleotides IR-N2 and CK22. The probe was radioactively labeled with α – [³²P] dCTP employing the PrimeIt II random labeling kit (Stratagene) according the manufacturer's instructions, dissolved in blocking buffer and allowed to bind for 20h at 57°C under over head agitation.

Finally, the membrane was washed two times for 30 min with 2xSSC containing 0.1% sodium dodecyl sulfate and exposed to an x-ray film (AGFA) for 48 h at -80°C.

Oligonucleotides:

IR-N2: TCT GCA TAC TTT ACC TCC CG

CK22: GCT CGC ACG CGC GAG GTA G

5.6 General protein analyzing methods

5.6.1 SDS-PAGE

Sodium dodecyl sulfate –polyacrylamide (SDS-PAGE) gel electrophoresis is used to resolve proteins according to their size under denaturing conditions, i.e. in the presence of SDS and β -mercaptoethanol. The polyacrylamide gel comprises a resolving gel in which the proteins are resolved according to their size and a stacking gel which serves to concentrate proteins to enter the resolving gel at the same time. The following protocol is used to pour 2 gels for the Protran system (BIORAD):

<u>Resolving gel:</u>	1.5 M Tris-HCl pH 8.8	2.5 ml
	20 % SDS	50 μ l
	16% ammonium persulfate	60 μ l
	TEMED	10 μ l

PAA [%]	18	12	10	8	7	6
30% (Roth)	6 ml	4 ml	3.33 ml	2.7 ml	2.33 ml	2 ml
H ₂ O	1.4 ml	3.4 ml	4 ml	4.7 ml	5.1 ml	5.4 ml

<u>Stacking gel (4% PAA):</u>	0.5 M Tris-HCl pH 6.8	1.25 ml
	20 % SDS	25 μ l
	16% APS	30 μ l
	TEMED	5 μ l
	30% PAA	0.7 ml
	H ₂ O	3 ml

<u>Electrophoresis running buffer:</u> (pH 8.3)	0.1% SDS 25 mM Tris 192 mM glycine
<u>2xSDS-sample buffer:</u>	2 ml 0.5 M Tris-HCl pH 6.8 1.6 ml Glycerol 1.6 ml 20% SDS 1.4 ml dH ₂ O 0.4 ml 0.05% (w/v) bromophenol blue 7 µl β-mercaptoethanol/100 µl

After the polymerization, the gel is fixed in the electrophoresis tank and filled with running buffer. Depending on the comb used, up to 40-50 µl sample resuspended in 2xsample buffer can be loaded and resolved. For the denaturation, the samples are boiled for 5 min and subsequently centrifuged to pellet the insoluble material (14,000 rpm 1 min). The resolving takes place at 160V. For the determination of the protein sizes, the broad range prestained protein marker is also loaded on the gel.

5.6.2 Coomassie staining

<u>Coomassie staining solution:</u>	1g Coomassie Blue R-250 45% methanol 45% H ₂ O 10% glacial acetic acid
<u>Coomassie destaining solution:</u>	45% methanol 45% H ₂ O 10% glacial acetic acid

Proteins resolved via SDS-PAGE can be fixed and stained by shaking in Coomassie Blue staining solution for approximately 30 min. By destaining with the destaining buffer, the excess dye can be removed.

5.6.3 Western blot

Western Blot Buffer: 25 mM Tris-HCl
 192 mM Glycin
 20% Methanol

The transfer of the resolved proteins onto nitrocellulose membranes (Schleicher & Schuell) was done with the Protran system (BIORAD) as well. In this system, the following setup (in this order) was made for the transfer: Sponge, Whatman paper, PAA-gel, nitrocellulose, Whatman-paper, Sponge. The transfer was carried out for 1h at 350 mA. Due to the high current, a cooling block was added to the transfer chamber to avoid overheating of the proteins. After the transfer, the nitrocellulose was blocked and incubated with the corresponding antibodies over night at 4°C. The following antibodies and blocking buffers were used in this work:

Blocking buffer 5% skim milk in 1xTBS (20 mM Tris, 150 mM NaCl, pH 7.5) 0.05%

Tween20:

anti - Erk1/2 (Stressgen, Victoria Canada, KAP-MA001) ¹	1:1000 in blocking buffer
anti- Erk (pTpY ^{185/187}) (Biosource Intl, Camarillo, Ca, USA) ¹	1:1000 in blocking buffer
anti-Erk2 (nanotools) ²	1:500 in blocking buffer
anti -Phospho – JNK MAPK (Promega) ¹	1:1000 in blocking buffer
anti - GST (Santa Cruz Biotechnologies, USA) ²	1:1000 in blocking buffer
anti – HA (Santa Cruz Biotechnologies, USA) ¹	1:1000 in blocking buffer
anti – myc (Santa Cruz Biotechnologies, USA) ²	1:1000 in blocking buffer
anti – HA (Cell Signaling, USA) ²	1:1000 in blocking buffer
anti – myc (Cell Signaling, USA) ²	1:1000 in blocking buffer
anti-phospho CREB (Cell Signaling, USA) ¹	1:1000 in blocking buffer
anti-phospho S6 (Cell Signaling, USA) ¹	1:1000 in blocking buffer
anti – Elp ²	1:1000 in blocking buffer

anti - EmIR _{intra} ¹	1:1000 in blocking buffer
anti – Flag - HRP (Sigma) ²	1:1000 in blocking buffer
anti-V5 antibody (Invitrogen) ²	1:2000 in blocking buffer
anti- phospho- HIGF-IR (Y ¹¹³¹)/HIR (Y ¹¹⁴⁶) ¹ (USBiological)	1:1000 in 5% BSA TBS 0.05% Tween 20
anti-insulin (Sigma) ²	1:2000 in blocking buffer

Blocking buffer 5% albumin (Applichem) in 1xTBS 0.05% Tween 20:

anti - phospho tyrosine (Cell Signal and Sigma) ²	1:2000 in 5% skim milk in 1xTBS 0.05% Tween 20
anti – Biotin - HRP (NEB) ²	1:1000 in blocking buffer

¹ polyclonal rabbit antibody

² monoclonal mouse antibody

The next day, the primary antibodies were removed and the blots were washed three times with 1xTBS 0.05 Tween 20 to remove unspecifically bound antibodies. For the storage at 4°C, sodium azide (NaN₃) was added to a final concentration of 0.02 – 0.05 % to the diluted primary antibodies. Then, the membrane was incubated for 1h at RT with a secondary antibody specific for the primary antibody. The following were used:

anti – mouse IgG – HRP (Jackson, Immuno Research)	1:10000 in blocking buffer
anti – rabbit IgG – HRP (Jackson, Immuno Research)	1:5000 in blocking buffer

Unbound secondary antibody were also removed by three 10 m in washing steps with 1xTBS 0.05% Tween20. Due to the horse radish peroxidase (HRP) coupled to the secondary antibody the membrane could be developed by chemiluminescence (ECL-Kit, Pierce) and the exposure of an x-ray film. Depending on the intensity of the signal, the film was exposed for 1 – 120 min. The films were developed with a Curix 60 automated developer (Agfa).

5.6.4 Determination of protein concentration

The concentration of proteins was determined with the BCA Protein Assay Kit (Pierce). Reagent A and B were mixed in a ratio of 50 : 1 to give the working solution. For each measuring to be done, 50 μ l of the protein solution of unknown concentration and 50 μ l of each bovine serum albumin (BSA) standard (50, 100, 200, 400, 600, 800, 1000 und 1200 μ g/ml) was mixed with 1 ml working solution. After a 30 min incubation step at 37°C, the absorption at 562 nm was determined in a spectrophotometer. Based on the absorption measured for the protein standards, the protein concentration of the samples was calculated.

5.6.5 Protease inhibitors and phosphatase inhibitors

The following stock solutions of protease inhibitors were use and stored at -20°C:

- PMSF (Roche): 100 mM in ethanol
- Aprotinin (Applichem): 10 mg/ml in H₂O
- Leupetin hemisulfate (Applichem). 1 mg/ml in H₂O
- Pepstatin A (Applichem) 1 mM ethanol

As phosphatase inhibitor, a 1M stock of sodium fluoride (Sigma) was made and stored at room temperature. The tyrosine phosphatase inhibitor sodium orthovanadate was made as a 100 mM stock solution with H₂O and stored at -20°C. For its full activation, the following protocol was used:

- the pH of the sodium orthovanadate stock was adjusted to 10 with either NaOH or HCl. The solution should have a yellow color
- the solution was boiled until the color disappeared
- after cooling down to room temperature, the pH was adjusted to 10
- the boiling and readjusting was repeated until the pH after the boiling stabilized at 10

5.7 Working with bacteria

5.7.1 Bacterial strains

E.coli DH5 α (Hannah et al.)

F' *endA1 hsdR17/r_k⁻,m_k⁻* supE44 thiE44 thi-1 λ recA1 gyrA relA1 Δ (*lacIZY-argF*)U169 deoR Φ 80*dlacZ* Δ M15

E.coli TOP10 (Invitrogen)

F' *mcrA endA1* Δ (*mrr-hsdRMS-mcrBC*) Φ 80*dlacZ* Δ M15 Δ *lacX74* recA1 deoR araD139 Δ (*ara-leu*)7697 galU galK rpsL (Str^R) endAI nupG

E.coli BL21 (Amersham)

B F', *ompT, hsdS* (*r_B⁻,m_B⁻*), gal, dcm

E.coli dam-4

GM1684 F' F-*lacIq*M15 pro+/dam-4 D (*lac-pro*)XIII thi-1 supE44 (relA1)

5.7.2 Media

Luria-Broth-Medium (LB-Medium)

LB Broth Base (Lennox L Broth Base) Invitrogen

LB-petri dishes

LB-Medium with 1,5% Bacto-Agar

SOC-Medium

Invitrogen

All bacteria were incubated at 37°C either in liquid medium or LB-agar plates supplemented with antibiotics depending on the transformed plasmid . In general 100 μ g/ml ampicilline or 50 μ g/ml kanamycine.

5.7.3 Transformation of bacteria

CaCl₂-competent cells

E. coli TOP10 (Invitrogen) were delivered chemically competent together with the pCR 2.1 TOPO TA-Kit. All other strains were made chemically competent according the CaCl₂-method. In brief, 350 µl of an *E. coli* LB over night culture were used as starter culture for a 50 ml LB culture and were incubated at 37°C and 225 rpm until a OD₆₀₀ of 0.45 - 0.5. Then, the culture is cooled at 4°C for 10 min and subsequently splitted in half. The bacteria were pelletized by a centrifugation step at 4°C (10 min, 8000 rpm). Each pellet was resuspended in 25 ml ice cold 100 mM CaCl₂ and again pelletized at 4°C (15 min, 6000 rpm). Each pellet was then resuspended in 2.5 ml ice cold 100 mM CaCl₂ and incubated on ice for at least 3h. Prior to aliquoting and storage at – 80°C, 0.3 volumes glycerol were added.

Transformation

For each transformation, 100 µl competent cells were incubated with the corresponding plasmid for approximately 1h on ice followed by a heat shock step (1 min, 42°C). The bacteria were then supplemented with 400 µl LB-medium and incubated for 1h at 37°C at 225 rpm. Finally, the bacteria are plated supplemented with the corresponding antibiotics (100µg/ml ampicilline or 50µg/ml kanamycine) and incubated at 37°C over night.

5.7.4 Recombinant expression of proteins in *E. coli*

5.7.4.1 pBAD/Thio-TOPO[®] vector and pBAD/TOPO[®] vector (Invitrogen)

The pBAD/Thio-TOPO[®] vector (Invitrogen) allows to clone the PCR amplified peptide coding regions via the TOPO-TA cloning system (Fig. 66). When the fragments are cloned under the conservation of the reading frame, the peptides are expressed with an N-terminal His-Patch thioredoxin (HP-thioredoxin) - and a C-terminal V5-tag and 6xHis tag. The HP-thioredoxin and 6xHis – can be used for the purification of the recombinant fusion protein by Immobilized Metal Affinity Chromatography under native conditions, while under denaturing conditions only the 6xHis – tag is capable to interact with the metal ions. The thioredoxin tag

also increases the translation efficiency and solubility of eukaryotic proteins expressed in *E.coli* and can be removed with the enterokinase. With an antibody (anti – V5 antibody, Invitrogen) recognizing the V5-epitope, the expressed fusion protein can easily be detected. For the maintenance and replication, the plasmid also contains a gene encoding for ampicilline resistance and a pUC origin of replication. The transcription of the fragment coding for the fusion protein is tightly regulated by the *araBAD* promoter (P_{BAD}) and the transcriptional regulator AraC which is also encoded on the pBAD/Thio-TOPO[®] vector. In the absence of arabinose, an AraC dimer binds to the promoter and blocks the transcription by creating a hairpin. The addition of arabinose induces a conformational change in the AraC dimer, releasing the DNA loop and enabling transcription.

The pBAD/TOPO[®] vector is identical to the pBAD/Thio-TOPO[®] vector, except that fusion proteins are synthesized lacking the N-terminal HP-thioredoxin tag.

For the induction of recombinant proteins with these vectors and their purification under denaturing conditions, the following procedure was applied..

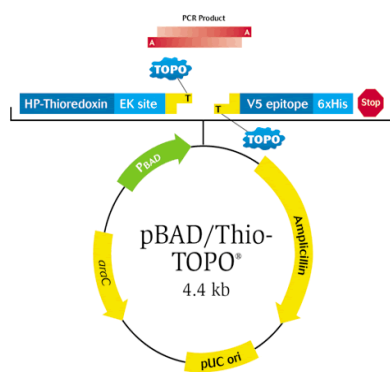


Fig. 66: pBAD/Thio-TOPO[®] vector (Invitrogen). This vector allows the expression of fusion proteins under the control of the inducible *araBAD* promoter (P_{BAD}) with an N-terminal **thioredoxin** tag which can be cleaved off at the Enterokinase (**EK**) site. A second tag, the **V5** epitope, is fused to the C-terminus followed by a **6xHis** tag. The former can be used to easily detect the fusion protein with the anti – V5 antibody and the latter to purify the fusion protein under native and denaturing conditions using Ni^{2+} loaded beads. The tags contribute approximately 16 kDa to the overall size of the fusion protein. For the selection and propagation in *E. coli* an **ampicilline** resistance and pUC origin of replication (**pUC ori**) are encoded on the plasmid. The transcriptional regulator of the P_{BAD} , AraC, is also encoded on the plasmid.

Vector specific oligonucleotides:

Trx forward: TTCCTCGACGCTAACCTG

pBAD reverse: GATTTAATCTGTATCAGG

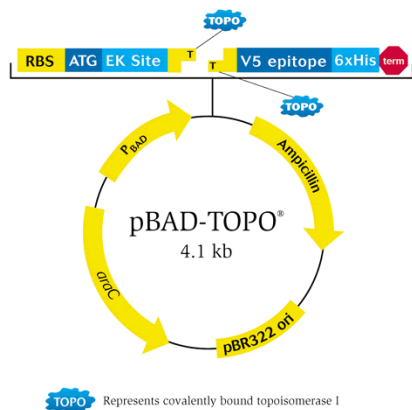


Fig. 67: pBAD/TOPO[®] vector (Invitrogen).

This expression plasmid is identical to pBAD/Thio-TOPO[®] vector, except that the fusion proteins are synthesized without a N-terminal HP-thioredoxin tag. For a detailed description, please refer to Fig. 66.

Vector specific oligonucleotides:

pBAD forward: ATGCCATAGCATTTTTATCC

pBAD reverse: GATTTAATCTGTATCAGG

A 20 ml LB ampicilline (100 μ g/ml) overnight culture was inoculated with the *E.coli* clone containing the corresponding expression plasmid and incubated at 37°C and 225 rpm. The next day, 10 ml over night culture were transferred into a 2 l flask containing 1 l of LB ampicilline (100 μ g/ml) and further incubated at 37°C and 225 rpm until a OD₆₀₀ of 0.5. At this point, arabinose was added to a final concentration of 0.2% to induce the expression of the fusion protein. After incubating 4h at 37°C and 225 rpm, the cells were pelleted by centrifugation (5000 rpm, 15 min) at 4°C. The supernatant was discarded and the pellet resuspended in 20 ml guanidine lysis buffer (6M Guanidine – HCl, 500 mM NaCl, 20 mM Na₃PO₄, pH of the solution was 7.8). The insoluble material was removed by a centrifugation step (12,000 rpm, 20 min at room temperature) and the supernatant transferred into a fresh tube. After the addition of another 5 ml lysis buffer, the remaining insoluble material was pellet by a further centrifugation step at room temperature (13,000 rpm, 20 min). The supernatant was again transferred to a fresh tube.

In the meantime, 2 ml slurry Ni²⁺-beads (ProBond[™] Resin, Invitrogen) per 1 l induction culture were washed three times with 1 ml lysis buffer to remove the preservative, and subsequently added to the supernatant. The binding of the 6xHis –tag to the metal ions was allowed to proceed over night at 4°C. For the purification of the fusion protein at room temperature, the suspension containing the Ni²⁺-beads was decanted into a PD-10 column (Amersham) and the solution ran through the column with 30 – 40 drops per minute. After the solution had completely dropped out, unspecific bound proteins were removed by washing the settled beads with 150 ml denaturing washing buffer (8M urea, 0.5 M NaCl, 20 mM

NaH₂PO₄; the pH of the solution was set to 5.8 immediately prior to usage, because urea is a strong base) per 2 ml slurry beads. The washing buffer dropped out of the column with 30 – 40 drops per minute. Specifically bound protein molecules were first eluted by resuspending the beads in 1 ml **denaturing elution buffer** (8M urea, 0.5 M NaCl, 20 mM NaH₂PO₄; the pH of the solution was set to 3.8 immediately prior to usage, because urea is a strong base) and a 10 min incubation. Then, the running through elution buffer was collected. This elution step was repeated once with 1 ml fresh denaturing elution buffer. The third and fourth elution steps were each carried out with 1ml of **imidazole elution buffer** (250 mM imidazole, 50 mM Na₂HPO₄, 300 mM NaCl, pH 8.0). To increase the amount of eluted proteins, a 10 min incubation step was also done. For the fifth elution step, 1 ml 0.5 M EDTA, pH 8.0 was added to the beads for 10 min. This buffer was also collected. The quality of the protein preparation was assessed by both Coomassie staining and Western blot analysis.

Finally, the metal chelating beads were regenerated by washing with 16 ml of each of the following buffers: 50 mM EDTA pH 8.0, 0.5 M NaOH, sterile H₂O, 5 mg/ml NiCl₂ and again sterile H₂O. For long-term storage at 4°C, 20% ethanol was added to the column.

5.7.4.2 pGEX-3X – Glutathione - S - Transferase fusion proteins

An alternative vector for the expression of proteins in *E.coli* is the pGEX-3X plasmid (Fig.68; Applied Biotech). The expression is under the control of the *tac* promoter and can be induced with IPTG (isopropyl-β-D-thiogalactopyranoside), a lactose analogue which is not metabolized within the cell. The recombinantly expressed proteins are synthesized with the glutathione S transferase (GST) of *Schistosoma japonicum* fused to their N-terminus. This tag contributes 26 kDa to the fusion protein and allows its affinity purification under native conditions by binding to immobilized glutathione, the substrate of GST. Due to the intrinsic factor Xa cleavage site, the GST tag can be removed.

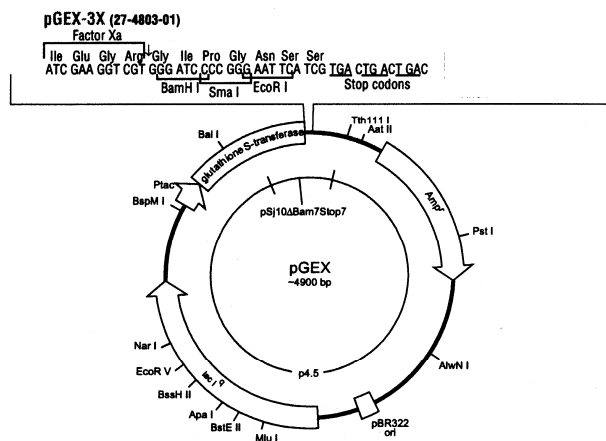


Fig. 68: pGEX-3X (Applied Biotech). This plasmid is suited to express recombinant proteins with an N-terminal Glutathione – S- Transferase (GST) tag under the control of the *tac* promoter in *E. coli*. The GST-tag contributes 26 kDa to the molecular weight of the fusion protein. For a tight expression control, the transcription regulator (**LacI**) is also encoded on the plasmid. Further, an ampicilline resistance (**Amp^r**) is also encoded and the plasmid contains an origin of replication (**pBR322 ori**).

pGEX-3X-vector oligonucleotides:

pGEX-3Xup: CGGGAGCTGCATGTGTCAG

pGEX-3Xdw: GGCAAGCCACGTTTGGTGG

Several protocols have been described for the purification of GST-fusion proteins, but the conditions have to be optimized for each protein to be purified. The following protocol has been used to induce and purify GST- fusion proteins for this work.

10 ml LB containing ampicilline (100 µg/ml) were inoculated with *E.coli* BL21 carrying the desired pGEX-3X expression plasmid. The next day, the over night culture was transferred into 1 l LB ampicilline (100 µg/ml) in a 2 l flask. This culture was incubated at 37°C at 200 rpm. At an OD₆₀₀ = 0.5, the expression of the fusion protein was induced with 0.2 mM IPTG. Since over expressed GST-fusion proteins might have the tendency to form inclusion bodies and, hence, to be insoluble, the induction was carried out in water bath at approximately 20°C at 200 rpm over night. After this induction period, the cells were pelleted at 4°C by centrifugation (10 min, 5,000 rpm). The supernatant was discarded and the pellet was immediately frozen on dry ice to destruct the bacterial wall. The frozen cell pellet was thawed by resuspending in 50 ml ice cold buffer 1 (0.4 M NaCl, 16 mM Na₂HPO₄, 4mM NaH₂PO₄; pH 7.3). The cells were then pelleted again by centrifugation (10 min, 5,000 rpm) and the supernatant was again discarded. In the next step, the pellet was resuspended in 20 ml ice cold buffer 2 (buffer 1 which contained 0.5 M instead of 0.4 M NaCl) which was further supplemented with 1% Triton – X100, 1mM PMSF, 10 µg/ml Aprotinin A, 1µg/ml Leupeptin hemisulfate and 1 µM Pepstatin A. Then, lysozyme (approximately 500 mg; Serva) was added and the cell suspension was incubated on ice for 10 min to digest the bacterial cell wall.

After the following ultrasonication step (when possible a French Press should be used), the insoluble material was removed by two consecutive centrifugation steps at 4°C. The first centrifugation was carried out for 10 min at 10,000 rpm. For the removal of any remaining insoluble material, the supernatant was centrifuged for another 10 min at 12,000 rpm and the pellet was also discarded. In the meantime, 1 ml glutathione beads (Glutathione Sepharose™ 4B, Amersham) were equilibrated by washing twice with buffer 1 and washing once buffer 2 containing 1% Triton – X100. The beads were then added to the cleared lysate and the binding of the GST to glutathione was allowed to proceed for 2h under over head agitation. This binding step and all following purification steps were carried out at 4°C. After the binding, the lysate with the glutathione beads were decanted into a PD-10 column and was allowed to run out with about 30 – 40 drops per minute. The settled beads were washed with 15 ml buffer 2 supplemented with 1% Triton – X100 to remove unspecifically bound proteins, while the specifically bound proteins were eluted with 1 ml of each of the following buffers. First, buffer 3 (25 mM glutathione, 100 mM Tris-HCl, pH 8.0) was added to the beads and the eluate was collected. The elution was repeated with buffer 4 (25 mM glutathione, 150 mM Tris-HCl, pH 8.0), buffer 5 (buffer 3 supplemented with 0.5 M NaCl) and buffer 6 (buffer 4 supplemented with 0.5 M NaCl). In the final, denaturing elution step, 2 ml guanidine lysis buffer (used for the denaturing purification of His-tagged proteins) was added to elute any remaining proteins from the beads. All eluates were analyzed on a SDS-PAGE followed by Coomassie staining and Western blotting with an anti – GST antibody (Santa Cruz). Essential for the isolation of the GST-fusion protein was that all solutions were pre-cooled to 4°C and that the bacterial culture was put on ice immediately at the end of the induction and never allowed to warm again.

5.7.4.3 Recombinant expression of ligand binding and intracellular domain of EmIR with the pBAD/Thio-TOPO® Vector in *E.coli* BL21

The coding regions of the ligand binding (EmIR_{LCL}) and the intracellular (EmIR_{intra}) domain of Emir were cloned into the pBAD/Thio-TOPO® vector for the expression in the *E.coli* strain BL21. The recombinantly expressed fusion proteins were purified under denaturing conditions as described above, two times dialyzed against 5 l 1xPBS and the protein concentration was determined using the BCA method (Pierce) and a bovine serum albumin

(BSA) standard. Each protein induction and purification was analyzed by SDS-PAGE followed by Coomassie staining and Western blotting with the anti-V5 anti antibody (Invitrogen) to identify the induced and purified protein and to analyze the quality of induction. For the cloning of the EmIR_{LCL} encoding fragment (residues 34 to 547), the cDNA fragment spanning from nt 146 to 1685 was amplified via PCR using Tag DNA-Polymerase and the oligonucleotides LCL dw and LCL up. The fragment (nt 3434 - 5296) which encodes EmIR_{intra} (residues 1129 – 1749) was amplified with the Taq DNA-Polymerase and the oligonucleotides CK5 and CK6. Initially, it had been planned to express the EmIR_{intra} domain in *E.coli* using the PinPoint Expression system (Promega). Since the cloning of the coding fragment had not been not successful, the amplified DNA fragment was cloned into the pBAD/Thio-TOPO[®] vector. Due to the original cloning strategies, CK5 and CK6 introduce a *Bam*H I and *Bgl* II restriction site into the PCR product. All plasmids were sequenced prior to the induction of protein expression to ascertain the correct insertion of the DNA-fragment and to exclude point mutations due to the PCR reaction.

Oligonucleotides:

LCL dw: GTCTTCGGTGGAAATCATAC

LCL up: GAAGCCGAGTTTGCCATTG

CK5: ATCGCTGGATCCATACATCGCATTCGAAAGAA

CK6: AACACAAGATCTTGAACAAGACGACCCATCACCGTCA

5.7.4.4 Expression of the extracellular and intracellular domain of EmIR with pGEX-3X in *E.coli* BL21

For the expression the extracellular (□) and intracellular domain as GST – fusion proteins, the fragment coding for the residues 33 – 776 (nt 146 - 2377) and 1146 – 1749 (nt 3485 - 5296), were amplified with the Taq DNA-Polymerase and the oligonucleotides CK35 & CK36 (1 min 94°C; 3 cycles: 20 s 61°C, 2 min 30 s 72°C; 27 cycles: 20 s 94°C, 30 s 63°C, 2 min 30 s 72°C; 10 min 72°C) and CK37 & CK 38(1 min 94°C; 3 cycles: 20 s 60°C, 2 min 30 s 72°C; 27 cycles: 20 s 94°C, 30 s 63°C, 2 min 30 s 72°C; 10 min 72°C) , respectively, and subsequently cloned via the Bam HI and Eco RI into the pGEX-3X expression vector. In case of CK36 and CK38, a stop codon was included to minimize the C-terminally added residues coded by the plasmid. After the sequencing of the expression plasmids, the expression of the fusion proteins EmIR α – GST and EmIR_{intra} - GST in *E.coli* BL21 was induced as described

above. After the purification under native conditions, SDS-PAGE followed by both Coomassie staining and Western blotting with an anti – GST antibody (Santa Cruz) was carried out to analyze the protein purification. Finally, the purified proteins were two times dialyzed against 5 l 1xPBS and then the concentration of the proteins was determined with the BCA method (Pierce).

Oligonucleotides:

CK35: GTCCCGTGGATCCGTCGGGTCTTCGGTGGAAATC

CK36: CCAAAGGAATTCTCAGGAGGCAGGAGAACTGCGAC

CK37: GAGTGGAGGATCCCTAACCCGGAGTACTGGCACG

CK38: GAACACAGAATTCTCAACAAGACGACCACCCATCACCG

5.7.4.5 Long-term storage of purified proteins

For the long-term storage of purified proteins, glycerol was added to a final concentration of 10% and aliquots were made. All samples were frozen on dry ice to reduce the formation of ice crystals and thawed in ice-water to reduce the damaging of the proteins. If possible, repeated freezing-thawing cycles were avoided.

5.8 Immunization of rabbits

White New Zealand Rabbits were immunized using the “Antibody-Multiplier, Ziege/ Kaninchen (ABM-ZK) komplett” and “Antibody-Multiplier, normal (ABM-N) inkomplett” from Linaris (Wertheim-Bettingen, Germany). The adjuvans were reconstituted with 2 ml 1xPBS containing the desired antigen, i.e. EmIR_{LCL} – thio or EmIR_{intra} – thio, at a concentration of 250 µg/ml. For the initial immunization, 1 ml of the ABM-ZK/ EmIR_{LCL} – thio or ABM-ZK/ EmIR_{intra} – thio was injected intravenously. At day 12 post-immunization, the antibody production was reboosted by injecting again 1 ml of the reconstituted ABM-ZK solution containing the antigen. After an incubation period of 14 d, i.e. at day 26 post-immunization, a second re-boost was carried out with 1 ml ABM-N/ EmIR_{LCL} – thio and ABM-N/ EmIR_{intra} – thio, respectively. While the rabbit immunized with EmIR_{LCL} – thio was sacrificed at day 45 and the final bleeding was done, the rabbit immunized with EmIR_{intra} – thio was boosted a third time with 1 ml reconstituted ABM-N. On day 59, the second rabbit

was sacrificed and the final bleeding was carried out. For the purification of the serum, the blood was allowed to clot for 30 – 45 min and the insoluble fraction was pelletized by centrifuging for 15 min at 2500 rpm and room temperature. The supernatant, i.e. the serum was taken off, aliquoted and stored at -20°C.

5.9 Expression of *E. multilocularis* proteins in heterologous systems

5.9.1 Expression of EmIR in S2 (*Drosophila*) – cells

pMT/V5 – His

The complete ORF encoding EmIR with its putative signal peptide (residues 2 - 1749) was amplified with the Pfu Turbo DNA-Polymerase (Stratagene) and the oligonucleotides CK 83 and CK84. This fragment was cloned into the pMT/V5-His expression plasmid (Invitrogen) via the *KpnI* and *XbaI* sites under conservation of the reading frame to give the plasmid pMT/V5 - **emir**. Recombinant protein expressed with this plasmid are synthesized with a C-terminal fused V5 and His-tag, which allow an easy detection with the V5-antibody and purification with Ni²⁺ beads, respectively. After the transfection into S2 –cells with calcium phosphate according to the manufacturer's instructions, the expression of the recombinant protein was analyzed by Western Blot analysis with the V5 – antibody.

pMTBip/V5 – His

In contrast to pMT/V5 – His, the pMTBip/V5 – His expression plasmid (Invitrogen) allows the expression of heterologous proteins with a signal peptide from *Drosophila melanogaster*. With the oligonucleotides CK98 and CK84, the ORF encoding EmIR but the putative signal peptide (aa 33 – 1749) was amplified, also with the Pfu Turbo DNA-Polymerase (Stratagene) and ligated into the pMTBip/V5 – His A plasmid via the *BglIII* and *XbaI* site. This plasmid, pMTBip/V5 – *emir*, was transfected into S2 cells according to the recommendations given by the manufacturer and the expression was detected as described for pMT/V5 – His.

For the synthesis of recombinantly expressed EmIR with a N-terminally fused Flag- tag (DYKDDDDK) besides the C-terminally fused V5 and His – tags, the plasmid pMTBip/V5 – *emir* was digested with *BglIII* and subsequently purified with the Qiagen's QIAquick® Gel

Extraction Kit. In the subsequent step, the linearized plasmid and the oligonucleotides Flag dw and Flag up were ligated with the T4 DNA ligase (NEB) over night at 16°C. Those complementary oligonucleotides encoded the Flag tag and had 5' overhangs which were complementary to the 3' overhangs of the linearized plasmid (Fig.69).

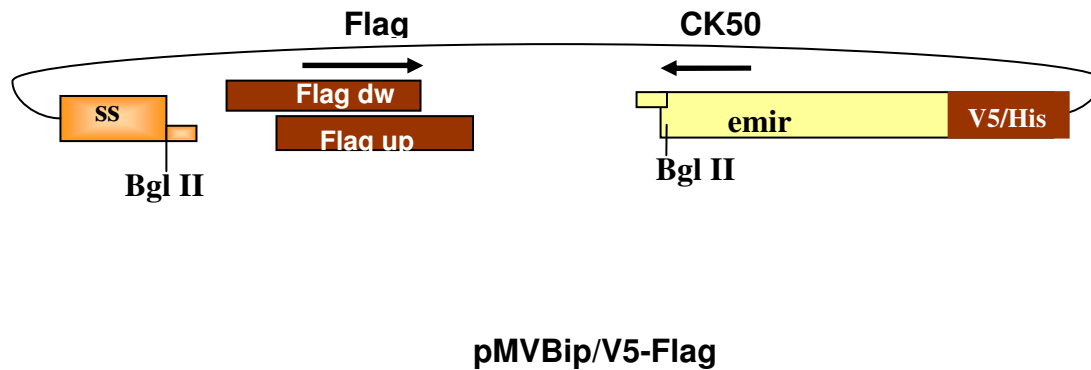


Fig. 69: Construction of the pMVBip/V5-Flag *emir* expression plasmid. The plasmid pMV/V5-*emir* was linearized via digestion with Bgl II and subsequently ligated with the oligonucleotides Flag dw and Flag up which encode the Flag tag and whose 5' ends are complementary to the 3' overhangs of the digested BglII site. The **Bgl II** restriction site, the signal sequence (ss) and the sequence of the *Echinococcus* insulin receptor (*emir*) are indicated. The arrows mark the oligonucleotides used for the PCR to control the insertion.

The ligated plasmids were then chemically transformed into *E. coli* TOP10 (Invitrogen) and selected on LB plates containing 100µg/ml Ampicilline over night at 37°C. The correct insertion of the oligonucleotides was first controlled by PCR employing the insert specific oligonucleotide Flag and *emir* specific oligonucleotide CK50. In case of the positive clones, the plasmids were purified with the Qiagen's QIAprep® Spin Miniprep Kit and sequenced. This plasmid was named pMVBip/V5-Flag *emir*.

Oligonucleotides used for the construction of the *Drosophila* expression vectors:

CK83: AGGCACGGTACCATGCCAAAATCGTCCTCTTATTC

CK84:ACAAAATCTAGAACAAGACGACCCATCACCGTC

CK98: CCGTCC AGATCT CGGGTCTTCGGTGGAAATC

Flag dw: GATCT GACTACAAGGACGACGATGACAAG

Flag up: GATCT CTTGTCATCGTCGTCCTTGTAGTC

Flag: GACTACAAGGACGACGATGAC

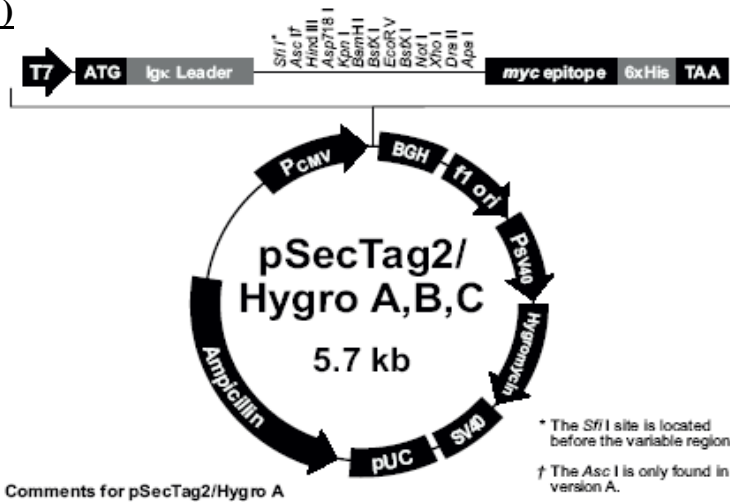
CK50: GTAAGAGGGCGTGATCGCG

5.9.2 Expression of EmIR in mammalian cells – human embryonal kidney (HEK293) cells

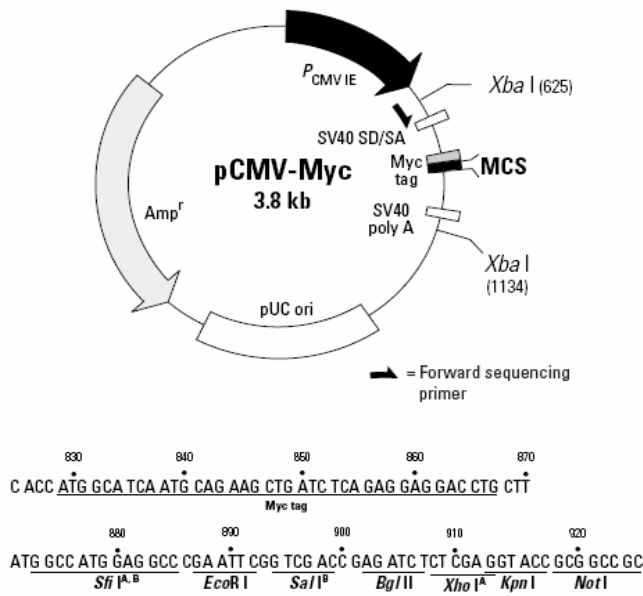
For the recombinant expression of proteins in the human embryonal kidney (HEK293) cell line, 2 expression systems were used (Fig.70). The pSecTag2/Hygro (Fig.70 A) system (Invitrogen) allows the expression of membrane anchored proteins under the control of the constitutively active human cytomegalovirus immediate-early promoter/ enhancer (P_{CMV}). The proteins being expressed with this system are synthesized with the murine Ig κ Leader sequence as the secretion signal fused to their N-terminus. The myc-tag and a 6xhistidine tag are C-terminally fused and enable the detection with an anti-myc antibody and purification with Ni^{2+} - beads. The second system (Fig. XX B) is suited for the expression of cytoplasmic proteins also under the control of the constitutively active P_{CMV} promoter. But in contrast to the pSecTag2/Hygro system, the recombinant proteins are expressed without a signal peptide and the myc or HA – tag is fused to the N-terminus. The corresponding expression vectors pCMV-myc/HA were from Clontech.

Fig. 70 (next page): Graphic view of mammalian expression vectors. All three vectors encode an ampicilline resistance (AmpR) and a pUC origin for the selection in *E. coli*. The transcription of the desired ORF is under the control of the constitutive P_{CMV} promoter. **A)** The pSecTag2/Hygro contains a fl origin and a gene coding for a hygromycin resistance under the control of the SV40 promoter for the selection of transfected mammalian cells. The recombinantly expressed proteins are made with the N-terminal fused murine Ig κ Leader sequence as export signal and a C-terminal fuses V5 and His-tag for the expression control via Western blotting and purification via metal affinity chromatography, respectively. **B,C)** The proteins are expressed with a N-terminal fused myc-tag (B) or HA-tag (C) which allows the expression control by Western blotting.

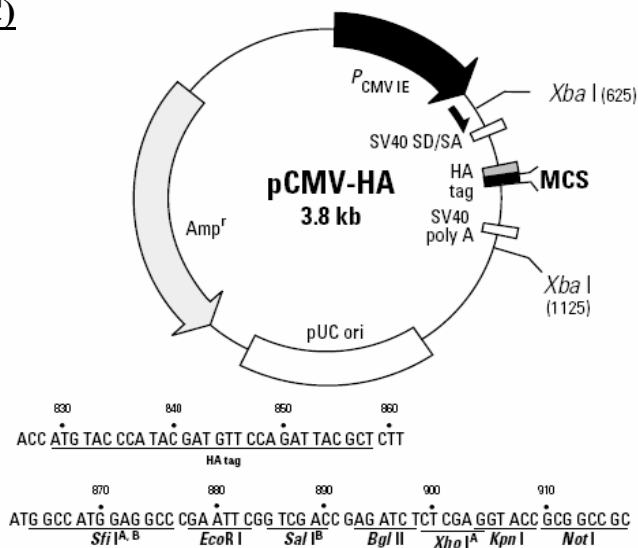
A)



B)



C)



pSec – *hir*

Total RNA was isolated from HepG2 cells, DNase I treated and reversely transcribed using the Omniscript (Qiagen) and the polydT oligonucleotide CD3RT. This first strand cDNA served as template to amplify the ORF of *hir* coding for the residues 28 – 1382. The PCR was carried out using the Phusion DNA-Polymerase (Finnzymes) and the oligonucleotides HIR12 (*Hind*III) and HIR13 (*Apa*I) and the following PCR conditions: 30 s 98°C; 5 cycles 10 s 98°C, 30 s 60°C, 2 min 10 s 72°C; 30 cycles 10 s 98°C, 30 s 63°C, 2 min 10 s 72°C; 10 min 72°C. The amplified fragment was cloned via the *Hind*III and *Apa*I site into pSecTag2/Hygro B and sequenced.

Oligonucleotides:

HIR12 (*Hind*III): GGCGCCAAGCTTCACCTGTACCCCGGAGAGG

HIR13 (*Apa*I): GAGGCAGGGCCCGGAAGGATTGGACGGAGGCT

pSec – *emir* Flag

For the expression of EmIR in HEK293 cells with the N-terminally fused Flag tag, the corresponding ORF was amplified with the oligonucleotides Flag *Sfi* and CK104 using the High Fidelity Expand PCR-System (Roche) and pMVBip/V5-Flag *emir* as template (94°C 2 min; 94°C 20s; 57°C 30s; 5min 10s 72°C; 30 cycles; 10min 72°C). The amplified fragment, *emir* – Flag, was cloned into the pCR 2.1TOPO TA cloning vector (Invitrogen) and sequenced using gene specific oligonucleotides. In the next step, *emir* – Flag was cloned via the *Sfi*I and *Xho*I restriction site into pSecTag2/Hygro A to give the expression plasmid pSec – *emir* Flag.

Oligonucleotides:

Flag *Sfi*: GTA TGG CCC AGC CGG CCG ACT ACA AGG ACG ACG ATG A

CK104: CAC AAA CTC GAG TAC AAG ACG ACC CAT CAC CG

pSec – emirLCL – hir Flag – chimera

The cDNA fragment ranging from nt xx to xx, encoding the amino acid residues 1-729 of EmIR was fused via PCR to the cDNA fragment encoding the amino acid residues 675 – xx of the human insulin receptor (HIR). The proof reading DNA-Polymerase Pfu Turbo was used in all following PCR reaction because an additional 3' A added by the Taq polymerases would introduce a frame shift after the fusion reaction. The so-called pSec – *emir*LCL – *hir* Flag – chimera was the following way (Fig.71):_In a first step and to preserve the N-terminal fused Flag tag, the cDNA fragment encoding the ligand binding domain and part of the fibronectin domain (aa 33- 729) of EmIR were amplified with the oligonucleotides Flag Sfi and CK106 with pSec – *emir* Flag as the template, while in the case of *hir*, the ORF encoding the residues 675 to 833 was amplified with the oligonucleotides HIR9 and HIR6 using pSec-*hir* as template. Both fragments were cut from an agarose gel and purified with the Qiagen's QIAquick® Gel Extraction Kit. The 9 most 5' nucleotides of CK106 and HIR9 are complementary to each other, i.e. the two oligonucleotides overlap in a total of 18 nucleotides, having a calculated melting temperature ($T_m = 4x(G+C)+2x(A+T)$) of 50°C. For the fusion of the two fragments, equal amounts were added to the PCR reaction mixture containing dNTPs, 1x Pfu Turbo buffer, U of Pfu Turbo DNA-Polymerase (Stratagene) and xx of the oligonucleotides Flag SfiI and HIR8. After an initial denaturing step (1 min 95°C), the complementary parts of the fragments were allowed to anneal (1 min 45°C) providing the Polymerase a 3' OH end to duplicate the still single stranded cDNA (2 min 40 s 72°C). Then, a standard PCR program was executed to amplify the fused cDNA fragment (20 s 95°C, 30 s 60°C, 3 min 72°C). After the separation on a 1xTAE 1% agarose gel, the PCR product of the correct size was cut, purified as described above and subsequently adenylated at its 3' ends to be able to clone it into the TOPO TA cloning vector (Invitrogen) to give the plasmid *emir* Flag – hir8 TOPO. To complete the chimera, the missing part of the *hir* cDNA had to be ligated to the *emir* Flag – hir8 fragment. The *hir* cDNA possessed a unique *Avr*II site which was not present in *emir*. Since *hir* had already been cloned into pSecTag2/Hygro via *Hind*III and *Apa*I, pSec-*hir* was digested with *Avr*II and *Apa*I to get the missing part of *hir* for the chimera. In the meantime *emir* Flag – hir8 TOPO was digested with *Sfi*I and *Avr*II. The two fragments were ligated via the *Avr*II site and, in the same tube, subsequently ligated into pSecHygroB via the *Sfi*I and *Apa*I sites. In the last step, the expression construct pSec – *emir*LCL – *hir* Flag – chimera was sequenced.

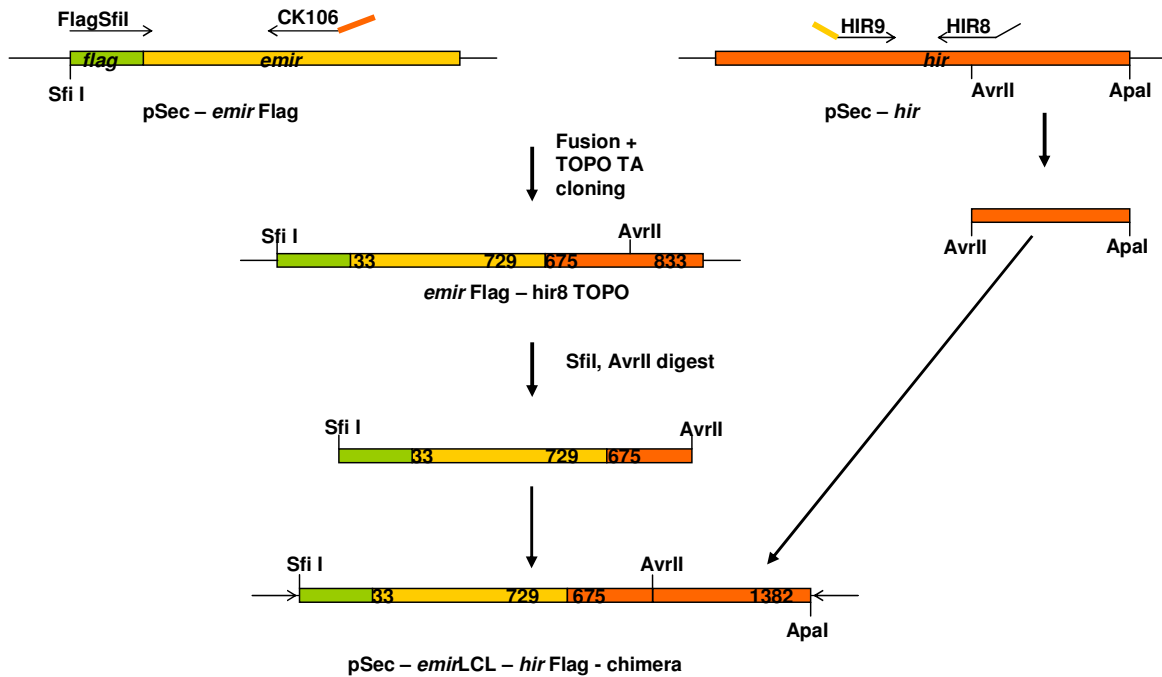


Fig.71: Schematic view of the cloning strategy for the expression plasmid pSec – emirLCL – hir Flag – chimera. The employed restriction sites are indicated. The numbers indicate the residues encoded by the limiting codons.

Oligonucleotides:

Flag Sfi: GTA TGG CCC AGC CGG CCG ACT ACA AGG ACG ACG ATG A

CK106: CCC TTT GA GCA AAA AAC AGA AGT CTC GGT A

hir emir

HIR9: TGTTTTTTG CTCAAAGGGCTGAAGCTCCC

Emir hir

HIR8: GTGACTGCA CCGTTCCTCAGGGGTGTCC

emir hir

pSec- hir-emir_{intra}

For the substitution of the intracellular domain of HIR with the putative intracellular domain of EmIR, the ORF coding for the residues 28 – 979 of HIR was amplified with the oligonucleotides HIR 12 and HIR 15 and subsequently cloned into the TOPO TA cloning vector (Invitrogen) to give the plasmid TOPO HIR12 - 15. While the former oligonucleotide introduced a HindIII restriction site at the 5' end, the latter introduced an *AcI* site at the

3'end. In case of EmIR, the ORF coding for the putative intracellular domain (aa 1133 – 1749) was amplified with the oligonucleotides CK107 and CK109 and also cloned into the TOPO TA cloning vector to obtain the plasmid TOPO CK107 – 109. The oligonucleotide CK109 introduced an ApaI site at the 3' end., whereas CK107 did not introduce any restriction site, because *emir* possesses an endogenous AclI site in the region coding for the juxtamembrane region (nt AACGTT³⁴⁵⁶). For the cloning of the fusion product into pHygroB via the HindIII and ApaI site, TOPO HIR12 – 15 was digested with HindIII and AclI, while TOPO CK107 – 109 was digested with AclI and ApaI. Both inserts were subsequently purified and, analogous to the construction of the pSec – *emir*LCL – *hir* Flag – chimera, ligated via the AclI restriction site and ligated into the pSec expression vector via the HindIII and ApaI restriction sites. This plasmid pSec- *hir-emir*_{intra} was also sequenced.

Oligonucleotides:

HIR12 (HindIII): GGCGCCAAGCTTCACCTGTACCCCGGAGAGG

HIR15 (AclI): CATCTGAACGTTTCTTTCTCAGGAATAGATAAATAC

CK107: GAGGAACGGTGCAGTCACAAGGTCTCAAG

CK109 (ApaI): CACAAAGGGCCCACAAGACGCCCATCACCG

Construction of the EmIR K1209A mutant

For the substitution of the lysine for an alanine at position 1209 in EmIR, the corresponding codon had to be changed from AAG to GCG. The point mutation was introduced via PCR. In a 50 µl containing 125 ng of each oligonucleotide CK90 and CK91, 10ng pSec – *emir* Flag, 2 µM dNTPs, 2.5 U Pfu Turbo DNA-Polymerase (Stratagene) were added and the following amplification program was executed: 95°C 1min, 95°C 50s, 60°C 50s, 68°C 11min, 18 cycles, and final elongation for 7min at 68°C. In the next step, the template DNA was digested over night at 37°C by adding 10U of *DpnI* (NEB) to the PCR reaction. *DpnI* digest only methylated DNA and therefore digest only the template DNA and not the PCR amplified DNA. The *DpnI* treated PCR product was chemically transformed into *E.coli* Top10 and plated on LB ampicilline (100µg/ml) plates to select for bacteria containing the religated PCR product. The presence of the plasmid in the grown clones was examined via a gene specific PCR. For the positive clones, the plasmid DNA was isolated with the Qiagen's QIAprep® Spin Miniprep Kit and the insert was completely sequenced to verify that only the intended point mutation had been introduced. Since a point mutation could also occur in the expression

plasmid, the insert was cut from the vector via the *SfiI* and *XhoI* restriction site, ligated into a freshly digested pSecTag2/Hygro. The expression plasmid was chemically transformed into *E.coli* Top10. For the selection on the plasmid, the cells were plated on LB Ampicilline (100µg/ml) plates and incubated at 37°C. The correct incorporation of the insert was analyzed via PCR using gene specific primer followed by sequencing.

alanine

CK90: GCT GCC ATC **GCG** ACG CTT TCT TC

CK91: GAA GAA AGC GTC **GCG** ATG GCA GC

5.9.3 Expression of EmFyn and EmRhoGAP in mammalian cells

pCMV-EmFyn-HA – constructs

The fragment coding for the SH4, SH3 and SH2 domain of EmFyn (nt 61 – 889; aa 1 – 276) was amplified with the Taq DNA Polymerase and the oligonucleotides EmFyn6 and EmFyn7 using the following amplification program: 30 s 95°C; 3 cycles 20 s 95°C, 30 s 61°C, 1 min 72°C; 27 cycles 20 s 95°C, 30 s 63°C, 1 min 72°C; 10 72°C. The amplified fragment was also ligated into the pCMV-HA vector to give the expression plasmid pCMV-*emfynSH4-3-2*-HA. The expression plasmid was sequenced before the transfection was carried out.

Oligonucleotides:

EmFyn 6 (*SfiI*): **GGCCATGGAGGCCATGGGAATTGTTTTACTTGCC**

EmFyn 7 (*SalI*): **GGTATAGTTCGACACACGGCTGCGATAGGCGAC**

pCMV-EmRhoGAP-myc

The ORF coding for full length EmRhoGAP (nt 102 – 1601) was PCR amplified with the oligonucleotides Z2-123-2 (*SfiI*) and Z2-123-3 (*XhoI*) using the Taq DNA Polymerase (NEB) and *emrhogap* which had been previously cloned into the pCR 2.1 TOPO vector (Invitrogen) as template. The following PCR program was used: 1 min 94°C; 3 cycles of 20 s 95°C, 30 s 59°C, 1 min 30 s 72°C; 27 cycles 20 s 95°C, 30 s 63°C, 1 min 30 s 72°C; 10 min 72°C. The oligonucleotides introduce a *SfiI* and a *XhoI* site at the 5' and 3' end of the fragment which

were used to ligate the fragment into pCMV-myc under the conservation of the reading frame. The corresponding expression plasmid was hence named pCMV-*emrhogap*-myc.

Oligonucleotides:

Z2-123-2 (SfiI): CACCGGCCATGGAGGCCATGGAATCTGACCCTGCGG

Z2-123-3 (XhoI): CGAGGTCTCGAGGGTGCGAACAAATACGCTCTC

5.9.4 Transfection of mammalian cells, lysis and immunoprecipitation

HEK293 cells were grown in DMEM 10%FCS, 100 U/ml Penicillin G/ Streptomycin (Pen/ Strep) at 37°C and 5% CO₂. The day prior to the transfection, the medium was removed and the cells were trypsinized for 10 min at 37°C. The cells suspension was then transferred into 5 ml DMEM 10% FCS, Pen/ Strep to inactivate the protease. The number of viable cells was determined by trypane blue staining and counting in a Neubauer chamber. 1.3×10^6 cells were seeded per well of a 6-well plate (Nunc) containing 5 ml DMEM 10%FCS, Pen/Strep and incubated at 37°C and 5% CO₂. The next day, the old medium was replaced by 4 ml fresh medium and the cells were further incubated. In the meantime, 10 µg of plasmid DNA was mixed with 62 µl 2M CaCl₂ and brought to a final volume of 500 µl with double distilled water. This solution was mixed and then slowly added to 500 µl 2x HEPES-Buffered Saline (HBS; 50mM HEPES, 1,5mM Na₂HPO₄, 280mM NaCl, pH 7,1). Subsequently, the transfection solution was shortly vortexed and incubated for 45 min at room temperature. Finally, the transfection solution was added drop wise to the medium and the cells were incubated for another 6 – 8 h. After this time, the medium was removed and fresh DMEM 10%FCS, Pen/Strep was added and the incubation was continued for another 48h.

When the stimulation of phosphorylation of the *emir*LCL – *hir* Flag – chimera by host factors was examined, the rich medium was replaced after 48h and replaced by medium containing only 0.2% FCS. After 4-5 h, the stimulus was added for the indicated time. Then, the medium was immediately removed and the cells were lysed in 200 µl 1xTBS lysis buffer (20 mM Tris, 150 mM NaCl, 1 mM NaVO₃, 1 mM EDTA, 10 mM NaF, 1 mM PMSF, 10 µg/ml Aprotin A, 1µg/ml Pepstatin hemisulfate, 1 µM Leupeptin, 1% Triton-X 100) under over head agitation for at least 1 h at 4°C. With a centrifugation step (15, 000 rpm; 15 min), the insoluble material was pelletized and the supernatant was taken off for the downstream applications.

The single transfection of pCMV-*emfyn*ΔCT-HA or co-transfection with pCMV-*emrhogap*-myc into HEK293 cells was carried out as for the receptor constructs, except that 1×10^6 cells were seeded in 6- well plates and that the 2xHBS was replaced by 2xBBS. In case of the co-transfections, 10 μg of each plasmid was used. The lysis was carried out as described above.

For immunoprecipitations, the lysate was brought to a final volume of 500 μl with fresh lysis buffer and the anti-myc and anti-HA (both Santa Cruz Biotechnologies) were added to a final dilution of 1:100. After rocking over night at 4°C, 40 μl slurry agarose G beads (Upstate) were equilibrated by washing three times with lysis buffer and then added to the lysate containing the antibody. After another 4-5h of overhead agitation, the antigen/antibody/protein G complex was precipitated by centrifugation (1 min 2500 rpm) at 4°C. Unspecific bound proteins were removed by three washing steps with 200 μl lysis buffer each. The washed complex was then resuspended in 80-100 μl 2 x SDS sample buffer containing β-mercaptoethanol, boiled for 5 min and then subjected to Western blot analysis.

5.10 Yeast Two Hybrid analysis

5.10.1 Media, buffers and yeast strains

Non-transformed *S. cerevisiae* AH109 (MATa, *trp1-901*, *leu2-3, 112*, *his3-200*, *gal4Δ*, *gal80Δ*, *LYS2::GAL1_{UAS}-GAL1_{TATA}-HIS3*, *GAL2_{UAS}-GAL2_{TATA}-ADE2*, *URA3::MEL1_{UAS}-MEL1_{TATA}-lacZ*) was maintained on YPDA plates and transferred on a fresh plate approximately every 2 – 3 weeks, incubated at 30°C for 2-3 days and then stored at 4°C.

YPDA:

20 g/l Difco Peptone

10 g/l yeast extract

20 g/l Bacto agar (for plates)

distilled H₂O ad 950 ml

The pH of the medium was set to 5.8 with 25% HCl (Merck) and then autoclaved. When the solution was cooled down to approximately 55°C, 50 ml of filter sterilized 40% Glucose (w/v) and 3 ml of a 1% adenine hemisulfate solution were added. The YPDA medium,

containing a final glucose concentration of 2% and adenine hemisulfate concentration of 0.003% was stored at room temperature, while plates were stored at 4°C.

For the selection of transformed AH109 and the detection of interaction, plates were made containing a specific selection medium. These single dropout (SD) media were made the following:

SD:

6,7 g Difco™ Yeast Nitrogen Base without Amino Acids

20 g Difco™ Bacto Agar

X g of the corresponding drop out (DO) supplement (Clontech) lacking the selective amino acid

dH₂O ad 950 ml

DO supplements (Clontech) :

- Leu/ - Trp DO Supplement (0.64 g/l)

- Ade/ - His/ - Leu/ - Trp DO Supplement (0.6 g/l)

The pH of this medium was also set to 5.8 and following the autoclaving step, 50 ml of 40% glucose (w/v) was added. Then plates were poured under sterile conditions. For the SD - His/ - Leu/ - Trp plates, the medium was set up as described above, except that it was additionally supplemented with 20 mg/l histidine HCl monohydrate (Sigma).

5.10.2 Matchmaker 3 GAL4 Two – Hybrid System

The Matchmaker 3 GAL4 Two – Hybrid System (Clontech) and *S. cerevisiae* AH109 (see above) were employed to analyze protein – protein interactions in further eukaryotic system. This system comprises two expression vectors, pGADT7 and pGBKT7 (Fig.72). Both vectors allow the expression of proteins under the control of the constitutively active ADH1 promoter with the difference that in case of p GADT7 the GAL4 activation domain (AD) and in case of pGBKT7 the GAL4 DNA-binding domain (BD) is fused to the N-terminus of the expressed protein. These vectors further differ in that the former encodes an ampicilline resistance and the LEU2 gene which allows the selection for bacteria and yeasts containing the plasmid in

the corresponding media, respectively. pGBKT7 instead encodes a kanamycine resistance and the TRP1 gene which allows a selection as well and also a differentiation form GADT7.

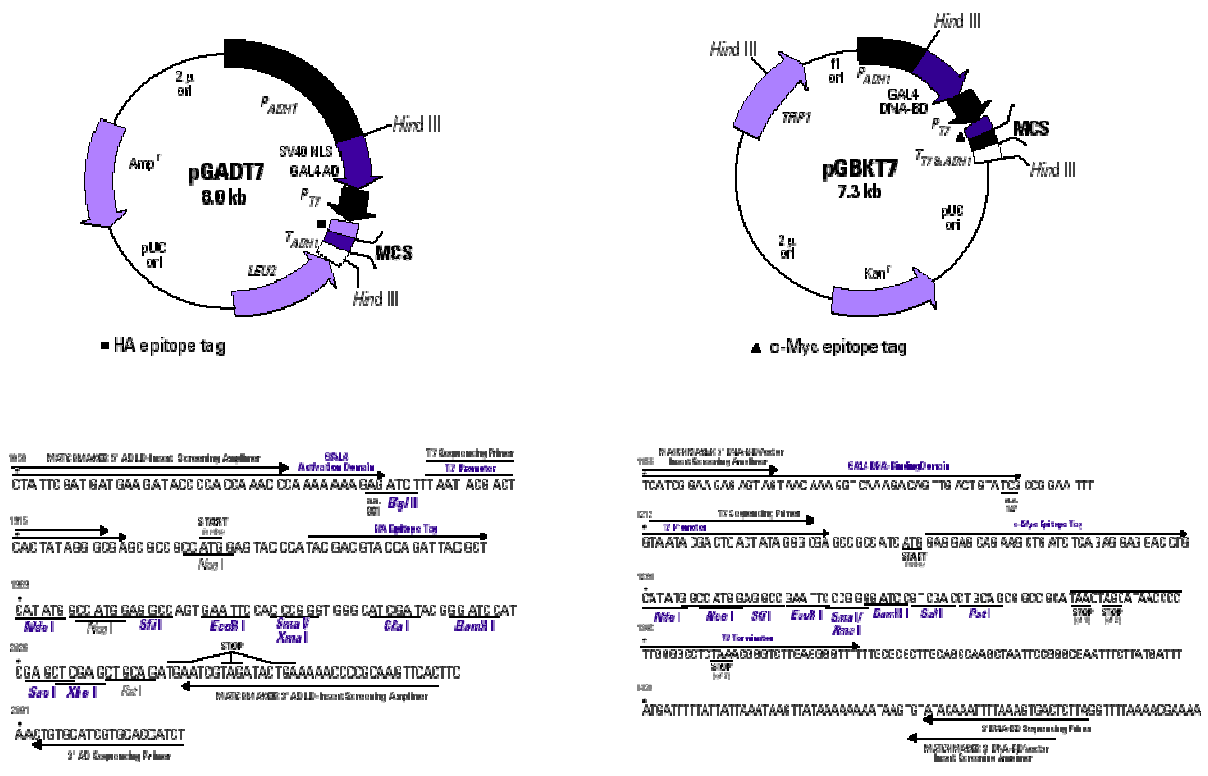


Fig. 72: Schematic view of the Yeast Two Hybrid expression vectors. In both vectors the expression of the cloned DNA fragment is under the control of the constitutive ADHI promoter (P_{ADHI}). **A)** With GADT7, the proteins are expressed with the N-terminally fused activation domain (AD) of the GAL4 transcription factor. It further codes for an ampicillin resistance (AmpR) and for leucine (Leu) as selection markers. **B)** With pGBKT7, the proteins are expressed with the N-terminally fused DNA binding domain (BD) of the GAL4 transcription factor. The encoded selection markers are a kanamycine (KanaR) resistance and the tryptophane (Trp) gene.

pGADT7 oligonucleotides:

T7-Sequencing Primer: TAATACGACTCACTATAGGGC

AD Sequencing Primer: AGATGGTGCACGATGCACAG

pGBKT7 oligonucleotides

T7-Sequencing Primer: TAATACGACTCACTATAGGGC

BD Sequencing Primer: TAAGAGTCACTTTAAATTTGTAT

5.10.3 Yeast transformation and analysis of protein interaction

The transformation of AH109 yeast cells was done according to Chen et al. [4], with some modifications. In brief, 100 ml YPDA were inoculated with 4-5 AH109 colonies being 2-3 mm in diameter and incubated at 30°C and 175-200 rpm. For 10 transformation reactions, the yeast cells from a 20 ml over night culture were pelletized by centrifuging for 5 min at 1000 rpm at room temperature. The supernatant was discarded and the pellet resuspended in 1 ml ONE-STEP-Buffer (0.2 M Lithium acetate, pH 7.5; 40% polyethylenglycol 3350; 100 mM dithiothreitol). The best transformation results were obtained when the buffer was freshly prepared from stock solutions with DTT being setup as 1 M stock and stored at – 20°C. For each transformation reaction, 0.5 – 1 µg of each plasmid were carefully mixed with 100 µl yeast cells resuspended in ONE-STEP Buffer. Following a heat shock step (30 min 45°C), the cells were plated on SD agar plates selecting for the transformed plasmids. Generally, after 2-3 days the first colonies were visible on the plates. For the interaction studies, only those colonies were used which had reached a diameter of at least 1 mm after 4 – 5 days to exclude false positive colonies. For the analysis of the interaction, those colonies were picked from the initial transformation plate and resuspended in 50 µl sterile 1xPBS to reach equal suspensions for the dropping on the interaction plates and to dilute away eventually contaminating medium from the initial plate. In a typical experimental setup, 5 µl of the suspension was dropped on the following SD agar plates under a sterile working bench:

SD – Leu/ - Trp for the selection on the plasmids

SD – His/ - Leu/ - Trp for the selection on interaction under medium stringency conditions

SD – Ade/ - His/ - Leu/ - Trp for the selection on interaction under high stringency conditions

The growth on these plates was daily checked and in general, growth on selecting plates could be observed after 4-6 days of incubation at 30°C in case of interacting fusion proteins. As a control for the quality of the plates and for a better evaluation of the growth of the transformed AH109, the control plasmids included in the Matchmaker system were also transformed. The expression of the large T antigen of the SV-virus as BD-fusion (T-BD) and human p53 as AD-fusion (p53-AD) in a AH109 cells results in a strong interaction and hence, the transformed yeast cells should grow on interacting plates under any stringency condition (positive control). With human lamin C, a protein is expressed as BD- fusion (lamin C – BD)

which barely interacts with any other protein, even p53. Therefore, yeasts expressing those two proteins should not grow on interaction plates but on plates only selecting for the plasmids and serve therefore as negative control. The growth of yeast on interaction plates expressing the proteins to be analyzed was judged in comparison to the positive and negative control.

5.10.4 Cloning of Yeast Two Hybrid constructs

5.10.4.1 EmFyn constructs

EmFyn-SH4-3-2

The ORF coding for EmFyn lacking the tyrosine kinase domain and the C-terminal tail (nt 61 – 889; aa 1 – 276) was also amplified from the cloned full length *emfyn* using Taq DNA-polymerase (NEB). The oligonucleotide used were EmFyn1 (NdeI) and EmFyn2 (EcoRI) and the reaction conditions were: 1 min 94°C; 3 Cycles 20 s 94°C, 30 s 61°C, 1 min 72°C; 22 cycles 20 s 94°C, 30 s 63°C, 1 min 72°C; 10 min 72°C. The amplified fragment was cloned via the NdeI and EcoRI restriction sites into the pGADT7 and pGBKT7 plasmid.

EmFyn-SH2

The oligonucleotides EmFyn3 (NdeI) and EmFyn2 (EcoRI) were employed to amplify the cDNA fragment (nt 578 – 889) coding for the EmFyn-SH2 domain (aa 173 – 276) from the cloned full length *emfyn* cDNA. The PCR was carried out with the Taq DNA-Polymerase (NEB) with the following PCR program: 1 min 94°C; 3 Cycles 20 s 94°C, 30 s 61°C, 30 s 72°C; 22 cycles 20 s 94°C, 30 s 63°C, 30 s 72°C; 10 min 72°C. The amplicon was also cloned via the NdeI and EcoRI restriction sites into the pGADT7 and pGBKT7 plasmid.

Oligonucleotides:

EmFyn1 (NdeI): GCAAGTCATATGATGGGGAATTGTTTTACTTGCCAC

EmFyn2 (EcoRI): GGTATAGAATTCACACGGCTGCGATAGGCGAC

EmFyn3 (NdeI): GCTGTACATATGGGTCTGTCTACACAAATGGAAGC

EmFyn5 (SalI): GGCCAGTCGACAAAGATGTCGATGAGGTTGTGG

5.10.4.2 EmRhoGAP constructs

EmRhoGAP

As a control to verify the amino acid sequence of EmRhoGAP, the ORF coding for the full length protein was amplified via PCR from a cDNA preparation of *in vitro* cultivated metacystode vesicles of the *E. multilocularis* isolate H95. For the first strand synthesis, total DNase I treated RNA was reversely transcribed with the Omniscript Kit (Qiagen) as described above). The PCR was carried out with NEB's Taq DNA polymerase and the oligonucleotides Z3-123- 3 (XhoI) and Z3-123-4 (NdeI) under the following conditions: 1 min 94°C; 3 Cycles 20 s 94°C, 30 s 59°C, 1 min 30 s 72°C; 22 cycles 20 s 94°C, 30 s 63°C, 1 min 30 s 72°C; 10 min 72°C. Like the *emfyn* constructs, the amplified fragment was ligated into pGADT7 and pGBKT7 and the sequenced.

Oligonucleotides:

Z3-123- 3 (XhoI): CGAGGTCTCGAGGGTGC GAACAAATACGCTCTC

Z3-123-4 (NdeI): GCTAAGCATATGGAATCTGACCCTGCGGTTAC

5.10.4.3 EmIR and HIR constructs

EmIRintra WT and EmIRintra (K1209A)

For the expression of the EmIR wild type and K1209A intracellular domain (aa 1129 – 1749) with the N-terminal fused BD-domain, the fragment ranging from nt – was amplified with the oligonucleotides CK92 and CK97 employing the Taq DNA polymerase (NEB) with pSec-*emir* and pSec *emir*(K1209) as template. The fragments obtained with the PCR program 1 min 94°C; 3 cycles 20 s 94°C, 30 s 52°C, 2 min 72°C; 27 cycles 20 s 94°C, 30 s 56°C, 2 min 72°C; 10 min 72°C were then cloned into pGBKT7 via the NdeI and BamHI site and subsequently sequenced. For the elimination of additional residues at the C-terminus a codon complementary to stop codon was included in CK97. The corresponding expression plasmids were pGBKT7- *emir*_{intra} and pGBKT7- *emir*_{intra}K1206A.

Oligonucleotides:

CK92 (NdeI): ATCGCTCATATGATACATCGCATTCGAAAGAA

CK97 (BamHI): GAACACGGATCCTCAACAAGACGACCCATCACCG

EmIRA172intra

For the deletion of the fragment coding for the additional 172 aa in EmIR's kinase domain two oligonucleotides were designed binding immediately 5' and 3' of the fragment to be deleted. CK99 faces upstream and is complementary to nt 3776 – 3799 of the coding strand, whereas CK100 faces downstream and corresponds to nt 4316 – 4340 of the coding strand. CK99 was phosphorylated at their 5' end with the T4 polynucleotide kinase (T4PNK) using the following setup:

CK99 (50 μ M)	6 μ l
T4PNK (10U/ μ l)	1 μ l
ATP (50 mM)	1 μ l
PNK 10x buffer	5 μ l
H ₂ O	37 μ l

After the phosphorylation of 1h at 37°C, the 5' phosphorylated oligonucleotides were purified with the nucleotide removal kit (Qiagen). In the following PCR, the fragment (nt 3434 – 3799) coding for the residues 1129 – 1250 was amplified with the Pfu Turbo DNA-Polymerase (Stratagene) and the oligonucleotides CK92 and 5'phosphorylated CK99. The templates were pGBKT7- *emir_{intra}* and pGBKT7- *emir_{intra}K1206A* and the reaction conditions were: 1 min 94°C; 25 cycles 20 s 94°C, 30 s 63°C, 30 s 72°C; 10 min 72°C. The amplified fragments (CK92-99 and CK92-99 K1209A) were resolved on a 2% agarose 1xTAE gel and purified with the Gel Extraction Kit (Qiagen). In a second PCR setup (1 min 94°C; 25 cycles 20 s 94°C, 30 s 63°C, 1 min s 72°C; 10 min 72°C) the fragment (nt 4316 – 5296) coding for the residues 1423 – 1749 was amplified with the Pfu Turbo DNA Polymerase and the oligonucleotides CK100 and the CK97 using pGBKT7- *emir_{intra}* as template. The amplified (CK100-97) fragment was also cut from a 2% agarose 1xTAE gel and purified. In the next step, both CK92-99 and CK92-99 K1209A were ligated over night at 16°C to CK100-97 with T4 DNA-ligase (NEB) and served as template for a PCR with the Phusion DNA-Polymerase (Finnzymes) and the oligonucleotides CK92 and CK97. The reaction conditions were 30 s

98°C; 35 cycles 10 s 98°C, 30 s 63°C, 45 s 72°C; 10 min 72. The amplified fragment was the cloned via its NdeI and BamHI site into pGBKT7 to give the expression plasmids pGBKT7-*emir_{intra} ΔI72* and pGBKT7-*emir_{intra} ΔI72K1206A*. Both plasmids were subsequently sequenced.

Oligonucleotides:

CK99: TGGGGAGCACTTGCTCACGATGAA

CK100: CTGTTCGTGGTGATGGAGCTGATGG

HIR_{intra}

With pSec-HIR as template, the ORF the intracellular domain (aa) of the human insulin receptor (HIR) was amplified using the Pfu Turbo DNA polymerase (Stratagene) and the oligonucleotides HIR-3 and HIR-4 according to the following PCR program: 2 min 94°C; 3 cycles 20 s 94°C, 30 s 55°C, 1 min 20 s 72°C; 27 cycles 20 s 94°C, 30 s 60°C, 1 min 20 s 72°C; 10 min 72°C. In the next step, this fragment was cloned via the NdeI and SalI restriction site into the pGBKT7 plasmid. A stop codon was included in HIR-4 to minimize the additional residues added to the C-terminus of HIR's intracellular domain.

Oligonucleotides:

HIR-3 (NdeI): GTGATTCATATGATTTATCTATTCCTGAGAAAGAG

HIR-4 (SalI): CGGTAGGTCGACTTAAGGAAGGATTGGACCGAG

5.11 Expression of *insulin* and *igf-I* in hepatocytes

The rat hepatocyte cell line (Reuber cells, RH-) and the human hepatocyte cell line (HepG2) were cultivated in Dulbecco's Minimal Essential Medium (DMEM) with L-Glutamine but without pyruvate (Biometra) supplemented with 10% fetal calf serum (Biometra) and 10U/ml Penicillin G/ Streptomycin at 37°C and 5% CO₂. When the cells reached approximately 80-90% confluence, the medium was removed and the cells were trypsinized (Trypsine/EDTA) for 10 min at 37°C. Then 10 ml fresh DMEM 10% FCS was added. 0.5 – 1 ml of the resuspended cells were used to inoculate a 20 ml new culture in a (Nunc). For the isolation of total RNA, a 75 cm² cell culture flask was inoculated as described and the cells were allowed

to grow until 80% confluence. After the removal of the medium, the cells were carefully washed with ice cold PBS and then solubilized with trypsin/EDTA for 10 min at 37°C. Then 4 ml ice cold DMEM 10% FCS were added to resuspended the cells. Following a centrifugation step at 4°C (1000 rpm, 5 min), the supernatant was discarded and the pellet washed twice with ice cold 1xPBS. Total RNA was then isolated with RNeasy kit (Qiagen). For the first strand cDNA, 2 µg of DNase I treated total RNA isolated from RH- and HepG2 with the RNease Kit (Qiagen) were reversely transcribed with the Omniscript Kit (Qiagen) according to the manufacturer's instructions. This first strand cDNA was used as template in a standard PCR using Taq DNA-Polymerase (NEB) and gene specific oligonucleotides. For the analysis of the expression of *insulin* in RH-, the oligonucleotides rat ins1 and rat ins2 were used. The reaction conditions were: 2 min 94°C; 40 cycles: 20 s 94°C, 30 s 55°C, 1 min 72°C; 10 min 72°C. The PCR products were analyzed on a 2% agarose gel followed by ethidium bromide staining. The expression of *insulin* and *igf-I* in HepG2 was already analyzed before with the oligonucleotides CK7 x CK8b and CK9 x CK88 [5].

Oligonucleotides:

CK7: TCTGCC **CATATG** GGACCGGAGACGCTCTGCGG

CK8b: AGGAGG **GAATTC** CTA CATCCTGTAGTTCTTGTTCC

CK9: CCAGCC **CATATG** TTTGTCAACCAACACCTGTGCG

CK88: CTGCAGGCTGCCTGCACCAG

rat ins 1: CTATCTTCCAGGTCATTGTTC

rat ins 2: GTTGCAGTAGTTCTCCAGTTG

5.12 Working with *E. multilocularis*

5.12.1 *E. multilocularis* isolates

The isolates of *E. multilocularis* used in this work were H95, MP1 and 7030. The isolate H95 originated from a primary infection of *Meriones unguiculatus* with oncospheres, while the isolate MP1 was obtained by surgery from the Munich Patient 1. MP1 further differs from H95 in almost a complete absence of protoscoleces. The isolate 7030 originated from a Javanese monkey and is characterized by the formation of many protoscoleces.

5.12.2 Cultivation of *E. multilocularis in vivo*

- Medium:
- * Dulbecco's Minimal Essential Medium with L-Glutamine, Glucose and without pyruvate (DMEM, Biochrom)
 - * 10% fetal calf serum (GIBCO; heat inactivated at 58°C for 30 min)
 - * 100 U/ml Penicillin G/Streptomycin (Pen/Strep, Biochrom)

Despite all advantages in the *in vitro* cultivation of *E. multilocularis* metacystode vesicles, they need to be passaged from a secondarily infected *M. unguiculatus* to another for long term maintenance as described [2]. In brief, 2 to 4 months post infection, the infected gerbil is killed with CO₂ and the parasitic material is isolated from the peritoneum under sterile conditions. The parasitic material is then cut into small pieces and grinded through a sterile metal kitchen/tea sieve. The grinded material is then washed with 1xPBS several times. An 16h treatment at 4°C with 10 µl/ml Ciprobay 400 and/or 100U/ml Penicillin G/Streptomycin was done before the grinded material is further used. After the antibiotics have been removed by several washes with 1xPBS and the grinded material has been gravity pelletized, 0.2 – 0.8 ml were injected with a syringe (0.9 gauge) into a new *M. unguiculatus*. The start of an *in vitro* coculture is described in the next point.

5.12.3 Cultivation of *E. multilocularis* in vitro

The methods for the *in vitro* cultivation of *E. multilocularis* have outstandingly improved by the work of Markus Spiliotis. The *in vitro* cultivation of metacestode vesicles under coculture and axenic conditions were done as described in detail [2] and are therefore described only briefly for a better understanding of the experimental setup.

Cocultivation with host cells

Grinded material which has been treated with antibiotics and washed with 1xPBS (see above) is used to start an *in vitro* coculture with a method modified from the originally described method which uses hepatocytes embedded between 2 layers of collagen [6]. Approximately 1 ml of the grinded material is resuspended in 50 ml medium (DMEM with L-Glutamine but without pyruvate, 10% FCS, 100U/ ml Penicillin G/Streptomycin) and transferred into a 75 cm² cell culture flask. Then, 1x10⁷ freshly trypsinized rat hepatocytes (RH-) are added and the metacestode material is incubated at 37°C and 5% CO₂. The medium is replaced after 10 – 20d and then weekly by allow the metacestode material to pellet by gravity in a 50 ml Falcon. The supernatant is discarded and the falcon is filled with fresh medium transferred back into the used cell culture flask and some drops of freshly trypsinized RH- are also added. After 1-3 weeks the first metacestode vesicles can be detected. From this point on, the medium is replaced once to three times a week by carefully decanting the culture through a tea sieve and resuspending in fresh medium containing freshly trypsinized RH-. When the metacestode vesicles reach a diameter of 3 – 5 mm, they can be used for expression and stimulation experiments.

Axenic cultivation without host cells

The axenic cultivation of metacestode vesicles in the absence of hepatocytes has been developed by Spiliotis et al. [2,7]. In brief, previously cocultivated metacestode vesicles with a diameter of 2-4 mm are cleared of debris by sieving and washing with 1xPBS. These vesicles (approximately 10 ml total volume) are adapted to the growth without hepatocytes by incubation at 37°C in a 75 cm² cell culture flask containing 50 ml medium which has been preconditioned by hepatocytes. This medium is made by adding 1-4x10⁶ RH- cells into a 150 cm² cell culture flask containing 50 ml DMEM 10% FCS and the incubation for 7d at 37°C

and 5% CO₂. At this point, the medium is removed and the insoluble material is removed by a centrifugation step (5 min, 1000xg). The supernatant is additionally sterile filtered (0.2 µm) and either immediately used or stored at -20°C. It is essential that the preconditioned medium is supplemented immediately prior to the usage with reducing agents (100 µM L-cysteine, 10 µM bathocuproinedisulfic acid, 0.01% β-mercaptoethanol). Another critical point is the presence of a nitrogen phase. The metacystode vesicles are transferred into a new cell culture flask containing fresh preconditioned medium to remove any remaining hepatocytes which settle and grow on the bottom of the old flask. After 3- 6 changes of the medium, the metacystode vesicles should be adapted to the axenic growth conditions which can be controlled by a control of the shape of the vesicles in the light microscope.

For an experiment in the presence or absence of certain compounds, axenic metacystode vesicles of the same lot were used. The compounds were always added freshly from stock solutions to the preconditioned medium.

5.12.4 Isolation of protoscoleces

Protoscoleces were always isolated from parasitic material obtained from a freshly sacrificed *Meriones unguiculatus*. As in the case of passaging into a new animal, the parasitic material was mechanically grinded through a standard kitchen sieve and then extensively washed with 1xPBS to remove insoluble material and host cells. In a next step, the protoscoleces were loosen from the metacystodes by mechanical stress, i.e. the grinded parasitic material was suspended with 1xPBS until a 40-50% (w/v) suspension and shook for about 10 min at room temperature. Then, the suspension was decanted through a polyester filter tissue (pore size 150 µm) and washed with 1xPBS. The flow through, which contained the protoscoleces was collected and subsequently decanted through another polyester filter tissue (pore size 30 µm). The protoscoleces retained on the filter but the calcium bodies passed through. Following a further washing step with 1xPBS, the protoscoleces were transferred into a 15 cm petri dish filled with 1xPBS. The protoscoleces gathered in the middle of the petri dish by gentle circular movements und could be easy collected with a 1000 µl pipette.

When RNA or protein was analyzed, the protoscoleces were pelletized by centrifugation and the supernatant was discarded. For the in vitro activation, the protoscoleces were gravity pelletized and then the supernatant was removed.

5.12.5 *in vitro* activation of protoscoleces

The *in vitro* activation of protoscolices was carried out according to Smyth and Davies [8] with modifications in the following way. First, isolated protoscolices with a total volume of 500 – 1000 μ l were incubated for 30 min at 37°C and approximately 125 rpm in 25 ml pepsin solution. This solution was made by bringing the pH of DMEM (Biochrom) lacking FCS to 2 with 25% HCl and then dissolving pepsin (Sigma # P6887) to a final concentration of 0.05%. The solution was sterilized with a sterile filter (0.2 μ m). After the incubation period, the protoscolices were rinsed well with sterile prewarmed 1xPBS. When the protoscolices were gravity pelletized, the supernatant was discarded and 25 ml of sodium taurocholate solution was added for 3h at 37°C and an agitation of 125 rpm. For this solution, sodium taurocholate (Sigma # T4009) was dissolved in DMEM without FCS to a final concentration of 0.2% and subsequently filter sterilized (0.2 μ m). Then, the protoscolices were rinsed with at least 400 - 500 ml prewarmed 1xPBS to remove any remaining activation solution. The activation of protoscolices was analyzed by comparing the number of evaginated protoscolices in a light microscope prior and after the treatment to the negative control, in which protoscolices were incubated like the activated ones but in DMEM alone. At this point, the protoscoleces were resuspended in 2xSDS sample buffer containing β -mercaptoethanol for the Western Blot analysis of protein expression using specific antibodies. For the semi quantitative RT-PCR analysis of gene expression, total RNA was isolated, DNase I treated and reversely transcribed described. The obtained cDNA was the template for PCR analysis using gene specific oligonucleotides as described under 5.12.14.

5.12.6 Protein synthesis and secretion into both the medium and hydatid fluid is upregulated by host factors

The metacestode vesicles of the isolate H95 were treated as described above, except that they were incubated in DMEM 1% FCS (supplemented with 100 μ M L-cysteine, 10 μ M bathocuproinedisulfic acid, 0.01% β -mercaptoethanol) at 37°C and 5% CO₂ for 16h to down regulate protein synthesis. After this incubation period, the metacestode vesicles were washed three times with pre-warmed 1xPBS to remove the starving medium. In the next step, 1 ml of the following media containing 20 μ Ci of the [³⁵S]-Met label was added to the washed metacestodes vesicles.

- preconditioned medium (cMEM)
- DMEM 10% FCS
- DMEM 1% FCS
- DMEM 1% FCS + 10 nM human insulin
- DMEM 1% FCS + 100 nM human insulin
- DMEM 1% FCS + 1 μ M human insulin

Then, the parasite vesicles were kept at 37°C and 5% CO₂ for 24h. At this time point, the medium was removed and the proteins were immediately precipitated by adding an equal volume of ice cold 20% TCA, followed by incubating on ice for 30 min and centrifuging for 15 min at 13,000 x g at room temperature. The supernatant with the non-incorporated label was discarded and the pellet was washed once with 300 μ l ice cold acetone. After an additional centrifugation step, the supernatant was discarded again and the pellet was air-dried. Finally, the pellet was resuspended in one volume 1xPBS and 10 μ l was used to measure the incorporated label in the scintillation counter. The metacystode vesicles were washed three times with ice cold 1xPBS to remove any remaining medium and subsequently disrupted by passing carefully several times through a blue tip. The cells and the insoluble material were separated from the crude hydatid fluid by a centrifuging step (2 min, 13,000 x g) and 1 μ l of the latter was used for the scintillation counter. The cells were solubilized by adding 150 μ l of 1xSDS-Buffer and heating to 100 °C for 5 min. Subsequently, the insoluble fraction was pelletized by an additional centrifugation step (1 min, 13,000 x g) and 2 μ l of the supernatant were analyzed in the scintillation counter.

5.12.7 Phosphorylation of parasite proteins is induced by insulin and IGF-I

Co-cultivated metacystodes of the isolate H95 were washed with 400 ml prewarmed 1xPBS and 12 cysts of 2-3 mm in diameter, giving a total volume of approximately 1 ml, were manually picked and transferred into a 15 ml Falcon tube (BD Biosciences). The picked cysts were then analyzed in the light microscope for integrity and the absence of brood capsules. After the excess 1xPBS had been removed, DMEM (0.2% FCS, Pen/Strep) lacking phosphate and pyruvate was added and supplemented with 300 μ Ci/ml [³²P]-phosphoric acid (Hartmann-Analytic). This phosphate free DMEM was made according the ingredient list supplied by the

manufacturer using only biochemical grade substances. The final phosphate and pyruvate free DMEM was sterilized by filtering through a 0.2 μm membrane filter (Nalgene) and stored at 4°C until use. After 20h incubation at 37°C and 5% CO₂, 100 nM insulin and 100 nM IGF-I were added. After 10 min at 37°C and 5% CO₂, the cysts were put on ice and carefully physically disrupted. The cysts were then pelletized by centrifuging for 10 min at 13,000 rpm and the supernatant discarded. In the next step, 1 ml lysis buffer (20 mM Tris-HCl, pH 8.0; 150 mM NaCl; 1 mM EDTA pH 8.0; 1% Triton X-100; 2% sodium deoxycholate; 1 mM Na₃VO₄; 10 mM NaF; 1 mM PMSF; Aprotinin; Leupeptin Hemisulfate; Pepstatin A) was added to each sample and the pelletized cysts were rocked overhead for 2h. Then, the insoluble fraction was removed by a centrifugation step (10 min; 13,000 rpm) executed at room temperature. The resulting supernatant was saved, an equal volume of 2xSDS sample buffer containing β -mercaptoethanol was added and then boiled for 5 min. The protein phosphorylation was analyzed by resolving the proteins via SDS-PAGE (12% PAA). After the transfer onto a nitrocellulose the phosphorylated proteins were detected by autoradiography using an intensifier screen and exposing the x-ray film (Fuji) at -20°C overnight.

5.12.8 *in vitro* phosphorylation of EmIR

5.12.8.1 *in vitro* phosphorylation assay

This assay was adapted from Vicogne et al. [9] and will be described in detail. Cocultivated metacystode vesicles of the *E. multilocularis* isolate H95 (3-5 mm in diameter) were analyzed for the absence of brood capsules in the light microscope. The vesicles were then decanted through a sieve and intensively washed with prewarmed 1xPBS. In the next step, the metacystode vesicles were incubated in DMEM 0.2% FCS (supplemented with 10U/ml Penicillin G/Streptomycin, 100 μM L-cysteine, 10 μM bathocuproinedisulfic acid, 0.01% β -mercaptoethanol) for 16 – 24h at 37°C and 5% CO₂. After this period, the vesicles were washed again with prewarmed 1xPBS and intact vesicles were transferred manually with a cut blue tip into a 15 ml falcon tub (2 ml per experimental condition). The excess 1xPBS was removed and 0.5 ml homogenization buffer (20 mM Tris-HCl, pH 7.5; 150 mM NaCl; 1 mM EDTA pH 8.0; 1% Triton X-100; 1 mM Na₃VO₄; 10 mM NaF; 1 mM PMSF; 10 $\mu\text{g/ml}$ Aprotinin A, 1 $\mu\text{g/ml}$ Pepstatin A, 1 μM Leupeptin hemisulfate) was added per 1 ml intact

vesicles. The vesicles were then carefully mechanically homogenized. For a complete homogenization, a gentle overhead agitation step was carried out for 1h at 4°C. The membrane fraction was then pelleted by a centrifugation step (3000 rpm, 3 min) at 4°C. The supernatant was discarded and the pellet carefully resuspended in fresh homogenization buffer (0.5 ml per 1 ml intact vesicles). The suspension was aliquoted in 1.5 ml caps and either human insulin (Hoechst) or human IGF-I (recombinant hIGF-I, Immunotools) were added to a final concentration of 100 nM. After 10 min at 37°C the membrane fraction was pelleted by a centrifugation step (3000 rpm, 3 min) carried out at RT. For the *in vitro* phosphorylation, the membrane fraction was carefully resuspended in 300 µl kinase buffer (50 mM Tris pH 7.5; 2mM MnCl₂; 15 mM MgCl₂; 0.1% Triton X-100; 1 mM Na₃VO₄; 10 mM NaF; 1 mM PMSF; 10 µg/ml Aprotinin, 1µg/ml Pepstatin A, 1 µM Leupeptin hemisulfate) containing 250 µM HIR-Inhibitor or an equal volume of DMSO, the inhibitor's solvent. After 30 min at 37°C, the kinase buffer was supplemented with 50 µM [³²P] γ-ATP (4.4 µl of 110 TBq/mmol). The phosphorylation was carried out for 40 min at 30°C, after which the membrane fraction was pelleted by centrifuging for 5 min at 13000 rpm and room temperature. After the supernatant had been discarded, 1 ml lysis buffer (20 mM Tris-HCl, pH 8.0; 150 mM NaCl; 1 mM EDTA pH 8.0; 1% Triton X-100; 2% sodium deoxycholate; 1 mM Na₃VO₄; 10 mM NaF; 1 mM PMSF; 10 µg/ml Aprotinin, 1µg/ml Pepstatin A, 1 µM Leupeptin hemisulfate) was added on each pellet. For the lysis of the membrane bound proteins, the samples were rocked over head at 4°C for at least 1h. The insoluble material was then pelleted by a centrifugation step (5 min, 13000 rpm) carried out at room temperature and EmIR's β - subunit was then immunoprecipitated from this supernatant with the EmIRintra immune serum (1:100). After overhead agitation over night at 4°C, 60 µl agarose G-beads (Upstate) were equilibrated by three times washing in 1xTBS pH 8.0, 1% Triton X-100 and were transferred to the lysate. The agitation was continued for another 4-5 h. Then, the protein G – antibody/antigen – complex was pelleted by centrifuging for 1 min at 2,500 rpm. The supernatant was removed and the pellet washed three times with cold lysis buffer lacking sodium deoxycholate. 100 µl 2xSDS-sample buffer containing β-mercaptoethanol were added on the agarose beads, followed by boiling for 5 min. The phosphorylation of the immunoprecipitated proteins were analyzed by SDS-PAGE (8% PAA), followed by a transfer onto a nitrocellulose membrane. The phosphorylation was detected by autoradiography employing a X-ray film (Fuji).

5.12.8.2 Stimulation of EmIR with insulin in intact vesicles

The metacestode vesicles were incubated in low serum medium for 16h as described above. In the next step, intact vesicles with a total volume of 2 ml were manually picked per stimulus and transferred into a 15 ml Falcon. The excess 1xPBS was removed and 2 ml fresh DMEM (0.2% FCS) supplemented with 100 nM human insulin was added. After 10 min, the vesicles were put on ice and the medium was removed. The vesicles were then carefully mechanically disrupted and pelleted by centrifugation (1 min, 13000 rpm) at 4°C. The pellet was solubilized in 1 ml lysis buffer (see above) and overhead agitation for at least 1h at 4°C. The insoluble material was removed by centrifugation for 15 min and 13000 rpm at 4°C. The immunoprecipitation with the anti-EmIRintra serum was carried out as above and analyzed by SDS-PAGE (8% PAA) and Western blotting with the anti-EmIRintra serum. The tyrosine phosphorylation of the EmIR β -subunit was analyzed by Western blotting using an anti-phospho tyrosine antibody (P-Tyr 100, Cell Signal).

5.12.8.3 Effect of HIR tyrosine kinase inhibitor HNMPA-(AM)₃ on

E. multilocularis metacestode vesicles

Cocultivated metacestode vesicles (isolate H95) were washed with 250 ml prewarmed 1xPBS and then, 4 vesicles of 3-4 mm in diameter were manually picked for each setup and transferred into a 15 ml Greiner tube. After the light microscopical verification of the integrity of the cysts, the excess 1xPBS was removed and 1 ml DMEM 10% FCS, Pen/Strep containing either 250 μ M HNMPA-(AM)₃ or an equal volume of the inhibitor's solvent, DMSO, was added. The vesicles were incubated at 37°C and 5% CO₂ and daily controlled in the light microscope. An identical setup was exerted with axenic vesicles supplementing the axenic cultivation medium with 250 μ M HNMPA-(AM)₃ or the corresponding volume of DMSO. For the determination of the minimal effective concentration of HNMPA-(AM)₃ three washed vesicles of the isolate H95 were transferred into a 15 ml Greiner tube for each setup. The excess 1xPBS was again removed and DMEM 10% FCS, Pen/Strep supplemented with 1, 5, 10, 25, 50, 100, 200 and 250 μ M inhibitor was added to the cysts. The control was supplemented with a volume of DMSO corresponding to the largest volume of inhibitor added, i.e. 1 μ l. At the indicated time points, the integrity of the vesicles was documented by photography using an inverse microscope and an alkaline phosphatase assay as described by

Stettler et al. [10] was exerted, with the exception that the incubation step was carried out over night to increase the sensitivity of the assay.

5.12.8.4 Effect of HIR tyrosine kinase inhibitor HNMPA-(AM)₃ on EmMPK-1

In vitro cocultivated metacestodes of the *E. multilocularis* isolate H95 were washed with 300 ml prewarmed 1xPBS. Prior to manual picking, the metacestode vesicles were controlled in the light microscope for integrity and absence of brood capsules. Only those vesicles with a diameter of 2-3 mm were picked. For each setup, vesicles with a total volume of 1 ml were used. After the removal of the excess 1xPBS, 2 ml DMEM (10%FCS, 100U/ml Penicillin G/Streptomycin) supplemented with 10, 25 and 50 μ M HNMPA-(AM)₃ were added to the metacestode vesicles. As control, the inhibitor was omitted and an equal volume of DMSO, the inhibitors solvent, was added to the rich medium. The metacestode vesicles were then incubated at 37°C and 5% CO₂ for the indicated time, after which the medium was removed and they were carefully mechanically disrupted. The membrane fraction was pelletized by centrifuging 5 min at 13,000 rpm and subsequently resuspended in 300 μ l 2xSDS-sample buffer containing β -mercaptoethanol. Following a 5 min boiling and a 1 min centrifugation step at 13,000 rpm, the soluble proteins were resolved via SDS-PAGE and the phosphorylation of EmMPK-1 was analyzed by Western blot analysis using the anti-Erk1/2 and anti-phospho-Erk1/2 antibodies.

5.12.8.5 EmMPK-1 is activated by human insulin as well as human IGF-I

In vitro cocultivated metacestodes of the *E. multilocularis* isolate H95 were washed with prewarmed 1xPBS and then transferred into DMEM 0.2% FCS, Pen/Strep, containing the supplements used in the axenic culture and incubated for 2d at 37°C and 5% CO₂. Then, the metacestodes were washed again with prewarmed 1xPBS and metacestodes with a diameter of 2-3 mm were picked. For each setup, metacestodes with a total volume of 0.5 ml were transferred into a 15 ml Greiner tube and controlled in the light microscope for integrity and the absence of brood capsules. The excess 1xPBS was removed and 1 ml of the starving medium was added to the metacestodes. Prior to the stimulation with human insulin or human IGF-I (either 100 nM for 30 min), the metacestode vesicles were preincubated with the inhibitor (in general 250 μ M) for 1h at 37°C and 5% CO₂. When no inhibitor was added, the medium was supplemented with an equal volume of DMSO. At the end of the stimulation, the

tubes were put on ice, the metacestodes carefully disrupted and the pelletized cellular fraction resuspended in 150 μ l 2xSDS-sample buffer containing β -mercaptoethanol and boiled. The phosphorylation of EmMPK-1 was analyzed by Western blotting with the anti-Erk1/2 and anti-phospho-Erk1/2 antibody.

5.12.8.6 Human insulin stimulates the expression of *egfd*

Metacestode vesicles of the *E. multilocularis* isolate H95 were cocultivated until a diameter of 3-5 mm. They were then washed with prewarmed 1xPBS and transferred into DMEM 0.2% FCS, Pen/Strep containing the supplements used in the axenic cultivation system []. After 4d at 37°C and 5% CO₂, the metacestodes were washed again with prewarmed 1xPBS and only those were manually transferred into 15 ml tubes which had appeared intact in the light microscope and did not have brood capsules. Metacestodes with a total volume of 1 ml per setup were picked. The excess 1xPBS was replaced by 2 ml DMEM Pen/Strep lacking FCS. After supplementing with human insulin, the metacestode vesicles were incubated at 37°C, 5% CO₂ for 24h. Then the medium was removed and the metacestode vesicles were washed with 10 ml ice cold 1xPBS. For the isolation of total RNA with the RNeasy kit (Qiagen), the metacestodes were carefully mechanically disrupted and centrifuged for 1 min at 14,000 rpm. The supernatant was discarded and the pellet resuspended in 600 μ l RLT-buffer and mixed well by transferring several times through a blue tip. Following a further centrifugation step (1 min; 14,000 rpm), the supernatant was loaded on a RNA column and further treated according the manufacturer's instructions. The RNA was eluted with 40 μ l RNase free water. The eluate was then used for a second elution step, to increase the amount of isolated total RNA. For the elimination of any contaminating chromosomal DNA, the isolated RNA was digested 50 μ l with DNase I (Roche) in 50 μ l containing (10 U DNase I; 5 mM MgSO₄; 0.1 M sodium acetate) for 1h at 37°C and subsequently purified employing a fresh RNeasy column as described in the manual. The purified RNA was eluted with 30 μ l RNase free H₂O and reversely transcribed using Qiagen's Omniscript kit and CD3RT oligonucleotide according to the manufacturer's recommendations. For the analysis of gene expression, a dilution series of the cDNA was made and the expression of the genes of interest was compared to the expression of *elp* [96]. All PCRs were carried out using Taq DNA Polymerase (NEB) in a standard experimental setup. The expression of *emfyn* was analyzed using the oligonucleotides and the following reaction conditions: 1 min 94°C; 40 cycles: 20 s 95°C, 30 s 59°C, 1 min 30 s 72°C; 10 min 72°C. In case of *emrhogap*, the oligonucleotides Z2-123-1

and Z2-123-2 were used and the reaction conditions were as follows: 1 min 94°C; 40 cycles: 20 s 95°C, 30 s 64°C, 1 min 30 s 72°C; 10 min 72°C. The expression of *emegfd* was assessed with the oligonucleotides WF5-DW2 and WF5-UP3 and the following reaction conditions: 2 min 94°C; 35 cycles: 20 s 94°C, 30 s 60°C, 1 min 72°C; 10 min 72°C. With the oligonucleotides CK95 and CK97 and the reaction conditions 2 min 94°C; 5 cycles: 20 s 94°C, 30 s 56°C, 30 s 72°C; 40 cycles: 20 s 94°C, 30 s 60°C, 30 s 72°C 10 min 72°C the expression of *emir* was assessed, in case of *elp* the PCR was carried out with the oligonucleotides Em10dw and Em10 up and the following reaction conditions: 2 min 94°C; 30 cycles: 20 s 94°C, 30 s 57°C, 30 s 72°C; 10 min 72°C. All PCR products were analyzed by agarose gel electrophoresis followed by staining with ethidium bromide.

Oligonucleotides:

emfyn:

Z3-159N: TGGCGCGTCACTTGAGGA

Z3-159C: ATCCTCGGGTCGTGCTGA

emrhogap:

Z2-123-1: CTCGACTGGGTATTATCCAGG

Z2-123-2: GACCATGACCTCGAAGGTAGG

emegfd:

WF5 DW1: CGAAATCGGGTGCGACAGCATAGG

WF 5 UP3: GATTAATCAAAAGTGCCACAAATGC

emir:

CK95 (NdeI): CTCTATCATATGGCACCTCGCTTCGCAGACGC

CK97 (BamHI): GAACACGGATCCTCAACAAGACGACCCATCACCG

elp:

Em10up: GACCATACTTGGCAACACAGG

Em10dw: CAGGATCTCTTCGATCAAGTG

5.12.8.7 Immunohistochemistry and electron microscopy

For immunohistochemistry analysis done together with Dennis Tappe, the tissue material was transferred into cryotubes (Nunc) filled with “Tissue-Tek” (Sakura) and shock frozen in liquid nitrogen. The frozen material was cut into 5-7 μm thick sections in a cryo-microtome (2800 Frogcut, Reichert-Jung), transferred on a microscope slide and fixed in ice-cold acetone for 10 – 20 min. After the specimen had been air-dried, it was washed with 1xPBS and blocked with 20% goat serum in 1xPBS for 30 min at room temperature. The incubation with the primary antibody, anti-EmIR_{intra} serum (1:500 in blocking buffer), was carried out overnight at 4°C. Following three 10 min washing steps with PBS 0.05% Tween 20 (PBST), the secondary antibody, anti-rabbit-Horseradish peroxidase (HRP) (1:200 in blocking buffer), was allowed to bind for 30 min at room temperature. Unbound secondary antibodies were removed by three washing steps with 1xPBST (10 min each). The HRP reaction was initiated by adding DAB-substrate (6 mg 3,3'-diaminobenzidine/ml 1xPBS supplemented with 15 μl H₂O₂; Sigma). After 10 – 30 s of incubation at room temperature, the reaction was terminated by washing with H₂O. The nuclei were visualized by a 3 min staining with hematoxylin (Supplier, concentration) followed by a washing step with H₂O. The blue color was allowed to develop further in H₂O. The reaction was stopped by embedding the specimen in “Histomount” (Shandon, Frankfurt, Germany).

The electronmicroscopical and immunofluorescence analysis of EmIR using the anti-EmIR_{intra} serum was done by Dr. Andrew Hemphill, University of Bern, Switzerland.

5.12.8.8 Isolation of hydatid fluid and measuring of insulin and IGF-I concentration

For the isolation of hydatid fluid, *in vitro* cultivated metacestodes with a diameter of approximately 5 mm (or larger) were decanted through a sterile sieve and washed carefully with at least 300 ml cold 1xPBS. Then, the metacestodes were carefully transferred into 1xPBS and either 3 metacestodes transferred into a 1.5 ml tube containing 1xPBS. The hydatid fluid was isolated by puncturing the metacestodes with a fine needle (0.4 gauge) followed by sucking out the fluid with a syringe. For the removal of any cells from the hydatid fluid, a centrifugation step (5 min; 14,000 rpm) at 4°C was carried out and the

supernatant transferred into a fresh tube. The hydatid fluid from identical experimental setups were pooled and stored at -20°C in 300 µl aliquots until further usage.

The concentrations of insulin and IGF-I in the hydatid fluid were determined with the Insulin-Immulate[®] and IGF-I - Immulate[®] System. For each measuring, 300 µl of undiluted hydatid fluid were used.

5.12.8.9 Uptake of insulin-biotin

Cocultivated *E. multilocularis* metacestode vesicles of the isolate H95 (diameter 5 mm) were incubated for 4d in DMEM 0.2% FCS, 100 U/ml Penicillin/Streptomycin supplemented 100 µM L-cysteine, 10 µM bathocuproinedisulfic acid, 0.01% β-mercaptoethanol. In the next step, the metacestode vesicles were washed with 300 ml prewarmed 1xPBS and only intact vesicles were picked and transferred into a 15 ml tube. After the excess 1xPBS had been removed, 2 ml of conditioned medium A1 supplemented with 100 nM biotinylated insulin (Sigma) was added. At the indicated time points, the incubation medium was removed and saved, and the metacestodes washed with ice-cold 1xPBS. The hydatid fluid was isolated and as described and an equal volume of 2xSDS sample buffer without β-mercaptoethanol was added. The uptake of insulin-biotin was examined by SDS-PAGE (18% PAA, 7M urea) followed by Western blotting with the anti-biotin HRP antibody (NEB). In brief, after the transfer, the nitrocellulose membrane was blocked for 1h with 5% BSA in 1xTBS 0,05% Tween 20 (1xTBST) at room temperature. The antibody (1:1000 in blocking buffer) was allowed to bind over night at 4°C. The next day, unbound antibody was removed by three washes with 1xTBST at room temperature. The blot was developed with the ECL-kit from Pierce and an x-ray film (Fuji).

5.13 IR orthologs of other cestodes

The *E. granulosus* cDNA was made by reverse transcription of DNase I digested total RNA using Qiagen's Omniscript and the CD3RT oligonucleotide as described above. The total RNA was isolated from parasitic material using the RNeasy Kit (Qiagen) as described above. The same kit was used to isolate total RNA from *in vitro* cultivated (in DMEM 10% FCS, 100U/ml Penicillin/Streptomycin) *T. crassiceps* metacestode vesicles according to the procedure described for *E. multilocularis*. The isolated RNA was DNase I treated and reverse transcribed with using Omniscript and the CD3RT oligonucleotide. The *T. solium* phage library was kindly provided by Prof. Brehm. The PCR using the oligonucleotides CK35&CK36 and CK37&CK38 which span the coding fragments for residue 33 – 776 and 1146 and 1749 of EmIR, respectively, was carried out using Taq DNA Polymerase (NEB) in standard PCR setup and the cDNAs as template. The reaction conditions were 1 min 94°C; 3 cycles: 20 s 61°C, 2 min 30 s 72°C; 27 cycles: 20 s 94°C, 30 s 63°C, 2 min 30 s 72°C; 10 min 72°C for CK35&CK36 and 1 min 94°C; 3 cycles: 20 s 94°C, 20 s 60°C, 2 min 30 s 72°C; 27 cycles: 20 s 94°C, 30 s 63°C, 2 min 30 s 72°C; 10 min 72°C for CK37 & CK 38. The PCR products were then diluted 1:50 with PCR grade H₂O and 2-5 µl were used in the nested PCR employing Taq DNA Polymerase. The first nested PCR was done with the oligonucleotides EmIGFRdw & EmIGFRup spanning the coding region for the EmIR residues 32 – 744 using the following reaction conditions: 2 min 94°C; 5 cycles: 30 s 94°C, 30 s 55°C, 2 min 72°C; 30 cycles: 30 s 94°C, 30 s 60°C, 2 min 72°C; 10 min 72°C. The second nested PCR was done using the oligonucleotides CK49&CK50 spanning the *emir* fragment from nt 141 – 1265 and the reaction conditions: 2 min 94°C; 30 cycles: 30 s 94°C, 30 s 57°C, 1 min 30 s 72°C; 10 min 72°C. The third nested PCR was carried out with the oligonucleotides CK93&CK96 (spanning the fragment from nt 3549 to nt 4883) using the reaction conditions: 2 min 94°C; 5 cycles: 30 s 94°C, 30 s 52°C, 2 min 72°C; 35 cycles: 30 s 94°C, 30 s 57°C, 2 min 72°C; 10 min 72°C.

All PCR products were analyzed by gel electrophoresis and purified using the Qiagen Gelex Purification Kit as described. The purified products were clones into pCR2.1 Topo TA cloning vector (Invitrogen) and subsequently sequenced using the provided vector specific and designed gene specific oligonucleotides.

Oligonucleotides:CK35: GTCCCGT**GGATCC**GTCCGGTCTTCGGTGGAAATCCK36: CCAAAG**GAATTCTC**AGGAGGCAGGAGAACTGCGACCK37: GAGTGGAG**GATCC**CTAACCCGGAGTACTGGCACGCK38: GAACACAG**AATTCTCA**ACAAGACGACCACCCATCACCGEmIGFRdw: GTCCCG **GAATTC** TGTCGGGTCTTCGGTGGAAATCEmIGFRup: GAATGGA **GGATCC** TCAATGCGGTGACAGAGAAGCAGTCC

CK49: GTCAACACCACGGCAGCTG

CK50: GTAAGAGGGCGTGATCGCG

CK93 (NdeI): GACAT**CCATATG**CTGAATTTCCGTCATCCTCTTGCK96 (BamHI): GGCGA**AGGATCCTCA**AAGGAGATAGAGGAGGTGCAG

Tc1: GCTCTTCAGTTTATCCGCTG

Ts2: GCTGGTTGGAGGCCAGTGAG

6 References

- [1] Sambrook J, Fritsch EF, Maniatis T. *Molecular Cloning, A LABORATORY MANUAL SECOND EDITION*, Cold Spring Harbor Laboratory Press 1989
- [2] Spiliotis M. Untersuchung zur *in vitro* Kultivierung und Charakterisierung von MAP-Kinase-Kaskade-Komponenten des Fuchsbandwurmes *Echinococcus multilocularis*. Dissertation zur Erlangung des naturwissenschaftlichen Doktorgrades der Bayerischen Julius-Maximilians-Universität Würzburg, Februar 2006
- [3] Brehm K., Jensen K., Frosch M. mRNA trans-splicing in the human parasitic cestode *Echinococcus multilocularis*. *J Biol Chem* 2000; 275: 38311 - 38318
- [4] Chen DC, Yang BC, Kuo TT. One step transformation of yeast in stationary phase. *Curr Genet* 1992; 21:83-84
- [5] Konrad C. Molekulare Charakterisierung und Funktionsanalyse einer Rezeptorkinase der Insulin/IGF – Familie des Fuchsbandwurms *Echinococcus multilocularis*. Diplomarbeit an der Fakultät für Biologie der Julius-Maximilians-Universität Würzburg, Juli 2002
- [6] Jura H, Bader A, Hartmann M, Maschek H, and Frosch M. Hepatic Tissue Culture Model for Study of Host-Parasite Interactions in Alveolar Echinococcosis. *Infection and Immunity* 1996; 64:34848-3490
- [7] Spiliotis M, Tappe D, Sesterhenn L, Brehm K. Long-term *in vitro* cultivation of *Echinococcus multilocularis* metacestodes under axenic conditions. *Parasitol Res* 2004; 92(5):430-432
- [8] Smyth JD, Davies Z. *In vitro* culture of the strobilar state of *Echinococcus granulosus* (sheep strain): a review of basic problems and results. *Int J Parasitol* 1974; 4(6):631 – 644
- [9] Vicogne J, Cailliau K, Tulasne D, Browaeys E, Yan YT, Fafeur V, Vilain JP, Legrand D, Trolet J, Dissous C. Conservation of epidermal growth factor receptor function in the human parasitic helminth *Schistosoma mansoni*. *J Biol Chem*.2004; 279(36):37407-37407
- [10] Stettler M, Siles-Lucas M, Sarciron E, Lawton P, Gottstein B, Hemphill A. *Echinococcus multilocularis* alkaline phosphatase as a marker for metacestode damage induced by *in vitro* drug treatment with albendazole sulfoxide and albendazole sulfone. *Antimicrob Agents Chemother*. 2001;45(8):2256-2262
- [11] Erwin DH. The origin of bodyplans. *Am. Zool*.1999; 39: 617 - 629
- [12] Thompson RCA., Lymbery AJ, editors. *Echinococcus* and Hydatid Disease. Wallingford, UK: CAB International 1995:411-463
- [13] Thompson RCA and McManus DP. Towards a taxonomic revision of the genus *Echinococcus*. *Trends in Parasitology* 2002; 18(10): 452 – 457
- [14] Dixon JB. Echinococcosis. *Comp.Immun. Microbiol. Infect. Dis*. 1997; 20(1): 87-94
- [15] Rausch RL, and Bernstein JJ. *Echinococcus vogeli* sp. n. (Cestoda: Taeniidae) from the bush dog, *Speoathus venaticus* (Lund). *Zeitung für Tropenmedizin und Parasitologie* 1972;23:25-34
- [16] Chap Z, Ishida T, Chou J, Hartley CJ, Entman ML, Brandenburg D, Jones RH, Field JB. First-pass hepatic extraction and metabolic effects of insulin and insulin analogues. *Am J Physiol* ;252(2 Pt 1):E209-217
- [17] Seitz HM und Frosch M. Der kleine Fuchsbandwurm. Erreger der alveolären Echinokokkose. In: Deutsches Ärzteblatt. Deutscher Ärzte-Verlag 1994; 38:3-8

- [18] Morar R, Feldman C. Pulmonary echinococcosis. *Eur Respir J* 2003; 21: 1069 - 1077
- [19] Lethbridge RC. The biology of the oncosphere of cyclophyllidean cestodes. *Helminthological Abstracts Series* 1980; A49:59-72
- [20] Smyth JD. *The Physiology of Cestodes*. Oliver and Boyd, Edinburgh 1969
- [21] Rausch RL and D'Alessandro A. Histogenesis in the metacestode of *Echinococcus vogeli* and mechanism of pathogenesis in polycystic hydatid disease. *Journal of Parasitology* 1999; 85:410-418
- [22] Lanier AP, Trujillo DE, Schantz PM, Wilson JF, Gottstein B, and McMahon BJ. Comparison of serological test for the diagnosis and follow-up of alveolar hydatid disease. *Transactions of the Royal Society of Tropical Medicine and Hygiene* 1988; 37:609-615
- [23] Ingold K, Bigler P, Thormann W, Cavaliero T, Gottstein B and Hemphill A. Efficacies of albendazole sulfoxide and albendazole sulfone against in vitro cultivated *Echinococcus multilocularis* metacestodes. *Antimicrobial Agents and Chemotherapy* 1999; 43:1052-1061
- [24] Gottstein B, and Hemphill A. Immunopathology of echinococcosis. In: *Chemical immunology, immunopathogenic aspects of disease induced by helminth parasites*. Freedman DO (ed.). Karger, Basel, Switzerland 1997;177-208
- [25] Khan AZ, Siboo R, Gomersall M, and Faucher M. Cystolytic events and the possible role of germinal of germinal cells in metastasis in chronic alveolar hydatidosis. *Ann Trop Med Parasitol* 1993;77:497-512
- [26] Ueda T, Watanabe-Fukunaga R, Fukuyama H, Nagata S, Fukunaga R. Mnk2 and Mnk1 are essential for constitutive and inducible phosphorylation of eukaryotic initiation factor 4E but not for cell growth or development. *Mol Cell Biol* 2004; 24(15): 6539-6549
- [27] Rausch RL, and Wilson JF. Rearing of the adult *Echinococcus multilocularis* Leuckart, 1863, from sterile larvae from man. *Am J Trop Med Hyg* 1973;22:357-360
- [28] Amman R, Eckert J. Clinical diagnosis and treatment of echinococcosis in humans. In: Thompson RCA, Lymbery AJ, editors. *Echinococcus and Hydatid Disease*. Wallingford, UK: CAB International 1995:411-463
- [29] Rausch RL, Wilson JF, Schantz PM, McMahon BJ. Spontaneous death of *Echinococcus multilocularis*: cases diagnosed serologically (by Em2 ELISA) and clinical significance. *Am J Trop Med Hyg* 1987; 36: 576 - 585
- [30] Reuter S, Kratzer W, Kurz S, Wellinghausen N, Kern P. Sonderdruck: Chemotherapie der alveolären Echinokokkose mit Benzimidazolen. In: *Medizinische Klinik* 1998;93(8)
- [31] Amman RW, Eckert J. Cestodes: Echinococcus. In: Weinstock JV, editor. *Parasitic diseases of the liver and intestines*. Philadelphia, PA: Saunders. 1996; 655-689
- [32] Xiao N, Qiu J, Nakao M, Li T, Yang W, Chen X, Schantz PM, Craig PS, Ito A. *Echinococcus shiquicus*, a new species from the Qinghai-Tibet plateau region of China: discovery and epidemiological implications. *Parasitol Int* 2006; 55 Suppl: S233-236
- [33] Schantz PM, Chai J, Craig PS. Epidemiology and control of hydatid disease. In: Thompson RCA, Lymbery AJ, editors. *Echinococcus and hydatid disease*. Wallingford: CAB International 1995;233-331
- [34] Brehm K, Kern P, Hubert K, and Frosch M. *Echinococcus* from Every Angle. *Para Today* 1999; 15:351-352
- [35] Romig T, Kratzer W, Kimmig P, et al. Römerstein Study Group. An epidemiologic survey of human alveolar echinococcosis in southwestern Germany. *Am J Trop Med Hyg* 1996; 61:566-573

- [36] Eckert J, Conraths FJ, Tackmann K. Echinococcosis: an emerging or re-emerging zoonosis? *Int J Para* 2000; 30:1283-1294
- [37] Hofer S, Gloor S, Müller U, Mathis A, Hegglin D, Deplazes P. High prevalence of *Echinococcus multilocularis* in urban red foxes (*Vulpes vulpes*) and voles (*Arvicola terrestris*) in the city of Zürich, Switzerland. *Parasitology* 2000;135-142
- [38] Robert Koch Institut, Epidemiologisches Bulletin Nr. 15, 2006
- [39] Claeys I, Simonet G, Poels J, Van Loy T, Vercammen I, De Loof A, Broeck JV. Insulin-related peptides and their conserved signal transduction pathway. *Peptides* 2002; 23:807-816
- [40] Gross DJ, Villa-Komaroff L, Kahn CR, Weir GC, and Halban PA. Deletion of a Highly Conserved Tetrapeptide Sequence of the Proinsulin Connecting Peptide (C-Petide) Inhibits Proinsulin to Insulin Conversion by Transfected pituitary Corticotroph (AtT20) Cells. *J Biol Chem* 1989;264:21486-21490
- [41] Cheatham B, and Kahn RC. Insulin Action and the Signaling Network. *Endocrine Reviews*. 1995; 16:117-142
- [42] Jones Ji, Clemmons DR. Insulin-like growth factors and their binding proteins: biological actions. *Endocr. Rev* 1995; 1:3-34
- [43] Rosen CJ, and Pollak M. Circulating IGF-1: New Perspectives for the New Century. *TEM* 1999; 10:136-141
- [44] Sandhu MS, Dunger DB, Giovannucci EL. Insulin, insulin-like growth factor-I (IGF-I), IGF binding proteins, their biologic interactions, and colorectal cancer. *J Natl Cancer Inst.* 2002 Jul 3;94(13):972-980
- [45] Leever SJ. Growth control: invertebrate insulin surprises! *Curr Biol.* 2001; 11(6):R209-212
- [46] Pierce SB, Costa M, Wisotzkey R, Devadhar S, Homburger SA, Buchman AR, Ferguson KC, Heller J, Platt DM, Pasquinelli AA, Liu LX, Doberstein SK, Ruvkun G. Regulation of DAF-2 receptor signaling by human insulin and ins-1, a member of the unusually large and diverse *C. elegans* insulin gene family. *Genes Dev.* 2001; 15(6):672-86.
- [47] Hanks SK, Quinn AM, Hunter T. The protein kinase family: conserved features and deduced phylogeny of the catalytic domains. *Science* 1988; 241(4861):42-52
- [48] Zwick E, Bange J, Ullrich A. Receptor tyrosine kinases as targets for anticancer drugs. *Trends Mol Med* 2002; 8(1):17-23.
- [49] Ullrich A, Schlessinger J. Signal transduction by receptors with tyrosine kinase activity. *Cell* 1990; 61(2):203-212.
- [50] White MF, Kahn CR. The insulin signaling system. *J Biol Chem* 1994; 269(1):1-4.
- [51] LeRoith D, Werner H, Beitner-Johnson D, Roberts CT Jr. Molecular and cellular aspects of the insulin-like growth factor I receptor. *Endocr Rev* 1995; 16(2):143-163
- [52] Shier P, Watt VM. Primary structure of a putative receptor for a ligand of the insulin family. *J Biol Chem.* 1989; 264(25):14605-14608.
- [53] Hänze J, Berthold A, Klammt J, Gallaher B, Siebler T, Kratzsch J, Elmlinger M, Kiess W. Cloning and sequencing of the complete cDNA encoding the human insulin receptor related receptor. *Horm Metab Res.* 1999; 31(2-3):77-79.
- [54] Vicogne J, Pin JP, Lardans V, Capron M, Noel C, Dissous C. An unusual receptor tyrosine kinase of *Schistosoma mansoni* contains a Venus Flytrap module. *Mol Biochem Parasitol.* 2003; 126(1):51-62

- [55] Fernandez-Almonacid R, Rosen OM. Structure and ligand specificity of the *Drosophila melanogaster* insulin receptor. *Mol Cell Biol*. 1987; 7(8):2718-2727
- [56] Ruan Y, Chen C, Cao Y, Garofalo RS. The *Drosophila* insulin receptor contains a novel carboxyl-terminal extension likely to play an important role in signal transduction. *J Biol Chem*. 1995; 270(9):4236-4243
- [57] Yamaguchi T, Fernandez R, Roth RA. Comparison of the signaling abilities of the *Drosophila* and human insulin receptors in mammalian cells. *Biochemistry* 1995; 34(15):4962-8.
- [58] Zhang B, Roth RA. The insulin receptor-related receptor. Tissue expression, ligand binding specificity, and signaling capabilities. *J Biol Chem*. 1992; 267(26):18320-8.
- [59] Schaeffer HJ and Weber MJ. Mitogen-Activated Protein Kinases: Specific Messages from Ubiquitous Messengers. *Molecular And Cellular Biology*. 1999; 2435 – 2444.
- [60] Sasaoka T, Kobayashi M. The functional significance of Shc in insulin signaling as a substrate of the insulin receptor. *Endocr J* 2000; 47(4):373-831
- [61] Dupont J, LeRoith D. Insulin and insulin-like growth factor I receptors: similarities and differences in signal transduction. *Horm Res* 2001; 55 Suppl 2:22-26
- [62] Najjar SM, Blakesley VA, Li Calzi S, Kato H, LeRoith D, Choice CV. Differential phosphorylation of pp120 by insulin and insulin-like growth factor-1 receptors: role for the C-terminal domain of the beta-subunit. *Biochemistry*. 1997; 36(22):6827-6834.
- [63] Kalloo-Hosein HE, Whitehead JP, Soos M, Tavare JM, Siddle K, O'Rahilly S. Differential signaling to glycogen synthesis by the intracellular domain of the insulin versus the insulin-like growth factor-1 receptor. Evidence from studies of TrkC-chimeras. *J Biol Chem*. 1997; 272(39):24325-24332. Erratum in: *J Biol Chem* 1997; 272(47):29984.
- [64] Urso B, Cope DL, Kalloo-Hosein HE, Hayward AC, Whitehead JP, O'Rahilly S, Siddle K. Differences in signaling properties of the cytoplasmic domains of the insulin receptor and insulin-like growth factor receptor in 3T3-L1 adipocytes. *J Biol Chem*. 1999; 274(43):30864-30873.
- [65] Nakae J, Kido Y, Accili D. Distinct and overlapping functions of insulin and IGF-I receptors. *Endocr Rev* 2001; 22(6):818-835
- [66] Hwang JB, Hernandez J, Leduc R, Frost SC. Alternative glycosylation of the insulin receptor prevents oligomerization and acquisition of insulin-dependent tyrosine kinase activity. *Biochimica et Biophysica Acta* 2000; 74 – 84
- [67] Yenush L, Fernandez R, Myers MG Jr, Grammer TC, Sun XJ, Blenis J, Pierce JH, Schlessinger J, White MF. The *Drosophila* insulin receptor activates multiple signaling pathways but requires insulin receptor substrate proteins for DNA synthesis. *Mol Cell Biol* 1996; 16(5):2509-17.
- [68] Fernandez R, Tabarini D, Azpiazu N, Frasch M, Schlessinger J. The *Drosophila* insulin receptor homolog: a gene essential for embryonic development encodes two receptor isoforms with different signaling potential. *EMBO J* 1995; 14(14):3373-3384.
- [69] Rogan MT, Hai WY, Richardson R, Zeyhle E, Craig PS. Hydatid cysts: does every picture tell a story? *Trends Parasitol*. 2006; 22(9): 431-438
- [70] Wu Q, Zhang Y, Xu J, Shen P. Regulation of hunger-driven behaviors by neural ribosomal S6 kinase in *Drosophila*. *Proc Natl Acad Sci U S A*. 2005; 102(37):13289-13294
- [71] Wu Q, Brown MR. Signaling and function of insulin-like peptides in insects. *Annu Rev Entomol*. 2006; 51:1-24

- [72] Roovers E, Vincent ME, van Kesteren E, Geraerts WP, Planta RJ, Vreugdenhil E, van Heerikhuizen H. Characterization of a putative molluscan insulin-related peptide receptor. *Gene* 1995; 162(2):181-188
- [73] Kimura KD, Tissenbaum HA, Liu Y, Ruvkun G. *daf-2*, an insulin receptor-like gene that regulates longevity and diapause in *Caenorhabditis elegans*. *Science* 1997; 277(5328):942-946
- [74] Xu X, Williams JW, Bremer EG, Finnegan A, Chong ASF. Inhibition of Protein Tyrosine Phosphorylation in T Cells by a Novel Immunosuppressive Agent, Leflunomide *J Biol Chem* 1995; 270: 12398 – 12403
- [75] Gregoire FM, Chomiki N, Kachinskas D, Warden CH. Cloning and developmental regulation of a novel member of the insulin-like gene family in *Caenorhabditis elegans*. *Biochem Biophys Res Commun.* 1998; 249(2):385-390
- [76] Gami MS, Wolkow CA. Studies of *Caenorhabditis elegans* DAF-2/insulin signaling reveal targets for pharmacological manipulation of lifespan. *Aging Cell* 2006; 5(1):31-37
- [77] Wolkow CA, Munoz MJ, Riddle DL, Ruvkun G. Insulin receptor substrate and p53 orthologous adaptor proteins function in the *Caenorhabditis elegans* *daf-2*/insulin-like signaling pathway. *J Biol Chem* 2002; 277(51):49591-4957
- [78] Greer EL, Brunet A. FOXO transcription factors at the interface between longevity and tumor suppression. *Oncogene* 2005; 24(50):7410-7425
- [79] Konrad C, Kroner A, Spiliotis M, Zavala-Góngora R, Brehm K. Identification and molecular characterisation of a gene encoding a member of the insulin receptor family in *Echinococcus multilocularis*. *International Journal for Parasitology* 2003; 33: 301–312
- [80] Spiliotis M, Kroner A, Brehm K. Identification, molecular characterization and expression of the gene encoding the epidermal growth factor receptor orthologue from the fox-tapeworm *Echinococcus multilocularis*. *Gene* 2003; 323:57-65
- [81] Kurzchalia TV, Ward S. Why do worms need cholesterol? *Nat Cell Biol* 2003; 5(8): 684-688
- [82] Spiliotis M, Tappe D, Bruckner S, Mosch HU, Brehm K. Molecular cloning and characterization of Ras- and Raf-homologues from the fox-tapeworm *Echinococcus multilocularis*. *Mol Biochem Parasitol* 2005; 139(2):225-237
- [83] Khayath N, Vicogne J, Ahier A, Younes AB, Konrad C, Trolet J, Viscogliosi E, Brehm K, Dissous C. Diversification of the insulin receptor family in the helminth parasite *Schistosoma mansoni*. *FEBS J.* 2007; 274(3): 659-676
- [84] Spiliotis M, Konrad C, Gelmedin V, Tappe D, Bruckner S, Mosch HU, Brehm K. Characterisation of EmMPK1, an ERK-like MAP kinase from *Echinococcus multilocularis* which is activated in response to human epidermal growth factor. *Int J Parasitol* 2006; 36(10-11):1097-1112
- [85] Spiliotis M, Brehm K. *Echinococcus multilocularis*: identification and molecular characterization of a Ral-like small GTP-binding protein. *Exp Parasitol.* 2004; 107(3-4):163-172
- [86] Zavala-Gongora R, Kroner A, Bernthaler P, Knaus P, Brehm K. A member of the transforming growth factor-beta receptor family from *Echinococcus multilocularis* is activated by human bone morphogenetic protein 2. *Mol Biochem Parasitol* 2006; 146(2):265-271
- [87] Zavala-Gongora R, Kroner A, Wittek B, Knaus P, Brehm K. Identification and characterisation of two distinct Smad proteins from the fox-tapeworm *Echinococcus multilocularis*. *Int J Parasitol* 2003; 33(14):1665-1677.
- [88] Brehm K, Wolf M, Beland H, Kroner A, Frosch M. Analysis of differential gene expression in *Echinococcus multilocularis* larval stages by means of spliced leader differential display. *Int J Parasitol.* 2003; 33(11):1145-1159.

- [89] Gelmedin V, Zavala-Gongora R, Fernandez C, Brehm K. *Echinococcus multilocularis*: cloning and characterization of a member of the SNW/SKIP family of transcriptional coregulators. *Exp Parasitol* 2005; 111(2):115-20.
- [90] Brehm K, Spiliotis M, Zavala-Gongora R, Konrad C, Frosch M. The molecular mechanisms of larval cestode development: first steps into an unknown world. *Parasitol Int* 2006; 55 Suppl: S15-21
- [91] Vogel M, Gottstein B, Müller N, Seebeck Z. Production of a recombinant antigen of *Echinococcus multilocularis* with high immunodiagnostic sensitivity and specificity. *Mol Biochem Parasitol* 1988; 31:117-128
- [92] Hemmings L, and McManus P. The isolation, by differential antibody screening, of *Echinococcus multilocularis* antigen gene clones with potential for immunodiagnosis. *Mol Biochem Parasitol* 1989; 33:171-182
- [93] Hemmings L, and McManus P. The diagnostic value and molecular characterisation of an *Echinococcus multilocularis* antigen gene clone. *Mol Biochem Parasitol* 1990; 44:53-62
- [94] Frosch PM, Geier C, Kaup FJ, Müller A, and Frosch M. Molecular cloning of an echinococcal microtrichal antigen immunoreactive in *Echinococcus multilocularis* disease. *Mol Biochem Parasitol* 1993; 58:301-310
- [95] Frosch PM, Frosch M, Pfister T, Schaad V, and Bitter Suermann D. Cloning and characterisation of an immunodominant major surface antigen of *Echinococcus multilocularis*. *Mol Biochem Parasitol* 1991;48:121-130
- [96] Brehm K, Jensen K, Frosch P, Frosch M. Characterization of the genomic locus expressing the ERM-like protein of *Echinococcus multilocularis*. *Mol Biochem Parasitol* 1999; 100:147-152
- [97] Lou M, Garrett TP, McKern NM, Hoyne PA, Epa VC, Bentley JD, Lovrecz GO, Cosgrove LJ, Frenkel MJ, Ward CW. The first three domains of the insulin receptor differ structurally from the insulin-like growth factor 1 receptor in the regions governing ligand specificity. *Proc Natl Acad Sci U S A* 2006; 103(33):12429-12934
- [98] Kjeldsen T, Andersen AS, Wiberg FC, Skou Rasmussen J, Schäffer L, Balschmidt P, Bach Møller K, Møller NPH. The ligand specificities of the insulin receptor and the insulin-like growth factor I receptor reside in different regions of a common binding site. *Proc Natl Acad Sci USA* 1997; 88: 4404-4408
- [99] Nilsen TW. Trans-Splicing of Nematode Premessenger RNA. *Annu Rev Microbiol* 1993; 47:413-440
- [100] Nilsen TW. Trans-Splicing: An update. *Mol Biochem Parasitol* 1995;75:1-6
- [101] Blumenthal T. Trans-splicing and polycistronic transcription in *Caenorhabditis elegans*. *Trends Genet* 1995; 11:132-136
- [102] Davis RE. Spliced Leader RNA Trans-splicing in Metazoa. *Parasitol Today* 1996; 12:33-40
- [103] Blaxter M, and Liu L. Nematode spliced leaders-ubiquity, evolution and utility. *Int J Parasitol.* 1996; 26:1025-1033
- [104] Donelson JE, Zeng W. A comparison of trans-RNA splicing in trypanosomes and nematodes. *Parasitol Today* 1990 Oct; 6(10):327-34.
- [108] Liu F, Lu J, Hu W, Wang SY, Cui SJ, Chi M, Yan Q, Wang XR, Song HD, Xu XN, Wang JJ, Zhang XL, Zhang X, Wang ZQ, Xue CL, Brindley PJ, McManus DP, Yang PY, Feng Z, Chen Z, Han ZG. New perspectives on host-parasite interplay by comparative transcriptomic and proteomic analyses of *Schistosoma japonicum*. *PLoS Pathog* 2006; 2(4):e29

- [109] Brehm K, Hubert K, Scitutto E, Garate T, Frosch M. Characterization of a spliced leader gene and of trans-spliced mRNAs from *Taenia solium*. *Mol Biochem Parasitol* 2002; 122:100-105
- [110] Soni P, Lakkis M, Poy MN, Fernstrom MA, Najjar SM. The differential effects of pp120 (Ceacam 1) on the mitogenic action of insulin and insulin-like growth factor 1 are regulated by the nonconserved tyrosine 1316 in the insulin receptor. *Mol Cell Biol* 2000; 20(11):3896-3905.
- [111] Chaika OV, Chaika N, Volle DJ, Hayashi H, Ebina Y, Wang LM, Pierce JH, Lewis RE. Mutation of tyrosine 960 within the insulin receptor juxtamembrane domain impairs glucose transport but does not inhibit ligand-mediated phosphorylation of insulin receptor substrate-2 in 3T3-L1 adipocytes. *J Biol Chem* 1999; 274(17):12075-12080.
- [112] O'Neill TJ, Craparo A, Gustafson TA. Characterization of an interaction between insulin receptor substrate 1 and the insulin receptor by using the two-hybrid system. *Mol Cell Biol* 1994; 14(10): 6433-42
- [113] Uhlik MT, Temple B, Bencharit S, Kimple AJ, Siderovski DP, Johnson GL. Structural and evolutionary division of phosphotyrosine binding (PTB) domains. *J Mol Biol* 2005; 345(1):1-20
- [114] Cornford EM. Effects of insulin on *Schistosomium douthitti*. *Gen Comp Endocrinol* 1974; 23(3):286-293
- [115] Levi-Schaffer F, Smolarsky M. *Schistosoma mansoni*: effect of insulin and a low molecular-weight fraction of serum on schistosomula in chemically defined media. *Exp Parasitol* 1981; 52(3):378-385
- [116] Reiner DS, Hetsko ML, Gillin FD. A lipoprotein-cholesterol-albumin serum substitute stimulates *Giardia lamblia* encystation vesicle formation. *J Eukaryot Microbiol* 1995; 42(5): 622-627
- [117] Bogoyevitch MA, Court NW. Counting on mitogen-activated protein kinases--ERKs 3, 4, 5, 6, 7 and 8. *Cell Signal* 2004; 16(12):1345-1354
- [118] Torii S, Yamamoto T, Tsuchiya Y, Nishida E. ERK MAP kinase in G cell cycle progression and cancer. *Cancer Sci* 2006; 97(8):697-702
- [119] Peck J, Douglas G 4th, Wu CH, Burbelo PD. Human RhoGAP domain-containing proteins: structure, function and evolutionary relationships. *FEBS Lett*; 528(1-3):27-34
- [120] Wolf RM, Wilkes JJ, Chao MV, Resh MD. Tyrosine phosphorylation of p190RhoGAP by Fyn regulates oligodendrocyte differentiation. *J Neurobiol* 2001; 49(1):62-78
- [121] Taniguchi S, Liu H, Nakazawa T, Yokoyama K, Tezuka T, Yamamoto T. p250GAP, a neural RhoGAP protein, is associated with and phosphorylated by Fyn. *Biochem Biophys Res Commun.* 2003; 306(1):151-5.
- [122] Thomas SM, Brugge JS. Cellular functions regulated by Src family kinases. *Annu Rev Cell Dev Biol.* 1997; 13:513-609
- [123] Bromann PA, Korkaya H, Courtneidge SA. The interplay between Src family kinases and receptor tyrosine kinases. *Oncogene.* 2004; 23(48):7957-68
- [124] Wheeler AP, Ridley AJ. Why three Rho proteins? RhoA, RhoB, RhoC, and cell motility. *Exp Cell Res* 2004; 301(1):43-49
- [125] Mitin N, Rossman KL, Der CJ. Signaling interplay in Ras superfamily function. *Curr Biol* 2005; 15(14):R563-574
- [126] Okada S, Matsuda M, Anafi M, Pawson T, Pessin JE. Insulin regulates the dynamic balance between Ras and Rap1 signaling by coordinating the assembly states of the Grb2-SOS and CrkII-C3G complexes. *EMBO J* 1998; 17(9):2554-65.

- [127] Myagmar BE, Umikawa M, Asato T, Taira K, Oshiro M, Hino A, Takei K, Uezato H, Kariya K. PARG1, a protein-tyrosine phosphatase-associated RhoGAP, as a putative Rap2 effector. *Biochem Biophys Res Commun* 2005; 329(3):1046-1052
- [128] Boggan TJ, Eck MJ. Structure and regulation of Src family kinases. *Oncogene* 2004; 23(48):7918-7927
- [129] Sun XJ, Pons S, Asano T, Myers MG Jr, Glasheen E, White MF. The Fyn tyrosine kinase binds Irs-1 and forms a distinct signaling complex during insulin stimulation. *J Biol Chem* 1996; 271(18):10583-10587
- [130] O'Brien RM, Streeper RS, Ayala JE, Stadelmaier BT, Hornbuckle LA. Insulin-regulated gene expression. *Biochem Soc Trans* 2001; 29(Pt 4):552-558
- [131] Bravo DA, Gleason JB, Sanchez RI, Roth RA, Fuller RS. Accurate and efficient cleavage of the human insulin proreceptor by the human proprotein-processing protease furin. Characterization and kinetic parameters using the purified, secreted soluble protease expressed by a recombinant baculovirus. *J Biol Chem* 1994; 269(41):25830-25837
- [132] Lane MD, Ronnett GV, Kohanski RA, Simpson TL. Posttranslational processing of the insulin proreceptor. *Curr Top Cell Regul* 1985; 27: 279 - 292
- [133] Hwang JB and Frost SC. Effect of Alternative Glycosylation on Insulin Receptor Processing. *J Biol Chem* 2004; 274(32): 22813 – 22820
- [134] He HJ, Kole S, Kwon YK, Crow MT, Bernier M. Interaction of filamin A with the insulin receptor alters insulin-dependent activation of the mitogen-activated protein kinase pathway. *J Biol Chem*. 2003; 278(29):27096-27104
- [135] Paez-Espinosa V, Carvalho CR, Alvarez-Rojas F, Janeri L, Velloso LA, Boschero AC, Saad MJ. Insulin induces tyrosine phosphorylation of Shc and stimulates Shc/GRB2 association in insulin-sensitive tissues of the intact rat. *Endocrine* 1998;8(2):193-200
- [136] Thirone AC, Paez-Espinosa EV, Carvalho CR, Saad MJ. Regulation of insulin-stimulated tyrosine phosphorylation of Shc and IRS-1 in the muscle of rats: effect of growth hormone and epinephrine. *FEBS Lett* 1998; 421(3):191-196
- [137] Le MN, Kohanski RA, Wang LH, Sadowski HB. Dual mechanism of signal transducer and activator of transcription 5 activation by the insulin receptor. *Mol Endocrinol* 2002; 16(12):2764-2779
- [138] Bass J, Turck C, Rouard M, Steiner DF. Furin-mediated processing in the early secretory pathway: Sequential cleavage and degradation of misfolded insulin receptors. *PNAS* 2000; 97(22): 11905 – 11909
- [139] Resh MD. Fyn, a Src family tyrosine kinase. *Int J Biochem Cell Bio*. 1998; 30(11):1159-1162
- [140] Maegawa H, McClain DA, Freidenberg G, Olefsky JM, Napier M, Lipari T, Dull TJ, Lee J, Ullrich A. Properties of a human insulin receptor with a COOH-terminal truncation. II. Truncated receptors have normal kinase activity but are defective in signaling metabolic effects. *J Biol Chem* 1988; 263(18): 8912-8917
- [141] Kapp K, Schussler P, Kunz W, Grevelding CG. Identification, isolation and characterization of a Fyn-like tyrosine kinase from *Schistosoma mansoni*. *Parasitology* 2001; 122(Pt 3):317-327
- [142] Broome MA, Hunter T. The PDGF receptor phosphorylates Tyr 138 in the c-Src SH3 domain in vivo reducing peptide ligand binding. *Oncogene* 1997; 14(1):17-34
- [143] Proud CG. Regulation of protein synthesis by insulin. *Biochem Soc Trans*. 2006; 34(Pt 2):213-216
- [144] Shapiro SZ, Bahr GM, Hira PR. Analysis of host components in hydatid cyst fluid and immunoblot diagnosis of human *Echinococcus granulosus* infection. *Ann Trop Med Parasitol* 1992; 86(5):503-509.

- [145] Husted ST, Williams JF. Permeability studies on taenid metacestodes: I. Uptake of proteins by larval stages of *Taenia taeniaeformis*, *T. crassiceps*, and *Echinococcus granulosus*. *J Parasitol* 1977; 63(2):314-321
- [146] Hurd H. *Echinococcus granulosus*: a comparison of free amino acid concentration in hydatid fluid from primary and secondary cysts and host plasma. *Parasitology* 1989; 98 (Pt 1):135-143
- [147] Mamuti W, Sako Y, Xiao N, Nakaya K, Nakao M, Yamasaki H, Lightowlers MW, Craig PS, Ito A. *Echinococcus multilocularis*: developmental stage-specific expression of Antigen B 8-kDa-subunits. *Exp Parasitol* 2006; 113(2):75-82
- [148] Mitzner S, Klammt S, Stange J, Schmidt R. Albumin Regeneration in Liver Support — Comparison of Different Methods. *Therapeutic Apheresis and Dialysis* 2006; 10(2):108–117
- [149] Duckworth WC, Saudek CD, Henry RR. Why intraperitoneal delivery of insulin with implantable pumps in NIDDM? *Diabetes* 1992; 41(6):657-661
- [150] Gomes CM, Goto H, Magnanelli AC, Monteiro HP, Soares RP, Corbett CE, Gidlund M. Characterization of the receptor for insulin-like growth factor on *Leishmania* promastigotes. *Exp Parasitol* 2001; 99(4): 190-197
- [151] De Cesare D, Fimia GM, Sassone-Corsi P. Signaling routes to CREM and CREB: plasticity in transcriptional activation. *Trends Biochem Sci* 1999; 24(7):281-285
- [152] Peterson RT, Schreiber SL. Translation control: connecting mitogens and the ribosome. *Curr Biol* 1998; 8(7):R248-250
- [153] Bretscher A, Edwards K, Fehon RG. ERM proteins and merlin: integrators at the cell cortex. *Nat Rev Mol Cell Biol* 2002; 3(8):586-99
- [154] Gautreau A, Louvard D, Arpin M. ERM proteins and NF2 tumor suppressor: the Yin and Yang of cortical actin organization and cell growth signaling. *Curr Opin Cell Biol* 2002; 14(1):104-109
- [155] Louvet-Vallee S. ERM proteins: from cellular architecture to cell signaling. *Biol Cell* 2000; 92(5):305-316
- [156] Bretscher A, Chambers D, Nguyen R, Reczek D. ERM-Merlin and EBP50 protein families in plasma membrane organization and function. *Annu Rev Cell Dev Biol* 2000; 16:113-143
- [157] Thomas L. Labor und Diagnose. TH-Books Verlagsgesellschaft. 5. Auflage, 2000
- [158] Volund A. Conversion of insulin units to SI units. *Am J Clin Nutr* 1993; 58(5):714-715
- [159] Cromlish WA, Tang M, Kyskan R, Tran L, Kennedy BP. PTP1B-dependent insulin receptor phosphorylation/residency in the endocytic recycling compartment of CHO-IR cells. *Biochem Pharmacol* 2006; 72(10):1279-1292
- [160] Duckworth WC, Garcia JV, Liepnieks JJ, Hamel FG, Hermodson MA, Frank BH, Rosner MR. *Drosophila* insulin degrading enzyme and rat skeletal muscle insulin protease cleave insulin at similar sites. *Biochemistry* 1989; 28(6): 2471-2447
- [161] Kuo WL, Gehm BD, Rosner MR. Regulation of insulin degradation: expression of an evolutionary conserved insulin-degrading enzyme increases degradation via an intracellular pathway. *Mol Endocrinology* 1991; 5(10): 1457-1476
- [162] Perlman RK, Rosner MR. Identification of Zinc ligands of the insulin-degrading enzyme. *J Biol Chem* 1994; 269: 33140 – 33145
- [163] Heck MMS and Earnshaw WC. Topoisomerase II: A Specific Marker for Cell Proliferation. *The Journal of Cell Biology* 1986; 103: 2569-2581

- [164] Scholzen T and Gerdes J. The Ki-67 Protein: From the Known and the Unknown. *Journal of Cellular Physiology* 2000; 182: 311-322
- [165] Colman H, Giannini C, Huang L, Gonzalez J, Hess K, Bruner J, Fuller G, Langford L, Pelloski C, Aaron J, Burger P, Aldape K. Assessment and prognostic significance of mitotic index using the mitosis marker phospho-histone H3 in low and intermediate-grade infiltrating astrocytomas. *Am J Surg Pathol* 2006; 30(5):657-664
- [166] Knobloch J, Kunz W, Grevelding CG. Quantification of DNA synthesis in multicellular organisms by a combined DAPI and BrdU technique. *Dev Growth Differ* 2002; 44(6):559-563
- [167] Abramoff MD, Magelhaes PJ, Ram SJ Image Processing with ImageJ. *Biophotonics International* 2004; 11(7): 36-42
- [168] Baltensperger K, Lewis RE, Woon CW, Vissavajhala P, Ross AH, Czech MP. Catalysis of serine and tyrosine autophosphorylation by the human insulin receptor. *Proc Natl Acad Sci U S A* 1992; 89(17): 7885-7889
- [169] Saperstein R, Vicario PP, Strout HV, Brady E, Slater EE, Greenlee WJ, Ondeyka DL, Patchett AA, Hangauer DG. Design of a selective insulin receptor tyrosine kinase inhibitor and its effect on glucose uptake and metabolism in intact cells. *Biochemistry* 1989; 28(13):5694-701
- [170] Sciutto E, Fragoso G, Fleury A, Lacleste JP, Sotelo J, Aluja A, Vargas L, Larralde C. *Taenia solium* disease in humans and pigs: an ancient parasitosis disease rooted in developing countries and emerging as a major health problem of global dimensions. *Microbes Infect* 2000; 2(15):1875-1890
- [171] Stettler M, Fink R, Walker M, Gottstein B, Geary TG, Rossignol JF, Hemphill A. *in vitro* parasitocidal effect of Nitazoxanide against *Echinococcus multilocularis* metacestodes. *Antimicrob Agents Chemother* 2003; 47(2):467-474.
- [172] Matsumoto J, Muller N, Hemphill A, Oku Y, Kamiya M, Gottstein B. 14-3-3- and II/3-10-gene expression as molecular markers to address viability and growth activity of *Echinococcus multilocularis* metacestodes. *Parasitology* 2006; 132(Pt 1):83-94
- [173] Osman A, Niles EG, Verjovski-Almeida S, LoVerde PT. *Schistosoma mansoni* TGF-beta receptor II: role in host ligand-induced regulation of a schistosome target gene. *PLoS Pathog.* 2006; 2(6):e54
- [174] Smyth JD. *Echinococcus granulosus* and *Echinococcus multilocularis*: *in vitro* culture of their strobilar stages from protoscoleces. *Angew Parasitol.* 1979; 20: 137 – 147
- [175] Edwin F, Wiepz GJ, Singh R, Peet CR, Chaturvedi D, Bertics PJ, Patel TB. A historical perspective of the EGF receptor and related systems. *Methods Mol Biol.* 2006; 327:1 - 24
- [176] Kim J, Ahn S, Guo R, Daaka Y. Regulation of Epidermal Growth Factor Receptor Internalization by G Protein-Coupled Receptors. *Biochemistry* 2003; 42: 2887 – 2894
- [177] Hoyne PA, Elleman TC, Adams TE, Richards KM, Ward CW. Properties of an insulin receptor with an IGF-1 receptor loop exchange in the cysteine-rich region. *FEBS Letters* 2000; 269: 57 – 60
- [178] Riedel H, Dull TJ, Schlessinger J & Ullrich A. A chimeric receptor allows insulin to stimulate tyrosine kinase activity if epidermal growth factor receptor. *Nature* 1986; 324: 68 – 70
- [179] Gryseels B, Polman K, Clerinx J, Kestens L. Human schistosomiasis. *Lancet* 2006; 368(9541):1106-1118
- [180] Garcia HH, Gonzalez AE, Evans CA, Gilman RH; Cysticercosis Working Group in Peru. *Taenia solium* cysticercosis. *Lancet* 2003; 362(9383):547-556
- [181] Julenius K, Mølgaard A, Gupta R and Brunak S. Prediction, conservation analysis and structural characterization of mammalian mucin-type O-glycosylation sites. *Glycobiology* 2005; 15:153 – 164

- [182] Blom N, Sicheritz-Ponten T, Gupta R, Gammeltoft S, Brunak S. Prediction of post-translational glycosylation and phosphorylation of proteins from the aminoacid sequence. *Proteomics* 2004; 4(6): 1633 – 1649
- [183] Wick KR, Werner ED, Langlais P, Ramos FJ, Dong LQ, Shoelson SE, Liu F. Grb10 inhibits insulin-stimulated insulin receptor substrate (IRS)-phosphatidylinositol 3-kinase/Akt signaling pathway by disrupting the association of IRS-1/IRS-2 with the insulin receptor. *J Biol Chem* 2003; 278: 8460 – 8467
- [184] Altschul SF, Madden TL, Schäffer AA, Zhang J, Zhang Z, Miller W, Lipman DJ. Gapped BLAST and PSI-BLAST: a new generation of protein database search programs. *Nucleic Acids Res* 1997; 25: 3389-3402
- [185] Thompson JD, Higgins DG, Gibson TJ. CLUSTAL W: improving the sensitivity of progressive multiple sequence alignment through sequence weighting, position-specific gap penalties and weight matrix choice. *Nucleic Acids Res* 1994; 22(22): 4673-5680
- [186] Gottstein B, Deplazes P, Aubert M. *Echinococcus multilocularis*: immunological study on the "Em2-positive" laminated layer during in vitro and in vivo post-oncospherical and larval development. *Parasitol Res* 1992; 78(4):291-297
- [187] Hemphill A, Gottstein B. Immunology and morphology studies on the proliferation of in vitro cultivated *Echinococcus multilocularis* metacestodes. *Parasitol Res* 1995; 81(7): 605-614
- [188] Ottensmeyer FP, Beniac DR, Lua RZT, Yip CC. Mechanism of transmembrane signaling: insulin binding and the insulin receptor. *Biochemistry* 2000; 39:12103-12112
- [189] Hanke JH, Gardner JP, Dow RL, Changelian PS, William H. Brissette, Weringer EJ, Pollok BA, Connelly PA. Discovery of a Novel, Potent, and Src Family-selective Tyrosine Kinase Inhibitor. *J Bio Chem* 1996; 271: 695 - 701
- [190] van der Geer P, Hunter T, Lindberg RA. Receptor protein-tyrosine kinases and their signal transduction pathways. *Annu Rev Cell Biol* 1994; 10:251-337
- [191] Pautsch A, Zoepfel A, Ahorn H, Spevak W, Hauptmann R, and Nar Herbert. Crystal Structure of Bisphosphorylated IGF-1 Receptor Kinase: Insight into Domain Movements upon Kinase Activation. *Structure* 2001; 9:955-965
- [192] Ebina Y, Araki E, Taira M, Shimada F, Mori M, Craik CS, Siddle K, Pierce SB, Roth RA, Rutter WJ. Replacement of lysine residue 1030 in the putative ATP-binding region of the insulin receptor abolishes insulin- and antibody-stimulated glucose uptake and receptor kinase activity. *Proc Natl Acad Sci U S A* 1987; 84(3):704-708
- [193] Dey BR, Frick K, Lopaczynski W, Nissley SP, Furlanetto RW. Evidence for the direct interaction of the insulin-like growth factor I receptor with IRS-1, Shc, and Grb10. *Mol Endocrinol* 1996; 10(6): 631 – 641
- [194] Avruch J, Khokhlatchev A, Kyriakis JM, Luo Z, Tzivion G, Vavvas D, Zhang XF. Ras activation of the Raf kinase: tyrosine kinase recruitment of the MAP kinase cascade. *Recent Prog Horm Res* 2001;56:127-155
- [195] Bader AG, Kang S, Zhao L, Vogt PK. Oncogenic PI3K deregulates transcription and translation. *Nat Rev Cancer* 2005; 5(12):921-929
- [196] Valverde AM, Benito M, Lorenzo M. The brown adipose cell: a model for understanding the molecular mechanisms of insulin resistance. *Acta Physiol Scand* 2005; 183(1):59-73
- [197] Jope RS, Johnson GV. The glamour and gloom of glycogen synthase kinase-3. *Trends Biochem Sci* 2004; 29(2): 95-102
- [198] Letunic I, Copley RR, Pils B, Pinkert S, Schultz J, Bork P. SMART 5: domains in the context of genomes and networks. *Nucleic Acids Res* 2006; 34(Database issue):D257-60

- [199] Seecef RL, Dewhurst S. Insulin is a *Drosophila* hormone and acts to enhance the differentiation of embryonic *Drosophila* cells. *Cell Differ* 1974; 3(1):63-70
- [200] Esch GW. *Taenia crassiceps*: insulin and carbohydrate metabolism in larval forms. *Exp Parasitol* 1969; 25(1): 210-216
- [201] Gustafson TA, He W, Craparo A, Schaub CD, O'Neill TJ. Phosphotyrosine-dependent interaction of SHC and insulin receptor substrate 1 with the NPEY motif of the insulin receptor via a novel non-SH2 domain. *Mol Cell Biol* 1995; 15(5): 2500-2508
- [202] Cheatham B, Kahn CR. Cysteine 647 in the insulin receptor is required for normal covalent interaction between α - and β -subunits and signal transduction. *J Biol Chem* 1992; 267: 7108-7115
- [203] Sparrow LG, McKern NM, Gorman JJ, Strike PM, Robinson CP, Bentley JD, and Ward CW. The Disulfide Bonds in the C-terminal Domains of the Human Insulin Receptor Ectodomain. *J Biol Chem* 1997; 272: 29460-29467
- [204] Kozak M. An Analysis of 5'-Noncoding Sequences from 699 Vertebrate Messenger RNAs. *Nucleic Acids Res* 1987; 15: 8125-8148
- [205] Zarudnaya MI, Kolomiets IM, Potyahaylo AL, Hovorun DM. Downstream elements of mammalian pre-mRNA polyadenylation signals: primary, secondary and higher-order structures. *Nucleic Acids Res* 2003; 31(5):1375-1386
- [206] Bjellqvist B, Hughes GJ, Pasquali C, Paquet N, Ravier F, Sanchez J-C, Frutiger S & Hochstrasser DF. The focusing positions of polypeptides in immobilized pH gradients can be predicted from their amino acid sequences. *Electrophoresis* 1993, 14, 1023-1031
- [207] Johnstone CN, Castellvi-Bel S, Chang LM, Bessa X, Nakagawa H, Harada H, Sung RK, Pique JM, Castells A, Rustgi AK. ARHGAP8 is a novel member of the RHOGAP family related to ARHGAP1/CDC42GAP/p50RHOGAP: mutation and expression analyses in colorectal and breast cancers. *Gene* 2004; 336(1):59-71
- [208] Barfod ET, Zheng Y, Kuang WJ, Hart MJ, Evans T, Cerione RA, Ashkenazi A. Cloning and expression of a human CDC42 GTPase-activating protein reveals a functional SH3-binding domain. *J Biol Chem* 1993; 268(35):26059-26062
- [209] Li SS. Specificity and versatility of SH3 and other proline-recognition domains: structural basis and implications for cellular signal transduction. *Biochem J* 2005; 390(Pt 3):641-653
- [210] Puntervoll P, Linding R, Gemünd C, Chabanis-Davidson S, Mattingsdal M, Cameron S, Martin DMA, Ausiello G, Brannetti B, Costantini A, Ferrè F, Maselli V, Via A, Cesareni G, Diella F, Superti-Furga G, Wyrwicz L, Ramu C, McGuigan C, Gudavalli R, Letunic I, Bork P, Rychlewski L, Küster B, Helmer-Citterich M, Hunter WN, Aasland R & Gibson T J. ELM server: a new resource for investigating short functional sites in modular eukaryotic proteins. *Nucleic Acids Res* 2003; 31: 3625-3630
- [211] Shang X, Zhou YT, Low BC. Concerted regulation of cell dynamics by BNIP-2 and Cdc42GAP homology/Sec14p-like, proline-rich, and GTPase-activating protein domains of a novel Rho GTPase-activating protein, BPGAP1. *J Biol Chem* 2003; 278(46): 45903-45914
- [212] Nassar N, Hoffman GR, Manor D, Clardy JC, Cerione RA. Structures of Cdc42 bound to the active and catalytically compromised forms of Cdc42GAP. *Nat Struct Biol* 1998; 5(12):1047-1052
- [213] Gamblin SJ, Smerdon SJ. GTPase-activating proteins and their complexes. *Curr Opin Struct Biol* 1998; 8(2):195-201
- [214] Seewald MJ, Korner C, Wittinghofer A, Vetter IR. RanGAP mediates GTP hydrolysis without an arginine finger. *Nature* 2002; 414: 662 – 666

- [215] Chakrabarti PP, Suveyzdis Y, Wittinghofer A, Gerwert K. Fourier Transform Infrared Spectroscopy on the RapRapGAP Reaction, GTPase activation without an Arginine Finger. *J Biol Chem* 2004; 279: 46226 – 46233
- [216] Liang X, Lu Y, Wilkes M, Neubert TA, Resh MD. The N-terminal SH4 region of the Src family kinase Fyn is modified by methylation and heterogeneous fatty acylation: role in membrane targeting, cell adhesion, and spreading. *J Biol Chem* 2004; 279(9): 8133-8139
- [217] Burgaya F, Garcia-Fernandez J, Riutort M, Baguna J, Salo. Structure and expression of Spk-1, an src-related gene product found in the planarian *Dugesia (G) tigrina*. *Oncogene* 1994; 9(4):1267-1272
- [218] Stover DR, Furet P, Lydon NB. Modulation of the SH2 binding specificity and kinase activity of Src by tyrosine phosphorylation within its SH2 domain. *J Biol Chem* 1996; 271(21):12481-12487
- [219] Kulansky Poltilove RM, Jacobs AR, Renfrew Haft C, Xu P, Taylor SI. Characterization of *Drosophila* Insulin Receptor Substrate. *J Biol Chem* 2000; 275: 23346 – 23354
- [220] Zhang B, Zheng Y. Negative regulation of Rho family GTPases Cdc42 and Rac2 by homodimer formation. *J Biol Chem* 1998; 273(40):25728-25733
- [221] Chen JC, Zhuang S, Nguyen TH, Boss GR, Pilz RB. Oncogenic Ras leads to Rho activation by activating the mitogen-activated protein kinase pathway and decreasing Rho-GTPase-activating protein activity. *J Biol Chem* 2003; 278(5):2807-2818
- [222] van de Vijver KK, Hokke CH, van Remoortere A, Jacobs W, Deelder AM, Van Marck EA. Glycans of *Schistosoma mansoni* and keyhole limpet haemocyanin induce hepatic granulomas in vivo. *Int J Parasitol* 2004; 34(8):951-961
- [223] Narumiya S, Yasuda S. Rho GTPases in animal cell mitosis. *Curr Opin Cell Biol* 2006; 18(2):199-205
- [224] Shi Y, Massague J. Mechanisms of TGF-beta signaling from cell membrane to the nucleus. *Cell* 2003;113(6): 685-700
- [225] Beall MJ, Pearce EJ. Transforming growth factor-beta and insulin-like signalling pathways in parasitic helminths. *Int J Parasitol* 2002; 32(4): 399-404
- [226] Maizels RM, Balic A, Gomez-Escobar N, Nair M, Taylor MD, Allen JE. Helminth parasites--masters of regulation. *Immunol Rev* 2004; 201: 89-116
- [227] Dissous C, Khayath N, Vicogne J, Capron M. Growth factor receptors in helminth parasites: signalling and host-parasite relationships. *FEBS Lett* 2006; 580(12): 2968-2975
- [228] Zang X, Taylor P, Wang JM, Meyer DJ, Scott AL, Walkinshaw MD, Maizels RM. Homologues of human macrophage migration inhibitory factor from a parasitic nematode. Gene cloning, protein activity, and crystal structure. *J Biol Chem* 2002; 277: 44261-44267
- [229] Beall MJ, Pearce EJ. Human transforming growth factor-beta activates a receptor serine/threonine kinase from the intravascular parasite *Schistosoma mansoni*. *J Biol Chem* 2001; 276(34): 31613-31619
- [230] Shilo BZ. Regulating the dynamics of EGF receptor signaling in space and time. *Development* 2005; 132(18): 4017-4027
- [231] Eckert J, Deplazes P. Biological, epidemiological, and clinical aspects of echinococcosis, a zoonosis of increasing concern. *Clin Microbiol Rev* 2004; 17(1): 107-135
- [232] Garcia HH, Del Brutto OH; Cysticercosis Working Group in Peru. Neurocysticercosis: updated concepts about an old disease. *Lancet Neurol* 2005; 4(10): 653-661

7 Publications

Original Articles

Konrad C, Tappe D, Spiliotis M, Brehm K. Host insulin activates the insulin receptor in *Echinococcus multilocularis* and affects longevity. [in preparation]

Konrad C, Frosch M, Schubert-Unkmeir A. Integrin-linked kinase is involved in *Neisseria meningitidis* invasion of endothelial cells. [in preparation]

Czapek F, **Konrad C**, Frosch M, Schubert-Unkmeir A. *N.meningitidis* dissociates occludin from brain endothelial tight junctions. [in preparation]

Khayath N, Vicogne J, Ahier Arnaud, Younes A.B., **Konrad C**, Trolet J, Viscogliosi E, Brehm K and Dissous C. Diversification of the insulin receptor family in the helminth parasite *Schistosoma mansoni*. *FEBS J* 2007; 274(3): 659-676

Spiliotis M, **Konrad C**, Gelmedin V, Tappe D, Bruckner S, Mosch HU, Brehm K. Characterisation of EmMPK1, an ERK-like MAP kinase from *Echinococcus multilocularis* which is activated in response to human epidermal growth factor. *Int J Parasitol* 2006; 36(10-11): 1097-112

Konrad C, Kroner A, Spiliotis M, Zavala-Gongora R, Brehm K. Identification and molecular characterisation of a gene encoding a member of the insulin receptor family in *Echinococcus multilocularis*. *Int J Parasitol*. 2003; 33(3): 301-12.

Kastaniotis AJ, Mennella TA, **Konrad C**, Torres AM, Zitomer RS. Roles of transcription factor Mot3 and chromatin in repression of the hypoxic gene ANB1 in yeast. *Mol Cell Biol*. 2000; 20(19): 7088-98.

Review Article

Brehm K, Spiliotis M, Zavala-Gongora R, **Konrad C**, Frosch M. The molecular mechanisms of larval cestode development: first steps into an unknown world. *Parasitol Int*. 2006;55 Suppl:S15-21.

Congresses/Meetings**2006**

Brehm K, Spiliotis M, Zavala-Gongora R, **Konrad C**, Gelmedin V, Schäfer T, Epping K. Hormonal cross-talk between parasite and host in alveolar echinococcosis.

58. Tagung der Deutschen Gesellschaft für Hygiene und Mikrobiologie, Würzburg, Germany, 1.-4.10.2006

Konrad C, Spiliotis M, Brehm K. Host insulin stimulates growth and development of *Echinococcus multilocularis* via activation of the parasite's insulin receptor orthologue EmIR.

58. Tagung der Deutschen Gesellschaft für Hygiene und Mikrobiologie, Würzburg, Germany, 1.-4.10.2006

C. Konrad, M. Spiliotis & K. Brehm. The *Echinococcus multilocularis* insulin receptor EmIR is activated by host insulin.

22. Jahrestagung der Deutschen Gesellschaft für Parasitologie
Vienna, Austria, 22.02.-25.02.2006

Zavala-Gongora R, Spiliotis M, **Konrad C**, Knaus P & Brehm K

Host-parasite cross-communication via TGF- β and insulin signaling systems in alveolar echinococcosis.

22. Jahrestagung der Deutschen Gesellschaft für Parasitologie
Vienna, Austria, 22.02.-25.02.2006

2005

Brehm K, Spiliotis M, Zavala-Gongora R, **Konrad C** & Bernthaler B

Do evolutionary conserved molecules mediate an interaction between *Echinococcus multilocularis* and its mammalian host?

Hydra-Meeting on Molecular and Cellular Biology of Helminth Parasites, Hydra, Greece, 06.09.-11.09. 2005

Spiliotis M, Zavala-Gongora R, **Konrad C**, Caballero-Gamiz R, Kroner A, Gelmedin V & Brehm K

Receptor kinases and the MAP-kinase cascade of *Echinococcus multilocularis* as possible targets for chemotherapy.

6th Drug Development Seminar on Antiparasitic Chemotherapy; Bernhardt-Nocht-Institut für Tropenmedizin, Hamburg, Germany, 28.04.-29.04.2005

2004

Konrad C, Spiliotis M, Zavala-Gongora R, Kroner A, Tappe D & Brehm K

Functional characterization of insulin-, EGF- and TGF- β signaling systems in *Echinococcus multilocularis* and their role in host-parasite-interplay.

56. Jahrestagung der Deutschen Gesellschaft für Hygiene und Mikrobiologie, Münster, Germany, 26.09-29.09.2004

Konrad C, Kroner A, Tappe D, Spiliotis M, Zavala-Gongora R & Brehm K

Identification and characterization of an insulin receptor homologue from *Echinococcus multilocularis*. 21. Jahrestagung der Deutschen Gesellschaft für Parasitologie; Würzburg, Germany, 17.03.-20.03.2004. *International Journal of Medical Microbiology* (2004) 293 (Suppl. No. 38) 113

Konrad C, Spiliotis M, Zavala-Gongora R, Kroner A & Brehm K

Signal transduction systems of *Echinococcus multilocularis* and their role in parasite development and host-parasite interaction.

XXIst International Congress of Hydatidology, Nairobi, Kenia, 16.08.-21.08.2004

Spiliotis M, Zavala-Gongora R, **Konrad C**, Kroner A & Brehm K

Molecular characterization of the fox-tapeworm *Echinococcus multilocularis* and the host-parasite interplay in alveolar echinococcosis. International Symposium „Threat of Infection“, Würzburg, Germany, 25.07.-28.07.2004

2002

Konrad C, Spiliotis M, Kroner A, Frosch M & Brehm K

The *Echinococcus multilocularis* larval stage expresses surface receptor tyrosine kinases with high homology to mammalian EGF- and IGF-receptors. *Joint annual Meeting of the German and Dutch Societies for Parasitology*; Lübeck-Travemünde, Germany, 20-23.03.2002

Konrad C, Kroner A, Frosch K & Brehm K

Charakterisierung und funktionelle Analyse einer Tyrosinkinase der IGF/Insulin-Rezeptor familie aus *Echinococcus multilocularis*. *Statusworkshop der Fachgruppe „Eukaryontische Krankheitserreger“ der Deutschen Gesellschaft für Hygiene und Mikrobiologie*; Hannover, Germany, 08.-09.02.2002

Spiliotis M, Zavala-Gongora R, **Konrad C**, Kroner A, Frosch M & Brehm K

Signal transduction systems of *Echinococcus multilocularis* and their possible role in host-parasite communication.

54. Jahrestagung der Deutschen Gesellschaft für Hygiene und Mikrobiologie; Heidelberg, Germany, 06.-10.10.2002; *International Journal of Medical Microbiology* (2002) 292: 257.

Brehm K, Spiliotis M, Zavala-Gongora R, Kroner A, **Konrad C**, Günthel D & Frosch M

Towards a characterization of the hormone-based interaction between the cestode *Echinococcus multilocularis* and its intermediate host.

International Meeting on „Molecular and Cellular Biology of Helminth Parasites“, Hydra, Greece, 14-19.09.2002

2001

Spiliotis M, Kroner A, **Konrad C**, Frosch M & Brehm K

Characterization of receptor tyrosine kinases and Ras/MAPK cascade signal transduction elements of the fox – tapeworm *Echinococcus multilocularis*. 53. Jahrestagung der Deutschen Gesellschaft für Hygiene und Mikrobiologie; Aachen, Germany, 30.09.-04.10.2001; *International Journal of Medical Microbiology* (2001) 291: P193.

8 Curriculum vitae

- Since 02/2007
 Institute for Parasitology and Virology
 University of Zürich
 Research associate in the group of PD Dr. Adrian B. Hehl: Vesicle maturation and protein sorting in *Giardia lamblia*.
- 07/2006 – 01/2007
 Institute for Hygiene and Microbiology
 Julius – Maximilians Universität, Würzburg
 Research associate in the group of Dr. Alexandra Schubert-Unkmeir: analysis of the infection of human brain endothelial cells with *Neisseria meningitidis*.
- 08/2002 – 06/2006
 Institute for Hygiene and Microbiology
 Julius – Maximilians Universität, Würzburg
 Group of Prof. Dr. Klaus Brehm

 PhD – thesis: “Molecular analysis of insulin signaling mechanisms in *Echinococcus multilocularis* and their role in the host-parasite interaction in the alveolar echinococcosis.”
- 10/1996 – 07/2002
 Studies of Biology at the Julius – Maximilians Universität, Würzburg with the major subject Microbiology and minor subjects Biochemistry and Cellular/ Developmental Biology;
 Diploma grade: A („sehr gut“)

 Diploma thesis: ”Molekulare Charakterisierung und Funktionsanalyse einer Rezeptorkinase der Insulin/IGF – Familie des Fuchsbandwurms *Echinococcus multilocularis*” in the group of Prof. Dr. Klaus Brehm
- 10/15/1998
 Intermediate examination (Diplom-Vorprüfung),
 grade: A („sehr gut“)
- 09/1999 – 06/2000
 enrolled as a non-degree graduate student at SUNY Albany, NY, USA
 Research on the regulation of hypoxic genes in *Saccharomyces cerevisiae* in the laboratory of Prof. Richard S. Zitomer
- 10/1995 – 10/1996
 Social Service (Zivildienst) in Würzburg
- 09/1986 – 06/1995
 Friedrich-Koenig-Gymnasium in Würzburg
 A-level (Abitur) 06/30/1995

09/1982 – 07/1986

Adalbert-Stifter Grundschule in Würzburg

12/27/1975

date of birth

Zürich, 21.2.2007

Christian Konrad